LASER DESORPTION IONIZATION FOURIER TRANSFORM ION CYCLOTRON RESONANCE (L.D.I.-F.T.-I.C.R.) MASS SPECTROMETRIC STUDIES OF SOME UNDERIVATIZED BACTERIAL OLIGOSACCHARIDES

by

ZAMAS LAM

B. Sc. (Hons.) Thames Polytechnic, London, England, 1984

M. Sc. University of British Columbia, Canada, 1987

A THESIS SUBMITTED IN PARTIAL FULFILLMENT OF

THE REQUIREMENTS FOR THE DEGREE OF

DOCTOR OF PHILOSOPHY

in

THE FACULTY OF GRADUATE STUDIES

(DEPARTMENT of CHEMISTRY)

We accept this thesis as conforming

to the required standard

THE UNIVERSITY OF BRITISH COLUMBIA

Nov 1989

In presenting this thesis in partial fulfilment of the requirements for an advanced degree at the University of British Columbia, I agree that the Library shall make it freely available for reference and study. I further agree that permission for extensive copying of this thesis for scholarly purposes may be granted by the head of my department or by his or her representatives. It is understood that copying or publication of this thesis for financial gain shall not be allowed without my written permission.

Department of Chemistry

The University of British Columbia
Vancouver, Canada

Date 28th Nov, 1989

DE-6 (2/88)

ABSTRACT

This thesis describes the novel application of laser desorption ionization Fourier transform ion cyclotron resonance (l.d.i.-F.t.-i.c.r.) mass spectrometry for determining the sequence of underivatized oligosaccharides. As a starting point, four model oligosaccharides obtained from bacteriophage degradation of the corresponding bacterial capsular polysaccharides were analyzed. The experiments progressed from a linear pentasaccharide (*Klebsiella* K44), to a linear pentasaccharide containing an acid-labile pyruvic acid (*Klebsiella* K3), to a linear tetrasaccharide containing an acetamido hexose and an acid-labile neuraminic acid (*E. coli* K9), and finally to a "3+1" branched tetrasaccharide containing an lactic acid ether and a base-labile *O*-acetate (*Klebsiella* K22). The glycosidic bond and significant ring cleavage fragmentations observed in the mass spectra could be used for the sequencing of all three linear oligosaccharides. Furthermore, these unusual ring-cleaved fragments also provided some tentative indication on the positions of linkage on several monosaccharide residues.

The fragments derived from these model oligosaccharides were used to propose a logical interpretation of the l.d.i.-F.t.-i.c.r. mass spectra of commercially available polysaccharide reported by others. Polysaccharides that have similar primary and tertiary structures gave similar mass spectra. This may be rationalized by the fact that fragmentation occurred at the sample layer or the selvedge. Consequently, the mass spectra reflected the primary and tertiary structures of the polysaccharides in the solid state.

Finally, this l.d.i.-F.t.-i.c.r. technique was employed to sequence an unknown oligosaccharide obtained by anhydrous hydrogen fluoride degradation of the bacterial capsular polysaccharide. It was concluded that the unknown sample is composed of two tetrasaccharides with the same carbohydrate components, but with one structure substituted with serine and the other with threonine. Furthermore, indirect evidence suggests that the amino acids are linked to the carboxylic acid group of the hexuronic acid. However, two possible structures could be proposed for these oligosaccharides.

The experimental results showed that l.d.i.-F.t.-i.c.r. mass spectrometry is well suited for the analysis of underivatized oligosaccharides, where the abundant ring fragments observed, can be used for a tentative indication of positions of linkage information. Furthermore, the high resolution data can be used to confirm the presence of unusual sugars and substituents.

TABLE OF CONTENTS

LIST OF TABLES

LIST OF FIGURES

LIST OF MASS SPECTRA

LIST OF ABBREVIATIONS

CPS	-	capsular polysaccharide
LPS	-	lipopolysaccharide
PMAA	-	partially methylated alditol acetate
Gal	-	galactose
Glc	-	glucose
Man	-	mannose
Rha	-	rhamnose
GalA	-	galacturonic acid
GalNAc	-	2-acetamido-2-deoxygalactose
GlcA	-	glucuronic acid
GlcNAc	-	2-acetamido-2-deoxyglucose
deoxyHex	-	deoxyhexose
Hex	-	hexose
HexA	-	hexose uronic acid
HexNAc	-	acetamido hexose
Kdo	-	2-keto-3-deoxy-manno-octulonsonic acid
NeuNAc	-	N-acetyl neuraminic acid
Ac	-	acetyl
pyr	-	pyruvic acid acetal
g.c.	-	gas chromatography
m.s.	-	mass spectrometry
^{252}Cf-p.d.	-	Californium-252 plasma desorption
c.i.	-	chemical ionization
d.c.i.	-	desorption chemical ionization
e.i.	-	electron ionization
f.a.b.	-	fast atom bombardment
f.d.	-	field desorption
F.t.-i.c.r.	-	Fourier transform ion cyclotron resonance
l.d.i.	-	laser desorption ionisation
l.s.i.m.s.	-	liquid secondary ion mass spectrometry
t.o.f.	-	time-of-flight
amu	-	atomic mass unit
eV	-	electron volt
f.i.	-	fragment ion
m/z	-	mass to charge ratio
n.m.r.	-	nuclear magnetic resonance

ACKNOWLEDGMENTS

I would like to express my sincere gratitude to the following:

Professors Guy G.S. Dutton and Melvin B. Comisarow under whose guidance this research was conducted, for their patient, inspiration and very enthusiastic discussion on various academic and non-academic topics during my course of studies. Professor Dutton in particular for his financial support for the various ICSs, IMSC and CIC conferences that he so actively encourages me to attend. Professor Comisarow for his financial support for the ASMS conference.

Dr. Günter K. Eigendorf for his encouragment and the opportunity to learn some of the mass spectrometric techniques in his laboratory. And his staffs for the weekly Friday nutrients.

To the numerous graduate students (Drs. Andrew V.S. Lim, Linda M. Beynon, Ms. Sandra Taylor), post-doc. (Dr. Neil Ravenscroft), visiting scientists (Drs. Haralambos Parolis, Lesley A.S. Parolis, Stephen K. Ng and Ms. Paola Cescutti) in the Department of Chemistry for their friendship and general assistance. In particular, to Linda, Neil, Paola and Sandra for their helpful discussions and in the perparation of this thesis.

Drs. Asgeir Bjaranson (Science Institute, University of Iceland) and David A. Weil (Nicolet Analytical Instruments) for running the l.d.i.-F.t.-i.c.r. spectra. Nicolet Analytical Instruments for the loan of the FTMS-2000.

The Department of Chemistry (U.B.C.) for their financial support in the form of a Research Assistantship and the Faculty of Graduate Studies (U.B.C.) for a Travel Award.

To the friends in Vancouver (in particular B & B & B) for their kindness, comfort and encouragement that have made the past five years so extremely enjoyable.

Delicated with love and gratitude to:

my parents

LAM CHE HIM & CHIU KAI YIN

my sister and niece

SYLVIA & LAURA TO

CHAPTER I

INTRODUCTION

INTRODUCTION

Carbohydrates are a group of naturally occurring biological materials which have been known to man since prehistoric times and are still being used as both anabolic materials and as a readily available food source. Carbohydrates are composed of polyhydroxy aldehydes, ketones, alcohols, acids, or simple derivatives thereof. They can be linked into chains by acetal linkages to form oligo- or poly-saccharides. No sharp distinction is drawn between oligo- and poly-saccharides, for their structures are similar and only the molecular weights are different. The term "oligosaccharides" usually implies carbohydrates with two to nine monosaccharide residues in each molecule. Polysaccharides (PS) are defined as those carbohydrate polymers that contain periodically repeating structures in which the dominant inter-unit linkages are of the *O*-glycosidic types. Polysaccharides containing only one type of monosaccharide unit are called homopolysaccharides or homoglycans, examples of which are cellulose and chitin. Polysaccharides containing different monosaccharide units are termed heteroglycans.

Plants are composed of 50 to 80% (dry weight) of carbohydrates, found exclusively as polysaccharide polymers. Although the principal building material of higher animals is proteins, carbohydrates are often found associated with proteins (e.g., glycoproteins, proteoglycans and peptidoglycans), as well as with other materials to form glycolipids, lipopolysaccharides (LPS), teichoic and nucleic acids[1]. In some lower animals the major constituent of the exoskeleton is chitin, which is a polymer of *N*-acetylated glucosamine.

Carbohydrates in nature can serve either a structural role or as a source of energy (e.g., glycogen and starch). Structural polysaccharides can be divided into two main classes: i) the fibrous polysaccharides, such as cellulose and chitin; or ii) the gel-forming matrix polysaccharides, such as pectin. Furthermore, complex carbohydrates are essential in biological recognition processes and protection.

As early as 300 A.D., man exploited naturally occurring carbohydrates in the food industry. Nowadays, the thickening and gelling properties of carbohydrates are used to control the texture, flavor, appearance and color of food. Carbohydrates also play a major role

in the cosmetic, textile, paper and paint industries; they are recently being utilized as drilling fluids in the petroleum industry[2]. Readily accessible mono- or di-saccharides can also be used as starting materials in the synthesis of complex chiral compounds[3].

Polysaccharides can usually be represented by an average or regularly repetitive structure. Plant polysaccharides are generally comprised of block polymers with no true sense of a repeating structure. One of the few plant homoglycans is cellulose, which is the polycondensation product of 1,4-linked β-D-glucopyranoses. Plant polysaccharides are mostly composed of heteroglycans of average block repeating units, therefore, are very difficult to characterize. On the other hand, a majority of microbial exopolysaccharides are composed of regular oligosaccharide repeating units. Thus, structural elucidation of these microbial oligosaccharides should lead to the complete structural characterization of the polysaccharides.

The recent resurgence of interest in carbohydrates is largely due to a greater understanding of their role in biological cell-cell recognition processes. Furthermore, the discovery of the highly glycosylated protein coat of the HIV virus has encouraged a large number of "non-carbohydrate" chemists to try their hand in this oldest branch of biological chemistry[4].

I.1 IMMUNOLOGICAL IMPORTANCE OF BACTERIAL EXOPOLYSACCHARIDES

The bacterial cell wall encloses the plasma membrane of the bacterium. Lipopolysaccharide (LPS) which exhibits both immunogenicity and full endotoxicity is a main component of the cell wall (10 to 15% dry weight). This species-specific LPS contains the somatic polysaccharide antigen and is called the bacterial O antigen.

In general, the outermost cell component of pathogenic microbes plays a critical role in the immune response. Many bacteria, both Gram-positive and Gram-negative, produce extracellular (exo-)polysaccharides either in the form of a discrete capsule surrounding the bacterial cell or in the form of loose slime unattached to the cell surface[5]. (Fig. I.1 is a schematic representation of the Gram-positive and Gram-negative cell walls of bacteria.)

This capsular polysaccharide (CPS) is called the K antigen and constitutes the principal antigen of most pathogenic microorganisms. For many years these microbial capsular polysaccharides were considered to function simply as energy reserves, structural polymers and to have merely a limited role in protection against phagocytosis. It is now well established that they are also essential in biological recognition where they: i) act as highly specific receptors for bacterial viruses (bacteriophages) and bacteriocins; ii) are immunogenic; and iii) are specific surface antigens[6]. These capsular polysaccharides also mask the cell wall O antigens and thus interfere with their serological detection[7]. Furthermore they also protect the bacteria against desiccation and the action of complement. Nevertheless, because these capsular polysaccharides are immunogenic, they play an important part in the immune response to bacterial infection.

Extensive reviews of the immunology of bacterial capsular polysaccharides have been published[8,9]. An animal's immunological defence system is based on its antibody molecules recognizing a portion of the structure of the bacterial polysaccharide antigens. These recognized partial structures are termed the immunodominant or immunodeterminant structures, and they may be monosaccharide units linked in a specific way or an oligosaccharide in a particular conformation or a non-carbohydrate substituent, e.g. pyruvic acid acetal, or *N*- and *O*- acetyls[10]. In acidic polysaccharides the immunodominant sugars are often the uronic acid residues. In the case of branched polysaccharides, the immunodeterminant is usually the side chain. Since capsular polysaccharides consist of regular oligosaccharide repeating units, the immunodominant structures are therefore expressed repetitively.

Several bacterial polysaccharides may share the same antigenic determinant, and can be recognized by the same antibody regardless of their origin. These immunologically related polysaccharides are said to cross-react serologically. Cross-reactions can be used to provide information about the structure of many polysaccharides[11-14].

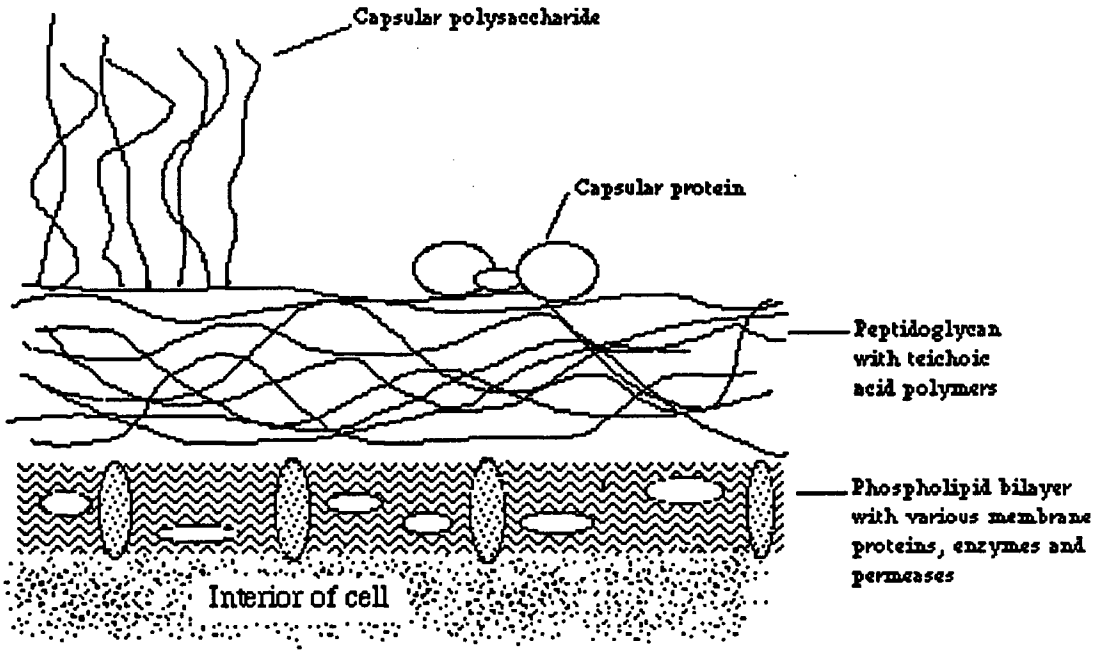

Cell envelope of the Gram-positive cell wall

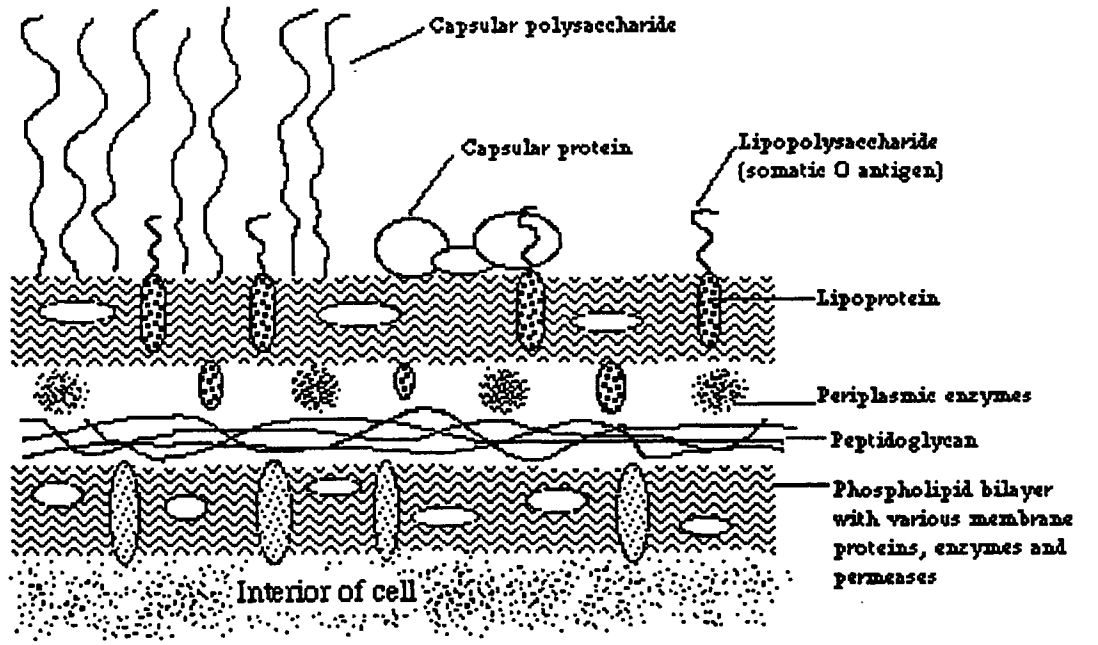

Cell envelope of the Gram-negative cell wall

Figure I.1 Schematic representations of Gram-positive and Gram-negative cell wall. Gram staining, perhaps the most widely used reaction in microbiology, was discovered by H.C.J. Gram (1884). It consists of staining heat-fixed smears with an aqueous solution of a basic gentian violet dye, mordanting with aqueous iodine, and then dehydration with ethanol. Those organisms that retain the blue-black dye are termed Gram-positives, and those which decolorized are termed Gram-negatives.

Both dead and live "attenuated" bacteria and toxins are commonly used as vaccines for disease prevention. Many exopolysaccharides coupled to carrier proteins can also be used as vaccines[8]. The first example dates from the 1940s, when bacterial polysaccharides were used to protect against pneumococcal infections[15]. Since then, many microbial polysaccharides have been shown to have non-cytotoxic antitumor properties, and hence have been extensively studied in cancer research[16,17].

Due to the immunological and serological importance of microbial exopolysaccharides, our laboratory has been part of an international collaborative program aimed at determining the molecular structures of these polysaccharides. This includes the characterization of their primary chemical structures as well as their tertiary structures in the solid and solution states. This is mainly achieved by using classical carbohydrate chemistry, combined with nuclear magnetic resonance spectroscopy (n.m.r.) and mass spectrometry (m.s.). With the advances of scientific instruments, a number of researchers are attempting to elucidate carbohydrate structures solely with the use of these spectroscopic techniques. The obvious advantages of this instrumental approach are the reduction in analysis time and sample quantity.

N.m.r. being a non-destructive technique is often favored for structural elucidation. Furthermore, there exists a large library of n.m.r. data which can be used as cross-references for unknown structures. The relatively large sample quantity needed (~ 10 to 20 mg) for n.m.r. analysis is sometimes prohibitory. On the other hand, mass spectrometry, although it is a destructive technique, often only requires sub-ng quantities. Therefore m.s. is becoming a more prominent tool in structural analysis, in addition to its more routine usage in molecular weight determination. Although the electron ionization (e.i.) mass spectra of alditol acetates and oligosaccharide alditols are well documented[18,19], there is a paucity of data relating to underivatized oligosaccharides.

The mass spectrometric investigations described in this and a previous dissertation[20] are specifically related to the structural characterization of *Klebsiella* and *E. coli* capsular polysaccharide antigens. In the previous studies[20], the preliminary investigation of some

desorption/ionization (desorption chemical ionization (d.c.i.), fast atom bombardment (f.a.b.) and laser desorption ionization Fourier transform ion cyclotron resonance (l.d.i.-F.t.-i.c.r.)) mass spectrometric techniques for the sequencing of both underivatized and derivatized oligosaccharides was presented. In this thesis, the application of l.d.i.-F.t.-i.c.r. mass spectrometry is extended to the sequencing and characterization of underivatized bacterial oligosaccharides obtained by specific chemical or enzymic degradation of bacterial capsular polysaccharides. As a starting point for the mass spectrometric studies, the application of l.d.i.-F.t.-i.c.r. to four underivatized model oligosaccharides is described in Section IV.3.1 to IV.3.8. These investigations served to illustrate the fragment ions formed using this technique and thus assisted in the analysis of the l.d.i.-F.t.-i.c.r. mass spectra of some commercial polysaccharides (Section IV.3.9). Finally the usefulness of this l.d.i.-F.t.-i.c.r. technique was evaluated by application to an unknown oligosaccharide which is described in Section IV.3.10 and IV.3.11. All the model oligosaccharides investigated were generated by specific degradation of the corresponding bacterial capsular polysaccharide. As capsular polysaccharides are comprised of a regular oligosaccharide repeating unit, the structural elucidation of the oligosaccharides may represent complete characterization of the native capsular polysaccharide.

Although this thesis is concerned with the analysis of pure carbohydrate compounds, it must be emphasized that any m.s. methods elaborated on bacterial carbohydrate antigens are directly transferable and relevant to other biological molecules containing sugars, such as glycoproteins and glycolipids.

CHAPTER II

CHEMICAL METHODS FOR STRUCTURAL ANALYSIS OF BACTERIAL CAPSULAR POLYSACCHARIDES

CHEMICAL METHODS FOR STRUCTURAL ANALYSIS OF POLYSACCHARIDES

The complete structural characterization of any carbohydrate material can be quite complex, due to the different permutations of sugar residues, glycosidic linkages, anomeric configurations and possible non-carbohydrate substituents that may be present. The normal analytical procedure involves: i) identification and quantitation of monosaccharide components; ii) analysis of non-carbohydrate substituents if present; and the determination of iii) absolute configuration; iv) anomeric configuration; v) ring size; vi) linkage position; vii) sugar sequence; and viii) tertiary structure. Although the present study did not involve traditional structural carbohydrate chemistry, this chapter will describe some of these more common, albeit complex procedures used for the structural elucidation of these polysaccharides in order to emphasize the usefulness and relative simplicity of the instrumental approaches.

II.1 ISOLATION AND PURIFICATION

The heterogeneity of capsular polysaccharide preparations arises from the other cell components. As capsular polysaccharides are soluble in water, the first step in its purification involves removal of non water-soluble components by high speed centrifugation. Extraction using dilute alkali is not normally used as the possibility exists for base-catalyzed degradation. Similarly, utilization of dilute acid increases the risk of hydrolysis of glycosidic linkages during isolation. LPS and nucleic acids can be separated from the capsular polysaccharides by liquid phenol precipitation from aqueous solvent[21]. In addition, LPS exists as micelles in aqueous solution and, therefore, can be removed during the centrifugation step. The polysaccharide in the supernatant can be separated from any proteins and nucleic acids present by addition of the supernatant to ethanol[22]. Because capsular polysaccharides are usually acidic, polysaccharides can be further purified by precipitation with potassium chloride[23], cupric acetate[24] or cetyltrimethylammonium bromide (Cetavlon)[25].

Purification by chromatographic techniques, such as gel filtration[26] or molecular sieve chromatography[27] on cross-linked dextrans are usually employed when dealing with milligram quantities of polysaccharide. Ion-exchange chromatography[28] is used for acidic polysaccharides, while affinity chromatography[29] is employed extensively for the purification of *N*-glycosidic glycopeptides[30].

The absence of heterogeneity, rather than the presence of homogeneity is used to established the purity of the polysaccharide. Purity is obtained where the isolate attains consistent chemical composition (such as sugar residues, analysis of particular functional groups and spectroscopic data) and the physical properties (optical rotation, gel chromatography[31] and electrophoresis[32,33]) of the isolate.

II.2 TOTAL SUGAR ANALYSIS

The initial step of structural characterization involves the total hydrolysis of polysaccharide into its component monosaccharides. As all sugars are to some extent degraded by acid, the experimental conditions must be chosen with care. The choice of reagent depends very much on the nature of the sugars, the type of glycosidic bonds present and the general stability of the individual monosaccharide units to acid[34]. Therefore a series of experiments with different hydrolytic conditions have to be used to establish the true composition of the polysaccharide.

II.2.1 HYDROLYSIS IN AQUEOUS MEDIUM

Hydrolysis may be carried out successfully using hydrochloric and sulphuric acids. Although hydrochloric acid is more easily removed than sulphuric acid, it usually causes greater degradation[35]. Therefore the volatile and easily removed trifluoroacetic acid has largely replaced mineral acids for aqueous hydrolysis[36]. For 2-acetamido-2-deoxy sugars, preliminary hydrolysis with acetic acid is usually carried out to avoid *N*-deacetylation[37]. Acetamido sugars can then be hydrolyzed with anhydrous hydrogen fluoride[38,39].

Although neutral sugars can be completely hydrolyzed with minimum degradation with 2 M trifluoroacetic acid at 100°C for 6-8 hours, other more acid labile saccharides, such as deoxysugars, ketoses and sialic acids are largely decomposed under these conditions, while 2-amino-2-deoxy sugars and uronic acids are incompletely hydrolyzed. Consequently, different acid strengths and exposure times are required in order to measure the exact number of monosaccharide residues in the oligosaccharide repeating unit.

II.2.2 HYDROLYSIS IN NON-AQUEOUS MEDIUM

Methanolysis with methanolic hydrogen chloride leads to the formation of methyl glycoside methyl esters and methyl glycosides, which stabilize the normally acid labile sugars, and thus is less destructive to deoxysugars and sialic acids[40,41].

In the case of polysaccharides containing uronic acid residues, methanolysis of the glycosidic bonds induces esterification of the uronic acid residue, which can then be reduced to its corresponding primary alcohol with sodium borodeuteride[42]. The mixture of methyl glycosides is hydrolyzed and converted into alditol acetate derivatives to be analyzed by gas chromatography (g.c.).

Although some polysaccharides are insoluble in aqueous solution (e.g. cellulose), the acetylated derivatives are readily soluble in acetic anhydride-acetic acid mixture. Acetolysis of the peracetylated material with a catalytic amount of sulphuric acid has the advantage of cleaving 1→6 linkages, which are more resistant than the other linkages to acid hydrolysis. Sialic acid linkages are usually very stable to the above process, leading to the isolation of sialic acid containing oligomers[43].

II.2.3 CHARACTERIZATION OF THE MONOSACCHARIDES

Conventional qualitative analytical techniques involve paper chromatography[44,45], thin-layer chromatography[46] and paper electrophoresis[47]. Spectrometric analysis permits classification into broad groups[48,49]. Gas chromatography[34,50], high performance liquid chromatography[51] (h.p.l.c.) and m.s. are increasingly popular for the quantification of

monosaccharides. G.c. methods require the sugar to be derivatized to impart volatility, whereas h.p.l.c. can be performed on the underivatized, hydrolyzed monosaccharides or oligosaccharides.

II.2.4 REDUCTION OF URONIC ACID FOR G.C. ANALYSIS

Polysaccharides containing uronic acid residues are difficult to analyze for the following reasons: i) the carboxylic function cannot be easily analyzed by g.c. or h.p.l.c.; ii) the glycosidic bond of the uronic acid is resistant to acid hydrolysis; and iii) incomplete periodate oxidation results from electrostatic repulsion between the periodate and the carboxylate ion (discussed in Section II.5.3). The best approach to use in the investigation of acidic polysaccharides involves reduction of the carboxylic function to the primary alcohol, though the pH of the reaction medium has to be rigidly controlled.

Normally an aqueous solution of the acidic polysaccharide is treated with a water-soluble carbodiimide to give *O*-acylisourea, which is then reduced with sodium borohydride[52]. This procedure, unlike methanolysis, leaves all glycosidic linkages intact. The uronic acid residues can also be reduced, after methanolysis, to the methyl glycoside methyl ester with sodium borodeuteride[42]. Another approach involves reduction of the permethylated polysaccharide, usually with lithium aluminum deuteride in tetrahydrofuran[53]. The reduction of the uronic acid using the deuteride approach, has the added advantage of labelling the acidic sugar which can be identified by the different g.c. retention time, as well as the increase in mass observable in the mass spectrum.

II.2.5 DETERMINATION OF ABSOLUTE CONFIGURATION

Routine use of chromatographic and spectrometric methods cannot distinguish between enantiomers, therefore, polarimetric measurements are employed: i) optical rotation $[\alpha]_D$; and ii) circular dichroism measurement of the alditol acetates or the partially methylated alditol acetates[54]. The use of optically active alcohols (e.g., (-)-2-butanol[55], (+)-2-octanol[56]) to convert the enantiomers to diastereomers, followed by g.c. separation of the volatile

derivatives, such as acetates or trimethylsilyl ethers can be achieved in milligram quantities. Enzymatic assay can presently only be used for a few sugars (e.g., D-glucose oxidase[57] and D-galactose oxidase[58].)

II.2.6 DETERMINATION OF ANOMERIC CONFIGURATION

The monosaccharides can be either α- or β- linked in the polysaccharide. The assignment of the anomeric configurations to specific linkages can be achieved by: i) the use of specific exoglycanase enzymes (e.g., α- or β- glucosidase)[59]; ii) measurement of the coupling constants and chemical shifts in the n.m.r. spectra (discussed in Section III.1.1); iii) the use of chromium trioxide oxidation on the peracetylated material, where the β-linked saccharides are preferentially degraded[60].

II.3 METHYLATION ANALYSIS

The second step in the characterization of polysaccharides involves the determination of the positions of substitution of each individual monosaccharide residue. This is accomplished by methylation analysis, where the free hydroxyl groups of the polysaccharide are protected by etherification (methylation), followed by hydrolysis, reduction and acetylation. The partially methylated alditol acetate (PMAA) derivatives obtained are then separated by g.c. and identified by g.c.-m.s. The information obtained can also be used to plan appropriate degradation methods for the polysaccharide into small oligosaccharide fragments. Nevertheless, methylation analysis does not provide information on the sequence or the anomeric linkages.

The most commonly used methylation procedure was developed by Hakomori[61]. Methylation can be achieved by treating the polysaccharides with the strong base dimethyl methylsulphinyl methanide (sodium dimsyl, formed by the reaction of sodium hydride with dimethyl sulphoxide) and followed by addition of methyl iodide. Hakomori methylation leads to esterification of uronic acids, pyruvate residues and *N*-methylation of acetamide groups in amino sugars.

Dimsyl can also be generated using potassium *tert*-butoxide[62], potassium hydride[63] and butyllithium[64]. These reagents generally produce dimsyl as efficiently as sodium hydride, and are more rapid, convenient and safer. These methods also result in less interfering peaks in g.c.-m.s. analyses of methylated polysaccharides.

The latest methylation procedure involves the use of methyl iodide, a solid base (sodium hydroxide) and DMSO[65]. Excellent yields of permethylated products can be obtained in a very short reaction time, and non-carbohydrate peaks are not observed in the chromatogram.

The use of a strong base during methylation causes removal of base-labile substituents (e.g., acetates), resulting in loss of substitution information. Nevertheless, *O*-acyl groups can be detected using the Prehm[66] methylation procedure, where the polysaccharide is dissolved in trimethyl phosphate and then methylated with methyl trifluoromethane sulphonate using 2,6-di-(*tert*-butyl) pyridine as the proton scavenger.

If undermethylation is suspected, then complete methylation can be obtained by treating the partially methylated polysaccharide with silver oxide and methyl iodide[67]. A second treatment by the Hakomori procedure will cause β-elimination of any uronic acid residue present. Polysaccharides containing uronic acid can be carboxyl-reduced before (carbodiimide reduction[52]) or after (lithium aluminium deuteride[53]) the permethylation steps.

The usual cause of undermethylation is the incomplete dissolution of the sample. Some polysaccharides like cellulose, are insoluble in DMSO; however, these can be methylated with a N-methylmorpholine-N-oxide (MMNO)-DMSO mixture. Solubility can also be improved by using the free acid form of the polysaccharide, by ultrasonication and by heating to ~ 50°C before methylation.

The methylated product is recovered by dialysis or partition between water and chloroform. Infrared spectroscopy is used to check for completeness of methylation (absence of hydroxyl absorption at 3600 cm^{-1}).

II.4 ANALYSIS OF NON-CARBOHYDRATE SUBSTITUENTS

The most common non-carbohydrate substituents in bacterial polysaccharides are the base-labile acetates and acid-labile acetal-linked pyruvate groups. If present, these non-carbohydrate substituents usually function as the antigenic determinants[10]. Therefore, determination of the location of these groups is of paramount importance. The presence of pyruvate is best identified and quantified by n.m.r. spectroscopy (discussed in Section III.1). The positions of linkage can be obtained by comparing the g.c.-m.s. data from the methylation analysis of the pyruvylated and the de-pyruvylated polysaccharide.

The *N*-acetyl group is usually associated with 2-acetamido-2-deoxyhexoses and is considered to be part of the sugar. Identification and quantification of the number of *O*-acetyl groups per repeating unit of a capsular polysaccharide can be measured from its ^{1}H-n.m.r. spectrum (discussed in Section III.1). Fast atom bombardment (f.a.b.)[68] mass spectrometry can be used to determine to which monosaccharide residues the *O*-acetyl groups are attached[69], however, the exact positions of linkage can only be attained by Prehm methylation[66] or the de Belder and Normann procedure[70]. Methylation using a strong base will cause de-*O*-acetylation, therefore, pertrifluoroacetyl derivatives are normally used in f.a.b.-m.s.[69] for the location of *O*-acetyl groups.

II.5 DEGRADATION OF POLYSACCHARIDES INTO SMALL OLIGOSACCHARIDES

Specific cleavages of polysaccharides into small oligosaccharide fragments, followed by isolation and characterization of these units are the established methods for polysaccharide sequencing. A number of specific degradation methods have been developed over the years. These include: partial acid hydrolysis, β-elimination[71,72], periodate oxidation[73] and enzymic degradation[74].

II.5.1 PARTIAL ACID HYDROLYSIS

Partial acid hydrolysis is the most common procedure for cleaving polysaccharide into smaller fragments. The mode of cleavage is dependent on the different rates of hydrolysis of

different glycosidic linkages[75]. The factors affecting the rates of hydrolysis depend on: ring size, configuration, conformation, positions of linkage, position of saccharide within the primary structure and any non-carbohydrate substituents present. Uronic acids and amino sugars are generally more resistant to acid hydrolysis than neutral sugars, and therefore, oligosaccharides containing these two residues are frequently isolated. The disadvantages of acid hydrolysis are: i) the possible loss of acid-labile substituents; ii) that partial hydrolysis usually gives non-specific cleavages, and therefore, a mixture of oligosaccharides is generated. Nevertheless, the mixture of oligosaccharides generated by this method, after permethylation, can be analyzed by g.c.-c.i.-m.s. to give sequence information on the polysaccharide itself[76].

II.5.2 β-ELIMINATION

Any methylated polysaccharides containing 4-*O*-substituted uronic acids will undergo β-elimination when treated with a strong base, such as dimsyl anion[71,72]. If the uronic acid is in the side chain, the resultant new polysaccharide can give an indication of where and how the acid is linked. On the other hand, if the uronic acid residue is in the main chain, this will result in fission of the polysaccharide and the oligosaccharides generated can provide information on the saccharide residues adjacent to the uronic acid residue. The oligosaccharides can also be used for m.s. sequencing of the PS[20,77].

II.5.3 PERIODATE OXIDATION/SMITH DEGRADATION

Water-soluble polysaccharides containing 1,2-diol and 1,2,3-triol systems can be degraded by periodate oxidation[78,79]. However, polysaccharides containing uronic acid residues will be incompletely oxidized due to the electrostatic repulsion between the periodate and the carboxylate ion. Therefore, the polysaccharides should be reduced using the carbodiimide procedure[52]. The oxidation can be monitored by spectrophotometry[80] or by titration of the liberated formic acid and formaldehyde[81] from a 1,2,3-triol. The resultant

polyaldehyde is usually reduced to the polyalcohol to prevent hemiacetal formation of the highly reactive aldehydes. This procedure is often mis-identified as the Smith degradation[82].

The Smith degradation involves periodate oxidation of the polysaccharide, reduction of the polyaldehyde, and a mild acid hydrolysis of the resultant polyalcohol at room temperature to cleave acyclic acetal linkages and leave the remaining glycosidic linkages intact[82]. Information on the oxidized saccharide can be obtained from the resultant aglycones (e.g., a 4-*O*-substituted hexopyranose will produce a 2-*O*-tetritol and a 2-*O*-substituted hexopyranose will produce a 2-*O*-glycerol). The hydrolysis step can be monitored by g.c. analysis of the trimethylsilyl derivatives of the product[83].

II.5.4 BACTERIOPHAGE DEGRADATION

Bacteriophages are serotype-specific viruses that first infect and then propagate within the bacterium thus destroying the host cell[84-86]. They are often designated by the Greek letter ϕ, followed by the number of the serotype of the host strain. The absorption of the phage to its receptor is highly specific, where the exopolysaccharide acts as a receptor for phage binding[87]. The phage-associated endoglycanases depolymerize this exopolysaccharide, and subsequent penetration of the host cell by the phage is followed by the release of viral DNA[88].

The use of these phage-borne enzymes for depolymerization of bacterial capsular polysaccharides allows the isolation of selectively cleaved oligosaccharides corresponding to one or more oligosaccharide repeating units (termed P1, P2, etc.)[74]. Furthermore, acid- and base-labile non-carbohydrate substituents remain intact on the oligosaccharide. This is usually difficult to achieve using chemical means of degradation. Fig. II.1 shows a schematic diagram of selective bacteriophage (ϕ) cleavages of a capsular polysaccharide to give P1 and P2 units. The characterization of the repeating oligosaccharides represents the structural elucidation of the polysaccharide itself; thus oligosaccharides generated by bacteriophage degradation are excellent substrates for mass spectrometric studies[89].

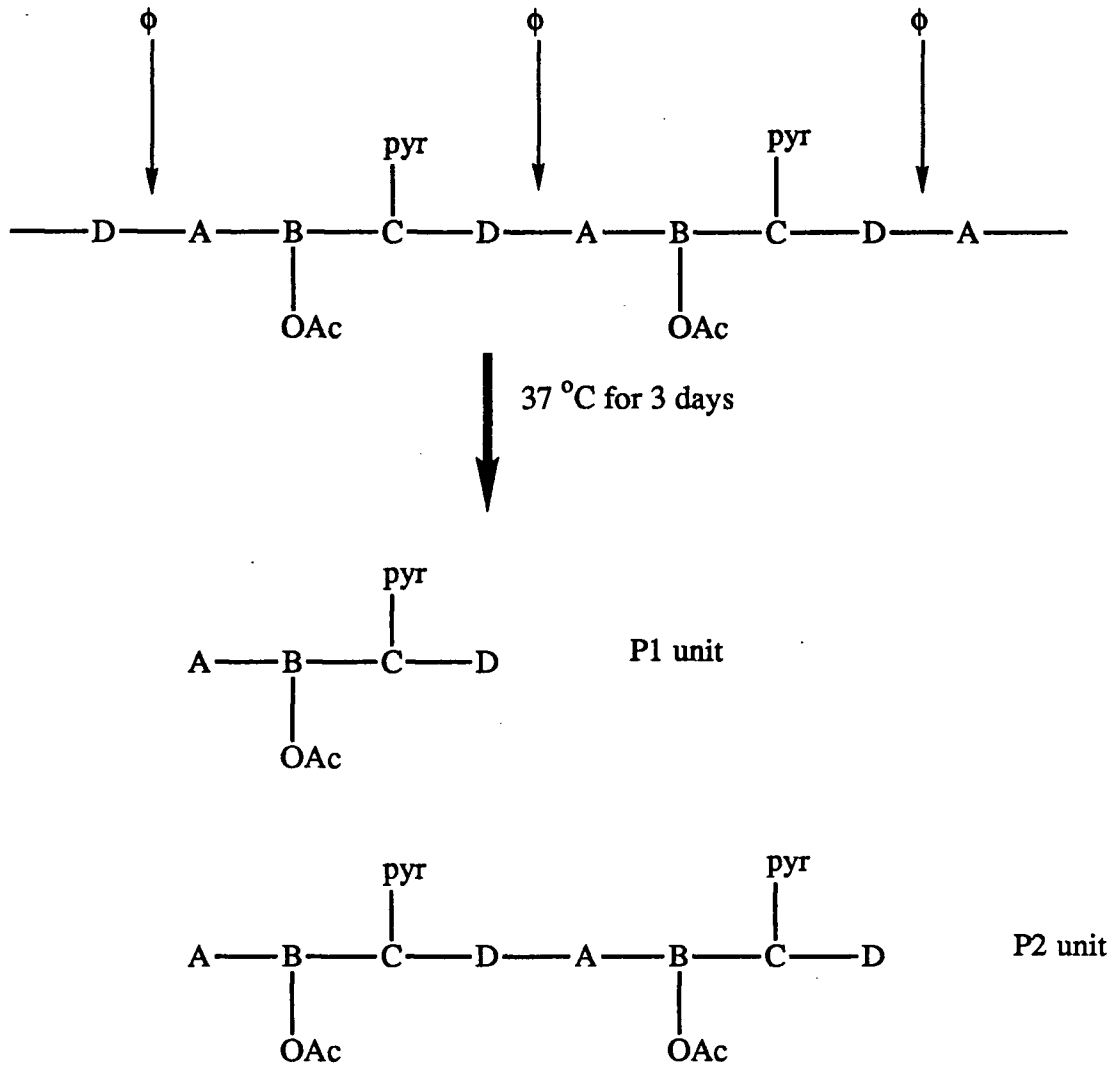

Fig.II.1 Schematic diagram to illustrate bacteriophage (ϕ) degradation of a capsular polysaccharide (made up of tetrasaccharide repeating unit) to give P1 (tetrasaccharide) and P2 (octasaccharide) units. Note that base- or acid-hydrolysis will remove either the *O*-acetyl or the pyruvic acid acetal groups respectively, with loss of substituent information. The P2 unit contains all the information required to elucidate the structure of the CPS, while P1 unit contains only partial (3/4) information.

CHAPTER III

INSTRUMENTAL METHODS USED IN CARBOHYDRATE ANALYSIS

INSTRUMENTAL METHODS USED IN CARBOHYDRATE ANALYSIS

The advance in analytical instrumentation, has generated a phenomenal improvement in instrumental techniques. Moreover, with the introduction of pulsed Fourier transform spectroscopy and superconducting magnets, complete characterization of polysaccharides may be possible in the near future by both n.m.r. and m.s.

III.1 NUCLEAR MAGNETIC RESONANCE SPECTROSCOPY

N.m.r. being a non-destructive physical technique is used extensively in carbohydrate chemistry for structural, configurational and conformational analyses[90-93]. The traditional n.m.r. experiments have been conducted in solution, but recent solid state experiments using cross polarization-magic angle spinning are developing as the technique improves[94]. The most useful one-dimensional n.m.r. parameters in carbohydrate chemistry are: i) chemical shifts; ii) relative integral intensities; iii) coupling constants; and iv) proton spin-lattice relaxation times (T_1)[95,96].

In recent years, two dimensional n.m.r. techniques have became more prominent in structural elucidation[97,98]. Complete characterization can be achieved using a combination of classical methods and high field n.m.r[99]. The n.m.r. approach suffers from the main disadvantage of requiring a relatively large amount of material (~ 10 to 20 mg).

III.1.1 CHEMICAL SHIFTS

The chemical and magnetic environment of a nucleus governs its chemical shifts (δ). The δ value is usually referenced to acetone and expressed relative to tetramethylsilane. The δ scale can be divided into three main regions for a ^1H spectrum and four for a ^{13}C spectrum:
i) The anomeric region - ^1H: H-1 α-anomers δ 5.5 to 5.0 and β-anomers δ 5.0 to 4.5; ^{13}C: α-pyranoses δ 98 to 103, β-pyranoses δ 103 to 106 and furanoses δ 106 to 109.
ii) The ring proton region - the ^1H spectrum is not well resolved (δ 3.0 to 4.5). In contrast, the ^{13}C spectrum can be used to assign linkage position. A free primary alcohol gives a

signal at δ 60 to 62. If it is substituted then the signal shifts downfield by 7 to 10 ppm. The rest of the ring carbons resonate between δ 65 to 80.

iii) The high field region where the methyl groups of pyruvate (depending on the R or S stereochemistry of the acetal[100], ^{1}H: ~ δ 1.5; ^{13}C: δ 17 to 25,); acetate (^{1}H: δ 2.0 to 2.2; ^{13}C: δ 20 to 25) and 6-deoxyhexoses (^{1}H: ~ δ 1.3; ^{13}C: δ 16 to 18) can be detected.

iv) The carboxy and carbonyl region which is only observed for ^{13}C spectra: ~ δ 170.

III.1.2 RELATIVE INTEGRAL INTENSITIES

A quantitative estimation of the ratio of α- to β-anomers, the number of 6-deoxyhexoses, pyruvate and acetate in the repeating oligosaccharide unit can be accomplished by measuring the relative integrals of the appropriate signals in the ^{1}H polysaccharide spectrum. Due to saturation and the nuclear Overhauser enhancement (n.O.e.) effect, quantitation with a proton decoupled ^{13}C spectrum is not reliable. Nevertheless, by counting the number of ^{13}C signals with the same number of hydrogen atoms in the spectrum the number of sugar residues per repeating unit can be determined.

Oligosaccharides mutarotate, and exhibit two signals (α- and β-) for the "mixture" of reducing sugar. Therefore, the degree of polymerization of an oligosaccharide can be determined by comparing the number of anomeric signals to those of the reducing sugar.

III.1.3 COUPLING CONSTANTS

Coupling constants (J values) arise from spin-spin coupling between two or more nuclei possessing magnetic moments. The coupling constant is mediated by the bonding electrons, and its magnitude is dependent on the type of chemical bond, the bond angle, the nature of the two nuclei and their distance. Therefore, coupling constants are used extensively for configurational and conformational analyses. The Karplus equation describes the relationship of J to the torsional angle (Ø) of the coupled nuclei[101]. The value is maximum when Ø is 0° or 180° and minimum at Ø of 90°. For a pyranosyl system, the splitting of transdiaxial protons

is ~ 8 to 12 Hz, while equatorial-equatorial and equatorial-axial protons have coupling constants of ~ 1 to 3 Hz and ~ 1 to 6 Hz respectively.

III.2 GAS CHROMATOGRAPHY

Although the separation and identification of saccharides is now dominated by g.c.-m.s., paper chromatography is still used for initial identification of the sugar residues from the color formed by reaction with *p*-anisidine HCl together with their R_f values[102].

The principle of gas liquid chromatographic separation depends on the partition of volatile components between a mobile gas phase and a stationary liquid phase. In modern capillary columns, the liquid phase is directly bonded onto the fused silica column wall. These wall coated open tubular columns provide excellent separation of compounds previously very difficult or impossible to separate on packed columns. Therefore, capillary g.c. is an excellent quantification and quantitation method for sugars. The flame ionization detector provides a large linear dynamic range for measuring both high and low concentration samples. As the availability of gas chromatographs fitted with mass selective detectors increases, g.c.-m.s. may play an even more important role in structural analysis.

Because carbohydrates are non-volatile, and thus are not directly amenable to g.c. analysis, they must therefore be chemically derivatized. The two most common derivatives used in g.c. analysis are the trimethylsilyl (TMS) and the alditol acetate (AA) derivatives[103,104]. Medium polarity columns, such as DB-17™ (100% methylphenyl-polysiloxane, J&W Scientific) or DB-225™ (50% cyanopropylmethyl-(50%)-methylphenyl-polysiloxane, J&W Scientific) are normally used for g.c. separation. Although trimethylsilyl derivatives are readily formed, the presence of a multiplicity of peaks due to the many isomeric forms (α-, β-, furanose and pyranose forms) complicates the chromatogram. Therefore, alditol acetate derivatization is commonly used because it generates a simple chromatogram and it facilitates easier quantification without using response factors[105]. Several comprehensive reviews on g.c. and g.c.-m.s. of alditol acetates have been published[18,34]. For co-eluting partially methylated alditol acetates (PMAAs), their partially

ethylated alditol acetates can be used[106]. There is little published data on methylated amino sugars, except for the common 2-acetamido-2-deoxyhexoses[107,108]. Amino sugar derivatives have longer retention times than their corresponding neutral sugars. It should be noted that when working with the simple regular repeating units of microbial capsular polysaccharides, exact quantification is not critical, rather the ratio of the sugar species to each other is more important.

Oligosaccharides generated by the different chemical or enzymic methods are chiefly separated by paper chromatography, followed by g.c.-m.s analysis of the hydrolyzate as the PMAA derivatives. However, for oligosaccharides with similar R_f value or molecular weights, the separation can be incomplete. Therefore, g.c.-c.i.-m.s. using non polar columns, such as a DB-1™ (100% dimethyl-polysiloxane, J&W Scientific) is becoming more prominent for the simultaneous separation and characterization of permethylated oligosaccharides[76,109,110]. Nevertheless, both g.c. and c.i.-m.s. data on oligosaccharides are not readily available. Furthermore, the volatility and thus molecular weight limit imposed by g.c. makes separation of high molecular weight oligosaccharides difficult, although, the new generation of high temperature non-polar columns has demonstrated the potential of g.c. separation with a number of malto-oligosaccharides[110].

III.3 MASS SPECTROMETRY

Due to their high molecular weights (~ 10^6 daltons), direct use of mass spectrometric methods for the analyses of capsular polysaccharides is at present not realistic. Thus, mass spectrometry in the past has played a small role in polysaccharide analysis, largely being limited to the use of g.c.-m.s. for detection and identification of derivatized monosaccharides obtained by chemical degradation of the biopolymers. Nevertheless, the molecular weight of the oligosaccharides generated by specific degradation of capsular polysaccharides is well within the mass detection range of modern mass spectrometers. Furthermore, in the last two decades a number of novel desorption/ionization techniques have been developed which enable very polar non-volatile compounds to be analyzed without prior derivatization. The

different desorption and/or ionization techniques used include: field desorption (f.d.)[111], desorption chemical ionization (d.c.i.)[112], Californium-252 plasma desorption (^{252}Cf p.d.)[113], laser desorption ionization Fourier transform ion cyclotron resonance (l.d.i.-F.t.-i.c.r.)[114], thermospray[115], fast atom bombardment (f.a.b.)[67] and liquid secondary ion mass spectrometry (l.s.i.m.s.)[116]. Although mass spectrometry is a destructive chemical technique, the quantity required for analysis is often in the sub-ng level. Therefore, a number of researchers in the bacterial capsular polysaccharide field, including ourselves, are exploiting this powerful combination of desorption mass spectrometry and specific degradation to sequence the repeating oligosaccharide.

It is important to note that historically, m.s. was and still is used in carbohydrate chemistry primarily for characterizing monosaccharide derivatives separated by g.c.[18]. Mass spectral identification is achieved by cross-referencing with reference spectra of all the common PMAA derivatives (Section III.3.1.1)[18]. Although previous workers have attempted to characterize oligosaccharides by m.s., these experiments were not successful due to the low volatility of the samples even with derivatization[19,117]. Earlier, it was hoped that m.s. could be used to distinguish the different positions of linkage for each individual monosaccharide residue. The only ionization technique available at that time was electron ionization (e.i.), but this method, unfortunately, causes a lot of fragmentation and was found to be useful only for the analysis of low mass permethylated oligosaccharides. Furthermore, the analysis of these very complicated mass spectra was too superficial in comparison to the well-documented methylation analysis. With the development of novel desorption/ionization techniques, it was possible to desorb and ionize large oligosaccharides. Nevertheless, in f.a.b., l.s.i.m.s. and ^{252}Cf p.d., fragmentations occur predominantly at the glycosidic bonds, due to the low energy transferred to the carbohydrate molecules, and the only information obtained from these ionization techniques is the molecular weight and the sequence information. The lack of ring cleavage fragmentations implies that no information can be obtained on the different stereoisomers, substitution patterns or anomeric configurations. Tandem mass spectrometry, such as f.a.b.-m.s.-.m.s., was carried out by a number of

workers on mono- or di-saccharides to obtain extra structural information relating to substitution patterns or anomeric configurations[118-121]. However, most correlations were based on the relative intensities of different peaks, which can sometimes be misleading. Although f.a.b. analysis can locate a monosaccharide residue which carries a substituent, it is incapable of defining the exact position of the linkage. The positions of linkage for these non-carbohydrate substituents are normally determined by e.i.-m.s. of the derivatives of the hydrolysate obtained from chemical degradation. Therefore, for any single m.s. technique to totally characterize oligosaccharides, it is important that it provides the following: i) glycosidic bond cleavages for sequencing; and ii) carbon backbone cleavages to provide information on the substitution patterns. The importance of carbon backbone cleavage data for providing linkage information is illustrated in Section IV.3.6.

So far, no single mass spectrometric technique can be used to distinguish stereoisomers of different monosaccharide units (e.g., glucose *vs* galactose). One possible method is by reaction mass spectrometry, where simple mono- and di-saccharides react with borate additives in the f.a.b. matrix to give specific complexes[122]. The different stereoisomeric complexes gives different spectra and the hexose identity can then be obtained by correlating the relative intensities of different peaks. However, a simpler classical carbohydrate method to characterize monosaccharide residues is methylation analysis (Section II.3 and III.2). Methylation analysis provides the following information: i) the identity of the monosaccharide residues; ii) the positions of linkage of each monosaccharide residue; iii) the structural pattern of the oligosaccharide, e.g., linear or branched; and iv) the identity of the branch point monosaccharide residue. Therefore, the general instrumental approach to analyze an unknown oligosaccharide requires the characterization of the monosaccharide residues with methylation analysis and then the sequencing of the oligosaccharide by n.m.r. or m.s.

Mass spectrometers in general consist of four components: a) the ion source, where the sample is transferred to the gas phase and ionized; b) the analyzer, where the ions are mass analyzed according to their mass to charge ratio; c) the detector, where the mass-resolved ion beams are detected, amplified and their intensity recorded; d) the vacuum system, which

provides a stable environment for the above processes. A detailed review of mass spectrometry will not be discussed here, although, a few of the most frequently used techniques are described in the following sections.

III.3.1 ELECTRON IONIZATION

The basic process whereby a molecule is ionized under electron impact is:

$$M_{(g)} + e^- \rightarrow M_{(g)}^{+\cdot} + 2e^-$$

This is the most common procedure used for generating ions in the gas phase. When electrons collide with neutral particles, the collisions can be elastic or inelastic. For elastic collisions the impact velocity is relatively low, and no appreciable loss of energy of the electrons is detected. At higher impact velocities the neutral particles are excited and the collisions become inelastic, but these neutral particles are not charged and hence not detected. Above the ionization potential (~ 12 eV for most molecules), many configurational changes are possible, with ionization and dissociation being most prominent. Above 25 eV, doubly charged ions and fragmentation can occur. The maximum of the ion intensity *vs* electron energy curve is located approximately at 70 eV. Thus, e.i.-m.s. utilizes mainly 70 eV energy electrons. The excess energy acquired by the molecule causes it to undergo single or multi-stage fragmentation; consequently, molecular ions are rarely observed for non-volatile materials.

E.i.-m.s. is, therefore, performed primarily on volatile, low mass samples, such as monosaccharide alditol acetate derivatives (discussed in Section III.3.1.1). Higher mass samples will frequently decompose thermally or fragment such that structural information is lost. Although molecular ions of derivatized oligosaccharides can be generated with low eV electron ionization, the positive radical molecular ions (i.e. an odd-electron species) are normally unstable and therefore, not observed. Chizhov and Kochetkov[117] have reported a series of e.i. fragmentation patterns for cyclic permethylated sugars and proposed nomenclature for these ionization pathways. Cleavage of the glycosidic bond gives rise to fragments of the A series, the C-1,C-2 bond to the C, D, F, H and K series, the C-4,C-5

bond to the J, H, B and D series (Fig. III.1 and III.2). A number of workers have attempted to use these fragmentation patterns for structural characterization of permethylated oligosaccharides with varying degrees of success[19,123].

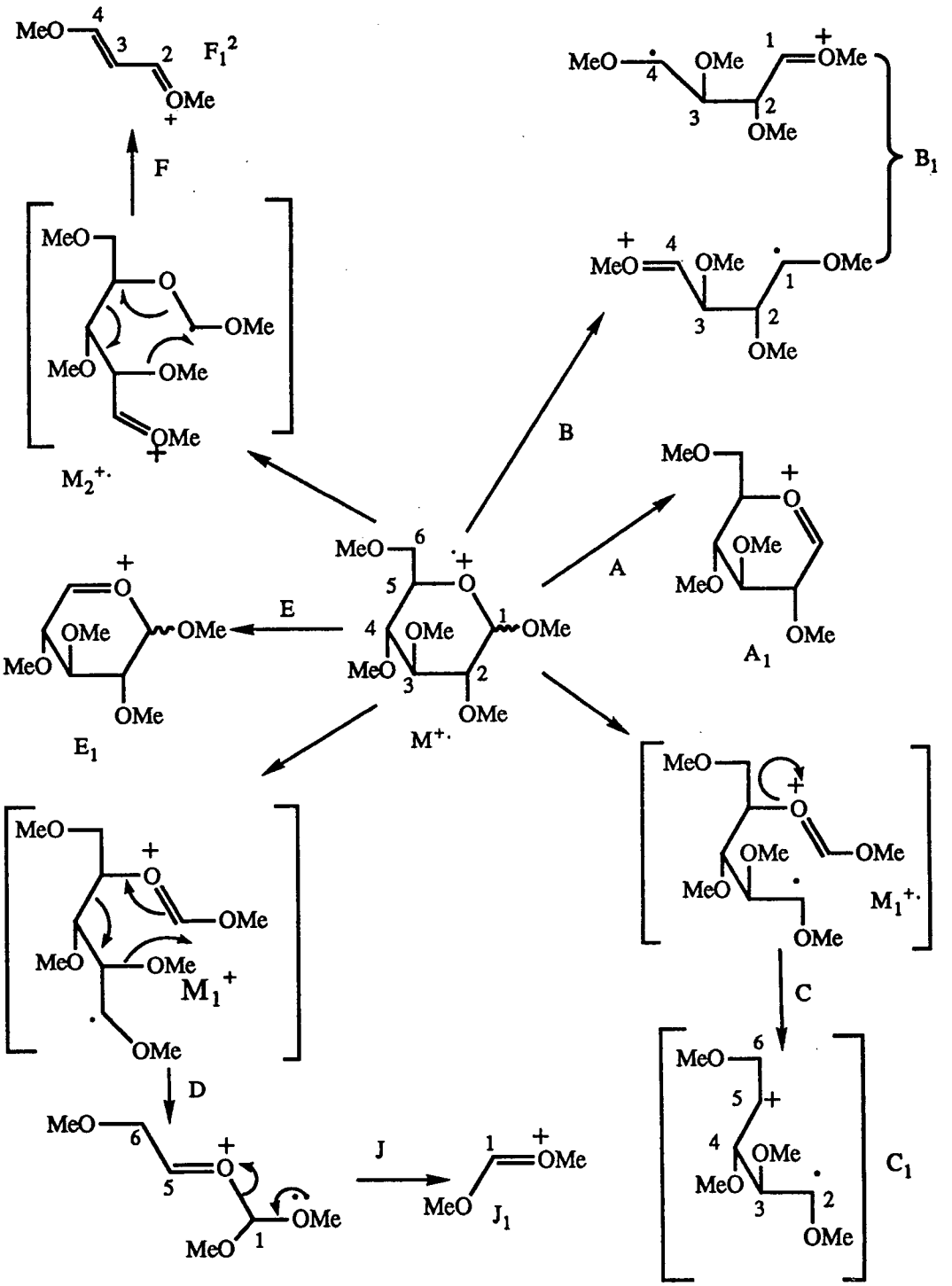

Fig.III.1 Some fragmentation patterns of a permethylated hexose proposed by Chizhov and Kochetkov[117].

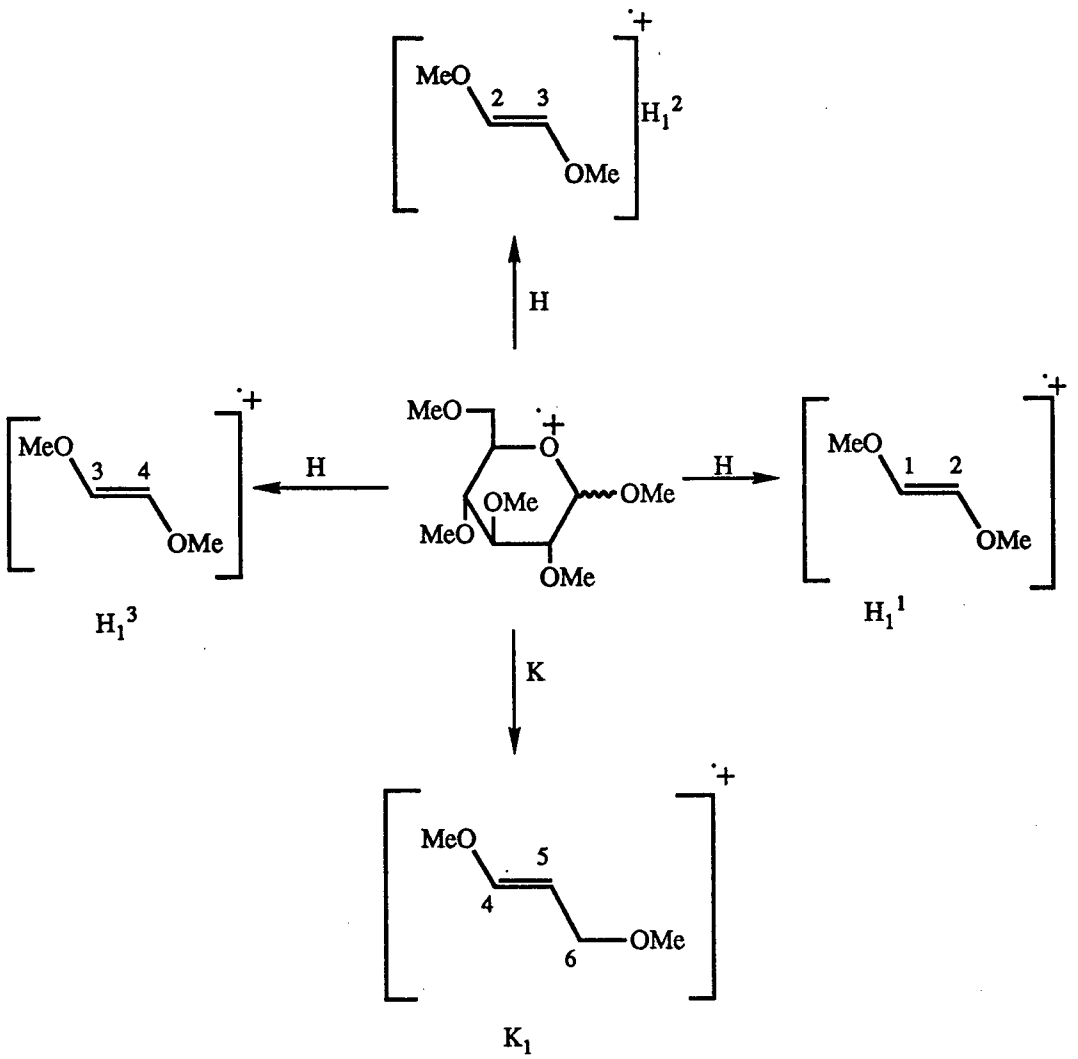

Fig.III.2 Some fragmentation patterns of a permethylated hexose proposed by Chizhov and Kochetkov[117].

III.3.1.1 E.I.-M.S. OF PERMETHYLATED ALDITOL ACETATES

Of all the carbohydrates, it is the alditol derivatives that exhibit the simplest mass spectrometric fragmentation patterns[18]. The following generalizations can be applied to the mass spectra of PMAAs.

i) Derivatives with the same substitution pattern generate very similar mass spectra. Therefore, the mass spectrum of D-mannitol hexaacetate is representative of all the peracetylated hexitols.

ii) No molecular ion is observed for e.i., and the base peak is customarily m/z 43 (C_2H_3O).

iii) Primary fragments result from α-cleavage of the carbon backbone, with the relative intensities of the ions decreasing with increasing molecular weight.

iv) The fission between carbon atoms is determined by the stability of the resulting radical, with the methoxylated radical being more stable than the acetoxylated radical. The primary fragmentation of amino alditol acetates largely depends on the substitution of the acetamido group. Preferred bond cleavages are in the following order.

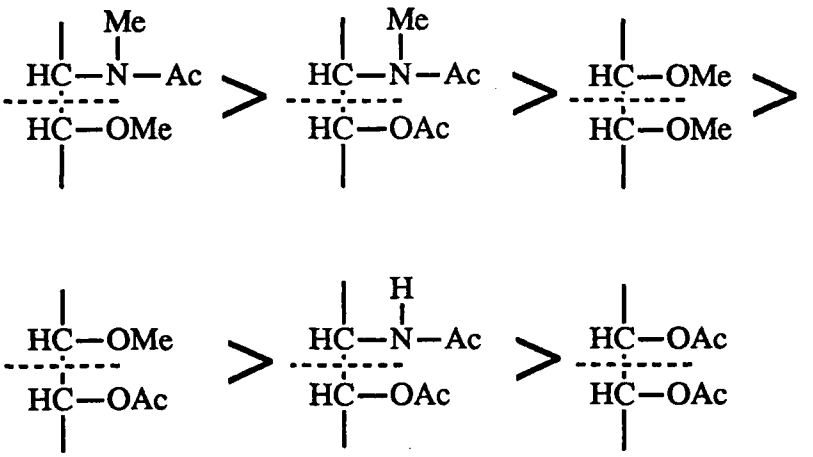

Fig. III.3 Preferred order of fragmentation for partially methylated alditol acetates[18].

v) Secondary fragments are obtained by single or consecutive loss of acetic acid (60 amu), acetamide (59), ketene (42), methanol (32) or formaldehyde (30).

Deuterium labelling studies using sodium borodeuteride or lithium aluminum deuteride can be used to identify the reducing end of an oligosaccharide and to distinguish an acidic residue from the neutral sugars by reduction, prior to sugar analysis by g.c.-m.s.

For g.c.-m.s. analysis of partially methylated alditol acetates, both the g.c. retention time and the fragmentation pattern are important. The retention time is especially crucial when different epimers are under investigation (e.g., glucose *vs* mannose). Fig. III.4 illustrates the fragmentation pattern of a typical PMAA (e.g., 1,5,6-tri-*O*-acetyl-2,3,4-tri-*O*-methylglucitol, mw = 350 amu)[18].

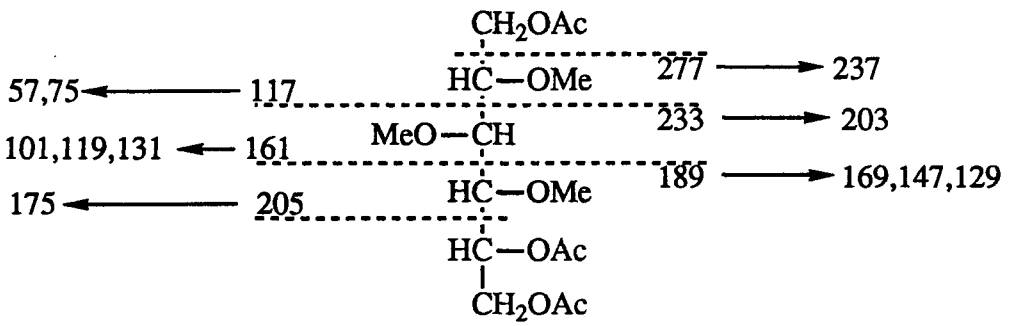

Fig.III.4 Fragmentation pattern of 1,5,6-tri-*O*-acetyl-2,3,4-tri-*O*-methylglucitol, as proposed by Lindberg *et al*[18].

III.3.2 CHEMICAL IONIZATION/DESORPTION CHEMICAL IONIZATION

Chemical ionization was first introduced in 1966[124]. It was developed directly from fundamental studies of gas phase ion/molecule reactions. In essence, the reagent gas which is present in large excess (1000 x) is ionized by electron impact. This is followed by ion/molecule reactions between the primary ions and the neutral reagent gas which produces the c.i. reagent ions. As a result of collisional relaxation, the c.i. reagent ions have a much lower energy than the ionizing electrons, consequently c.i. is a milder form of ionization. The mode of ionization is a type of Lewis acid-Lewis base reaction, where the molecule is converted to a relatively low energy even-electron species. Therefore, an abundance of pseudo-molecular ions can be observed.

The most widely used positive-ion reagent gas systems are those which yield Brønsted acids[125]. The major reaction mode of the Brønsted acids, BH^+, is proton transfer to give initially the protonated molecule MH^+.

$$BH^+ + M \rightarrow MH^+ + B$$

In principle, the BH^+ ions can also react by hydride ion abstraction or by charge exchange.

$$BH^+ + M \rightarrow [M - H]^+ + BH_2 \text{ (or } B + H_2)$$

$$BH^+ + M \rightarrow M^{+\cdot} + BH^{\cdot} \quad \text{(or } B + H^{\cdot})$$

By selecting the appropriate reagent gas, pseudo-molecular ions may be observed in the presence of fragment ions, with similar fragmentation patterns obtained from e.i.-m.s. For carbohydrates, the most common c.i. reagent gas used is ammonia and the pseudo-molecular ion observed in the positive-ion mode is generally $M+NH_4^+$. Positive-ion chemical ionization using methane as the reagent gas usually gives the fragment ion $(M+H-AcOH)^+$, i.e., $(M-59)^+$. Although c.i.-m.s. can directly analyze underivatized oligosaccharides, the molecular weight limit of such samples is fairly low, hence derivatization is normally carried out for m.s. analysis. G.c.-c.i.-m.s. analysis of permethylated oligosaccharides, obtained by partial acid hydrolysis, has been used successfully for the sequencing and characterization of capsular polysaccharide[76].

Another method of increasing the abundance of the pseudo-molecular ions is to desorb materials from sample probes which are positioned directly within the reagent plasma (d.c.i.)[112]. Since desorption chemical ionization still involves heating and sample-surface interaction, pyrolysis can still be a problem. Nevertheless, d.c.i. is frequently used for the sequencing of permethylated oligosaccharides[126]. Furthermore, structural information may be obtained if Chizhov's fragment ions are observed.

III.3.3 FAST ATOM BOMBARDMENT/LIQUID SECONDARY ION MASS SPECTROMETRY

Mass spectrometric analysis of ions produced by bombarding surfaces with ions in the keV energy range is well established as a surface technique[127]. The early applications of

secondary ion mass spectrometry (s.i.m.s.) were mostly in fundamental studies which utilized the fact that s.i.m.s. provides high absolute sensitivity for many surface components. Furthermore, s.i.m.s. unlike some other available techniques, could detect hydrogen and could determine the isotopic composition of elements on the surface[128]. S.i.m.s. was first shown to be a very sensitive technique for detection and identification of organic compounds in 1976[129]. The main disadvantage of s.i.m.s. is the radiation damage caused by the exciting primary ion beam. This damage can be minimized by operating in the "static mode", in which the surface is bombarded at an extremely low primary ion current density. Hence, during the analysis only a small probability exists for a surface area damaged by the impact of an ion to be struck by another primary ion during measurement.

The secondary ions formed can be either atomic or molecular. Formation of molecular ions can be accomplished by three different processes: i) cationization and anionization (these result from chemical reaction during or following the concurrent production of metal ions and the liberation of organic molecules by sputtering or by thermal vaporization); ii) electron transfer (the resulting anion and cation radicals $M^{-\bullet}$ and $M^{+\bullet}$, can be observed in s.i.m.s. spectra, sometimes associated with fragment ions which correspond to known products of their unimolecular dissociation); and iii) the direct sputtering of organic molecular ions from the solid to the gas phase[130]. These ions arise by momentum transfer from the primary ions.

All s.i.m.s. spectra show high abundances of pseudo-molecular ions that allow determination of molecular weight. Secondary ion yields are strongly dependent on the substrate and the properties of the primary beam, with the highest parent-like emissions obtained from compounds deposited on noble metal substrates and utilising a Cs^+ ion beam.

With few exceptions, low-energy bombardment of solids has used keV ion beams rather than neutrals, largely as a matter of experimental convenience since ion beams in this energy range are relatively easy to produce[131]. It is generally understood that the approaching ion is neutralized by long-range electron transfer as it approaches the surface so that the major effects of the impact would be the same for neutrals as for singly charged ions[132].

F.a.b. was first developed in 1981[68] and is presently the most common desorption/ionization technique used for the sequencing of biological molecules[133,134]. Secondary ions are produced by bombarding the sample in a liquid matrix with a primary neutral beam (Ar^0 or Xe^0) in the 8 kV energy range produced by charge exchange neutralization of an ion beam. It is now well established that the presence or absence of charge on the impacting primary particle has little effect on the desorption process, but the use of the neutral beam is somewhat more convenient with magnetic instruments in which the ion source is at high potential[135]. Nevertheless, the increase in secondary ion intensities resulting from the use of a 20 to 30 kV ion beam (Cs^+) has convinced a lot of the original f.a.b. spectrometrists to work with liquid secondary ion mass spectrometry (l.s.i.m.s.)[136].

With the use of the liquid matrix the requirement for working in the "static mode" to avoid radiation damage on the surface is removed. The beam current density used is several orders of magnitude larger than those of s.i.m.s. and the spectra are stable for up to 30 minutes[137]. The reason for this is that the matrix presents a mobile, constantly renewed surface to the bombarding beam, which continously replenishes undamaged sample molecules to be ionized. However, substantial radiation damage to the matrix does occur[138]. One disadvantage of the liquid matrix is that a very high background is produced by the ionization of the matrix and its radiation products. Also clustering of the matrix with sample ions is observed with formation of mixed cluster ions when impure samples or mixtures are analysed.

Mass spectral data showed that the same secondary ions are produced whether the sample is in a liquid or solid matrix. The distribution of the secondary ions is representative of the composition of the liquid phase. If odd-electron species are just as stable in solution as even-electron species they can be detected just as easily. Although the ion production mechanism can be considered as identical in f.a.b. and s.i.m.s., a solid matrix usually leads to more fragmentation due to the process of primary energy dissipation. Solutes, molecules and ions are less tightly bound in liquids and the energy dissipation occurs mainly as translation instead of as vibration of the matrix[139]. This may lead to the ejection of larger solvated

clusters where energy dissipation can easily be accomplished by excessive loss of solvent molecules without breaking intramolecular bonds[140]. Bombarding with lower energy primary particles has been found to increase the extent of fragmentation probably via the ejection of smaller clusters where the energy dissipation by solvent loss is less efficient. The size distribution of the ejected clusters, depending on the primary beam conditions, could be reflected in the degree of fragmentation.

The second aspect in which solid and liquid matrix differ is related to the dynamic nature of the liquid sample. The liquid matrix must be considered to be mobile in the spectra-recording time scale. Hence, f.a.b. can reflect the equilibria of the solution; it has been used to measure acidity constants, stability constants, and to monitor enzyme reactions[141,142].

A situation of particular importance occurs when the solvent-solute interactions are strong enough to induce heterogeneities in the distribution of species within the liquid matrix. If one solute behaves like a surfactant, a concentration gradient will develop, resulting in the enrichment of the surface with this compound. This behaviour is not confined to certified surfactants such as the long chain quarternary ammonium salts but also occurs with amino acids and dipeptides[143,144].

A crucial step in the f.a.b. technique is the choice of a suitable matrix composition[145-147]. The same solute can produce ions that vary in abundances by orders of magnitude as the matrix composition is altered. Some general requirements concerning the solvent properties of the matrix are summarised as follows: i) The sample must be soluble in the matrix. ii) Only low-vapour pressure solvents can be used in the vacuum of the mass spectrometer. Volatile solvents could in principle be employed with high pumping rates, provided that stable surfaces could be obtained on the time scale of recording a spectrum. iii) The viscosity of the solvent must be low enough to ensure the diffusion of the solutes to the surface. iv) Ions from the matrix itself must be as unobstrusive as possible in the secondary ion mass spectrum. v) The matrix must be chemically inert; if specific ion formation reactions are used to promote secondary ion yield the reaction must be reproducible. The usual matrices used for carbohydrates are glycerol, thioglycerol or a 1:1 mixture of both. Frequently additives

such as 1% volatile acid (acetic and hydrochloric), NaCl and KBr are added to improve molecular ion intensity. However, cationization of the molecular ion will decrease fragmentation, with possible loss of sequence information. Although underivatized samples can be used, derivatization is frequently carried out to improve ion intensities. F.a.b. produces simple fragmentation patterns, with dehydration and glycosidic bond cleavage for underivatized samples, and primarily oxonium ion formation (Chizhov's A series) from derivatized materials.

III.3.4 LASER DESORPTION IONIZATION FOURIER TRANSFORM ION CYCLOTRON RESONANCE

D.c.i. and f.a.b. usually give abundant sequence information on derivatized oligosaccharides, however, they provide little or no information on either the positions of linkage between the saccharide residues or the anomeric configuration of the linkages[148]. Tandem mass spectrometric experiments, such as collisional activation dissociation (c.a.d.) experiments[119] and mass ion kinetic energy (m.i.k.e.s.) experiments[118] have been carried out on either permethylated disaccharides or methyl glycosides in an attempt to distinguish the position of linkage and the anomeric configuration. The commonly used derivatization methods are esterification of the reducing end with ethyl *p*-aminobenzoate[136] or reduction followed by either permethylation or peracetylation[148]. All these derivatization techniques can remove any acid/base labile substituents that may be present and structural information consequently will be lost[69].

It would be preferable to sequence native carbohydrates without having to use derivatization. The application of laser desorption for mass analysis of non-volatile and thermally labile biomolecules, such as oligosaccharides, glycosides, lipid A compounds and oligopeptides has been shown to be useful[149-160]. Most of the pseudo-molecular ions observed in positive-ion spectra were either cationized or protonated but the exact mechanism of desorption/ionization is still under investigation[161-169]. The potential of l.d.i.-F.t.-i.c.r. for the analysis of oligo- and poly-saccharides was demonstrated by Coates

and Wilkins[170,171]. From the l.d.i.-F.t.-i.c.r. mass spectra of nine commercially available polysaccharides they observed "*extensive fragmentation of the saccharide chains, from both within the sugar rings and between them ... . Although similarities are seen in the spectra of some compounds, each displays a characteristic fragmentation pattern.*"[151] Using the high resolution data obtained from the positive-ion l.d.i.-F.t.-i.c.r. mass spectra of an underivatized de-*O*-acetylated pentasaccharide derived from bacteriophage hydrolysis of *Klebsiella* K44 capsular polysaccharide, we have shown that l.d.i.-F.t.-i.c.r. can be used to sequence underivatized oligosaccharides (Appendix 1)[20,172]. Encouraged by these results, a systematic study involving application of positive- and negative-ion l.d.i.-F.t.-i.c.r. to a number of well characterized underivatized model oligosaccharides was initiated. These studies will be discussed in Section IV.3.1 to IV.3.8. Moreover, the fragmentation pattern observed for these underivatized model oligosaccharides can also be used to explain the polysaccharide mass spectra observed by Coates and Wilkins[171,173]. This will be discussed in Section IV.3.9. In Section IV.3.10 and IV.3.11, this l.d.i.-F.t.-i.c.r. technique was applied to an unknown oligosaccharide, and results obtained compared with those obtained by classic carbohydrate chemistry. The two different aspects of l.d.i.-F.t.-i.c.r. are discussed below.

III.3.4.1 LASER DESORPTION IONIZATION

Soon after the advent of the laser several mass spectrometrists realized the potential of a laser mass spectrometer combination[174]. The nature of the radiation produced by the laser has some specific properties, which makes the laser a highly attractive source for sample desorption. Laser radiation is coherent, monochromatic, directional and intense. The high intensity of a laser beam enables sample vaporation to be on a very short time scale. The direction of the beam is defined by the geometry of the lasing system. Generally, a beam with a diameter of a few millimeters and a very low divergence is generated. This low divergence facilitates the operation of the laser at a relatively long working distance from the sample, without severe radiation loss. Furthermore, the coherence and directional properties together enable focusing of the beam to a very small spot, thereby increasing the power density. The

monochromatic nature of the radiation leads to a narrow wavelength band. Although monochromaticity is an important factor in many other laser applications, no extentive use of this property can be made in laser desorption ionization (l.d.i.). In principle, with a tunable laser very accurate scanning of wavelength over the absorption bands of the sample can be performed and the effects of selective excitations can be studied. Nevertheless, using multiphoton mass spectrometry Schlag *et. al.* demonstrated that the isotopic species mono-^{13}C-benzene can be preferentially ionized in a natural isotopic mixture by shifting the wavelength by 1.6 cm^{-1} from the absorption band of light benzene[175]. This demonstrated that trace components in a mixture can be ionized without ionizing the major components if the intermediate-state spectrum shows sharp features at a resolution of 1 cm^{-1}. They also proposed that multiphoton ionization occurs only subsequent to multiphoton absorption into the final energtic state of the neutral molecule, further multiphoton absorption will lead to dissociation.

Laser radiation is produced either in pulses or continously[174]. The normal pulse range is from 1 μs to 1 ms. However, each pulse exhibits a fine structure and is effectively built up of a train of separate pulses 0.1 to 1 μs wide. By the so called Q-switching technique part of the total energy can be released in one short pulse of ~10 ηs duration. Even shorter pulses in the pico second range can be obtained with an additional mode-locking technique. Although the total energy in a pulse is kept low, a 1 μJ pulse of 10^{-8} s focused on 10^{-6} cm^2 from a Q-switched Nd-YAG laser leads to an instantaneous high power density of 10^8 Wcm^{-2}.

As a result of the energy transferred to the sample material, heating, melting, vaporization and ionization processes take place. Under severe conditions large amounts of substrate can be vaporized leaving a crater in the solid. Two classes of power density can be distinguished. With low power density (< 10^8 W cm^{-2}) evaporation of surface layers can be obtained, in the form of intact neutrals and ionized molecules. This evaporation process is reproducible, and can be looked upon as a thin vapour layer moving into the solid at a steady state. In the high power domain (> 10^8 W cm^{-2}) a high degree of irreproducibility is observed and mainly atomic and small molecular fragments in an ionized state are desorbed. After

vaporization, collision between neutral and primary ions in the plasma can lead to formation of secondary ions. The dominant process is cationization by alkali ions.

$$M_{(s)} + h\gamma \rightarrow M_{1(g)} + M_{2(g)} + M_{3(g)} + \text{etc...}$$

Due to the pulse nature of the ion current generated, special mass analyzers are required with emphasis on the scan speed and signal registration. Spectrometers equipped with time-of-flight detectors have been most frequently used because of their ability to record a complete spectrum for each laser generated ion pulse and high transmission. The major drawback of this system is the relative low dynamic range of the recording system due to the inherently short sampling time[176]. Quadrupole mass filter and scanning magnetic sector type instruments have also been used, but are too slow to obtain a complete spectrum for each pulse[150,177]. Therefore high, repetitive rate lasers have been used recording only one mass peak per laser pulse. Magnetic analyzers, both single and double focusing instruments, can be efficiently applied employing simultaneous ion recording techniques such as photoplates and channelplate-camera systems[178,179]. Since Fourier transform ion cyclotron resonance (F.t.-i.c.r.)[180,181] mass spectrometry is an inherent pulse experiment which gives the whole mass spectrum at once[180-185], it is well suited for l.d.i. Gross *et al* first demonstrated the feasibility of l.d.i.-F.t.-i.c.r.[182].

III.3.4.2 FOURIER TRANSFORM ION CYCLOTRON RESONANCE

In a uniform magnetic field of strength "B", a moving ion of charge "z", and of mass "m", will be subjected to the Lorentz force, which is perpendicular to the direction of the ion, hence, constraining it to a circular orbit with its radius proportional to its velocity. This orbit will have a characteristic cyclotron frequency, ω, and the orbital motion can be described as

$$\omega = zB/m$$

The ion cyclotron resonance (i.c.r.) spectrometer measures the cyclotron frequencies of an ensemble of ions of differing masses (illustrated in Fig. III.5). The i.c.r. experiment is divided into two parts: i) excitation of cyclotron motion by an alternating electric field between the plates of a capacitor (illustrated in Fig. III.6); ii) detection of the excited cyclotron motion of

the ions (illustrated in Fig. III.6). The rotating ions induce an alternating current in an external circuit; the voltage induced across this circuit is the i.c.r. signal[183]. In a F.t.-i.c.r. spectrometer, all the ions are excited together by using a fast frequency sweep from a radio frequency oscillator. The i.c.r. signal from all the ions is then digitally sampled and Fourier transformed to give a mass spectrum[184,185]. This F.t.-i.c.r. concept was first demonstrated by Comisarow and Marshall in 1974[180,181].

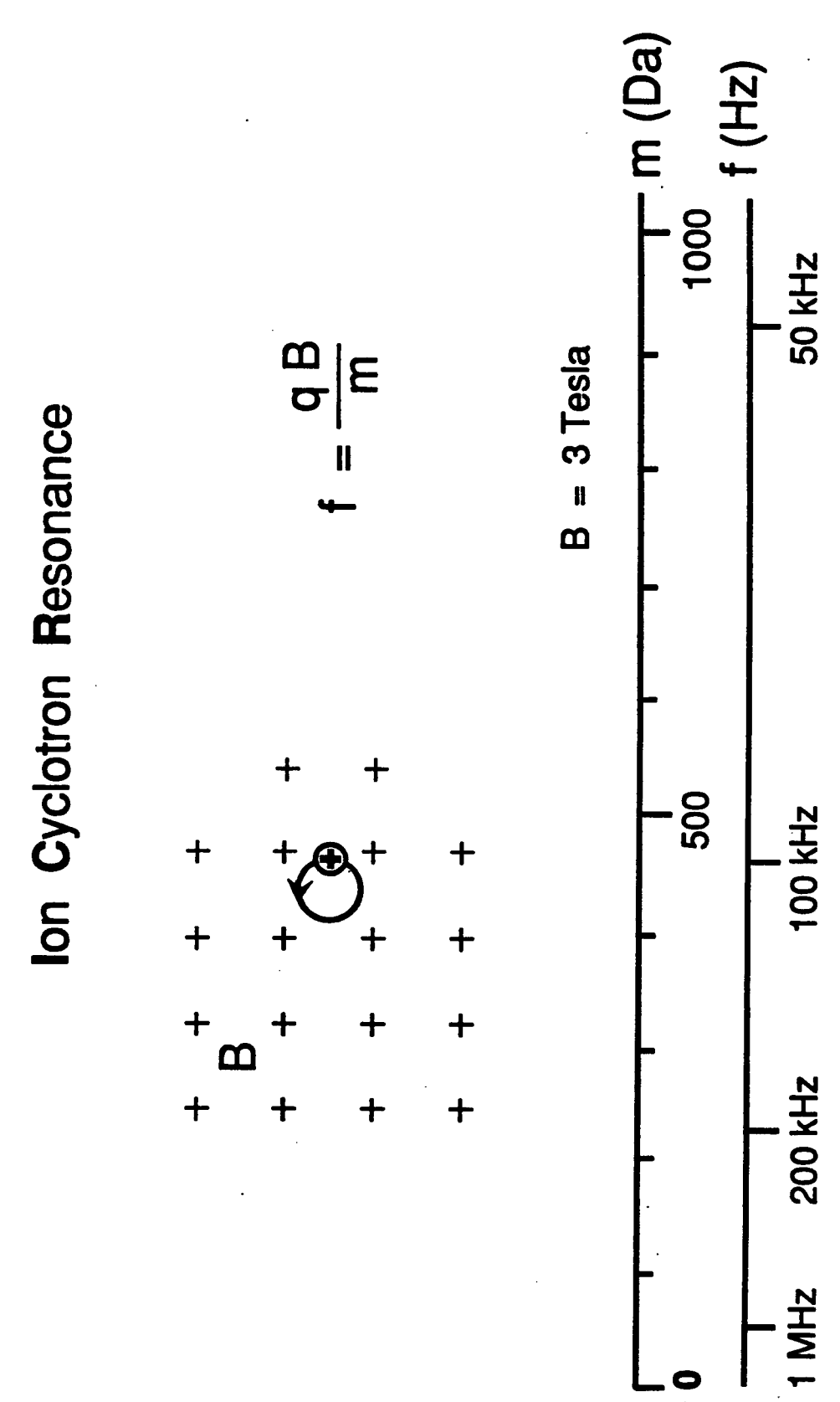

Fig.III.5 Schematic to illustrate the principle of ion cyclotron resonance mass spectrometry.

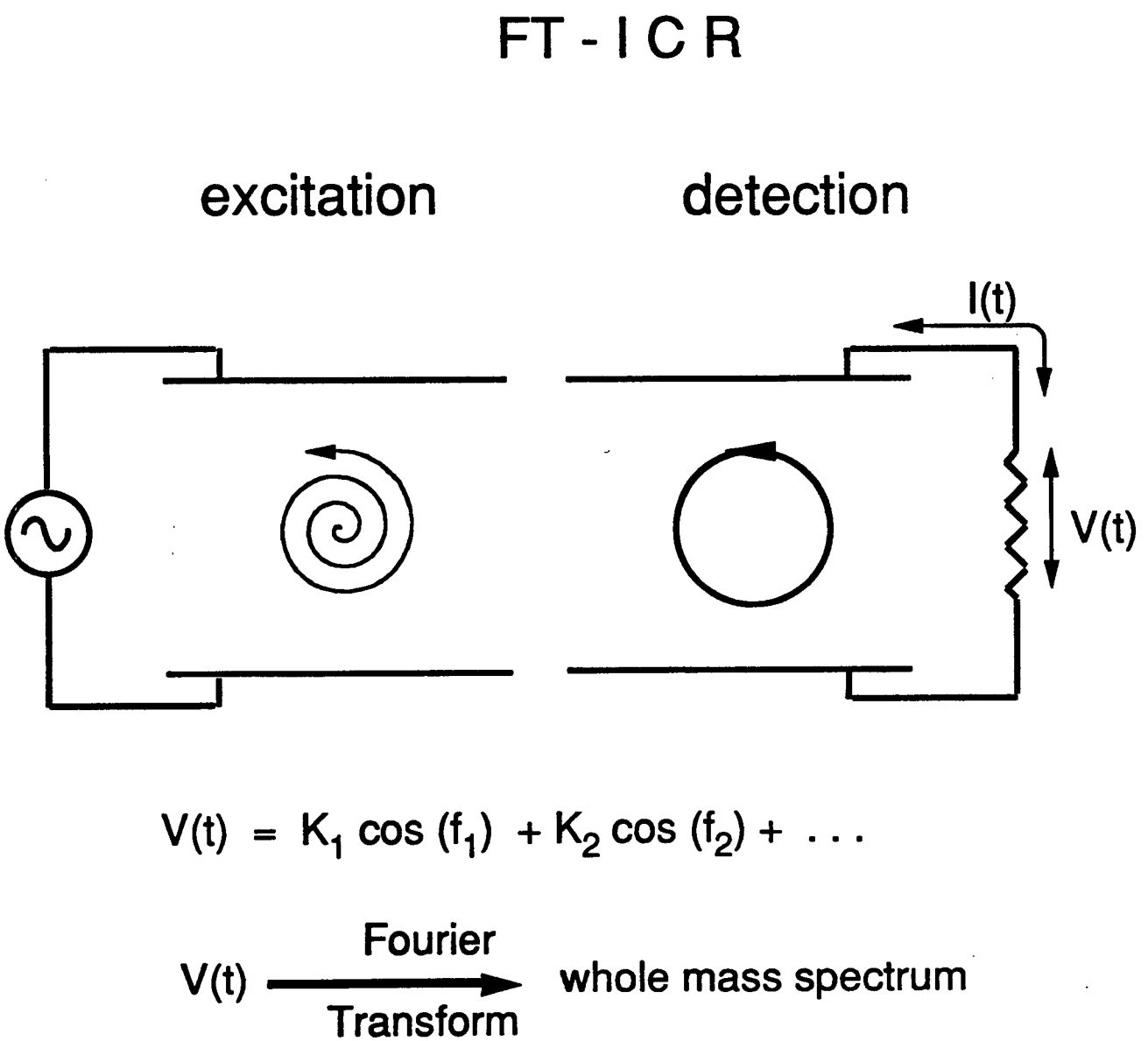

Fig.III.6 Schematic to illustrate the principle of Fourier transform ion cyclotron resonance mass spectrometry.

CHAPTER IV

LASER DESORPTION IONIZATION FOURIER TRANSFORM ION CYCLOTRON RESONANCE MASS SPECTROMETRY OF SOME UNDERIVATIZED OLIGOSACCHARIDES DERIVED FROM SPECIFIC DEGRADATION OF BACTERIAL CAPSULAR POLYSACCHARIDES.

LASER DESORPTION IONIZATION FOURIER TRANSFORM ION CYCLOTRON RESONANCE MASS SPECTROMETRY OF SOME UNDERIVATIZED OLIGOSACCHARIDES DERIVED FROM SPECIFIC DEGRADATION OF BACTERIAL CAPSULAR POLYSACCHARIDES.

IV.1 INTRODUCTION

The mass spectrometric investigations described in this and the previous M. Sc. thesis[20] are specifically related to the structural characterization of *Klebsiella* and *E. coli* capsular polysaccharide antigens. In the previous studies[20], a preliminary investigation was carried out on three different types of desorption/ionization mass spectrometry (desorption chemical ionization (d.c.i.), fast atom bombardment (f.a.b.) and laser desorption ionization Fourier transform ion cyclotron resonance (l.d.i.-F.t.-i.c.r.)) for the sequencing of oligosaccharides. It was demonstrated that positive-ion l.d.i.-F.t.-i.c.r. mass spectrometry could be used to sequence an underivatized pentasaccharide obtained by bacteriophage degradation of the bacterial capsular polysaccharide[172] (Appendix 1). Furthermore, the ring fragments observed could be used to provide some tentative indication on the positions of linkage. Encouraged by these results, the application of both positive- and negative-ion l.d.i.-F.t.-i.c.r. to this and other underivatized oligosaccharides generated by specific degradation of the native bacterial capsular polysaccharide was further investigated.

This thesis seeks to characterize the abundant ring fragmentation patterns observed in the l.d.i.-F.t.-i.c.r. spectra of model underivatized oligosaccharides (Section IV.3.1 to Section IV.3.8). The experiments progressed from a linear pentasaccharide (*Klebsiella* K44), to a linear pentasaccharide containing an acid-labile pyruvic acid acetal (*Klebsiella* K3), to a linear tetrasaccharide containing an acetamido hexose and a sialic acid (*E. coli* K9), and finally to a "3+1 branched" tetrasaccharide containing a base-labile *O*-acetyl group and a lactic acid ether (*Klebsiella* K22). Using the fragmentation patterns observed from these model underivatized oligosaccharides, a logical interpretation could be proposed for the mass spectra of commercial polysaccharides published by Coates and Wilkins[171] (Section IV.3.9). In Section IV.3.10 and IV.3.11, the results obtained from l.d.i.-F.t.-i.c.r. of an unknown

oligosaccharide are presented, and compared to the structure obtained by classic carbohydrate chemistry. In Section IV.4, all the mass spectral data presented in this thesis was correlated to project possible uses of l.d.i.-F.t.-i.c.r. in carbohydrate chemistry.

It must be emphasized that the focus of this thesis is not to illustrate that l.d.i.-F.t.-i.c.r. mass spectrometry can be used as a stand-alone method for the complete characterization of carbohydrate materials. But rather it serves to illustrate that l.d.i.-F.t.-i.c.r. may be used to minimize the amount of classic carbohydrate chemistry required to elucidate the structure of an oligosaccharide sample.

IV.2 EXPERIMENTAL PROCEDURES

All the oligosaccharides discussed in this thesis are obtained by bacteriophage or anhydrous hydrogen fluoride degradation of the native capsular polysaccharide. Due to the experimental approach in the isolation of capsular polysaccharide, the acidic component, such as hexuronic acid and pyruvic acid acetal have alkali halide as the counter ion. Therefore, the mass spectra reflect the amount of sodium and/or potassium ion associated with the oligosaccahride samples.

Mass spectra were obtained by Drs. Asgeir Bjarnason and David A. Weil at Nicolet Analytical Instruments, with a Nicolet FTMS-2000 mass spectrometer equipped with a dual cell, a 3.0 T superconducting magnet and a Nicolet laser desorption interface. The laser was a Tachisto 216 pulsed CO_2 laser operating as a stable resonator with aperture-controlled beam characteristics. Equipped with a total reflector, the laser delivers up to 2 J in a 40 ηs wide pulse emitting at λ = 10.59 micron. Output energy can be controlled by adjusting the aperture and was estimated to be on the order of 0.05 J per pulse for these experiments. The spot size of the focused laser beam on the probe tip was of the order of 100 microns.

Approximately 100 n mol. of the sample, dissolved in 50 μL of methanol/water mixture, was used for mass analyses. Typically, each sample was examined three times: once with no dopant, once with KBr or NH_4Br dopant and once with KBr/NaCl or NH_4Br/NaCl dopant. This solution was transferred to and allowed to evaporate on the stainless steel tip of the

direct insertion probe of the mass spectrometer. The vacuum system was pumped down to ~ 1 x 10^{-8} torr after insertion of the sample probe, prior to mass analysis. After each laser pulse, the probe was rotated so that the laser always struck a fresh spot on the sample surface. After the laser pulse, a delay of 2 to 3 s was employed to reduce the pressure in the cell, before ion detection. Mass spectra were collected in the direct (broadband) mode[185] with a high frequency cutoff at 500 KHz (corresponding to a lower mass limit of ~ 90 amu). Normally, 64K-datapoint transients were collected and when the signals were weak, the spectra from several laser shots were averaged to increase the signal to noise ratio. Positive- and negative-ion spectra were obtained in each case. For exact mass measurements, the series of ions corresponding to $K_nBr_{n-1}^+$ or $K_nBr_{n+1}^-$ were used as internal mass calibrants. When these ions were absent or weak, a few peaks in the oligosaccharide spectra that could be assigned with certainty were used as internal calibrants. After data collection, the sample was 'recovered', doped with successive solutions of methanolic KBr and NaCl and rerun as necessary. Actual sample consumption was thus limited to several picomoles for each laser shot.

IV.2a DATA ANALYSES

The data analyses of the l.d.i.-F.t.-i.c.r. spectra were carried out as follows:

i) The baseline noise level was first determined and all peaks above twice the baseline noise were considered to be real signals. All the spectra in this thesis have an average baseline noise of less than 5% of the base peak.

ii) The highest-mass peaks in each spectrum were taken to represent the pseudo-molecular ions, which indicate the number of residues present in the oligosaccharide. All masses resulting from glycosidic bond cleavages gave "whole saccharide" structures which could then be used to derive a number of possible sequences for the oligosaccharide. In the positive-ion spectra, the ions are typically cationized (either from the added alkali salt or by salt present in the sample). Deprotonated structures are the most common species in the negative-ion spectra. Nevertheless, some chloridation of high intensity peaks are sometimes observed.

In both the positive- and negative-ion spectra, many of the observed masses are assigned to dehydrated formulae, formed by loss of one or more water molecules.

iii) Due to the ease of dehydration of oligosaccharides, it is important to distinguish whether the sample contains any anhydro-saccharide residues, or if such fragments are dehydration products formed during the desorption/ionization process. If the pseudo-molecular ions are dehydrated, then all the hydroxy groups on all the fragment ions have to be carefully accounted for.

iv) It should be noted that for a homoglycan, such as a mannan, the molecular formula for the molecule is $[(A)_n+18]$, where A is the molecular weight of the anhydro-residue, n is the degree of polymerization, and 18 represents the molecular weight of a water molecule. For example, the molecular formula of chitin is $[(203)_n+18]$, and the individual residues are separated by 203 amu in the mass spectrum. For each different class of saccharide residue, there are different mass separations. Consequently, the sequence of a heteroglycan can be obtained by adding the different mass separations. For a hexose, the mass separation is 162; for a deoxyhexose it is 146; for a hexuronic acid it is 176 and for an acetamido hexose it is 203.

v) After obtaining a number of possible sequences for the oligosaccharide, the mass errors for the peaks derived from glycosidic bond cleavage were then calculated. If the mass errors were too high (i.e. $\geq \pm 50$ ppm), a few peaks that can be assigned with certainty were used to recalibrate the spectra.

vi) The recalibrated masses were again correlated with proposed sequences. Any masses that were not assigned to glycosidic bond cleavage were then considered to be derived from ring cleavages. Thus, elemental formulae could be assigned and structure(s) proposed in the context of the most probable sequence to delineate the oligosaccharide.

vii) With the assumption that ring fragments were formed by simple ring cleavages, rather than extensive rearrangement of the monosaccharide residue, the ring fragments could then be used to elucidate the structure of the oligosaccharide in greater detail (i.e., positions of linkage). If possible, these fragments were then correlated to the known structure with

respect to anomeric configuration, epimeric stereochemistry, and ring size. The use of ring fragments in e.i. spectra for the determination of positions of linkage for low molecular weight permethylated oligosaccharides is well documented[19]. Nomenclature has long been proposed for these ring fragments by Chizhov and Kochetkov[117]. However, due to pyrolysis in both e.i. and c.i., underivatized oligosaccharides have not been studied extensively.

viii) The error limits of high resolution data according to some mass spectrometrists have to be below ± 10 ppm[186], therefore, the mass errors in some of the spectra presented in this thesis are too high to be considered "proper" high resolution results. Nevertheless, due to the nature of carbohydrate materials (which are predominantly made up of carbon, hydrogen, oxygen and nitrogen, all of a certain ratio), ultra-high mass resolution is not required, as the low resolution data limits the number of possible monosaccharide residues in the sample.

IV.3 RESULTS AND DISCUSSIONS

In the interpretation of l.d.i.-F.t.-i.c.r. spectra of oligosaccharides, it is not always essential for all the ions to be assigned exact structures. The low resolution spectra provide a framework of limited possibilities for the oligosaccharide sequences. Therefore, only selected ions of high intensity, in the high resolution spectra need be assigned to structures for complete sequencing. The structures of these ions are "whole oligosaccharides" attached to one or more sub-monosaccharide units (ring fragments). In some cases, two or more possible structures could be rationalized for a particular ion with the same elemental composition. The structures could be derived from different oligosaccharides attached to different ring fragments, or the same oligosaccharide attached to one or more ring fragments. Generally, only one of these structures exists in the framework designated by the low resolution spectra. If however, both of these structures were possible, then either both structures or only the most "weighted" probable structure contribute to the intensity of the ion. This "weighting" process was predominantly determined by whether: i) the ring fragment could be derived from a particular part of a monosaccharide residue; ii) the ring fragments in

the structures have been observed previously; and iii) the same ring fragment exists in the spectrum derived from different monosaccharide residues.

The ring fragments observed are usually unsaturated and can be categorized into four different types: one-carbon, two-carbon, three-carbon and four-carbon fragments. Each of these can be further divided into sub-groups, with differing compositions of oxygen or hydrogen atoms. Any unsaturated structure can be written in a cyclic or a chain form. In this study most of these unsaturated fragments are arbitrarily drawn as the cyclic form as no mechanistic studies have been carried out to identify their exact structure. Furthermore, no charges are placed on any part of the fragment structures, but the figure captions will indicate what types of alkaline ion attachment was involved in providing the ion charge.

For any four-carbon ring fragment structures, it is possible to propose alternative structures with two-carbon fragments attached to each terminal of the oligosaccharide. However, the presence of multiple ring fragment structures imply that the oligosaccharides were energetic enough to undergo multiple fragmentation at both termini. Therefore, single ring fragmentation was usually assumed to have occurred, and the presence of multiple ring fragment structures were considered only if no simple single ring fragments could be assigned.

IV.3a NOMENCLATURE

Although a systematic nomenclature has been proposed recently for higher oligosaccharides (which is similar to the nomenclature for protein fragmentation)[187], it can not be used to designate fragmentations of a homoglycan. Therefore, in this thesis, the fragmentation products were designated with a different "cleavage label". The two-carbon fragments were considered to be derived from **M**-, three-carbon from **P**- and four-carbon fragments from **N**-series cleavages. Any subscript designated to a particular series merely serves to denote the sub-group with differing compositions for oxygen and hydrogen atoms. The superscripts ^{0}, ^{1}, ^{2} or ^{3} denotes none, one, two or three unit of dehydration.

IV.3b DESORPTION MECHANISM

Laser-induced desorption of organic solids has been shown to be essentially a rapid heating effect resulting in flash evaporation of neutrals and ions which subsequently can undergo gas phase ion-molecule reactions[155,157,167,188,189]. A number of workers have measured the kinetic energy spread of the laser desorbed ions, which supports this "thermal desorption" model[155,188,190,191]. The long neutral[192] and ion[152,155,192,193] emission time after a short laser pulse also strongly strengthen this thermal model for the desorption mechanism. Cotter *et. al.* using a 40 ηs laser pulse observed the emission life-time of ions to be 1 μs, while neutrals were still observed after 100 μs, which suggested that cationization or deprotonation of the neutrals will be the dominant species observed in the mass spectra[192].

IV.3c FRAGMENTATION MECHANISM

After the initial desorption of the oligosaccharides from the sample layer, fragmentation of the oligosaccharides can occur either in the gas phase or in the desorption plume (also termed as the selvedge) by ion-molecule reactions, or even in the sample layer if excess thermal energy is deposited by the laser pulse. Ionization processes, such as cation ion attachment in the positive-ion mode and deprotonation in the negative-ion mode can occur either before or after the primary and secondary fragmentations.

Using repetitive laser desorption mass spectrometry on the disaccharide, sucrose Heresh observed a series of oligosaccharide (2 to 7 hexose units) fragment ions and with both glycosidic and ring cleavages[194]. The author suggested that the thermal energy deposited by the repetitive laser pulses, caused oligosaccharide polymerization and fragmentation in the sample layer, followed by desorption and ionization in the gas phase.

In contrast to Heresch's experiments, all the oligosaccharide mass spectra contained in this thesis were obtained by a single laser pulse on the sample. Therefore, due to the low molecular weight of the oligosaccharides and the relatively small energy transfer (as compared to Heresch's repetively laser experiments), all the samples investigated in this

thesis could be desorbed into the selvedge as the intact oligosaccharides, where primary and secondary ion-molecule reactions can occur .

In this thesis, all the ions observed in mass spectra are "even-electron" species, and are likely to undergo chemistry which is similar in the gaseous and aqueous phases. Consequently, for some of these frequently observed ring fragments, structures are proposed by analogy to known "even-electron" gas phase fragmentations[117] and "even-electron" solution chemistry. An example of this "even-electron" species approach for fragmentation is the glycosidic bond cleavage *via* protonation of the glycosidic oxygen, to generate the reducing end oligosaccharides, and the non-reducing end oligosaccharide oxonium ions as shown in Fig. IV.1. The proposed reaction scheme shows proton donation by water to a glycosidic oxygen. This is a bimolecular reaction, which could occur in the desorption plume following the laser pulse. Carbohydrates are highly hygroscopic and the sample handling procedure, involving dissolution in water/methanol and introduction *via* the solid probe followed by evaporation of the solvent, probably leaves sufficient water for the protonation reaction to occur.

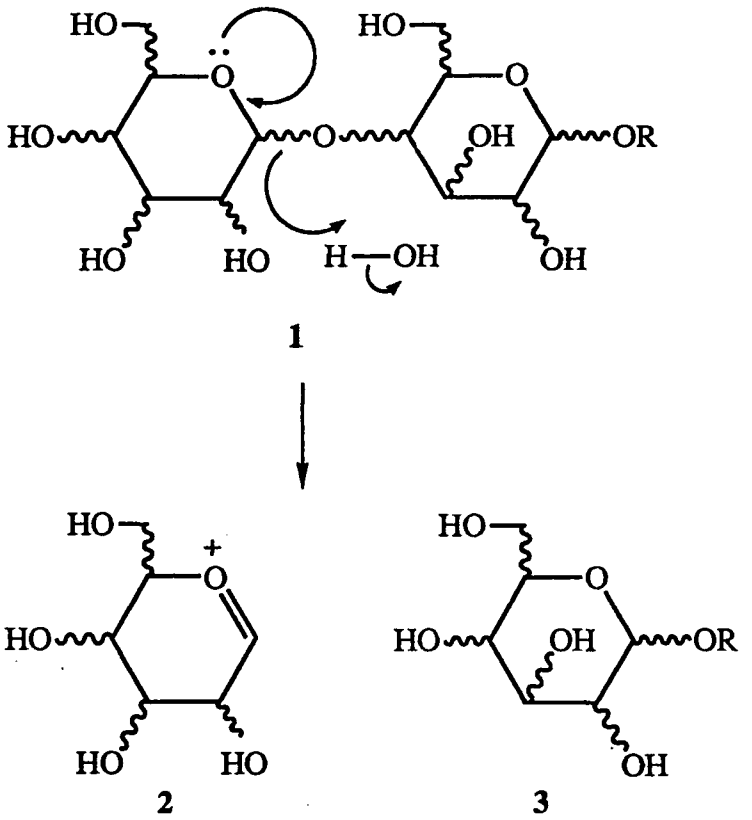

Fig.IV.1 Proposed glycosidic bond cleavage *via* protonation to give an oxonium ion and a reducing end fragment.

If fragmentation is a result of ionization followed by gas phase unimolecular or ion-molecule reactions, then the formation of the ring fragments would be strongly influenced by the first generation ions, and different ring fragments would be observed in the positive- and negative-ion modes. This assumption is supported by the positive- and negative-ion f.a.b.-m.s.-m.s. experiment on a series of underivatized monosaccharides, where the authors observed different ring fragments in the different modes, and they attributed the results to the different first generation ions obtained under the different modes[120]. On the other hand, if fragmentation occurs before ionization, then all the ring fragments observed in both the positive- and negative-ion spectra would be the same. In this thesis, the same ring fragments (with the exception of two) were observed in both positive- and negative-ion experiments. This suggests that ionization followed by gas phase ion-molecular reactions may not be the dominant fragmentation process, but rather fragmentation occurs before

ionization. However, once the desorbed fragments are in the gas phase further fragmentation could occur by ion-molecule reactions.

The only two ring fragments that were observed exclusively in the negative-ion mode are: $-C_3H_3O_4$ and $-C_3H_4O_3N$. These two ring fragments both contain an α,α-unsaturated system, therefore, deprotonation between the two double bond is very facile, and the deprotonated species would be much more stable than the corresponding cationized species. Hence, they were observed in relatively high abundance in the negative-ion spectra (Sections IV.3.4 & IV.3.6).

IV.3d RING FRAGMENTS

Due to the lack of literature data on ring-cleavage of underivatized oligosaccharide, the mass spectral data of all the oligosaccharides in this thesis has to be reviewed collectively in order to analyze the ring fragments. A general discussion of the different ring fragments is outlined in the following paragraphs in order to better understand the mass spectral interpretation presented in this thesis. More detailed analysis, and the way in which these ring fragments were used for structural characterization, will be discussed in subsequent sections.

The most common ring fragment in both positive- and negative-ion modes is the $-C_2H_3O_2$ fragment. This two-carbon ring fragment has been observed occasionally in both f.a.b and l.s.i.m.s. spectra[136,148]. The authors attributed this fragment to a C-1,C-2 centre or a C-3,C-4 centre (Fig. IV.2). Therefore these fragments are associated with both the reducing and the non-reducing end oligosaccharides. It should be noted that fragments containing a C-5,C-6 centre will also give a $-C_2H_3O_2$ ring fragment. Hence, the existence of a $-C_2H_3O_2$ fragment attached to a non-reducing end oligosaccharide implies that the ring cleaved hexose could be linked *via* position 3, 4, 5 or 6. Therefore the analytical aspect of the $-C_2H_3O_2$ ring fragment for determining positions of linkage is not very informative. However, if one of the H's were to be replaced by a substituent, then the two-carbon ring fragment might be useful for a tentative position-of-linkage assignment. In our previous study on

Klebsiella K44 oligosaccharide (Appendix 1), it was noted that a 2-linked rhamnose residue cleaved to give a $-C_2H_3O$ ring fragment, which may be interpreted to indicate 2-linked residues would be cleaved to give such a ring fragment.

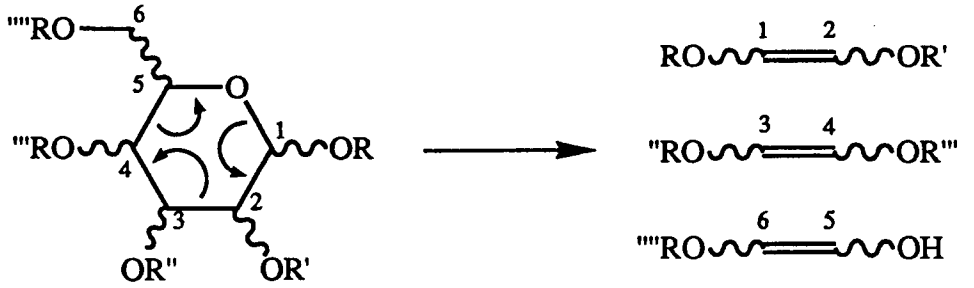

Fig.IV.2. Some ring cleavages giving two-carbon $-C_2H_3O_2$ fragments common to both positive- and negative-ion modes. Two of the products are of the structural type $C_2H_2O_2R_2$. If one of the R groups is replaced with a H atom, then the fragment formula will be $C_2H_3O_2$~R.

In this thesis, the three-carbon fragment, $-C_3H_5O_3$, was also abundant in both the positive- and negative-ion spectra. These $-C_3H_5O_3$ fragments could contain either a C-1,C-2,C-3 or C-2,C-3,C-4 or C-4,C-5,C-6,O-hemiacetal centre (Fig. IV.3). Fragments derived from the C-1,C-2,C-3 centre imply that the hexose is linked *via* position 1, 2 or 3 (1/2/3), while fragments derived from the C-2,C-3,C-4 centre imply that the hexose is linked *via* position 2, 3 or 4, similarly fragments derived from the C-4,C-5,C-6,O-hemiacetal centre imply that the hexose is linked *via* position 4, 5 or 6. Fragments derived from the C-1,C-2,C-3 and the C-4,C-5,C-6,O-hemiacetal centres imply that the hexose cleaves by breakage of the C-1,O-hemiacetal bond and the C-3,C-4 bond. However, if the first stage of the fragmentation is *via* glycosidic bond cleavage in the desorption plume, then the oxonium ion formed would have a double bond between C-1 and the ring oxygen (Fig. IV.1, structure 2). In this case, cleavage between the C-1,O-hemiacetal double bond would be unlikely. Therefore, we propose that if gas phase ion-molecule reactions play a prominant role in fragmentation of oligosaccharides, any $-C_3H_5O_3$ fragments attached to non-reducing end oligosaccharides are derived from the C-2,C-3,C-4 centre, which implies that the cleaved residue is linked *via* position 2, 3 or 4. If the non-reducing end oligosaccharide were to

undergo fragmentation to give a $-C_3H_5O_3$ fragment, then the three-carbon fragment would contain the C-1,C-2,C-3 centre.

If fragmentation occurs as a result of thermal pyrolysis in the desorption plume, then the cleavage would be influenced by the conformation of the oligomers in the solid state. Thus any of the three centres could contribute to a $-C_3H_5O_3$ fragment. All the oligosaccharide samples investigated in this thesis have degrees of polymerization lower than five, therefore as a result of the thermal energy deposited by the laser pulse, desorption of the intact oligosaccharides into the gas phase followed by fragmentation is possible. Therefore, we propose that if gas phase ion-molecule reaction plays a prominant role in fragmentation of lower oligosaccharides, any $-C_3H_5O_3$ fragments attached to non-reducing end oligosaccharides are derived from the C-2,C-3,C-4 centre, which implies that the cleaved residue is linked *via* position 2, 3 or 4.

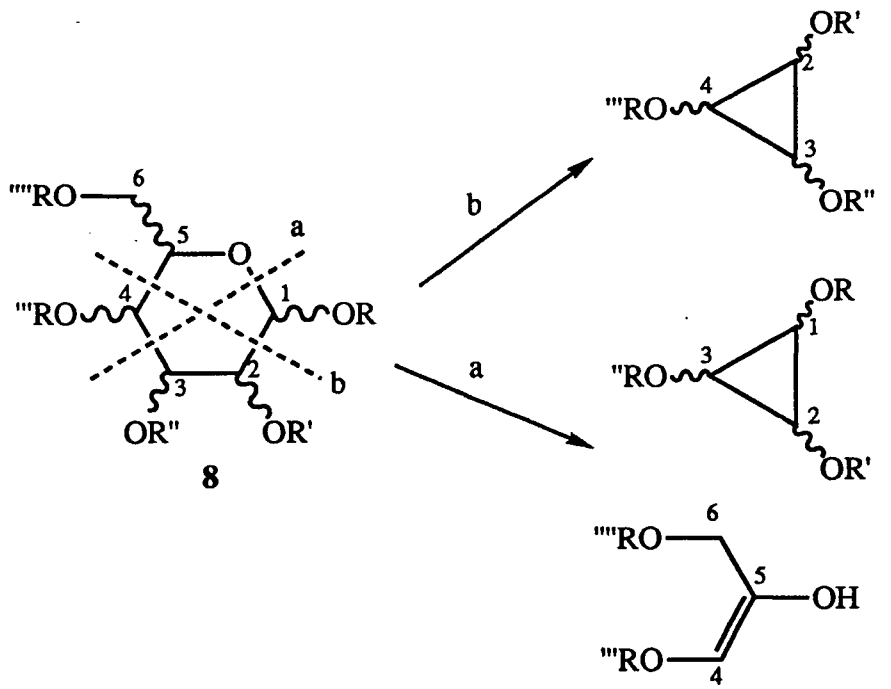

Fig.IV.3. Some ring cleavages giving three-carbon $-C_3H_5O_3$ fragments common to both positive- and negative ion modes. Two of the products are of the structural type $C_3H_3O_3R_3$. If two of the R groups are replaced with H atoms, then the fragment formula will be $C_3H_5O_3$~R. The structural formula of the other product is $C_3H_4O_3R_2$. If one of the R groups is replaced with a H atom, then the fragment formula will be $C_3H_5O_3$~R.

In a recent f.a.b.-m.s.-m.s. study of some monosaccharides[120], the authors suggested three different fragmentation reactions in the negative-ion mode for the formation of this $-C_3H_5O_3$ fragment containing the three centres discussed above. These fragmentation pathways all involve the initial deprotonation of the C-2 hydroxyl group. However, this $-C_3H_5O_3$ fragment was not observed in their positive-ion f.a.b.-m.s.-m.s. monosaccharide spectra. In contrast the ions containing this $-C_3H_5O_3$ fragment were relatively abundant in both the positive- and negative-ion l.d.i.-F.t.-i.c.r. spectra obtained in this study, suggesting that fragmentation occurred before ionization.

Another fragment seen in both positive- and negative-ion l.d.i.-F.t.-i.c.r. spectra is the $-C_4H_7O_3$ fragment, and this fragment could only be derived from the C-3,C-4,C-5,C-6 centre of a hexose (Fig. IV.4).

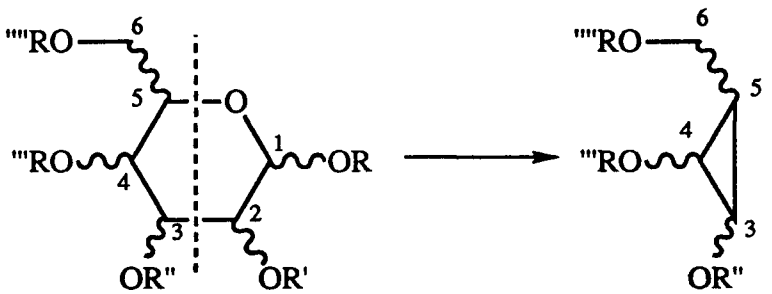

Fig.IV.4. Ring cleavage giving a four-carbon $-C_4H_7O_3$ fragment common to both positive- and negative-ion modes. If two of the R groups are replaced with H atoms, the fragment formula will be $C_4H_7O_3$~R.

Other ring fragments that have been observed in this thesis include: $-CHO_2$; $-C_2H_5O_2$; $-C_3H_3O_4$; $-C_3H_4O_3N$; $-C_4H_7O_4$; and $-C_4H_9O_3$. The possible analytical implications of these ring fragments will be discussed individually in the following sections.

The low resolution spectra and the "raw" high resolution tabulated spectra of the various oligosaccharides are listed in Appendix 2. The positive- and negative-ion spectra of each oligosaccharide are discussed in separate sections and accompanied by the "processed" high resolution data tables. These tabulated data include the observed mass (amu), calculated mass, relative intensity (%), mass error (ppm) and proposed carbohydrate structures, but will not include any alkali-halide clusters ions observed in the mass spectra.

The "whole oligosaccharide" fragments will be briefly mentioned in the text, however, the ring fragments will be discussed in more detail. Some masses could not be assigned to carbohydrate structures. Those with negative mass defect could be assigned to alkali-halide clusters from the KBr/NaCl matrix. Generally, all peaks considered to be signal ions could be assigned structures. In some spectra, a few ions are still to be structurally identified.

IV.3.1 NEGATIVE-ION L.D.I.-F.T.-I.C.R. SPECTRUM OF *Klebsiella* K44 DE-*O*-ACETYLATED OLIGOSACCHARIDE OBTAINED BY BACTERIOPHAGE DEGRADATION OF THE NATIVE CAPSULAR POLYSACCHARIDE

This linear pentasaccharide was chosen as the first example to demonstrate the application of l.d.i.-F.t.-i.c.r. to a linear oligosaccharide contain common sugars (Fig. IV.5). It was generated by bacteriophage degradation of the corresponding *Klebsiella* K44 capsular polysaccharide. The structure of the capsular polysaccharide is made up of a linear pentasaccharide repeating unit, consisting of one β-D-glucosyluronic acid, two α-L-rhamnose, one β-D-glucose and one 6-*O*-acetylated-α-D-glucose[195,196].

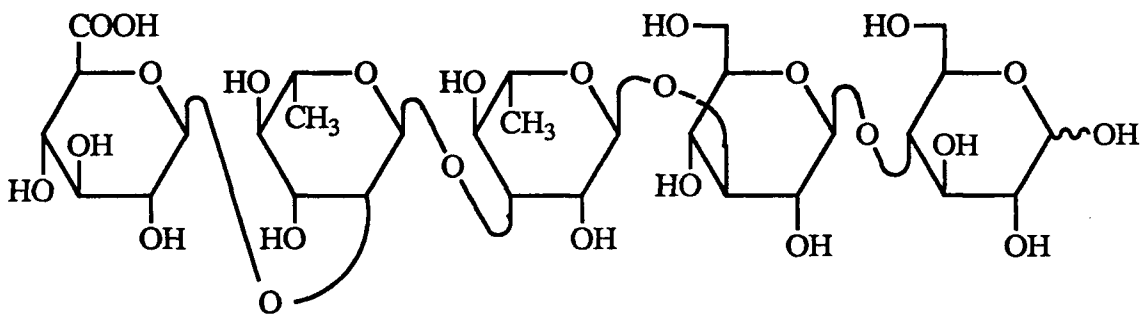

β-D-GlcA(1→2)-α-L-Rha(1→3)-α-L-Rha(1→3)-β-D-Glc(1→4)-D-Glc

Fig.IV.5. Structure of *Klebsiella* K44 de-*O*-acetylated oligosaccharide obtained by bacteriophage degradation of the capsular polysaccharide.

The negative-ion spectrum (Spec. IV.1 & IV.2) was dominated by KBr cluster-ions, however these inorganic ions were easily identifiable by their negative mass defect. Other than these inorganic ions and two other peaks (m/z 623.170 - 7% and 273.012- 8%), all the peaks above 5% could be assigned to carbohydrate structures (Table IV.1). Although the spectrum was recalibrated, the mass error of two fragments was still above 50 ppm (m/z 791.319, 5%, 92.0 ppm and 453.134, 10%, -60.7 ppm).

The low resolution mass spectral data indicated that the sample is a pentasaccharide, consisting of two hexoses *(2 x Hex)*, two deoxyhexose *(2 x deoxyHex)* and one hexuronic acid *(HexA)*. This pentasaccharide after successive glycosidic bond cleavages gave nine

different fragment structures: *(2deoxyHex)*; *(2Hex)*; *(Hex,deoxyHex)*; *(deoxyHex,HexA)*; *(Hex,2deoxyHex)*; *(2deoxyHex,HexA)*; *(2Hex,deoxyHex)*; *(2Hex,2deoxyHex)* and *(Hex,2deoxyHex,HexA)*. These fragments suggested that: i) the two hexose residues are contiguous; ii) the two deoxyhexose residues are adjacent; and iii) the hexuronic acid is a terminal residue and is linked to a deoxyhexose. Thus, the low resolution glycosidic bond cleavage data suggested two possible sequences for this linear pentasaccharide:

HexA→deoxyHex→deoxyHex→Hex→Hex

Hex→Hex→deoxyHex→deoxyHex→HexA

Four different types of ring fragment were observed, *viz*: $-C_2H_3O$, $-C_2H_3O_2$, $-C_2H_5O_2$ and $-C_3H_5O_3$. None of these fragments could be used conclusively to locate the reducing end of the oligosaccharide. However, from our previous positive-ion mass spectral data (Appendix 1), it was shown that the reducing residue is a hexose and the sequence is:

HexA→deoxyHex→deoxyHex→Hex→Hex

The fragment ion m/z 521.172 (7%) could be written as a deprotonated, di-dehydrated structure of a *(2deoxyHex,HexA)* unit linked to a $-C_3H_5O_3$ ring fragment. If the first step of fragmentation for this species is *via* oxonium ion formation, then the $-C_3H_5O_3$ ring fragment suggests that the cleaved hexose is linked to the deoxyhexose *via* position 2, 3 or 4. However, none of the other two-carbon ring fragments could be used to determine the positions of linkage for other monosaccharide residues. Therefore, the linkage information obtained from the negative-ion spectral data is:

HexA(1→?)deoxyHex(1→?)deoxyHex(1→2/3/4)Hex(1→?)Hex

Combining this information and the information obtained from the positive-ion spectral data detailed in Appendix 1: i) HexA(1→2)deoxyHex; ii) deoxyHex(1→3/4/5/6)Hex; and iii) Hex(1→3/4/5/6)Hex, gives:

HexA(1→2)deoxyHex(1→?)deoxyHex(1→3/4)Hex(1→3/4/5/6)Hex

The most interesting observation for this negative-ion spectrum is that the two-carbon ring fragments seem to reflect the stereochemistry of the anomeric centre of the monosaccharide residues. For the non-reducing oligosaccharide structures, the ring

fragments correlated with the anomeric configuration of the monosaccharide residue linked to the ring cleaved residue (Fig. IV.6). In this case, α-anomers gave a $-C_2H_5O_2$ fragment (cleavage from the 3-*O*-substituted-β-D-glucose residue and the 3-*O*-substituted-α-L-rhamnose residue), while β-anomers gave a $-C_2H_3O_2$ fragment (cleavage from the reducing end 4-*O*-substituted-D-glucose residue and the 2-*O*-substituted-α-L-rhamnose residue). For the reducing oligosaccharide structures, the ring fragments correlated with the anomeric configuration of the ring cleaved residue itself (Fig. IV.7). In this case, α-anomers gave a $-C_2H_3O$ fragment (cleavage from the 2-*O*-substituted-α-L-rhamnose residue and the 3-*O*-substituted-α-L-rhamnose residue), while β-anomers gave a $-C_2H_3O_2$ fragment (cleavage from the non-reducing end β-D-glucose residue and the 3-*O*-substituted-β-D-glucose residue).

It could be argued that the two-carbon fragments shown in Fig. IV.6 and IV.7 may indicate the configuration of the highest-numbered chiral carbon, i.e., a D- or L-series sugar, rather than the the configuration of the anomeric carbon. The fragmentation of a monosaccharide ring, however, is more likely to manifest itself as either a neighbouring-group effect (as observed in Fig. IV.6) or as a representation of the stereochemistry of the fragment centre (as observed in Fig. IV.7), rather than a reflection of the stereochemistry of a relatively distant group, i.e., C-5 in this case.

Although the pseudo-molecular ion showed one unit of dehydration, this oligosaccharide does not contain any anhydro-residues. The fragment ions m/z 689.2144 (deprotonated (*Hex,2deoxyHex,HexA*) unit attached to a $-C_2H_3O_2$ fragment) and 675.2143 (deprotonated (*2Hex,2deoxyHex*) unit attached to a $-C_2H_3O_2$ fragment) indicated that none of the monosaccharide residues are anhydro-derivatives. Therefore, the dehydration occurred during the desorption/ionization process.

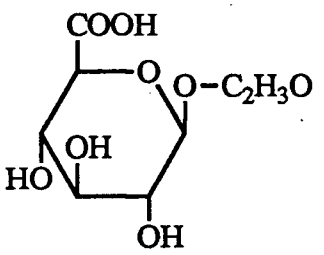

$C_2H_3O_2$ fragment attached to β-D-glucuronic acid

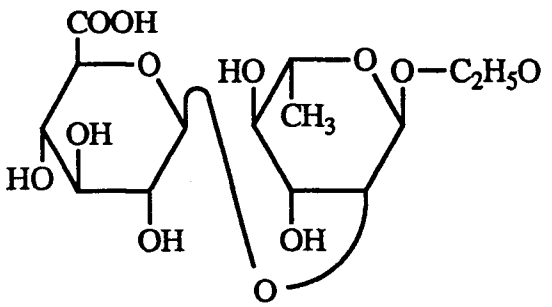

$C_2H_5O_2$ fragment attached to α-L-rhamnose

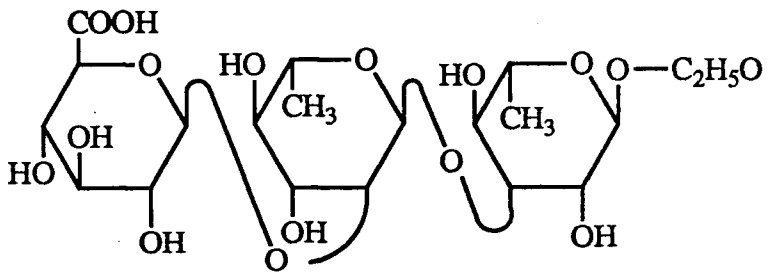

$C_2H_5O_2$ fragment attached to α-L-rhamnose

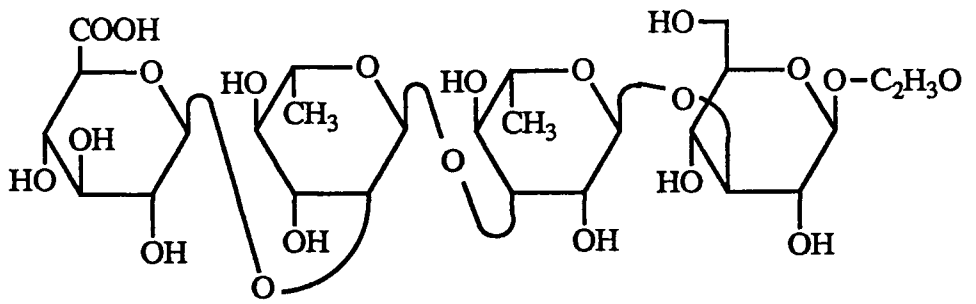

$C_2H_3O_2$ fragment attached to β-D-glucose

Fig.IV.6. Structures of the non-reducing end ring cleavage fragments obtained from negative-ion l.d.i.-F.t.-i.c.r. of *Klebsiella* K44 de-*O*-acetylated oligosaccharide. Deprotonation of these structures will give the corresponding ions.

β-D-glucose cleaved to give $C_2H_3O_2$ fragment

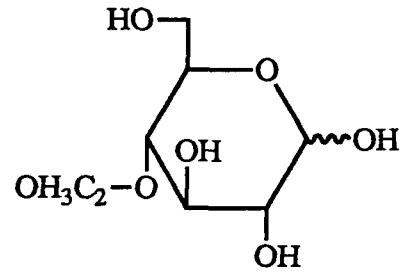

α-L-rhamnose cleaved to give C_2H_3O fragment

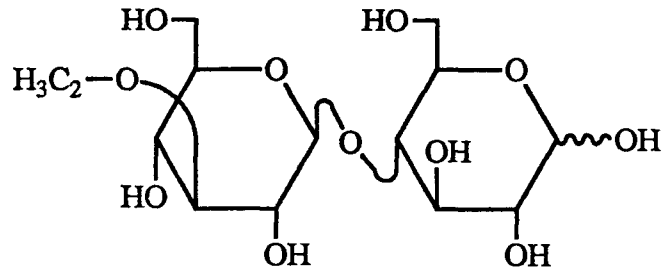

α-L-rhamnose cleaved to give C_2H_3O fragment

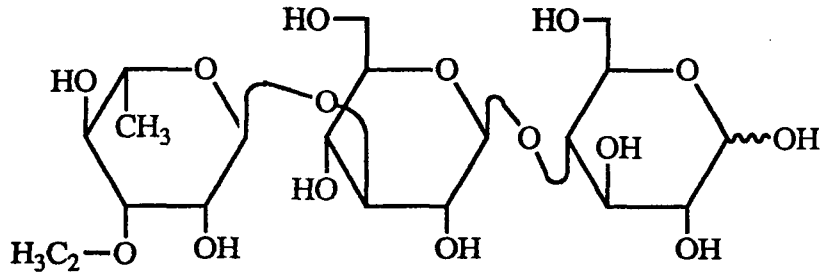

β-D-glucuronic acid cleaved to give $C_2H_3O_2$ fragment

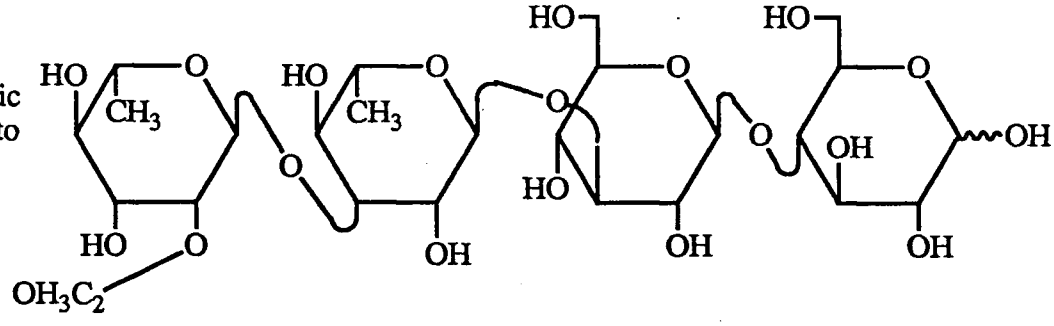

Fig.IV.7. Structures of the reducing end ring cleavage fragments obtained from negative-ion l.d.i.-F.t.-i.c.r. of *Klebsiella* K44 de-*O*-acetylated oligosaccharide. Deprotonation of these structures will give the corresponding ions.

TABLE IV.1

NEGATIVE ION LDI-FT-ICR FRAGMENT STRUCTURES OF *KLEBSIELLA* K44 DE-*O*-ACETYLATED OLIGOSACCHARIDE

Observed mass (amu)	*Calculated mass (amu)*	*Relative intensity (%)*	*Mass error (ppm)*	*Proposed structure*
791.319	791.246	5	92.0	[(2Hex,2deoxyHex,HexA)-H_2O-H]$^-$
689.214	689.214	5	0.6	[(Hex,2deoxyHex,HexA)+$C_2H_3O_2$-H]$^-$
675.214	675.235	11	-31.1	[(2Hex,2deoxyHex)+$C_2H_3O_2$-H]$^-$
629.170	629.194	7	-37.0	[(Hex,2deoxyHex,HexA)-H_2O-H]$^-$
623.170		7		?
615.224	615.214	5	15.9	[(2Hex,2deoxyHex)-H_2O-H]$^-$
555.196	555.193	7	5.4	[(Hex,2deoxyHex)+2$C_2H_3O_2$-H]$^-$
529.171	529.177	6	-10.6	[(2deoxyHex,HexA)+$C_2H_5O_2$-H]$^-$
521.172	521.151	7	39.1	[(2deoxyHex,HexA)+$C_3H_5O_3$-2H_2O-H]$^-$
513.160	513.183	14	-44.8	[(2Hex,deoxyHex)+C_2H_3O-H]$^-$
485.154	485.151	15	5.6	[(2deoxyHex,HexA)-H]$^-$
469.151	469.156	7	-12.2	[(2Hex,deoxyHex)-H_2O-H]$^-$
467.134	467.141	19	-14.8	[(2deoxyHex,HexA)-H_2O-H]$^-$
453.134	453.162	10	-60.7	[(Hex,2deoxyHex)-H_2O-H]$^-$
449.113	449.130	6	-38.4	[(2deoxyHex,HexA)-2H_2O-H]$^-$
383.120	383.119	7	2.4	[(deoxyHex,HexA)+$C_2H_5O_2$-H]$^-$
367.124	367.125	16	-2.7	[(2Hex)+C_2H_3O-H]$^-$
323.106	323.098	5	24.5	[(2Hex)-H_2O-H]$^-$
321.086	321.083	16	11.5	[(deoxyHex,HexA)-H_2O-H]$^-$
309.126	309.119	6	22.0	[(2deoxyHex)-H]$^-$
307.108	307.104	17	13.7	[(Hex,deoxyHex)-H_2O-H]$^-$
303.078	303.072	8	20.1	[(deoxyHex,HexA)-2H_2O-H]$^-$
291.110	291.109	18	4.5	[(2deoxyHex)-H_2O-H]$^-$
273.012		8		?
235.042	235.045	9	-14.5	[(HexA)+$C_2H_3O_2$-H]$^-$
221.069	221.067	16	11.8	[(Hex)+$C_2H_3O_2$-H]$^-$
203.057	203.056	6	5.9	[(Hex)+$C_2H_3O_2$-H_2O-H]$^-$
193.036	193.035	12	4.7	[(HexA)-H]$^-$
185.045	185.046	12	-2.7	[(Hex)+$C_2H_3O_2$-2H_2O-H]$^-$
179.059	179.056	11	14.5	[(Hex)-H]$^-$
175.028	175.025	9	16.6	[(HexA)-H_2O-H]$^-$
173.048	173.045	9	16.8	[(HexA)+$C_2H_3O_2$-CO_2-H_2O-H]$^-$
161.046	161.046	15	0.6	[(Hex)-H_2O-H]$^-$
145.052	145.051	21	6.9	[(deoxyHex)-H_2O-H]$^-$

IV.3.2 POSITIVE- AND NEGATIVE-ION L.D.I.-F.T.-I.C.R. SPECTRA OF MALTOSE AND CELLOBIOSE

To confirm the empirical observation of anomeric configuration correlating to mass fragments, the mass spectra of two underivatized disaccharides were obtained. These disaccharides were: maltose [α-D-glucose (1→4) D-glucose] and cellobiose [β-D-glucose (1→4) D-glucose] (Fig. IV.8).

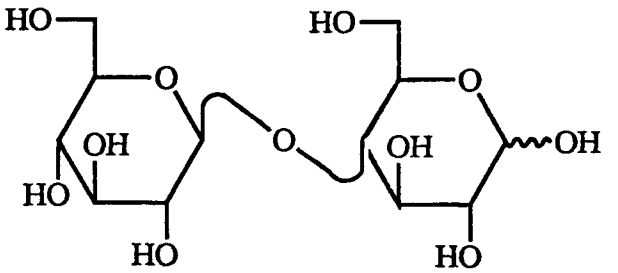

Cellobiose [β-D-Glc (1→4) D-Glc]

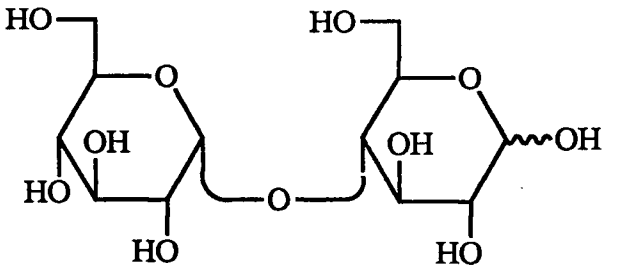

Maltose [α-D-Glc (1→4) D-Glc]

Fig.IV.8. Structure of the disaccharides:
maltose [α-D-Glc(1→4)-D-Glc] and cellobiose [β-D-Glc(1→4)-D-Glc]

There were no obvious differences between the positive- and negative-ion spectra of these disaccharides (Spec. IV.3-10; Table IV.2a-d). Although five different ring fragments were observed ($-C_2H_3O$, $-C_2H_3O_2$, $-C_3H_5O_3$, $-C_4H_7O_3$, $-C_4H_7O_4$), none of these fragments was characteristic for either disaccharide. The fragment $-C_4H_7O_4$ could have three possible structures, and could be linked either to the non-reducing or the reducing end (Fig. IV.9). A possible explanation for the very similar spectra observed, may be due to the thermal model

of laser desorption. As both disaccharides are of low molecular weight, they can be easily desorbed into the gas phase by the thermal energy deposited by the laser pulse. Due to the similar structures of the disaccharides, they could have similar gas phase unimolecular and ion-molecule reactions, thereby giving identical spectra.

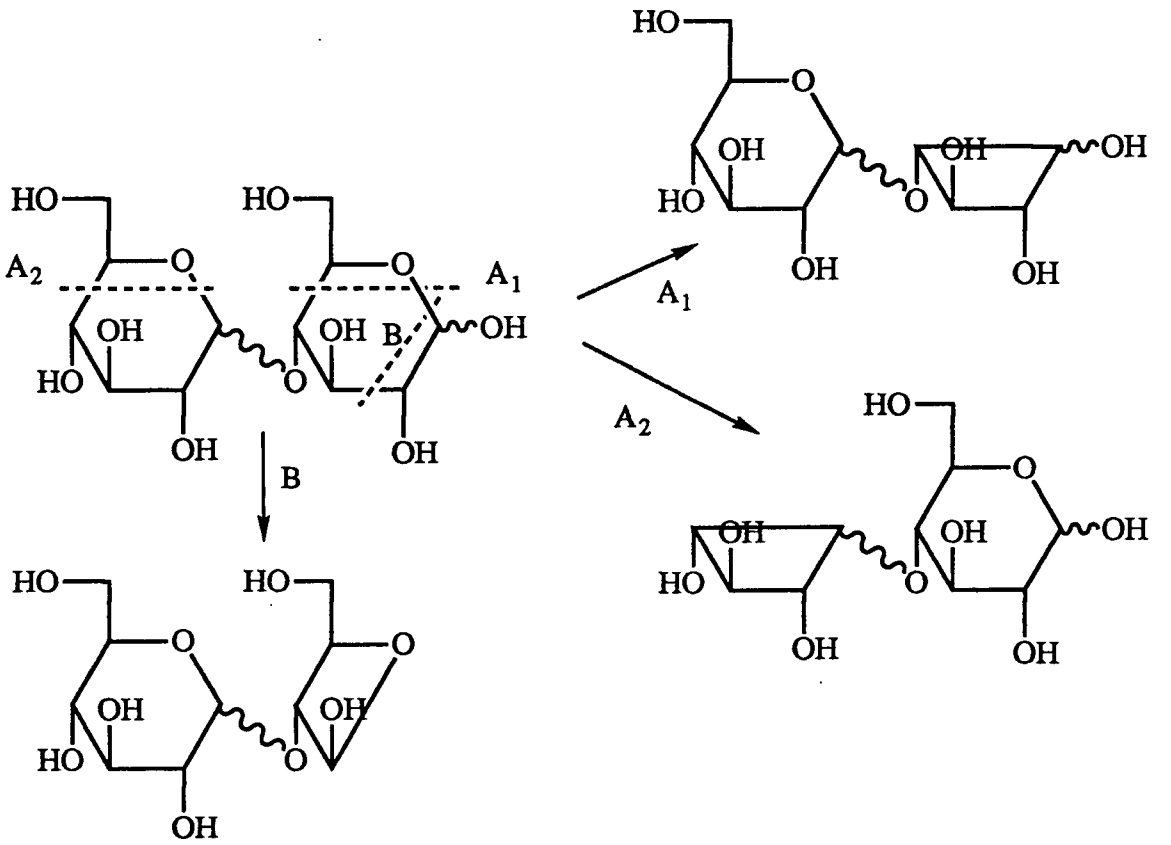

Fig.IV.9. Some ring cleavages giving R-$C_4H_7O_4$ fragments common to both positive- and negative-ion modes, containing either a C-1,C-2,C-3,C-4, or a C-3,C-4,C-5,C-6,O-hemiacetal centre.

TABLE IV.2a

POSITIVE-ION LDI-FT-ICR FRAGMENT STRUCTURES OF MALTOSE

Observed mass (amu)	*Calculated mass (amu)*	*Relative intensity (%)*	*Mass error (ppm)*	*Proposed structure*
381.081	381.079	24	5.3	$[(2Hex)+K]^+$
365.103	365.105	72	-6.8	$[(2Hex)-H_2O+K]^+$
325.114	325.113	24	3.3	$[(2Hex)-2H_2O+K]^+$
321.055	321.058	16	-11.5	$[(2Hex)+C_4H_7O_4+K]^+$
305.088	305.084	33	12.2	$[(2Hex)+C_4H_7O_4+Na]^+$
271.085	271.079	12	20.9	$[(2Hex)+C_4H_7O_3-H_2O+Na]^+$
265.096	265.092	14	14.1	$[(2Hex)+C_4H_7O_4-H_2O+H]^+$
247.084	247.081	13	10.8	$[(2Hex)+C_4H_7O_4-2H_2O+H]^+$
229.071	229.071	24	1.0	$[(2Hex)+C_4H_7O_4-3H_2O+H]^+$
187.061	187.060	17	5.0	$[(Hex)+C_2H_3O_2-2H_2O+H]^+$
169.051	169.050	11	7.4	$[(Hex)+C_2H_3O_2-3H_2O+H]^+$
163.061	163.060	56	4.3	$[(Hex)-H_2O+H]^+$

TABLE IV.2b

NEGATIVE-ION LDI-FT-ICR FRAGMENT STRUCTURES OF MALTOSE

Observed mass (amu)	*Calculated mass (amu)*	*Relative intensity (%)*	*Mass error (ppm)*	*Proposed structure*
341.124	341.109	21	43.8	$[(2Hex)-H]^-$
281.094	281.088	19	22.9	$[(Hex)+C_4H_7O_4-H]^-$
263.083	263.077	23	23.2	$[(Hex)+C_4H_7O_4-H_2O-H]^-$
251.083	251.077	25	24.2	$[(Hex)+C_3H_5O_3-H]^-$
221.071	221.067	58	21.4	$[(Hex)+C_2H_3O-H]^-$
179.060	179.056	100	20.6	$[(Hex)-H]^-$
161.049	161.046	70	20.4	$[(Hex)-H_2O-H]^-$
143.039	143.035	18	24.7	$[(Hex)-2H_2O-H]^-$
119.038	119.035	11	25.3	$[(C_4H_8O_4)-H]^-$
101.026	101.024	17	14.5	$[(C_4H_8O_4)-H_2O-H]^-$

TABLE IV.2c

POSITIVE-ION LDI-FT-ICR FRAGMENT STRUCTURES OF CELLOBIOSE

Observed mass (amu)	*Calculated mass (amu)*	*Relative intensity (%)*	*Mass error (ppm)*	*Proposed structure*
381.080	381.079	13	0.8	$[(2Hex)+K]^+$
365.110	365.105	50	13.1	$[(2Hex)-H_2O+K]^+$
325.127	325.113	15	44.6	$[(2Hex)-2H_2O+K]^+$
305.093	305.084	17	27.9	$[(2Hex)+C_4H_7O_4+Na]^+$
271.089	271.079	10	38.4	$[(2Hex)+C_4H_7O_3-H_2O+Na]^+$
229.074	229.071	9	15.3	$[(2Hex)+C_4H_7O_4-3H_2O+H]^+$
187.062	187.060	9	8.0	$[(Hex)+C_2H_3O_2-2H_2O+H]^+$
163.061	163.060	57	4.3	$[(Hex)-H_2O+H]^+$

TABLE IV.2d

NEGATIVE-ION LDI-FT-ICR FRAGMENT STRUCTURES OF CELLOBIOSE

Observed mass (amu)	*Calculated mass (amu)*	*Relative intensity (%)*	*Mass error (ppm)*	*Proposed structure*
377.129	377.086	15	115	$[(2Hex)+Cl]^-$
341.142	341.109	32	95.6	$[(2Hex)-H]^-$
263.091	263.077	36	53.6	$[(Hex)+C_4H_7O_4-H_2O-H]^-$
221.077	221.067	18	46.6	$[(Hex)+C_2H_3O-H]^-$
179.060	179.056	60	20.7	$[(Hex)-H]^-$
161.049	161.046	100	20.5	$[(Hex)-H_2O-H]^-$
143.039	143.035	15	24.5	$[(Hex)-2H_2O-H]^-$
101.026	101.024	12	14.8	$[(C_4H_8O_4)-H_2O-H]^-$

IV.3.3 POSITIVE-ION L.D.I.-F.T.-I.C.R. SPECTRA OF *Klebsiella* K3 OLIGOSACCHARIDE OBTAINED BY BACTERIOPHAGE DEGRADATION OF THE NATIVE CAPSULAR POLYSACCHARIDE

This linear oligosaccharide was chosen as it contains five common sugars and an acid-labile pyruvic acid acetal group (Fig. IV.10). The structure of the *Klebsiella* K3 capsular polysaccharide is made up of a "4+1" branched pentasaccharide repeating unit, consisting of one pyruvic acid acetal 4,6-linked to a α-D-mannose, one α-D-galactosyluronic acid, two α-D-mannose and one α-D-galactose. The branching pyruvylated mannose residue is linked to the branch point galactosyluronic acid residue[197]. The bacteriophage endoglycanase hydrolyze the galactose-galactosyluronic acid glycosidic linkages, therefore, generating a linear pentasaccharide repeating unit.

All peaks above 10% intensity of the base peak have been assigned to carbohydrate structures (Spec. IV.11 & IV.12). Listed in Table IV.3 are the tabulated high resolution mass spectral data for the oligosaccharide. These ions can be divided into two categories: i) fragment ions arising from glycosidic bond cleavages; and ii) fragment ions derived from ring cleavages. As the oligosaccharides obtained from the enzymic procedure were not desalted, multiple peaks were often observed for the same carbohydrate structures, such as m/z 907.202 (potassiated species) and 891.250 (the corresponding sodiated species).

The low resolution mass spectral data indicated that the capsular polysaccharide is made up of a pentasaccharide repeating unit, consisting of four hexoses *(4 x Hex)*, one hexuronic acid *(HexA)* and one pyruvic acid acetal *(pyr)*. From the high resolution data, the pseudo-molecular ion m/z 917.257 (11%) can be assigned to a sodiated, dehydrated *(4Hex,HexA,pyr)* structure. Although the other pseudo-molecular ions (m/z 913.199, 907.202, 891.250) were decarboxylated, they were not dehydrated, thus implying that the sample does not contain any anhydro-saccharides.

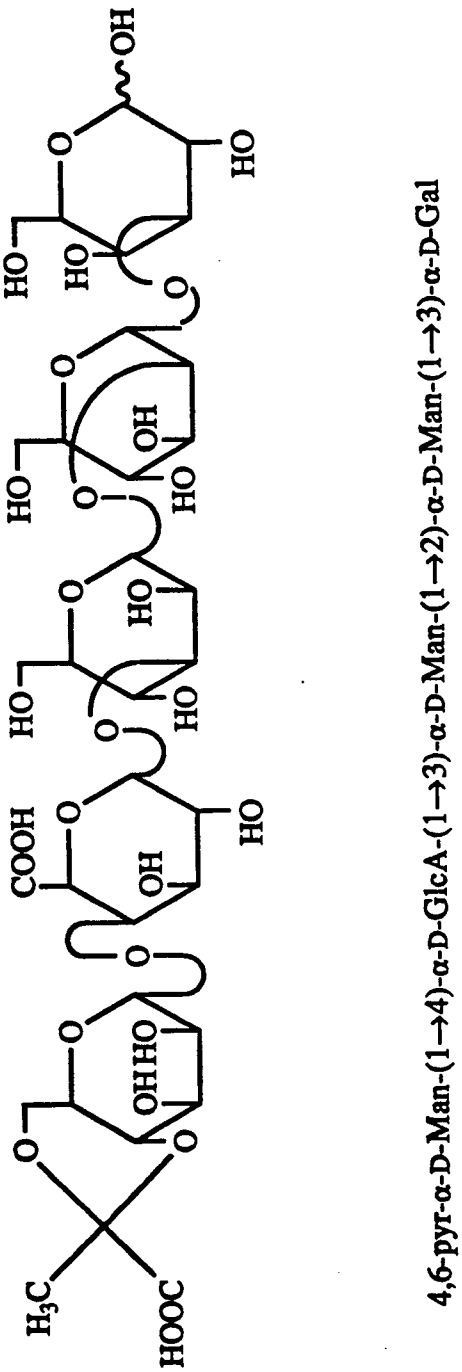

Fig.IV.10. Structure of *Klebsiella* serotype K3 oligosaccharide obtained by bacteriophage degradation of the capsular polysaccharide.

The pentasaccharide after successive glycosidic bond cleavages, gave seven different fragment structures: *(2Hex)*; *(3Hex)*; *(Hex,HexA)*; *(2Hex,HexA)*; *(3Hex,HexA)*; and *(3Hex,HexA,pyr)*. These fragments suggested that: i) the three hexose residues are contiguous; ii) the fourth hexose is a terminal residue and is linked to the other *(3Hex) via* the hexuronic acid residue; iii) the absence of *(2Hex,pyr) & (3Hex,pyr)* fragments suggested that the pyruvic acid acetal is located either on the fourth hexose unit or on the hexuronic acid. Thus, the low resolution glycosidic bond cleavage data suggested four possible sequences for this linear pentasaccharide:

Hex(pyr)→HexA→Hex→Hex→Hex

Hex→HexA(pyr)→Hex→Hex→Hex

Hex→Hex→Hex→HexA(pyr)→Hex

Hex→Hex→Hex→HexA→Hex(pyr)

Four different types of ring cleavage fragments were observed: $-C_2H_3O_2$, $-C_3H_5O_3$, $-C_4H_7O_3$, and $-C_4H_7O_4$. These ring fragments can be used to ascertain the location of labile substituents and alternative reducing end structures. The site of pyruvylation was deduced from the ring fragment, m/z 293.090 ($C_{11}H_{17}O_9$), which could be assigned to $[(Hex,pyr)+C_2H_3O_2+H]^+$. Thus, the pyruvic acid acetal is attached to the terminal hexose residue and not to the hexuronic acid. This further narrowed down the choice of possible sequences to:

Hex(pyr)→HexA→Hex→Hex→Hex

Hex→Hex→Hex→HexA→Hex(pyr)

Based upon the low resolution data, the high resolution spectrum contained two fragment ions, each of which could be assigned to more than one structure. The fragment ion m/z 609.155 ($C_{22}H_{34}O_{17}K$) could be assigned to:

$[(3Hex)+C_4H_7O_4-2H_2O+K]^+$

or $[(2Hex,HexA)+C_4H_9O_3-2H_2O+K]^+$

or $[(2Hex,HexA)+C_2H_3O_2+C_2H_3O-H_2O+K]^+$

or $[(2Hex,HexA)+2C_2H_3O+K]^+$

The fragment ion m/z 553.176 ($C_{20}H_{34}O_{16}Na$) could be assigned to:

$[(3Hex)+C_2H_3O+Na]^+$

or $[(2Hex)+C_4H_7O_4+C_4H_7O_3+Na]^+$

The $-C_4H_9O_3$ ring fragment is fully saturated. Since all the other observed ring fragments have one unit of unsaturation, it would seems that structures containing the saturated $-C_4H_9O_3$ ring fragment are less likely to exist than structures containing unsaturated $-C_4H_7O_4$. As discussed in Section IV.3.3, the approach in this study is to consider that four-carbon ring fragments are more likely than two two-carbon ring fragments in a particular structure. Therefore, it is assumed that structures with the $-C_4H_7O_4$ fragment are more likely, thus the fragment ions m/z 609 and 553 have been assigned to structures containing this fragment. It should be noted though that the structures containing $-C_2H_3O$ might contribute to the intensity of the fragment m/z 553.

Therefore, the proposed structure of the fragment ion m/z 553 is a sodiated *(2Hex)* unit sandwiched between $-C_4H_7O_4$ and $-C_4H_7O_3$ ring fragments. The $-C_4H_7O_3$ fragment can only be derived from the C-3,C-4,C-5,C-6 centre of a hexose, therefore, the sequence of this m/z 553 fragment is $C_4H_7O_4$-*(2Hex)*-$C_4H_7O_3$ (Fig. IV.11). The reverse of this sequence would imply a *(4Hex)* unit, which was not observed in the mass spectrum.

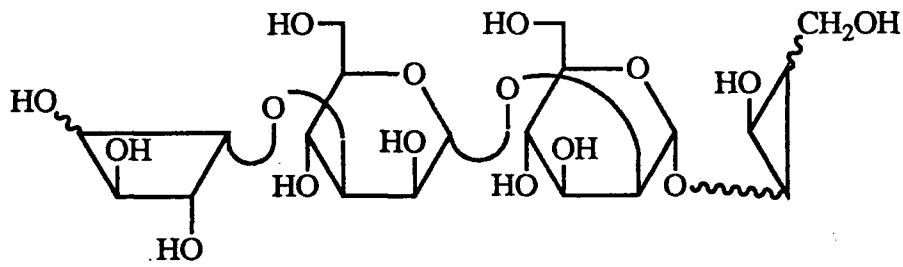

Fig.IV.11. Structure of fragment ion $C_4H_7O_4$-(2Hex)-$C_4H_7O_3$. Sodiation of this structure will give m/z 553.176.

Therefore, the sequence of the linear repeating pentasaccharide is:

Hex(pyr)→HexA→Hex→Hex→Hex

Further analyses of the ring structure also provide some tentative information on the positions of linkage. The fragment ion m/z 801.215 (21%) could be assigned to a sodiated, decarboxylated *(3Hex,HexA,pyr)* unit linked to a $-C_3H_5O_3$ ring fragment, implying that the cleaved residue is located at the reducing end, and probably linked *via* positions 2, 3 or 4. Subsequent, sequential loss of the non-reducing end hexose from this m/z 801 fragment would give fragment ion m/z 613.157 (21%) $\{[(2Hex,HexA)+C_3H_5O_3+Na]^+\}$, and with further loss of the hexuronic acid would give fragment ion m/z 437.130 (25%) $\{[(2Hex)+C_3H_5O_3+Na]^+\}$. It could be argued that the fragments m/z 613 and 437 could have been derived from the secondary and tertiary cleavage of a *(Hex→HexA→Hex→Hex)* tetrasaccharide unit. However, the mass spectral data did not show any other fragment ions that would favour one of these possibilities.

The reducing end hexose also fragmented to give a $-C_4H_7O_3$ unit which is derived from the C3-C4-C5-C6 centre (m/z 553.176, 13%). Therefore the position of linkage for the reducing end hexose is either at C-3 or C-4. Another observed four-carbon fragment, $-C_4H_7O_4$, derived from fragmentation of the galacturonic acid and attached to the reducing *(3Hex)* unit. However, immediate structural implication could not be drawn from this fragment. Unfortunately, the pentasaccharide did not undergo enough ring fragmentation for all the positions of linkage to be determined. Therefore the only information obtained from the positive-ion l.d.i.-F.t.-i.c.r. spectra for this oligosaccharide is:

Hex(pyr)(1→?)HexA(1→?)Hex(1→?)Hex(1→3/4)Hex

TABLE IV.3

POSITIVE-ION LDI-FT-ICR FRAGMENT STRUCTURES OF *Klebsiella* K3 OLIGOSACCHARIDE OBTAINED BY PHAGE DEGRADATION

Observed mass amu	*Calculated mass amu*	*Relative intensity %*	*Mass error ppm*	*Proposed structure*
917.257	917.238	10	20.2	$[(4Hex,HexA,pyr)-H_2O+Na]^+$
913.199	913.241	11	-45.7	$[(4Hex,HexA,pyr)-CO_2-H+2Na]^+$
907.202	907.233	29	-33.9	$[(4Hex,HexA,pyr)-CO_2+K]^+$
891.250	891.259	57	-9.5	$[(4Hex,HexA,pyr)-CO_2+Na]^+$
801.215	801.227	21	-15.6	$[(3Hex,HexA,pyr)+C_3H_5O_3-CO_2+Na]^+$
745.184	745.201	13	-22.7	$[(3Hex,HexA)+C_2H_3O_2+Na]^+$
729.204	729.206	24	-2.6	$[(3Hex,HexA,pyr)-CO_2+Na]^+$
719.155	719.164	19	-12.5	$[(3Hex,HexA)+K]^+$
711.188	711.196	20	-10.8	$[(3Hex,HexA,pyr)-CO_2-H_2O+Na]^+$
703.186	703.190	50	-6.1	$[(3Hex,HexA)+Na]^+$
685.174	685.180	17	-8.3	$[(3Hex,HexA)-H_2O+Na]^+$
641.182	641.190	17	-13.3	$[(3Hex,HexA)-CO_2-H_2O+Na]^+$
613.157	613.159	21	-2.5	$[(2Hex,HexA)+C_3H_5O_3+Na]^+$
609.155	609.143	27	20.4	$[(3Hex)+C_4H_7O_4-2H_2O+K]^+$
569.160	569.169	23	-16.3	$[(3Hex)+C_2H_3O_2+Na]^+$
553.176	553.174	13	3.7	$[(2Hex)+C_4H_7O_4+C_4H_7O_3+Na]^+$
549.142	549.140	18	3.2	$[(3Hex)-H+2Na]^+$
543.143	543.132	15	20.6	$[(3Hex)+K]^+$
541.137	541.138	22	-0.7	$[(2Hex,HexA)+Na]^+$
527.158	527.158	100	-0.8	$[(3Hex)+Na]^+$
523.127	523.127	21	0.0	$[(2Hex,HexA)-H_2O+Na]^+$
509.150	509.148	16	4.1	$[(3Hex)-H_2O+Na]^+$
479.142	479.137	11	9.9	$[(2Hex)+C_2H_3O_2+C_3H_5O_3+Na]^+$
437.130	437.127	25	6.9	$[(2Hex)+C_3H_5O_3+Na]^+$
421.095	421.095	26	-1.7	$[(Hex,HexA)+C_2H_3O_2+Na]^+$
365.106	365.106	35	2.2	$[(2Hex)+Na]^+$
363.099	363.092	17	17.6	$[(Hex,HexA)+C_2H_3O_2-2H_2O+H]^+$
361.079	361.074	12	13.9	$[(Hex,HexA)-H_2O+Na]^+$
347.099	347.095	11	10.9	$[(2Hex)-H_2O+Na]^+$
293.090	293.087	11	11.6	$[(Hex,pyr)+C_2H_3O_2+H]^+$
187.063	187.060	15	12.8	$[(Hex)+C_2H_3O_2-2H_2O+H]^+$

IV.3.4 NEGATIVE-ION L.D.I.-F.T.-I.C.R. SPECTRA OF *Klebsiella* K3 OLIGOSACCHARIDE

The negative-ion spectrum of *Klebsiella* K3 oligosaccharide (Spec. IV.13 & IV.14, Table IV.4) confirmed the sequence obtained from the positive-ion spectrum, and in addition, established one other position of linkage. The fragment ion m/z 497.110 (10%) could be assigned to a deprotonated *(Hex,HexA,pyr)* unit linked to a $-C_3H_5O_3$ ring fragment, implying that the cleaved residue was attached to the hexuronic acid, and is either linked *via* position 2, 3 or 4.

Another three-carbon ring fragment, $-C_3H_3O_4$, observed in the spectrum could be assigned to a species with two units of unsaturation. The fragment ions m/z 589.166 (6%), 571.142 (16%), and 553.142 (39%) were the deprotonated and the "successive" dehydration products of a *(3Hex)* unit linked to a $-C_3H_3O_4$ ring fragment (Fig. IV.12). This ring fragment was derived from the C-3,C-2,C-1,O-hemiacetal centre of the hexuronic acid. A simple mechanism that can be proposed for this fragmentation is illustrated in Fig. IV.13. This mechanism involves the formation of an α,α-unsaturated hydroxyl-keto-aldehyde structure at the C-3,C-2,C-1,O-hemiacetal centre.

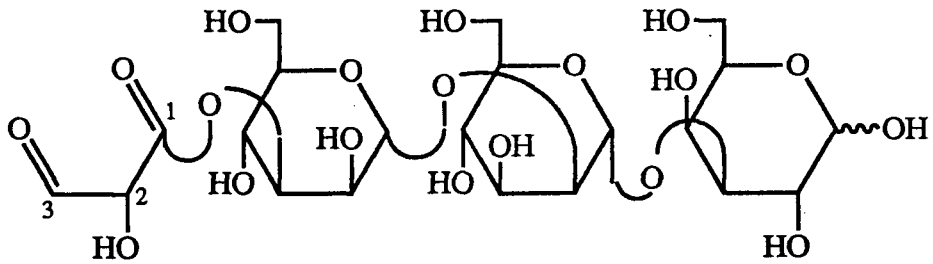

Fig.IV.12. Structure of fragment ion $C_3H_3O_4$-(3Hex). Deprotonation of this structure will give m/z 589.166. Successive dehydration of this ion gave fragment ions m/z 571.142, and 553.142.

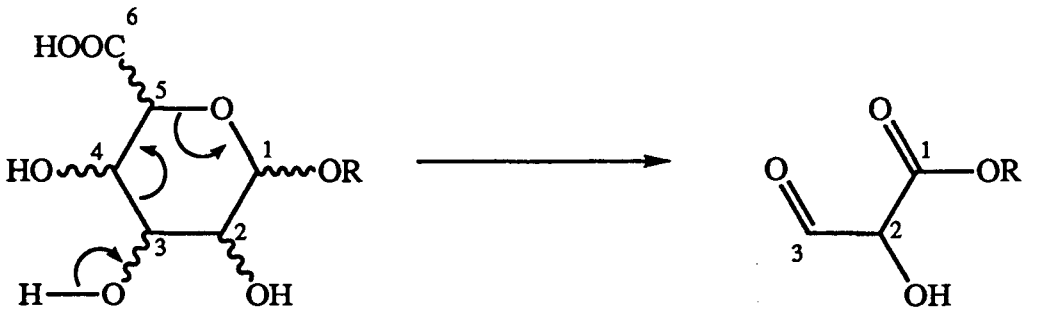

Fig.IV.13. Deprotonation of C-3 hydroxy hydrogen of the galacturonic acid and subsequent cleavages of the C-3,C-4 and C-5,O bonds.

Other than these two unique fragment ions and a greater abundance of dehydrated ions observed in the negative-ion spectrum, both the positive- and negative-ion spectra were very similar.

In conclusion, the positive- and negative-ion l.d.i.-F.t.-i.c.r. spectra provided the following sequence and linkage information:

Hex(pyr)(1→?)HexA(1→2/3/4)Hex(1→?)Hex(1→3/4)Hex

TABLE IV.4

NEGATIVE-ION LDI-FT-ICR FRAGMENT STRUCTURES OF *Klebsiella* K3 OLIGOSACCHARIDE OBTAINED BY PHAGE DEGRADATION

Observed mass amu	*Calculated mass amu*	*Relative intensity %*	*Mass error ppm*	*Proposed structure*
867.281	867.262	34	21.1	[(4Hex,HexA,pyr)-CO_2-H]$^-$
759.230	759.220	15	13.3	[(3Hex,HexA,pyr)+$C_3H_5O_3$-CO_2-3H_2O-H]$^-$
705.202	705.210	65	-10.4	[(3Hex,HexA,pyr)-CO_2-H]$^-$
703.192	703.194	14	-2.1	[(3Hex,HexA)+$C_2H_3O_2$-H_2O-H]$^-$
687.202	687.199	10	4.9	[(3Hex,HexA,pyr)-CO_2-H_2O-H]$^-$
679.196	679.194	36	3.3	[(3Hex,HexA)-H]$^-$
661.182	661.183	39	-2.4	[(3Hex,HexA)-H_2O-H]$^-$
643.179	643.173	6	10.1	[(3Hex,HexA)-2H_2O-H]$^-$
589.166	589.162	6	5.8	[(3Hex)+$C_3H_3O_4$-H]$^-$
585.164	585.167	11	-5.5	[(2Hex,HexA,pyr)+$C_2H_3O_2$-CO_2-H]$^-$
571.142	571.152	16	-16.6	[(3Hex)+$C_3H_3O_4$-H_2O-H]$^-$
559.155	559.152	5	5.6	[(2Hex,HexA)+$C_2H_3O_2$-H]$^-$
553.142	553.141	39	0.8	[(3Hex)+$C_3H_3O_4$-2H_2O-H]$^-$
543.158	543.157	7	1.5	[(2Hex,HexA,pyr)-CO_2-H]$^-$
525.148	525.146	13	4.0	[(2Hex,HexA,pyr)-CO_2-H_2O-H]$^-$
517.138	517.141	61	-5.2	[(2Hex,HexA)-H]$^-$
515.123	515.125	5	-5.6	[(Hex,HexA,pyr)+$C_3H_5O_3$+H_2O-H]$^-$
499.130	499.131	100	-1.7	[(2Hex,HexA)-H_2O-H]$^-$
497.110	497.115	10	-9.8	[(Hex,HexA,pyr)+$C_3H_5O_3$-H]$^-$
481.122	481.120	51	4.4	[(2Hex,HexA)-2H_2O-H]$^-$
397.098	397.099	31	-2.7	[(Hex,HexA)+$C_2H_3O_2$-H]$^-$
381.105	381.104	48	3.1	[(Hex,HexA,pyr)-CO_2-H]$^-$
379.087	379.088	55	-3.4	[(Hex,HexA)+$C_2H_3O_2$-H_2O-H]$^-$
355.088	355.088	7	-0.8	[(Hex,HexA)-H]$^-$
337.077	337.078	29	-2.1	[(Hex,HexA)-H_2O-H]$^-$
335.099	335.098	8	2.8	[(Hex,HexA)+$C_2H_3O_2$-CO_2-H_2O-H]$^-$
323.100	323.098	6	5.6	[(2Hex)-H_2O-H]$^-$
321.084	321.083	7	1.6	[(Hex,pyr)+$C_2H_3O_2$-H]$^-$
319.067	319.067	39	-1.8	[(Hex,HexA)-2H_2O-H]$^-$
303.073	303.072	5	3.8	[(Hex,pyr)+$C_2H_3O_2$-H_2O-H]$^-$
193.036	193.035	8	5.2	[(HexA)-H]$^-$
179.057	179.056	6	3.9	[(Hex)-H]$^-$
175.026	175.025	18	4.6	[(HexA)-H_2O-H]$^-$

IV.3.5 POSITIVE-ION L.D.I.-F.T.-I.C.R. SPECTRA OF *E. coli* K9 OLIGOSACCHARIDE OBTAINED BY BACTERIOPHAGE DEGRADATION OF THE NATIVE CAPSULAR POLYSACCHARIDE

This linear tetrasaccharide was chosen as it contains two common sugars, one amino sugar and an acid-labile sialic acid (Fig. IV.14). It was generated by bacteriophage degradation of the corresponding *E. coli* K9 capsular polysaccharide. The structure of the capsular polysaccharide is made up of a linear tetrasaccharide repeating unit, consisting of one β-D-galactose, one α-D-galactose, one *N*-acetyl β-D-galactosamine and one *N*-acetyl neuraminic acid[198].

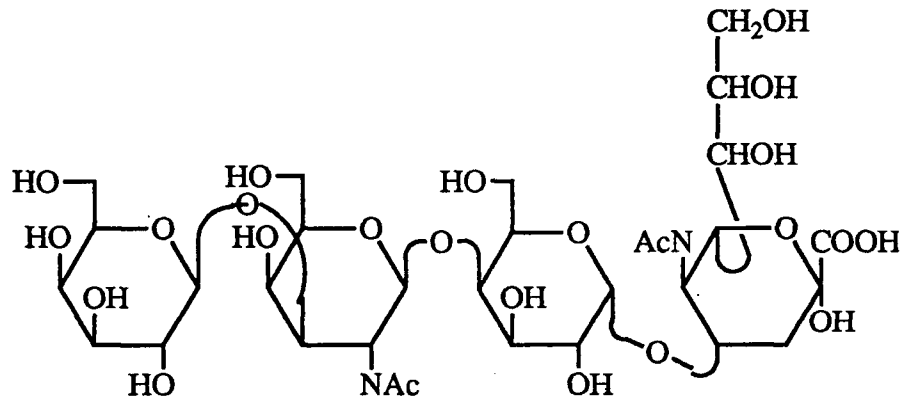

β-D-Gal(1→3)-β-D-GalNAc(1→4)-α-D-Gal(1→4) NeuNAc

Fig.IV.14. Structure of *Escherichia coli* serotype K9 oligosaccharide obtained by bacteriophage degradation of the capsular polysaccharide

No pseudo-molecular ions were observed in any of the positive-ion spectra (Spec. IV.15 & IV.16, Table IV.5). They showed only ions corresponding to *(2Hex,HexNAc)*, *(Hex,HexNAc)* and *(HexNAc)*. Although only limited structural information could be obtained from these spectra, they were consistent with the more detailed analysis obtained from the negative-ion spectrum.

TABLE IV.5

POSITIVE-ION LDI-FT-ICR FRAGMENT STRUCTURES OF *E. coli* K9 OLIGOSACCHARIDE OBTAINED BY PHAGE DEGRADATION

Observed mass amu	*Calculated mass amu*	*Relative intensity %*	*Mass error ppm*	*Proposed structure*
584.171	584.159	12	20.5	$[(2Hex,HexNAc)+K]^+$
568.188	568.185	34	5.8	$[(2Hex,HexNAc)+Na]^+$
550.176	550.174	11	3.6	$[(2Hex,HexNAc)-H_20+Na]^+$
388.120	388.122	100	-5.2	$[(Hex,HexNAc)-H_20+Na]^+$
			or	$*[(Hex,HexNAc)+C_2H_3O_2-H_20+Na]^+$
366.140	366.140	24	0.5	$[(Hex,HexNAc)-H_20+H]^+$
			or	$*[(Hex,HexNAc)+C_2H_3O_2-H_20+H]^+$
204.087	204.087	29	-0.5	$[(HexNAc)-H_20+H]^+$
			or	$*[(HexNAc)+C_2H_3O_2-H_20+Na]^+$
186.076	186.076	15	0.5	$[(HexNAc)-2H_20+H]^+$
			or	$*[(HexNAc)+C_2H_3O_2-2H_20+H]^+$

* Loss of a ketene from a *N*-acetylated amino sugar, $-C_2H_2O$

IV.3.6 NEGATIVE-ION L.D.I.-F.T.-I.C.R. SPECTRA OF *E. coli* K9 OLIGOSACCHARIDE

All peaks above 10% intensity of the base peak, with the exception of ten peaks, eight of which are alkali-halide clusters, have been assigned to the corresponding carbohydrate structures (Spec. IV.17 & IV.18). The high resolution mass spectral data for the oligosaccharide are listed in Table IV.6. The negative-ion mass spectrum was dominated by deprotonated structures. A number of even mass ions were observed suggesting that the analyte contains an odd number of nitrogen atoms[186].

Although fragments containing one nitrogen atom are easily identified by their even masses, the presence of *N*-acetyl sugars in oligosaccharide structures complicates the mass spectral analysis of the sugar. For example, a fragment at m/z 220.083 in the negative-ion spectrum reflects the elemental formula of $C_8H_{14}O_6N$, which is either a *N*-acetamido hexose or a hexosamine attached to a $-C_2H_3O_2$ ring fragment (Fig. IV.15). Therefore, extra care has to be taken when analyzing this type of compound.

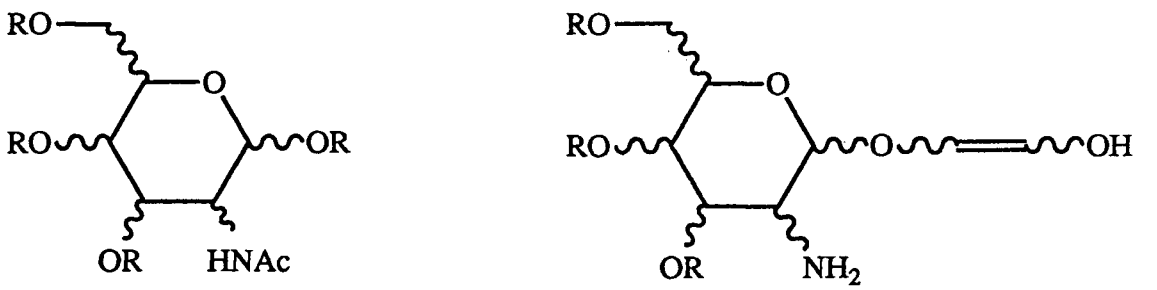

Acetamido hexose Amino hexose attached to a $C_2H_3O_2$ ring fragment

Fig.IV.15. Both *HexNAc* and *HexN-$C_2H_3O_2$* have the same elemental formula of $C_8H_{15}O_6N$

The low resolution mass spectral data imply that the capsular polysaccharide is made up of a tetrasaccharide repeating unit, consisting of two hexoses (2 x *Hex*), one *N*-acetamido hexose *(HexNAc)* and one *N*-acetyl neuraminic acid *(NeuNAc)*. The three main fragments observed after successive glycosidic bond cleavages were: *(2Hex,HexNAc)*; *(Hex,NeuNAc)*; *(Hex,HexNAc)*. These fragments suggest four possible sequences for this linear tetrasaccharide:

HexNAc→Hex→Hex→NeuNAc

NeuNAc→Hex→Hex→HexNAc

Hex→HexNAc→Hex→NeuNAc

NeuNAc→Hex→HexNAc→Hex

The fragment ion m/z 170.045 ($C_7H_8O_4N$, 38%) in the high resolution data could be a deprotonated, dehydrated $C_3H_4O_3N$+$C_4H_7O_3$ structure (Fig. IV.16), implying that a hexose residue is 3-, 4-, 5- or 6-linked to the amino hexose unit. The -$C_3H_4O_3N$ fragment probably has a similar structure to the -$C_3H_3O_4$ fragment (derived from cleavage of the hexuronic acid residue, Fig. IV.12) observed in the negative-ion spectra of *Klebsiella* K3 oligosaccharide.

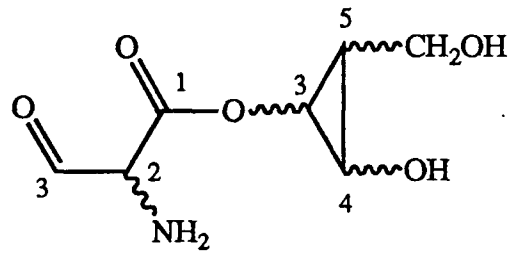

Fig.IV.16. Structure of fragment ion $C_3H_4O_3N$-$C_4H_7O_3$. Deprotonation and dehydration of this structure will give m/z 170.045. This structure suggested that a hexose is 3/4/5/6 linked to a hexosamine.

Fragment ions at m/z 626.182 (13%) indicated that the *NeuNAc* residue can be located either at the reducing or the non-reducing end of the sequence and is linked *via* positions 1, 2 or 4. Fragment ions at m/z 497.192 (21%), 467.172 (32%) and 407.153 (11%) are all derived from the same series with successive loss of C-9, C-8 and C-7 from the (*NeuNAc*) residue. This series demonstrated that the *NeuNAc* is linked via position 4 to the *(Hex,HexNAc)* unit. The fragment ion at m/z 395.159 (13%) confirms this inference (Fig. IV.17).

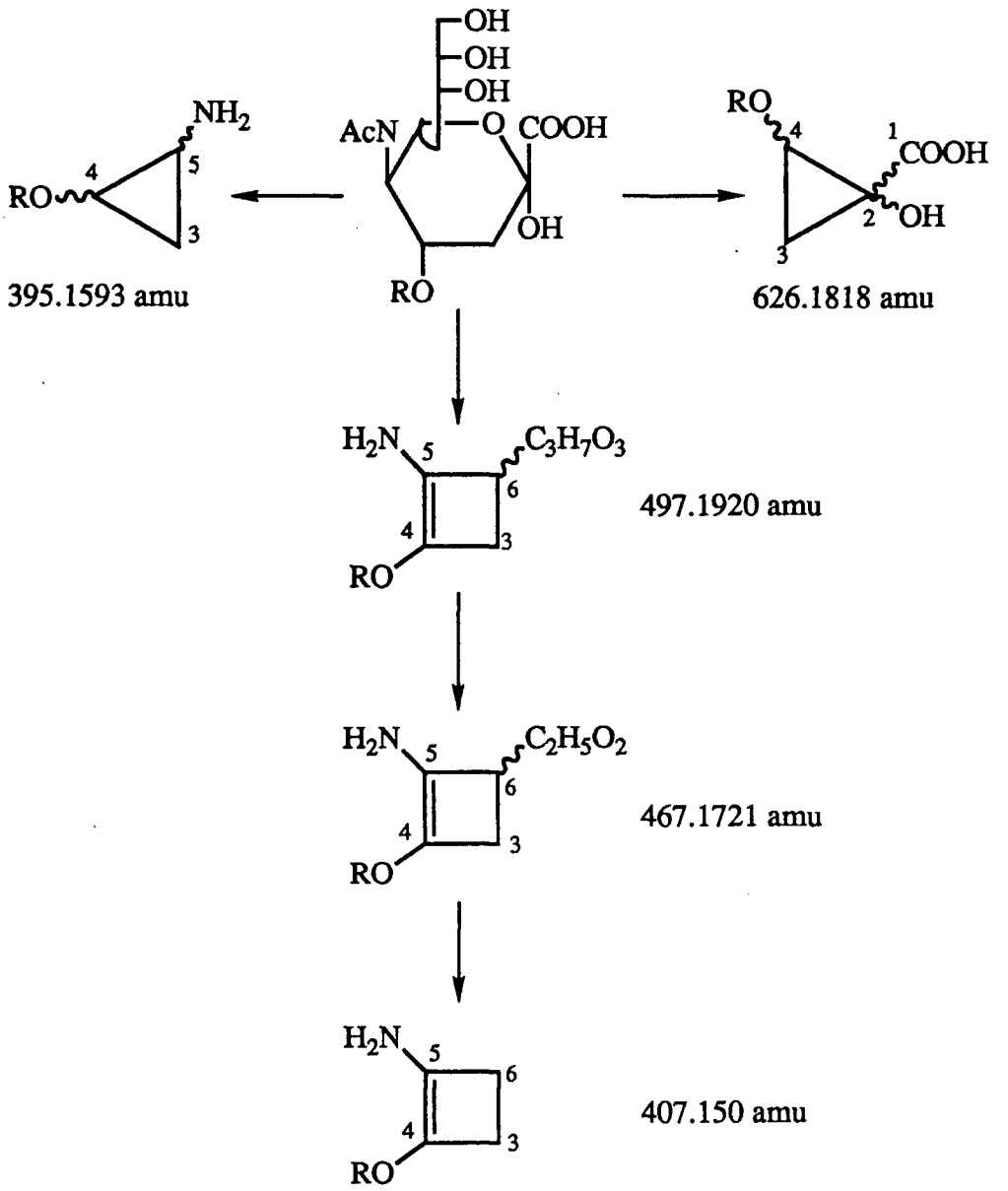

Fig.IV.17. Fragmentation of the R (1→4) NeuNAc unit. These structures implied that the neuraminic acid is located at the reducing end and is 4-linked to a (R=*Hex,HexNAc*) unit.

Therefore, the negative-ion l.d.i.-F.t.-i.c.r. spectrum provided the following sequence and linkage information:

Hex(1→?)HexNAc(1→3/4/5/6)Hex(1→4)NeuNAc

The pseudo-molecular ion m/z 817.274 could be assigned to the deprotonated, dehydrated tetrasaccharide. Therefore it is important to distinguish whether this tetrasaccharide contains any anhydro-saccharide. As the fragment ion m/z 264.094 could be

assigned to the deprotonated, decarboxylated *NeuNAc* residue, and the fragment ions m/z 497.199, 467.188, 407.167 and 395.167 could be assigned to the series of deprotonated *(Hex,HexNAc)* unit linked to ring fragments of *NeuNAc* , it is safe to assume that the anhydro-saccharide in the pseudo-molecular ion is the non-reducing end hexose residue. However, there was no peak that could confirm that the oligosaccharide contains an intrinsic anhydro-hexose or whether dehydration occurred during the desorption/ionization process.

TABLE IV.6

NEGATIVE-ION LDI-FT-ICR FRAGMENT STRUCTURES OF *E. coli* K9 OLIGOSACCHARIDE OBTAINED BY PHAGE DEGRADATION

Observed mass amu	*Calculated mass amu*	*Relative intensity %*	*Mass error ppm*	*Proposed structure*
817.274	817.273	24	0.7	[(2Hex,HexNAc,NeuNAc)-H_2O-H]$^-$
626.182	626.194	12	-19.2	[(2Hex,HexNAc)+$C_4H_5O_4$-H_2O-H]$^-$
			or	*[(2Hex,HexNAc)+$C_2H_3O_2$+$C_4H_5O_4$-H_2O-H]$^-$
580.163		11		?
526.178	526.178	20	-0.3	[(2Hex,HexNAc)-H_2O-H]$^-$
			or	*[(2Hex,HexNAc)+$C_2H_3O_2$-H_2O-H]$^-$
497.192	497.199	21	-13.8	*[(Hex,HexNAc)+$C_7H_{12}O_4N$-H]$^-$
496.197		10		?
484.166	484.167	14	-2.3	*[(2Hex,HexNAc)-H_2O-H]$^-$
467.172	467.188	32	-34.7	*[(Hex,HexNAc)+$C_6H_{10}O_3N$-H]$^-$
466.156	466.157	27	-0.5	*[(2Hex,HexNAc)-2H_2O-H]$^-$
462.111	462.120	12	-19.9	[(Hex,HexNAc)+$C_2H_3O_2$+^{37}Cl]$^-$
460.122	460.123	30	-0.9	[(Hex,HexNAc)+$C_2H_3O_2$+^{35}Cl]$^-$
452.134	452.141	16	-16.6	[(Hex,NeuNAc)-H_2O-H]$^-$
			or	*[(Hex,NeuNAc)+$C_2H_3O_2$-H_2O-H]$^-$
424.130	424.146	100	-37.4	[(Hex,HexNAc)+$C_2H_3O_2$-H]$^-$
410.152	410.130	12	51.7	*[(Hex,NeuNAc)-H_2O-H]$^-$
407.153	407.167	11	-34.8	*[(Hex,HexNAc)+C_4H_6ON-H]$^-$
395.159	395.167	13	-19.9	*[(Hex,HexNAc)+C_3H_6ON-H]$^-$
364.114	364.125	53	-30.3	[(Hex,HexNAc)-H_2O-H]$^-$
			or	*[(Hex,HexNAc)+$C_2H_3O_2$-H_2O-H]$^-$
290.088	290.088	34	0.0	[(NeuNAc)-H_2O-H]$^-$
			or	*[(NeuNAc)+$C_2H_3O_2$-H_2O-H]$^-$
272.075	272.078	15	-10.7	[(NeuNAc)-2H_2O-H]$^-$
			or	*[(NeuNAc)+$C_2H_3O_2$-2H_2O-H]$^-$
264.094	264.109	10	-56.1	[(NeuNAc)-CO_2-H]$^-$
			or	*[(NeuNAc)+$C_2H_3O_2$-CO_2-H]$^-$
262.088	262.093	18	-20.4	[(HexNAc)+$C_2H_3O_2$-H]$^-$
202.071	202.072	15	-6.6	[(HexNAc)-H_2O-H]$^-$
			or	*[(HexNAc)+$C_2H_3O_2$-H_2O-H]$^-$
170.045	170.046	38	-6.5	[($C_3H_4O_3N$+$C_4H_7O_3$)-H_2O-H]$^-$

* Loss of a ketene from a *N*-acetylated sugar, -C_2H_2O

IV.3.7 POSITIVE-ION L.D.I.-F.T.-I.C.R. SPECTRA OF *Klebsiella* K22 OLIGOSACCHARIDE OBTAINED BY BACTERIOPHAGE DEGRADATION OF THE NATIVE CAPSULAR POLYSACCHARIDES

The structure of *Klebsiella* K22 capsular polysaccharide is made up of a 2+2 branched tetrasaccharide repeating unit, consisting of one β-D-glucose, one 6-*O*-acetylated β-D-galactose, one α-D-glucose and one lactic acid ether-linked to an α-D-glucosyluronic acid[199], with the β-D-glucose and the 6-*O*-acetylated β-D-galactose in the main chain. The serotype specific bacteriophage K22 cleaves the main chain galactose-glucose glycosidic linkages, to generate a "3+1" branched structure (Fig. IV.18). Consequently, this tetrasaccharide was chosen for its interesting "3+1" structure, the base-labile *O*-acetyl group and the ether-linked lactic acid group.

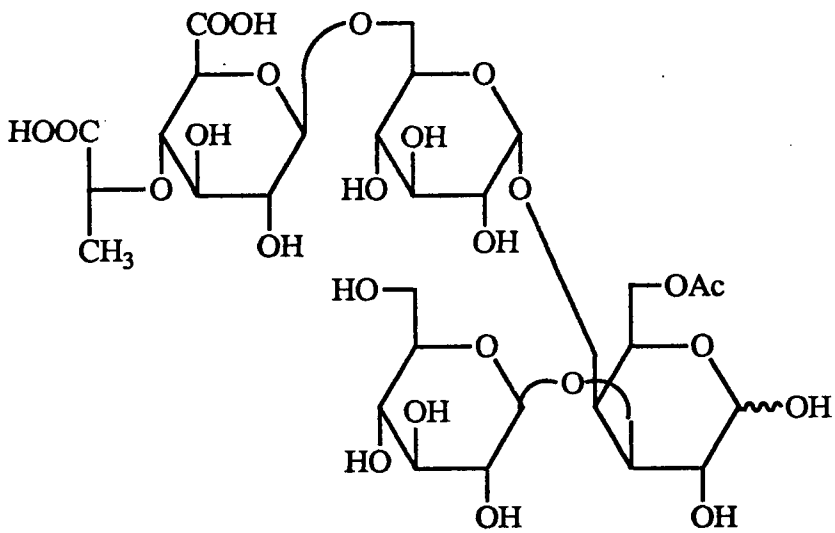

Fig.IV.18. Structure of *Klebsiella* serotype K22 oligosaccharide obtained by bacteriophage degradation of the capsular polysaccharide

The tabulated high resolution mass spectral data for the oligosaccharide are listed in Table IV.7. All peaks above 4% of the base peak can be assigned to carbohydrate structures (Spec. IV.19 & IV.20). The low resolution mass spectral data indicated that the oligosaccharide consists of three hexoses (3 x *Hex*), one hexuronic acid (*HexA*), one lactyl group (lac), and one acetyl group (*OAc*).

The tetrasaccharide, after successive glycosidic bond cleavages, gave three different fragment structures: (*Hex*); (*2Hex*) and (*3Hex*). These fragments suggested that: i) the three hexoses are linked together, and ii) the hexuronic acid is a terminal residue. The oligosaccharide generated by bacteriophage degradation of the native capsular polysaccharide have a 3+1 branched structure. Therefore, the low resolution glycosidic bond cleavage data suggested four possible sequences for this tetrasaccharide:

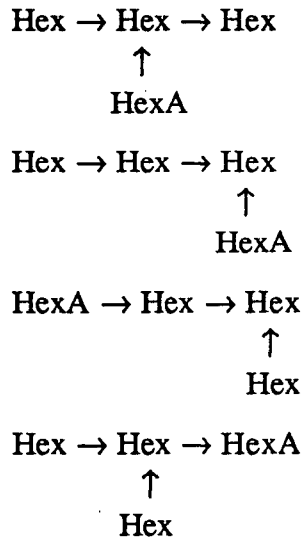

From the high resolution data, the fragment ion m/z 271.043 ($C_9H_{12}O_8Na$) could be assigned to two different sodiated, dehydrated structures: (*HexA,lac*) and (*Hex*)+$C_3H_3O_4$. The (*Hex*)+$C_3H_3O_4$ structure implies the formation of an α,α-unsaturated hydroxyl-keto-aldehyde structure at the C-3,C-2,C-1,O-hemiacetal centre (Fig. IV.19). This type of ring fragment has only been previously observed in negative-ion spectra but not in the positive-ion spectra (Sections IV.3.4 & IV.3.6). This can be rationized by the fact that the the C-2 hydrogen is acidic; and deprotonation of this α,α-unsaturated three-carbon fragment is facile under the desorption/ionization condition. Therefore, this α,α-unsaturated

three-carbon fragment will be unstable in the positive-ion mode. With this assumption, the fragment ion m/z 271 was assigned to the sodiated, dehydrated (*HexA,lac*) structure, implying that the lactyl group is attached to the hexuronic acid.

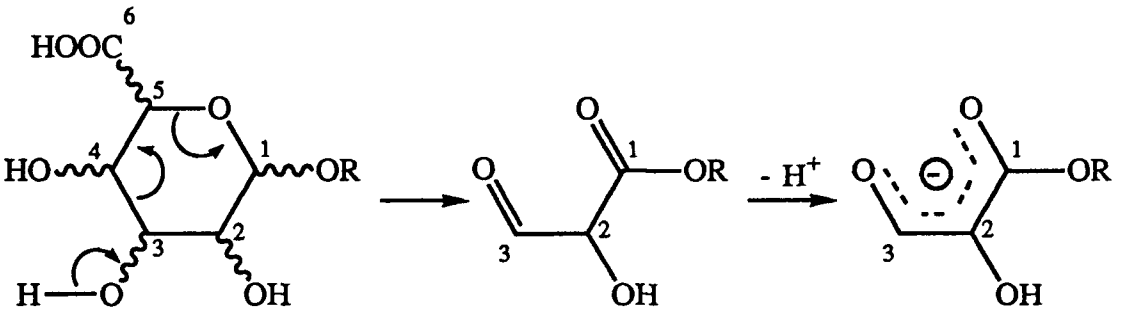

Fig.IV.19 Deprotonation of the C-3 hydroxy hydrogen of the glucuronic acid and subsequent cleavage of the C-3,C-4 and the C-5,O-hemiacetal bonds to give a keto-enol three-carbon -$C_3H_3O_4$ fragment, containing a C-1,C-2,C-3,O-hemiacetal centre. Due to the acidity of the C-2 hydrogen, this three-carbon fragment is unstable in the positive-ion mode.

The three structures (*Hex,OAc*); (*Hex*)+$C_2H_3O_2$; and (*HexA,lac*)-CO_2 all share the same elemental composition, $C_8H_{14}O_7$. These structures can be sub-units of larger structural fragments, such as fragment ions m/z 569.161 and 407.115. Due to this ambiguity in assignment, there is no direct evidence to locate the acetyl group or to obtain further sequence information on this 3+1 branched oligosaccharide. No fragments, however, could be assigned to a (*HexA,OAc*) or a (*HexA,lac,OAc*) structure, suggesting that the *O*-acetyl group is attached to one of the hexose residues.

TABLE IV.7

POSITIVE-ION LDI-FT-ICR FRAGMENT STRUCTURES OF *Klebsiella* K22 OLIGOSACCHARIDE

Observed mass amu	*Calculated mass amu*	*Relative intensity %*	*Mass error ppm*	*Proposed structure*
817.224	817.222	4	2.0	$[(3Hex,HexA,lac,OAc)+Na]^+$
585.143	585.143	29	0.2	$[(3Hex,OAc)+K]^+$
			or	$[(3Hex)+C_2H_3O_2+K]^+$
			or	$[(2Hex,HexA,lac)-CO_2+K]^+$
569.161	569.169	100	-14.1	$[(3Hex,OAc)+Na]^+$
			or	$[(3Hex)+C_2H_3O_2+Na]^+$
			or	$[(2Hex,HexA,lac)-CO_2+Na]^+$
543.130	543.132	15	-4.6	$[(3Hex)+K]^+$
527.155	527.158	51	-6.6	$[(3Hex)+Na]^+$
407.115	407.116	42	-2.0	$[(2Hex,OAc)+Na]^+$
			or	$[(2Hex)+C_2H_3O_2+Na]^+$
			or	$[(Hex,HexA,lac)-CO_2+Na]^+$
389.102	389.105	8	-8.1	$[(2Hex,OAc)-H_2O+Na]^+$
			or	$[(2Hex)+C_2H_3O_2-H_2O+Na]^+$
			or	$[(Hex,HexA,lac)-CO_2-H_2O+Na]^+$
365.105	365.106	24	-0.3	$[(2Hex)+Na]^+$
347.094	347.095	9	-2.0	$[(2Hex)-H_2O+Na]^+$
271.043	271.043	13	0.4	$[(HexA,lac)-H_2O+Na]^+$
205.070	205.071	26	2.0	$[(Hex,OAc)-H_2O+H]^+$
			or	$[(Hex)+C_2H_3O_2-H_2O+H]^+$
			or	$[(HexA,lac)-CO_2-H_2O+H]^+$
203.053	203.053	9	1.0	$[(Hex)+Na]^+$
187.060	187.060	23	0.0	$[(Hex,OAc)-2H_2O+H]^+$
			or	$[(Hex)+C_2H_3O_2-2H_2O+H]^+$
			or	$[(HexA,lac)-CO_2-2H_2O+H]^+$
145.049	145.050	4	-2.1	$[(Hex)-2H_2O+H]^+$

IV.3.8 NEGATIVE ION L.D.I.-F.T.-I.C.R. SPECTRA OF *Klebsiella* K22 OLIGOSACCHARIDE

Listed in Table IV.8 are the tabulated high resolution mass spectral data for the oligosaccharide. With the exception of three peaks (m/z 581.138 - 13%, 405.105 - 15%, and 215.032 - 12%) all peaks above 10% can be assigned to carbohydrate structures (Spec. IV.21 & IV.22). The pseudo-molecular ions confirmed the positive-ion data, that the oligosaccharide is made up of three hexoses, one hexuronic acid, one lactyl and one acetyl group.

As with the positive-ion mass spectra, the negative-ion mass spectral data of this oligosaccharide are very complicated due to the possible double and triple assignment of a number of fragment ions. This is due to the fact that the structures (*HexA,lac*) and (*Hex*)+$C_3H_3O_4$ share the same elemental composition ($C_9H_{14}O_9$), and the fact that deprotonation of both structures is equally facile in the negative-ion mode. Deprotonation can occur at the C-2 of the -$C_3H_3O_4$ ring fragment or at the carboxylic group of the hexuronic acid. The exact assignment of any ion containing a -$C_3H_3O_4$ ring fragment is of importance, as it will prove that the hexuronic acid is not located at the reducing end, thus reducing the number of possible sequences. No extra sequence information could be obtained from the negative-ion spectra.

TABLE IV.8

NEGATIVE-ION LDI-FT-ICR FRAGMENT STRUCTURES OF *KLEBSIELLA* K22 OLIGOSACCHARIDE

Observed mass (amu)	*Calculated mass (amu)*	*Relative intensity (%)*	*Mass error (ppm)*	*Proposed structure*
793.225	793.226	31	-1.0	[(3Hex,HexA,lac,OAc)-H]$^-$
775.208	775.215	10	-9.2	[(3Hex,HexA,lac,OAc)-H_2O-H]$^-$
751.213	751.215	10	-2.5	[(3Hex,HexA,lac)-H]$^-$
721.190	721.205	16	-20.5	[(3Hex,HexA,OAc)-H]$^-$
615.169	615.178	12	-14.3	[(2Hex,HexA,lac,OAc)+CHO_2-CO_2-H]$^-$
			or	[(2Hex,HexA,lac)+$C_2H_3O_2$+CHO_2-CO_2-H]$^-$
581.138		13		?
427.110	427.109	100	1.2	[(Hex,HexA,lac)-H]$^-$
			or	[(2Hex)+$C_3H_3O_4$-H]$^-$
409.099	409.099	52	0.7	[(Hex,HexA,lac)-H_2O-H]$^-$
			or	[(2Hex)+$C_3H_3O_4$-H_2O-H]$^-$
405.105		15		?
355.087	355.088	29	-4.8	[(Hex,HexA)-H]$^-$
349.075	349.078	13	-8.4	[(HexA,lac)+$C_4H_7O_4$-H_2O-H]$^-$
			or	[(Hex)+$C_3H_3O_4$+$C_4H_7O_4$-H_2O-H]$^-$
337.076	337.078	50	-5.9	[(HexA,lac)+$C_3H_5O_3$-H]$^-$
			or	[(Hex)+$C_3H_3O_4$+$C_3H_5O_3$-H]$^-$
			or	[(Hex,HexA)-H_2O-H]$^-$
319.066	319.067	15	-4.4	[(HexA,lac)+$C_3H_5O_3$-H_2O-H]$^-$
			or	[(Hex)+$C_3H_3O_4$+$C_3H_5O_3$-H_2O-H]$^-$
			or	[(Hex,HexA)-2H_2O-H]$^-$
277.056	277.057	11	-3.6	[(HexA)+$C_4H_7O_4$-H_2O-H]$^-$
275.077	275.077	22	-1.6	[(HexA,lac)+$C_3H_5O_3$-CO_2-H_2O-H]$^-$
			or	[(Hex,HexA)-CO_2-2H_2O-H]$^-$
265.057	265.057	13	0.0	[(HexA,lac)-H]$^-$
			or	[(Hex)+$C_3H_3O_4$-H]$^-$
247.044	247.046	30	-7.7	[(HexA,lac)-H_2O-H]$^-$
			or	[(Hex)+$C_3H_3O_4$-H_2O-H]$^-$
215.032		12		?
179.055	179.056	10	-6.7	[(Hex)-H]$^-$
175.023	175.025	12	-8.6	[(HexA)-H_2O-H]$^-$

In summary, the l.d.i.-F.t.-i.c.r. spectra of this 3+1 branched tetrasaccharide suggested four possible sequences **A**, **B**, **C** or **D**:

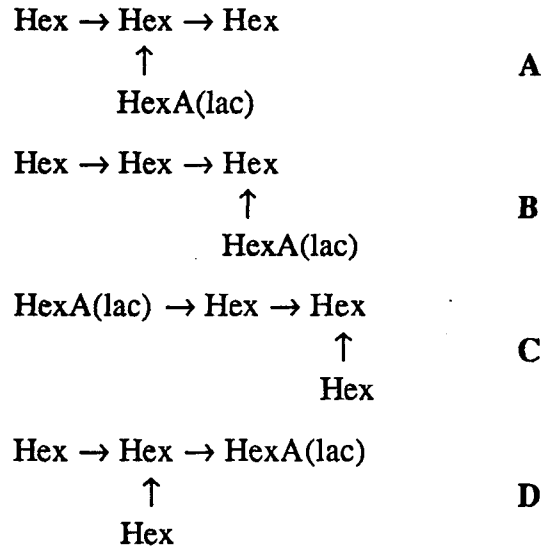

Because the structures (*HexA,lac*) and (*Hex*)+$C_3H_3O_4$, (*Hex,OAc*) and (*Hex*)+$C_2H_3O_2$ and (*HexA,lac*)-CO_2 share the same elemental formulae, the location of the *O*-acetyl group and the exact sequence of this "3+1" branched tetrasaccharide could not be determined. However, indirect evidence suggests that the *O*-acetyl group is attached to one of the hexose residues.

This ambiguous sequence information should not be looked upon as a drawback of the l.d.i.-F.t.-i.c.r. technique, as all single-stage mass spectrometric methods are unable to distinguish between alternative underivatized branched oligosaccharides.

The most effective mass spectrometric method for the sequencing of this branched structure is to analyze the permethylated and pertrifluoroacetylated derivatives[69]. This derivatization approach will encourage oxonium ion formation, which effectively "labels" the non-reducing end residues of the branched oligosaccharide (Fig. IV.20). Permethylation will remove all base-labile substituents, therefore, an ether-linked lactyl group will be stable to permethylation, while an ester-linked lactyl group will be removed. For this oligosaccharide, the lactyl group is ether-linked, therefore the non-reducing end permethylated (*HexA,lac*) will give an oxonium ion fragment m/z 305. Pertrifluoroacetylation has the added advantage

of not removing any *O*-acyl groups. Therefore, an acetylated residue could be distinguished from a non-acetylated residue due to the differences in the mass increment.

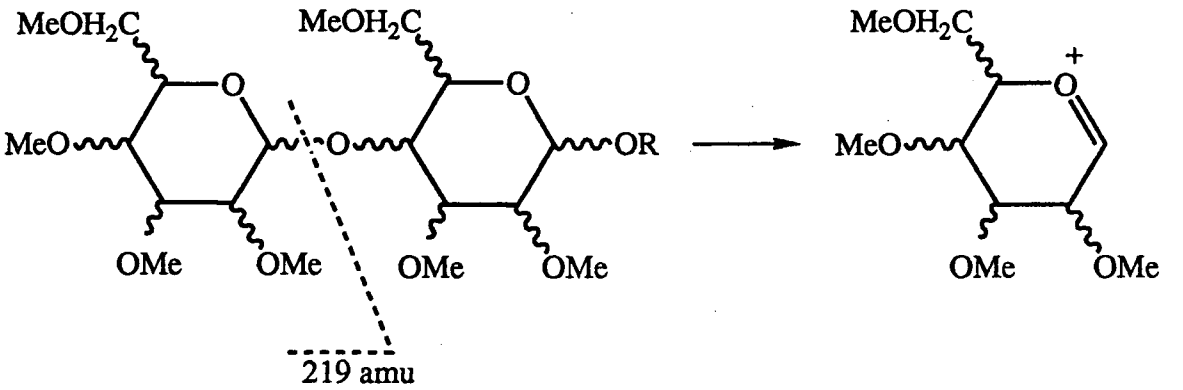

Fig.IV.20 A non-reducing end permethylated hexose residue will cleave to give an oxonium ion fragment of 219 mass unit.

In theory, each of the possible branched sequences has a characteristic permethylated oxonium ion fragment, therefore, the appearance of one of these fragments in the spectra will define the sequence. For example, **B** will give a (*2Hex*) fragment m/z 423, **D** will give a (*3Hex*) fragment m/z 627, **C** will give a (*Hex,HexA,lac*) fragment m/z 509, and **A** will give a (*2Hex,HexA,lac*) fragment m/z 713.

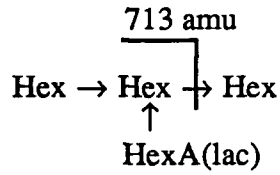

A

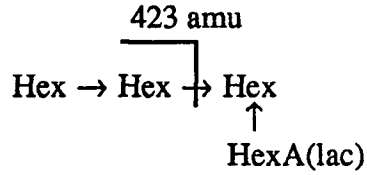

B

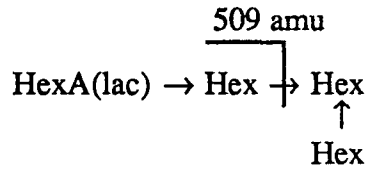

C

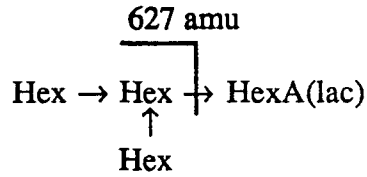

D

Similarly, the pertrifluoroacetylated 3+1 branched tetrasaccharide will also give characteristic pertrifluoroacetylated oxonium ion fragments. A non-reducing end (*HexA,lac*) will give a fragment m/z 428. A non-reducing end (*Hex*) will give a fragment m/z 547, while a non-reducing end (*Hex*) substituted with one *O*-acetyl group will give fragment m/z 493.

Therefore, in the case of pertrifluoroacetylated sample, **B** will give a (*2Hex*) fragment m/z 997, **D** will give a (*3Hex*) fragment m/z 1147, **C** will give a (*Hex,HexA,lac*) fragment m/z 878, and **A** will give a (*2Hex,HexA,lac*) fragment m/z 1328.

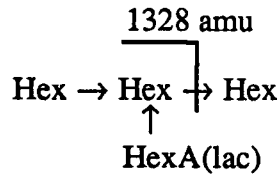

A

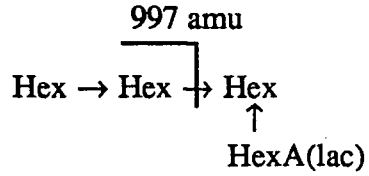

B

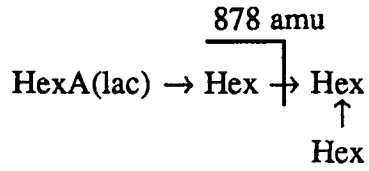

C

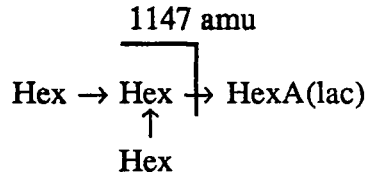

D

Furthermore, as pertrifluoroacetylation does not remove *O*-acetyl groups, any characteristic oxonium ion fragments that are 97 amu lower than expected, implies that the acetylated hexose is part of the oxonium ion. For example, in **A**, if the *O*-acetyl group is located on one of the non-reducing end hexoses, then the characteristic oxonium ion fragment will be m/z 1231. Furthermore, a fragment peak at m/z 547 indicates that the *O*-acetyl group is on the branching hexose, while a fragment peak at m/z 450 indicates that the *O*-acetyl group is on the non-reducing end hexose.

As structure **C** is the real sequence for this 3+1 branched oligosaccharide, the pertrifluoroacetylated oligosaccharide will give the following oxonium fragment ions : m/z 428, 547, 878, indicating that the *O*-acetyl group is not attached on any of these residues and, therefore, must be linked to the reducing end hexose.

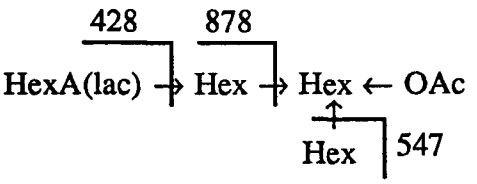

Although this Section illustrates that l.d.i.-F.t.-i.c.r. could not sequence this 3+1 underivatized branched tetrasaccharide, sequencing could, in principle, be accomplished with the derivatization methods as described above.

IV.3.9 STRUCTURAL ASSIGNMENTS FOR SOME COMMERCIAL POLYSACCHARIDES USING L.D.I.-F.T.-I.C.R.

Coates and Wilkins have demonstrated the potential of l.d.i.-F.t.-i.c.r. for the analysis of some commercial oligo- and poly-saccharides[170,171]. They categorized their polysaccharide mass spectral data by the differences in the "masses" of the ring fragments observed. Their results and interpretations are described in Section IV.3.9.A. Based on the l.d.i.-F.t.-i.c.r. studies of the four model underivatized oligosaccharides investigated in this thesis, mechanisms could be proposed for the formation of ring fragments observed by Coates and Wilkins in their polysaccharide mass spectra. These proposed mechanisms are detailed in Section IV.3.9.B.

IV.3.9.A SUMMARY OF L.D.I.-F.T.-I.C.R. FRAGMENTATION DATA ON POLYSACCHARIDES OBTAINED BY COATES AND WILKINS.

From the low resolution positive-ion l.d.i.-F.t.-i.c.r. mass spectra of nine commercially available polysaccharides[171] (locust bean gum, white dextrin, dextran, cellulose, starch, xanthan gum, agarose, agar and chitin) they observed

> *"extensive fragmentation of the saccharide chains, from both within the sugar rings and between them ... . Although similarities are seen in the spectra of some compounds, each displays a characteristic fragmentation pattern."*

The observed ion masses in their fingerprint mass spectra of polyhexoses can be described by the empirical formula

$$[(162)_n + X + K]^+ \quad \text{or} \quad [(Hex)_n + X + K]^+ \quad n = 1, 2, 3, \ldots \qquad (1)$$

where n corresponds to the number of hexose rings in the fragment ion, X corresponds to the mass of a ring fragment and K corresponds to a potassium ion attachment. For the polyhexoses analyzed, they observed sixteen series of fragment ions, with differing X, each of which was assigned an arbitrary label from A to R (Table IV.9). Fewer ion series were observed in the chitin spectrum than in the polyhexose spectra, primarily only those for which X = 0 (A), 60 (F), 74 (G), and 185. They noted that

TABLE IV.9

SUMMARY OF WILKIN'S ION SERIES A-R OF THE FORM $[(162)_n+X+K]^+$ FOR THE L.D.I.-F.T.-I.C.R. MASS SPECTRA OF SIX POLYHEXOSES

	% of relative abundance of series peaks (number of series peaks present)															
	A	B	C	D	E	F	G	H	J	K	L	M	N	P	Q	R
polyhexose	[0][b]	[18]	[24]	[42]	[44]	[60]	[74]	[84]	[88]	[90]	[102]	[104]	[120]	[126]	[144]	[148]
locust bean gum[a]	48 (4)	10 (2)		4 (2)		6 (2)								15 (3)	18 (4)	
white dextran	27 (5)	5 (3)		4 (4)	5 (4)	46 (7)					5 (4)		4 (3)		5 (4)	
dextran	15 (5)			4 (2)		65 (7)				8 (4)					9 (5)	
cellulose	26 (6)			10 (6)		47 (6)	3 (3)				5 (4)				6 (4)	
starch	19 (6)			6 (6)		31 (7)			8 (4)			24 (6)				11 (5)
xanthan gum	6 (2)		10 (4)	18 (5)		31 (5)		7 (3)			14 (4)			5 (3)	10 (4)	

[a]The entries in this table can be explained by using locust bean as an example. There are 4 peaks in its mass spectrum whose masses fit the A series pattern $[(162)_n + X + K]^+$. Thus, the number in parentheses in the A column entry is 4. The first number in this entry, 48, is obtained by summing the intensities of these peaks and dividing that sum by the sum of the intensities of all the ion peaks in the spectrum. The other entries in this table are obatined in the same way. [b]Numbers in brackets correspond to X in $[(162)_n + X + K]^+$.

"The series for which X = 185 is equivalent to the polyhexose series for which X = 144, shifted in mass reflect the acetylated amine substituent on carbon 2. The fact that the series for which X = 60 and X = 74 do not shift establishes that carbon 2 is not present in those fragments after cleavage across the sugar ring."

IV.3.9.B PROPOSED STRUCTURES AND REACTIONS PATHWAYS OF L.D.I.-F.T.-I.C.R. DATA ON POLYSACCHARIDES OBTAINED BY COATES AND WILKINS.

The most common ion series were A (X = 0), D (X = 42), F (X = 60), and Q (X = 144), with the A and F series ions being the most intense. These four series were observed in each of the mass spectra of the polysaccharides reported and thus are likely to be fragmentation patterns characteristic of hexose rings, rather than unique fingerprints of the individual polysaccharides. All the other ion series are probably derived from specific ring cleavages of each individual polysaccharide. When analyzing these data, comparison should be made between the spectra of similar polysaccharides, e.g., cellulose and chitin. Cellulose being the polymer of 1,4-linked β-D-glucose residues and chitin is poly- β-1,4-linked *N*-acetyl D-glucosamine.

Some insight into the chemical origin of the ions in the Coates-Wilkins A-R series is provided by writing their empirical formula (1) in a different form. For any polyhexose, their molecular formula can be written as

$$[(162)_n + 18] \qquad (2)$$

where n is the degree of polymerization, 162 being the molecular weight of a $C_6H_{10}O_5$ anhydro-hexose residue and 18 is the molecular weight of water. Successive loss of hexose residues in the mass spectrum of this polysaccharide would give rise to fragment ions whose formula is given by

$$[(162)_n + 18], \quad n = n\text{-}1, n\text{-}2, n\text{-}3, \ldots \qquad (3)$$

Loss of water from these ions would give rise to ions of the formula

$$[(162)_n + 18 - (18)_m], \qquad n = n, n\text{-}1, n\text{-}2, \ldots, m = 1, 2, 3, \ldots \qquad (4)$$

Ring cleaved oligohexoses in the mass spectrum would give rise to ions of the formula

$$[(162)_n + 18 - (18)_m + Y] \qquad n = n\text{-}1, n\text{-}2, n\text{-}3, \ldots, m = 0, 1, 2, \ldots \qquad (5)$$

where Y is the mass of the ring fragment.

Similarly, for any non-polyhexose homoglycan, the mass number, 162, would be replaced by the molecular weight of the anhydro-residue which makes up the homoglycan. Chitin, which is a poly- *N*-acetylated glucosamine would have a mass number of 203. Similarly, for a linear heteroglycan composed of two different saccharide residues alternately linked, the mass spectrum should reflect this alternating sequence. Agarose which is composed of galactose ($C_6H_{10}O_5$, 162) and 3,6-anhydrogalactose ($C_6H_8O_4$, 144) alternating in the chain, would reflect the following formula in the mass spectrum

$$[(162)_n + (144)_p + 18 - (18)_m + Y + Z] \qquad p = n\text{-}1, n, n+1 \qquad (6)$$

where n and p are the number of galactose and 3,6-anhydrogalactose residues in the chain respectively, m is the degree of dehydration, Y is the mass of the ring fragment derived from galactose and Z is the mass of the ring fragment derived from 3,6-anhydrogalactose.

Applying the ring fragment data obtained from the high resolution positive- and negative-ion l.d.i.-F.t.-i.c.r. experiments performed on model underivatized oligosaccharides and the known primary and tertiary molecular structure of the commercial polysaccharides, plausible mechanisms and corresponding structures are proposed for the reactants and products of fourteen of the sixteen ion series observed by Coates and Wilkins. These fourteen proposed structures/reactions are for the most frequently occurring high intensity peaks. In order to minimize confusion between the classical Kochetkov and Chizhov[117] **A** to **K** ion series on permethylated glycosides and the Coates-Wilkins series, in this thesis these latter new ion series are labelled from **L** onwards.

Following Kochetkov's convention, we label glycosidic bond cleavage of the saccharide chain the **L**-type fragmentation. Each ion in the Coates-Wilkins B (X = 18) series fits formula (3) and corresponds to the $\mathbf{L}^0$ fragmentation route shown in Fig. IV.1. The superscript ^{0} denotes no loss of a water molecule from the oligosaccharide (superscript ^{1}, ^{2} or ^{3} implies one, two or three unit of dehydration respectively). It should be noted that there are two ways in which the $\mathbf{L}^0$ cleavage can take place. One way places the ion charge on the

oligosaccharide at the non-reducing end, and the other places the charge on the reducing end oligomer. For any polyhexose, these two fragmentation paths give products which cannot be distinguished from each other.

Therefore, in order to determine the reducing end of the sequence of any oligosaccharide either i) the oligosaccharide would have to be "labelled" by chemical means, or ii) the oligomers would have to contain at least two different classes of monosaccharides at different locations. Furthermore, there must also be an abundance of ring cleavages to distinguish the reducing and non-reducing end residues.

Carbohydrates are easily dehydrated in the mass spectrometer, and the $\mathbf{L^1}$, $\mathbf{L^2}$ and $\mathbf{L^3}$ fragmentations are derived from the $\mathbf{L^0}$ fragmentations by successive loss of water molecules. $\mathbf{L^1}$, $\mathbf{L^2}$ and $\mathbf{L^3}$ fragmentations give rise to Coates-Wilkins A (X = 0), Q (X = 144) and P (X = 126) series ions respectively, which fit formula (4).

Results reported in this thesis indicate that unsaturated two-carbon fragments are the most abundant ring fragments. The reaction pathways giving two-carbon ring fragments are designated as the **M**-type fragmentation. The positive-ion spectrum of *Klebsiella* K44 oligosaccharide showed two different fragment structures derived from this **M** fragmentation. Namely, a 2-substituted rhamnose attached to the reducing oligosaccharide gave an unsaturated $-C_2H_3O$ ring fragment, while non 2-substituted monosaccharides gave rise to an unsaturated $-C_2H_3O_2$ ring fragment. The fragmentation forming $-C_2H_3O$ is labeled the $\mathbf{M_1}$ reaction. This could be visualized by the loss of the glycosidic oxygen linked at position-2 of the saccharide (Fig. IV.21). Similarly, it stands to reason that for a $-C_2H_3O$ ring fragment attached to a non-reducing oligosaccharide, either position-3 or position-4 would be substituted (Fig. IV.22). The Coates-Wilkins E (X = 44) series ions could be formed via an $\mathbf{M_1}$ fragmentation. These E series ions were of low intensity and were only observed in white dextrin. White dextrin is derived from starch, a poly- 1,4- and 1,6-linked α-D-glucose, by acid/heat treatment. It is known that this treatment causes rearrangements, and the possibility of some 2-, 3- or 4-linked units in white dextrin is conceivable[200].

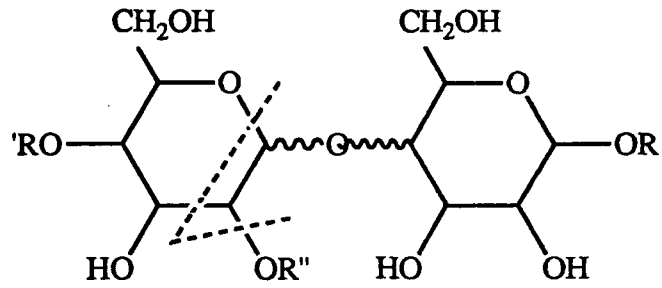

Fig.IV.20 Cleavage of a 2-substituted non-reducing residue to give a $-C_2H_3O$ fragment containing a C-1,C-2 centre.

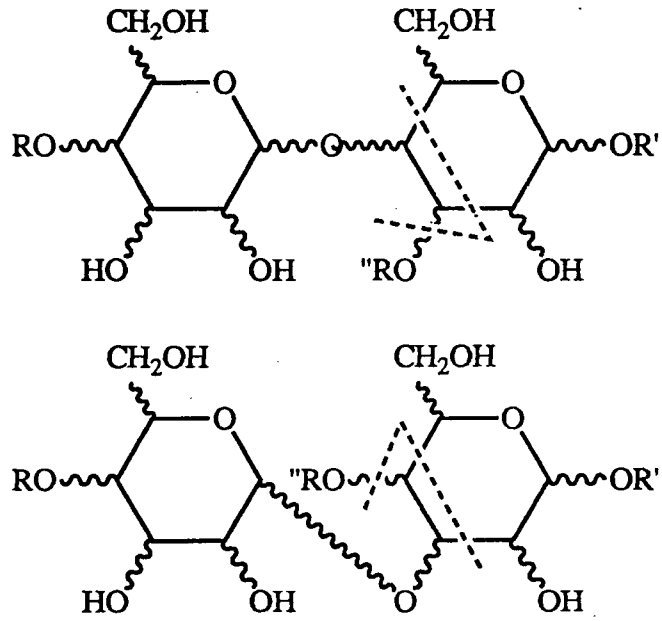

Fig.IV.22 Cleavage of a 3- and 4-substituted reducing residue to give $-C_2H_3O$ fragments containing the C-3,C-4 centre.

For glycosides that are not 2-linked, the formula for an unsaturated fragment from ring cleavage is $-C_2H_3O_2$ (Fig. IV.2). This ring cleavage is termed the $\mathbf{M_2}$ reaction. The $\mathbf{M_2^0}$ fragmentation gives rise to the Coates-Wilkins F (X = 60) series ions. Successive loss of water molecules from the $\mathbf{M_2^0}$ fragmentation products gives the $\mathbf{M_2^1}$ and the $\mathbf{M_2^2}$ products which correspond to Coates-Wilkins D series (X= 42) and C series (X = 24) ions respectively.

The Coates-Wilkins G series (X = 74) was observed only in cellulose (poly- 1,4-linked β-D-glucose) and chitin (poly- 1,4-linked β-D-*N*-acetyl glucosamine) spectra. This 74 mass unit represents a three-carbon fragment with one unit of unsaturation. As Coates pointed

out, the fact that this mass unit did not shift in the chitin spectrum suggested that C-2 was not present in the fragment. A probable structure of this three-carbon fragment is $-C_3H_5O_2$, containing the C-4,C-5,C-6 centre. This ring cleavage reaction is termed the $\mathbf{P_1}$-reaction. A possible reaction pathway is illustrated in Fig. IV.23.

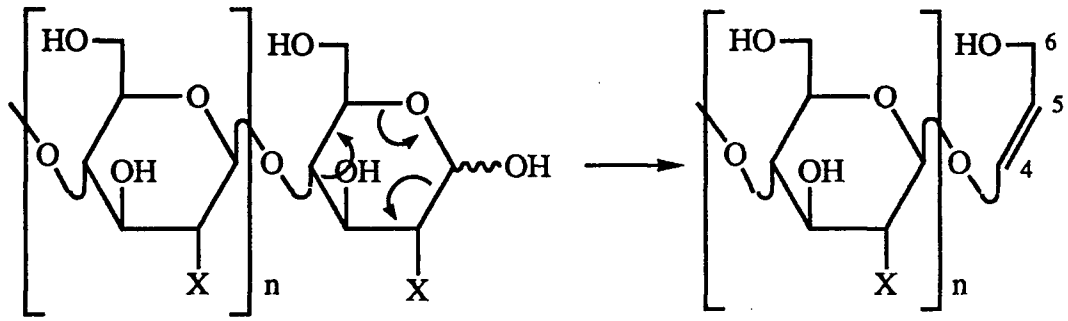

Fig.IV.23 Proposed reaction pathway for cellulose and chitin to give $-C_3H_5O_2$ ring fragment containing a C-4,C-5,C-6 centre. The substituent X on C-2 can be a hydroxy (cellulose) or an acetamido (chitin) group.

The Coates-Wilkins K series (X = 90, average intensity 8%) was observed only in dextran (poly- 1,6-linked α-D-glucose) spectra. This 90 mass unit could represent a $-C_3H_5O_3$ ring fragment containing either a C-1,C-2,C-3 or a C-4,C-5,C-6,O-hemiacetal centre. As suggested by Heresch[194] in his repetitive laser experiments on sucrose, the fragmentation could have occurred in the solid. Dextran being a highly polymerized carbohydrate material, would have fragmentation occurring more readily in the solid rather than in the gas phase, thus giving a $-C_3H_5O_3$ ring fragment containing a C-4,C-5,C-6,O-hemiacetal centre, linked to the non-reducing oligosaccharides. This ring cleavage is termed the $\mathbf{P_2}$-reaction. A possible pathway is illustrated in Fig. IV.24.

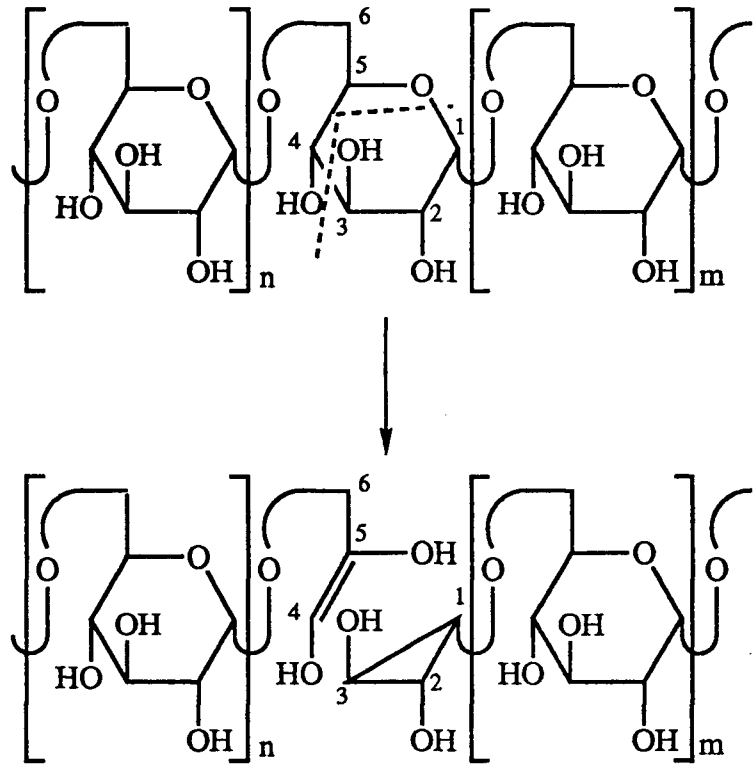

Fig.IV.24 Proposed reaction pathway for dextran (poly- α- 1,6-linked glucose) to give $-C_3H_5O_3$ ring fragments containing either a C-1,C-2,C-3 or a C-4,C-5,C-6,O-hemiacetal centre.

The Coates-Wilkins J series (X = 88, average intensity 8%) was observed only in the starch (poly- 1,4-linked α-D-glucose) spectrum. This 88 mass unit could represent two two-carbon ring fragments attached to the oligosaccharides. With the following assumptions that: i) ring cleavages of α-anomers give $-C_2H_3O$ fragments and residues linked to α-anomers give $-C_2H_5O_2$ fragments (negative-ion data on *Klebsiella* K44 oligosaccharide); and ii) fragmentation occurs before ionization, this 88 mass unit could be interpreted as "whole oligosaccharide" structures associated with a $-C_2H_3O$ ($\mathbf{M_1}$ reactions) fragment attached to the non-reducing end residue (derived from cleavages of a α-glucose unit) and a $-C_2H_5O_2$ ($\mathbf{M_3}$ reactions) fragment attached to the reducing end residue (derived from cleavages of a glucose residue linked to α-glucose residue) ring fragments. A possible pathway giving two ring fragments is illustrated in Fig. IV.25.

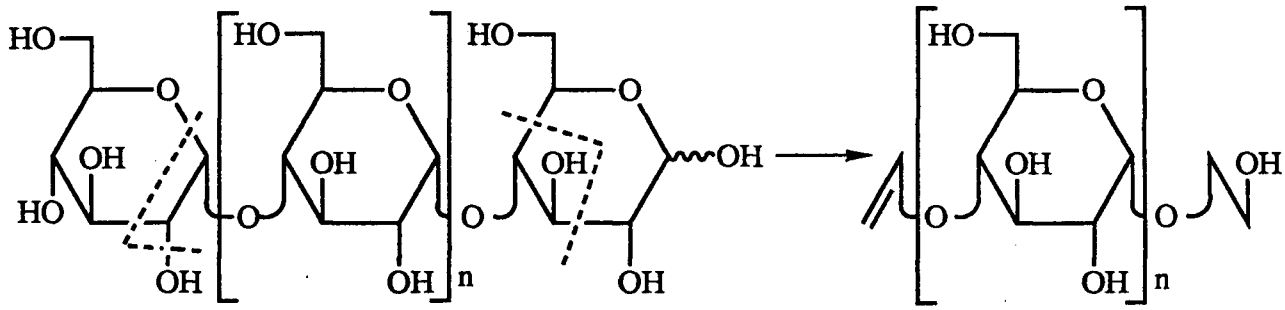

Fig.IV.25 Double ring cleavages of starch (poly- 1,4-linked α-D-glucose) to give a $-C_2H_3O$ (derived from cleavages of α-glucose residue) and a $-C_2H_5O_2$ (derived from cleavages of glucose unit linked to α-glucose residue) ring fragments.

The Coates-Wilkins L series (X = 102) was observed in the spectra of white dextrin (average intensity 5%), cellulose (average intensity 5%) and xanthan gum (average intensity 14%). Xanthan gum could be considered as cellulose, substituted on alternating glucose units by a trisaccharide composed of two mannose residues, one glucuronic acid residue, one *O*-acetate and one pyruvic acid acetal[201]. This 102 mass unit could represent a four-carbon ring fragment with two units of unsaturation, or two two-carbon ring fragments at both ends. Assuming that: i) ring cleavages of both β-anomers and residues linked to β-anomers give $-C_2H_3O_2$ fragments (negative-ion data on *Klebsiella* K44 oligosaccharide); ii) fragmentation occurs before ionization; and iii) xanthan gum gives a cellulose backbone after the initially loss of the side chain, this 102 mass unit could be interpreted to give two $-C_2H_3O_2$ ring fragments derived from cleavages of β-glucose and glucose residues linked to β-glucose (M_2 reactions). A possible pathway is illustrated in Fig. IV.26. This simplistic "β-anomers" argument could not be applied to white dextrin, whose exact structure is not known, as extensive rearrangement could have occurred during its formation by acid treatment of starch.

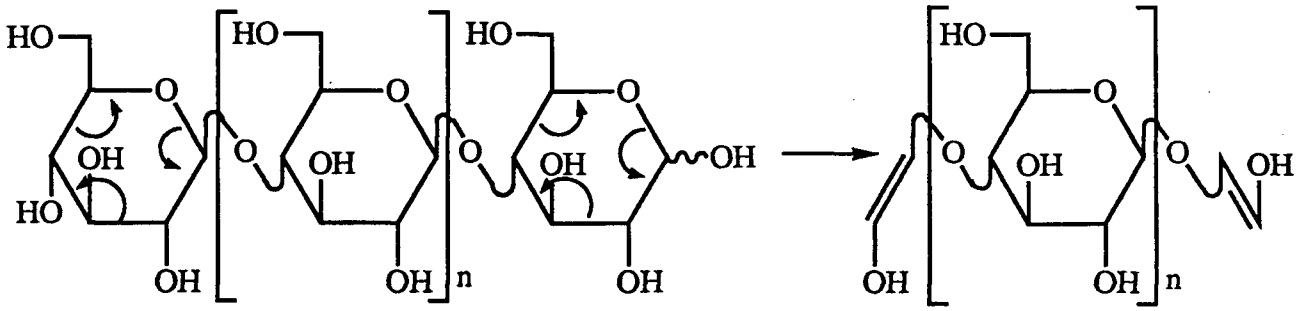

Fig.IV.26 Double ring cleavages of cellulose (poly- 1,4-linked β-D-glucose) to give two $-C_2H_3O_2$ ring fragments derived from cleavages of β-glucose and glucose linked to β-glucose.

The Coates-Wilkins M series (X = 104, average intensity 24%) was observed only in the starch (poly- 1,4-linked α-D-glucose) spectrum. This 104 mass unit could be interpreted as a $-C_4H_7O_3$ ring fragments containing a C-3,C-4,C-5,C-6 centre (Fig. IV.4). This ring cleavage reaction is termed the $\mathbf{N_2}$ fragmentation.

The Coates-Wilkins N series (X = 120, average intensity 4%) was observed only in the white dextrin spectrum. This 120 mass unit could be interpreted as a $-C_4H_7O_4$ ring fragment (as illustrated in Fig. IV.9). This ring cleavage reaction is termed the $\mathbf{N_3}$ fragmentation.

No structures could be proposed for the other two Coates-Wilkins series: H (X = 84) and R (X = 148). A summary of the proposed interpretation of Coates-Wilkins l.d.i.-F.t.-i.c.r. mass spectral data is listed in Table. IV.10.

It should be noted that while a particular ion formula in the Coates-Wilkins scheme allows its formation to be assigned to a specific reaction type, it is understood that the last reaction forming the ion does not necessarily have to be of that type. For example, consider an ion in the Coates-Wilkins C series. As argued above, the formation of this ion can be assigned to a reaction of the $\mathbf{M_2^2}$ type in which the ion is formed by a type $\mathbf{M_2}$ cleavage with additional loss of two water molecules. The last reaction forming this ion could have been a type $\mathbf{M_2^2}$ fragmentation, or it could have been a type $\mathbf{L^1}$ fragmentation preceded by a type $\mathbf{M_2^1}$ fragmentation. Similarly, an ion in the Coates-Wilkins P series (X = 126) could have been formed by a $\mathbf{L^3}$ reaction or three successive $\mathbf{L^1}$ reactions. Usually, several combinations of reactions can be written to account for the formation of any particular fragment ion.

M.s.-m.s. or other experiments, which delineate fragmentation pathways, will be needed to ascertain the precise sequence of reactions leading to each of the observed fragment ions.

TABLE IV.10

PROPOSED STRUCTURES AND LABELS, FOLLOWING KOCHETKOV'S CONVENTION

Proposed label following Kochetkov's convention	*Coates-Wilkins series*	*Mass of the sub-monosaccharide fragment, X*	*Structure of the ring fragments*	*Polysaccharide in which the ring fragment is prominant*	*For proposed fragmentation reaction and structure see Fig.*
L^1	A	0	Glycosidic bond cleavage	All polysaccharides	IV.1
L^0	B	18	Glycosidic bond cleavage	All polysaccharides	IV.1
M_2^2	C	24	R~$C_2H_3O_2$	Xanthan gum (10%)	IV.2
M_2^1	D	42	R~$C_2H_3O_2$	All polysaccharides	IV.2
M_1^0	E	44	R~C_2H_3O	White dextrin (5%)	IV.22
M_2^0	F	60	R~$C_2H_3O_2$	All polysaccharides	IV.2
P_1^0	G	74	R-$C_3H_5O_2$	Cellulose (3%) Chitin (10%)	IV 23
	H	84	?	Xanthan gum (7%)	
M_1^0,M_3^0	J	88	OH_3C_2-R-$C_2H_5O_2$	Starch (8%)	IV.25
P_2^0	K	90	R~$C_3H_5O_3$	Dextran (8%)	IV.3 ,IV.24
M_2^0,M_2^0	L	102	$O_2H_3C_2$-R-$C_2H_3O_2$	White dextrin (5%) Cellulose (5%) Xanthan gum (14%)	IV.26
N_2^0	M	104	R-$C_4H_7O_3$	Starch (24%)	IV.4
N_3^0	N	120	R~$C_4H_7O_4$	White dextrin (4%)	IV.9
L^3	P	126	Glycosidic bond cleavage	All polysaccharides	IV.1
L^2	Q	144	Glycosidic bond cleavage	All polysaccharides	IV.1
	R	148	?	Starch (11%)	

IV.3.10 NEGATIVE-ION L.D.I.-F.T.-I.C.R. SPECTRA OF *E. coli* K49 OLIGOSACCHARIDE OBTAINED BY ANHYDROUS HYDROGEN FLUORIDE HYDROLYSIS OF THE NATIVE CAPSULAR POLYSACCHARIDE

Anhydrous hydrogen fluoride degradation of capsular polysaccharides under sub-ambient temperatures (-40 to 0°C) is a selective chemical degradation method that cleaves predominantly only one specific type of linkage[38,202-205]. Therefore this method is analogous to bacteriophage degradation, which leads to the isolation of oligosaccharide repeating unit. Due to differences in the behavior of different linkages to different specific reagents, the CPS will cleave at different sites, thus generating different repeating oligosaccharides.

A number of specific degradation techniques were employed by Dr. L.M. Beynon in the structural characterization of the capsular polysaccharide from *E. coli* K49 bacteria. The particular oligosaccharide investigated in this Section was obtained by hydrolyzing *E. coli* K49 capsular polysaccharide with anhydrous hydrogen fluoride. The reaction was quenched by addition of methanol and the volatiles removed under nitrogen. The oligosaccharide thus obtained would have methyl esters of any free acidic groups (e.g., a hexuronic acid will give a methyl hexuronate) and a methyl glycoside at the reducing end of the newly generated oligosaccharide derived from the non-reducing end (Fig. IV.27).

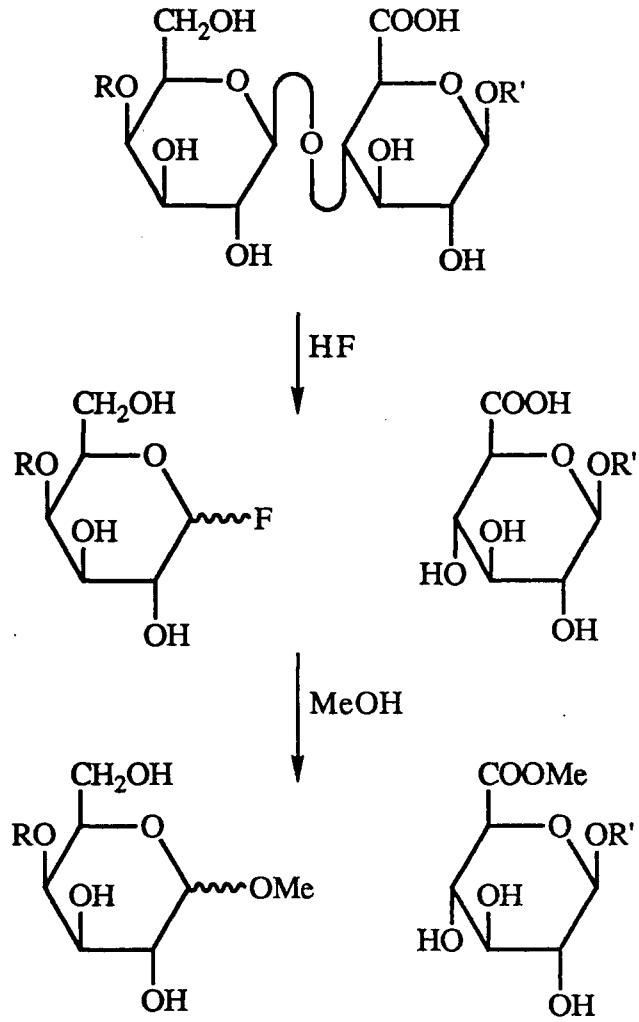

Fig.IV.27 Anhydrous hydrogen fluoride hydrolysis (methanol quenched) of a capsular polysaccharide to give a methyl glycoside and an oligosaccharide with a methyl hexuronate ester. Different hydrolytic conditions will give different oligosaccharides. In this diagram, the hydrolysis occurs between the galactose and glucuronic acid residues.

As discussed in Section II.1, all capsular polysaccharides are acidic, since they contain acidic sugar residues and/or acidic non-carbohydrate substituents. Although the most commonly found acidic sugars in CPS are hexuronic acid residues (HexA), some structures have been shown to contain either 2-keto-3-deoxy-manno-octulosonic acid (Kdo, $C_8H_{14}O_8$)[206-214] or *N*-acetylated neuraminic acid (NeuNAc, $C_{11}H_{19}O_9N$)[215-218]. A few CPS lack these acidic sugar residues, and their acidity is conferred by non-carbohydrate acidic substituents, such as pyruvic acid[219] or phosphates[220-225]. As most CPS are made up of simple sugars, the first approach in analyzing the mass spectra of *E. coli* K49 oligosaccharide

is to presume that the oligosaccharide repeating unit contains an acidic sugar residue, rather than an acidic non-carbohydrate substituent. The second approach is to assume that the oligosaccharide lacks any acidic monosaccharide residues but the acidity is conferred by phosphate groups. If however, both of these approaches do not give reasonable oligosaccharide structures, then, a pyruvic acid residue will be considered to be the sole acidic component. All these alternatives assume that the acidic component is present as the methyl ester. Therefore, the true molecular weight of the non esterified oligosaccharide would be at least 28 mass units lower than the pseudo-molecular ion (loss of CH_2 from the C-1 of the methyl glycoside and the other CH_2 from the methyl ester of the acidic component).

The negative-ion spectrum of *E. coli* K49 oligosaccharide (Spec. IV.23 and IV.24) showed a number of both even and odd mass peaks in the low mass region and a number of odd masses in the high mass region, suggesting that the oligosaccharide contains two nitrogen atoms[183]. One of the nitrogen atoms could be accounted for by an acetamido hexose adjacent to a hexose residue (m/z 364.123). However, none of the other peaks were easily identified. The high mass ions at m/z 835.280, 821.268 and 791.246 could be deprotonated pseudo-molecular ions. The ion at m/z 835 was assumed to be the deprotonated molecular ion, suggesting that the true molecular weight of the non-esterified oligosaccharide is 808 (836-28) amu. With these assumptions, the fragment ion m/z 821 was derived from m/z 835 by loss of a CH_2 group from either the C-1 of the reducing methyl glycoside or the methyl ester of the acidic component. Similarly, the fragment ion m/z 791 was derived from m/z 835 by loss of a molecule of carbon dioxide, suggesting that the oligosaccharide contains a carboxylic acid group. This carboxylic group is likely to be derived from C-6 of an acidic monosaccharide residue, implying that these groups are present rather than an acidic non-carbohydrate substituent, such as phosphate. However, methanol treatment would not leave any free carboxylic acid group in the oligosaccharide. Therefore, loss of a molecule of carbon dioxide from the oligosaccharide implies that either i) the ion m/z 835 is not the true deprotonated molecular ion, or ii) the analyte was not pure and contained more than one oligosaccharide.

Loss of a hexose residue from the ion m/z 835 will give a fragment ion at m/z 673.247, while loss of a hexose and a CH_2 unit will give a fragment ion at m/z 659.200. The existence of these two fragments showed that the non-reducing sugar is a hexose residue and that it does not carry any non-carbohydrate substituents. Similarly, loss of a hexose residue from the fragment ion m/z 791 will give m/z 629.214. It is interesting to note that all these six high mass ions (m/z 835, 821, 791, 673, 659 and 629) could be closely correlated with each other. This suggests that if the analyte were not pure, the different oligosaccharides must have similar structures.

As a result, the following assumptions were made in order to analyze the spectra: i) the oligosaccharide contains at least one hexose linked to an acetamido hexose; ii) the non-reducing end sugar is a hexose residue; iii) any non-carbohydrate substituents present are not linked to the non-reducing end hexose; iv) the oligosaccharide contains two nitrogen atoms; v) the oligosaccharide consists of mostly common 'neutral' monosaccharide residues (hexose, deoxyhexose and pentose); vi) the oligosaccharide contains one acidic monosaccharide residue (HexA, Kdo, NeuNAc); vii) the oligosaccharide contains two ~OMe groups attached to the C-1 of the reducing residue and to the carboxylate group of the acidic sugar; viii) the possible true molecular weight of one of the non-esterified oligosaccharides is 808 amu; ix) in addition to the one hexose and one acetamido hexose, the other component in the oligosaccharide must have one nitrogen atom. However, no assumptions were made as to whether the oligosaccharide was linear or branched.

An oligosaccharide with a molecular weight of 808 amu is likely to be a tetra- or penta-saccharide structure, consisting of one acidic sugar, one hexose, one acetamido hexose and one or two unknown components. The molecular weight of the anhydro disaccharide (*Hex,HexNAc*) is 365, and therefore, the molecular weight of the unknown components is 443 (808-365) amu. The oligosaccharide could be represented by the following structure:

Hex + HexNAc + X + Y + Z

where X is the acidic monosaccharide residue, and Y and Z are the other components

This 443 amu unit must contain an acidic monosaccharide residue, e.g., HexA, Kdo or NeuNAc. The molecular weight of an anhydro NeuNAc residue is 291 amu, which means that the fourth component has a molecular weight of 152 (443-291) amu. As NeuNAc contains one nitrogen atom, this 152 amu component would not contain any nitrogen. No common monosaccharide has a molecular weight of 152. Therefore, it seems unlikely that the analyte contains a NeuNAc residue.

Similarly, the molecular weight of an anhydro Kdo residue is 220 amu, which implies that the other component has a molecular weight of 223 (443-220) amu. As Kdo contains no nitrogen atom, this 223 amu component must contain one nitrogen atom. No known acetamido sugars have a molecular weight of 223 amu. The three most common 'normal' sugars are hexose, deoxyhexose and pentose. The molecular weights of their anhydro residues are 162 amu, 146 amu and 132 amu respectively. Therefore, the possible molecular weights of the nitrogen-containing components are 61 (223-162) amu, 77 (223-146) amu or 91 (223-132) amu respectively. If the bacteria incorporate any non-carbohydrate substituents into their capsular polysaccharide, then the substituent should be readily available from the food source. Amino acids, being the most readily available nitrogen compounds are the most likely non-carbohydrate substituents containing nitrogen. Furthermore, *E. coli* capsular polysaccharides have been shown to contain amino acids[226-228]. No naturally occurring amino acids have molecular weight of 61, 77, or 91 amu. Therefore, it is unlikely that the analyte contains a Kdo residue.

The molecular weight of an anhydro HexA residue is 176 amu, which means that the molecular weight of the nitrogen-containing component is 267 (443-176) amu. No known acetamido sugars have this mass. The three most common 'normal' sugars are hexose (162 amu), deoxyhexose (146 amu) and pentose (132 amu). Therefore, the possible molecular weights of the nitrogen-containing components are 105 (267-162) amu, 121 (267-146) amu or 135 (267-132) amu respectively. No naturally occurring amino acids have a molecular weight of 135 amu. However, 105 amu is characteristic of the hydroxyamino acid serine,

$H_2NCH(CH_2OH)COOH$; while 121 amu suggests the presence of the thioamino acid cysteine, $H_2NCH(CH_2SH)COOH$.

The above analysis gives two possible structures for the oligosaccharide. One structure is (*2Hex,HexA,HexNAc,2OMe*) substituted with serine ($C_{31}H_{52}O_{24}N_2$, 836.2911 amu) and the other is (*Hex,deoxyHex,HexA,HexNAc,2OMe*) substituted with cysteine ($C_{31}H_{52}O_{22}N_2S$, 836.2733 amu). None of the known *E. coli* capsular polysaccharides have been shown to contain cysteine residues However, some have been found to contain serine, and some of these CPS containing serine also showed partial incorporation of threonine, $H_2NCH(CH_3CHOH)COOH$[207-208]. This partial incorporation of both serine and threonine residues would explain the inconsistency observed in the higher mass peaks (m/z 791 and 629), as the fragment ions containing the different amino acid residues would be fourteen mass units apart. However, the tetrasaccharide substituted with cysteine cannot explain the high mass inconsistency, and is unlikely to be the true structure of the analyte, and thus is discounted.

There are five linear, nine 3+1 branched and two 2+1+1 branched carbohydrate structures possible for this 'serinated' tetrasaccharide:

Hex → HexNAc → HexA → Hex ~ OMe

Hex → HexNAc → Hex → HexA ~ OMe

Hex → HexA → HexNAc → Hex ~ OMe

Hex → HexA → Hex → HexNAc ~ OMe

Hex → Hex → HexNAc → HexA ~ OMe

HexNAc → Hex (Hex) → HexA ~ OMe

HexNAc → Hex → HexA (Hex) ~ OMe

Hex → HexNAc (Hex) → HexA ~ OMe

Hex → HexNAc → HexA (Hex) ~ OMe

Hex → HexA → HexNAc (Hex) ~ OMe

HexA → HexNAc (Hex) → Hex ~ OMe

HexA → HexNAc → Hex (Hex) ~ OMe

HexA → Hex (Hex) → HexNAc ~ OMe

HexA → Hex → HexNAc (Hex) ~ OMe

Hex → HexNAc (HexA) (Hex) ~ OMe

HexNAc → Hex (HexA) (Hex) ~ OMe

All structures would have a 'free' hexose residue located at the non-reducing end. The serine (Ser) or threonine (Thr) residue could be located on any of the HexNAc or HexA or the non-reducing end Hex residues. However, there were no masses that could be assigned to serine or threonine linked to either HexNAc or Hex or HexA. Furthermore, there is no indication of how the amino acid residues are linked to the carbohydrate backbone. The amino acid could be linked *via* an amide bond through the N-terminal to the hexuronic acid, or an ester bond through the hydroxyl group to the hexuronic acid or through the C-terminal to any hexose residues (Fig. IV.28).

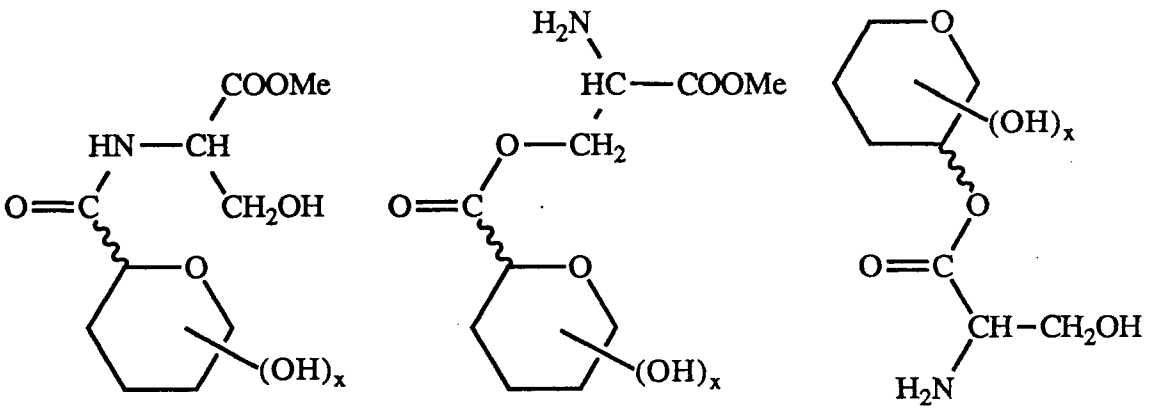

Amide bond through the N-terminal to the hexuronic acid

Ester bond through the hydroxyl group to the hexuronic acid

Ester bond through the C-terminal to C-2 of an hexose

Fig.IV.28 The serine residue could be linked to the carbohydrate backbone through any of the above linkages. The ester bond through the C-terminal was arbitrarily drawn at the C-2 of an hexose. None of the hydroxyl groups on the hexose ring are shown, due to the unknown positions of linkage. The carbomethoxy group in the first two structure arises from the methanolic work-up.

If one considers that the major amino acid substituent is serine, then the oligosaccharide, after glycosidic bond cleavages at all possible locations, would give the

following disaccharide fragment structures: (*HexNAc,Hex*); (*HexNAc,Hex,Ser*); (*HexNAc,Hex,OMe*); (*HexNAc,Hex,OMe,Ser*); (*HexNAc,HexA*); (*HexNAc,HexA,Ser*); (*HexNAc,HexA,OMe*); (*HexNAc,HexA,OMe,Ser*); (*HexNAc,HexA,2OMe,Ser*); (*Hex,HexA*); (*Hex,HexA,Ser*); (*Hex,HexA,OMe*); (*Hex,HexA,OMe,Ser*); (*Hex,HexA,2OMe,Ser*); (*2Hex*); (*2Hex,Ser*); and (*2Hex,Ser,OMe*). The fragment ions m/z 470.1435 and 456.1299 could be assigned to (*Hex,HexA,2OMe,Ser*) and (*Hex,HexA,OMe,Ser*) respectively. Dehydration of these ions gives fragments m/z 452.131 and 438.116. Moreover, the fragment ions m/z 369.107 could be assigned to (*Hex,HexA,OMe*), while simultaneous dehydration at two sites could give fragment ion m/z 333.078.

On the other hand, the fragment ion m/z 424.134 could be assigned to two different structures: [(*2Hex,Ser,OMe*)-H_2O-H]$^-$ or [(*Hex,HexNAc*)+$C_2H_3O_2$-H]$^-$. The ion series m/z 470, 456, 452, 438 and 369 strongly indicates that the serine residue is linked to the (*Hex,HexA*) disaccharide. Therefore, fragment ion m/z 424 is more likely to be [(*Hex,HexNAc*)+$C_2H_3O_2$-H]$^-$.

The ion series m/z 470 ,456, 452, 438, 369 and 333 suggests that the oligosaccharide has a serine residue linked to either a hexuronic acid and or a hexose at the reducing end. This effectively limits the oligosaccharide to the following six possible carbohydrate backbones:

Hex - HexNAc - HexA - Hex ~ OMe

Hex - HexNAc - Hex- HexA ~ OMe

HexNAc - Hex (Hex) - HexA ~ OMe

HexNAc - Hex - HexA (Hex) ~ OMe

Hex - HexNAc - HexA (Hex) ~ OMe

HexNAc - Hex (HexA) (Hex) ~ OMe

The three most prominent fragment ions (470.144 - 100%; 426.115 - 100%; 408.110 - 90%) in the spectra were all even masses, implying that they all contain one nitrogen atom. Most of the fragment ions observed in the spectrum could be explained by invoking either a

glycosidic bond or simple two-carbon ring cleavage argument. However, as the two very intense ions, m/z 426 and 408, could not be assigned by these simple fragmentations, they were assumed to be derived from more complex ring cleavages. Their nitrogens could be derived either from the amino sugar or the amino acid residue. The ion m/z 426.115 could be attributed to a deprotonated, deacetylated disaccharide (*HexA,HexNAc*) linked to a $-C_3H_5O_3$ ring fragment (Fig. IV.29). Dehydration of this ion would give the fragment m/z 408.110.

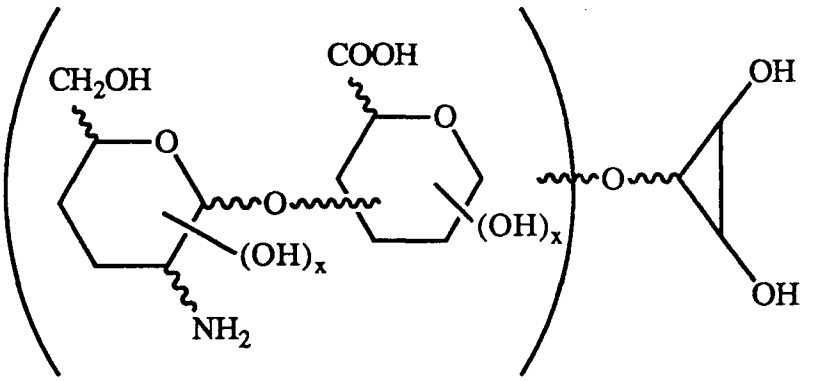

Fig.IV.29 Structure of fragment ion (*HexN,HexA*)~$C_3H_5O_3$. The hydroxyl groups of the monosaccharide residues are not shown. The -$C_3H_5O_3$ ring fragment could be attached to either the hexuronic acid or the amino hexose residues. Deprotonation of ion m/z 426.1146, and subsequent dehydration will give fragment m/z 408.1098.

From the mass spectra of all the model oligosaccharides in this thesis, no fragment ions were observed that have a ring-cleaved fragment linking two "whole" monosaccharide residues. Therefore, it is assumed that all ring fragments observed are associated with either the non-reducing or the reducing end. Hence, the two fragment ions m/z 425 and 408 suggest that the acetamido hexose is adjacent to the hexuronic acid residue. Therefore, the oligosaccharide backbone could only be the following linear and 3+1 branched structures:

Hex (1→?) HexNAc (1→?) HexA (1→?) Hex ~ OMe

Hex (1→?) HexNAc (1→?) HexA ~ OMe

?

|

1

Hex

All the fragment ions mentioned above can be fitted to a tetrasaccharide containing either serine or threonine residues, which suggests that there are a mixture of two oligosaccharides in the sample, one with a serine substituent and the other substituted with a threonine. The very slight differences in the oligosaccharide structures will make their complete separation and isolation of both components difficult. However, from the mass spectra there is no direct evidence to locate the exact position of the amino acid.

Nevertheless, there is some indirect evidence that points to the location and the linkage of the amino acid. i) It is postulated above that the amino acids are linked to either the hexuronic acid or the hexose residue. As discussed before, there are only three different ways that the amino acid could be linked (Fig. IV.26). If the amino acid is linked *via* the C-terminal to any hydroxyl group, then the 'free' C-6 of the uronic acid would be esterified during the work-up procedure, and the disaccharide fragment (*Hex,HexA,2OMe*) should be observed. No ions could be assigned to that structure. This may imply that the amino acid is linked to C-6 of the uronic acid, and loss of the esterifed amino acid would give fragment ion m/z 369 and 333, (*Hex,HexA,OMe*).

ii) The fragment ion m/z 791 was assigned to the deprotonated, decarboxylated structure (*2Hex,HexA,HexNAc,Thr,OMe*). This fragment could in theory be assigned to the deprotonated, decarboxylated structure (*2Hex,HexA,HexNAc,Ser,2OMe*). However, due to the work-up procedure, this assignment would imply that there were three sites of esterification (C-1 of the reducing monosacharide, C-6 of the hexuronic acid and the C-terminal of the amino acid) and the amino acids were linked *via* the N-terminal to a hydroxyl group of the oligosaccharide, which is unlikely. Therefore, the structure of the fragment ion m/z 791 could only be a tetrasaccharide substituted with a threonine residue. This suggests that the amino acid is linked to C-6 of the uronic acid, and loss of a $C_2H_2O_2$ unit from the esterified C-terminal of the 'threoninated' pseudo-molecular ion would give fragment ion m/z 791. Further loss of a hexose residue would give fragment ion m/z 629.

Therefore, the indirect evidence suggests that the amino acids are linked (either *via* the N-terminal or the hydroxyl group) to C-6 of the hexuronic acid.

The negative-ion l.d.i.-F.t.-i.c.r. fragment ions of the proposed tetrasaccharide structures substituted with serine and threonine residue are listed in Table IV.11. There are two ions (m/z 528.095 and 484.060) that could not be assigned exact structures, however, their masses suggest that both are chloridated fragments containing one nitrogen atom.

Table IV.11

NEGATIVE-ION LDI-FT-ICR FRAGMENT STRUCTURES OF *E. coli* K49 OLIGOSACCHARIDE OBTAINED BY ANHYDROUS HYDROGEN FLUORIDE HYDROLYSIS OF THE NATIVE CAPSULAR POLYSACCHARIDE (METHANOL QUENCHED)

Observed mass amu	*Calculated mass amu*	*Relative intensity %*	*Mass error ppm*	*Proposed structure*
835.280	835.284	34	-0.7	[(2Hex,HexA,HexNAc,Ser,2OMe)-H]$^-$
			or	[(2Hex,HexA,HexNAc,Thr,OMe)-H]$^-$
821.268	821.268	10	0.0	[(2Hex,HexA,HexNAc,Ser,OMe)-H]$^-$
			or	[(2Hex,HexA,HexNAc,Thr)-H]$^-$
791.246	791.294	40	60.8	[(2Hex,HexA,HexNAc,Thr,OMe)-CO_2-H]$^-$
673.247	673.231	30	24.4	[(Hex,HexA,HexNAc,Ser,2OMe)-H]$^-$
			or	[(Hex,HexA,HexNAc,Thr,OMe)-H]$^-$
659.200	659.215	16	-23.1	[(Hex,HexA,HexNAc,Ser,OMe)-H]$^-$
			or	[(Hex,HexA,HexNAc,Thr)-H]$^-$
629.214	629.241	27	-42.9	[(Hex,HexA,HexNAc,Thr,OMe)-CO_2-H]$^-$
528.095		13		?
484.060		11		?
470.144	470.152	100	-17.2	[(Hex,HexA,Ser,2OMe)-H]$^-$
			or	[(Hex,HexA,Thr,OMe)-H]$^-$
460.107	460.123	15	-35.4	[(Hex,HexNAc)+$C_2H_3O_2$+Cl]$^-$
456.130	456.136	22	-13.2	[(Hex,HexA,Ser,OMe)-H]$^-$
			or	[(Hex,HexA,Thr)-H]$^-$
452.131	452.141	19	-21.5	[(Hex,HexA,Ser,2OMe)-H_20-H]$^-$
			or	[(Hex,HexA,Thr,OMe)-H_20-H]$^-$
438.116	438.125	10	-21.2	[(Hex,HexA,Ser,OMe)-H_20-H]$^-$
			or	[(Hex,HexA,Thr)-H_20-H]$^-$
426.115	426.125	100	-25.2	*[(HexA,HexNAc)+$C_3H_5O_3$-H]$^-$
424.134	424.146	13	-28.5	[(Hex,HexNAc)+$C_2H_3O_2$-H]$^-$
408.110	408.115	90	-12.2	*[(HexA,HexNAc)+$C_3H_5O_3$-H_20-H]$^-$
400.086	400.102	12	-39.9	[(Hex,HexNAc)-H_20+Cl]$^-$
369.107	369.104	16	8.5	[(Hex,HexA,OMe)-H]$^-$
364.123	364.125	15	-4.9	[(Hex,HexNAc)-H_20-H]$^-$
333.078	333.083	15	-14.8	[(Hex,HexA,OMe)-2H_20-H]$^-$

* Loss of a ketene from an amino sugar, -C_2H_2O

IV.3.11 POSITIVE-ION L.D.I.-F.T.-I.C.R. SPECTRA OF *E. coli* K49 OLIGOSACCHARIDE

The positive-ion l.d.i.-F.t.-i.c.r. spectral data (Spec. IV.25 and IV.26, Table IV.12) were in accordance with the proposed sequences obtained from the negative-ion spectra. The fragment ions m/z 510.115, 494.154 and 466.116 confirmed that the amino acid residue was located on either the hexuronic acid or the hexose. The fragment ions m/z 432.160 (Fig. IV.30) and 464.128 (Fig. IV.31) are consistent with an acetamido hexose linked to the reducing end (*HexA,Hex*) residues. However, there was no indication of the exact location of the amino acids.

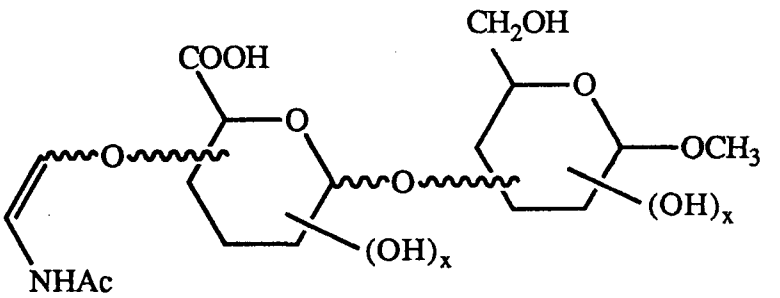

Fig.IV.30 Structure of fragment ion (Hex,HexA,OMe)+C_2H_3ONAc. Decarboxylation, and sodiation of this structure will give m/z 432.160. None of the hydroxyl groups on the hexose ring were drawn in, due to the unknown positions of linkage.

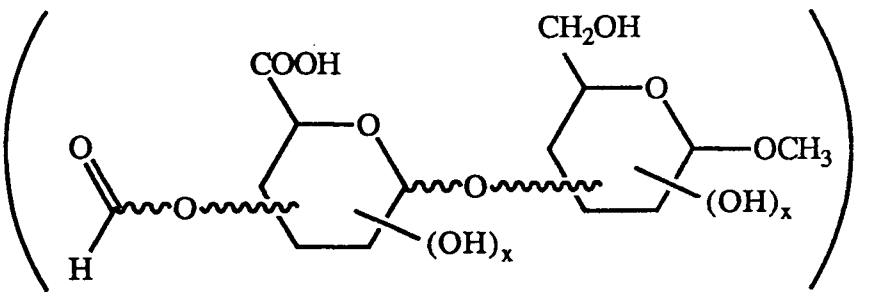

Fig.IV.31 Structure of fragment ion (Hex,HexA,OMe)+CHO_2. Addition of the threonine or serine+OMe residue, loss of two molecules of water, and subsequent sodiation will give m/z 464.128. None of the hydroxyl groups on the hexose ring were drawn in, due to the unknown positions of linkage.

Table IV.12

POSITIVE-ION LDI-FT-ICR FRAGMENT STRUCTURES OF *E. coli* K49 OLIGOSACCHARIDE OBTAINED BY ANHYDROUS HYDROGEN FLUORIDE HYDROLYSIS OF THE NATIVE CAPSULAR POLYSACCHARIDE (METHANOL QUENCHED)

Observed mass amu	*Calculated mass amu*	*Relative intensity %*	*Mass error ppm*	*Proposed structure*
845.024	845.265	18	-285.0	[(2Hex,HexA,HexNAc,Ser,OMe)+Na]$^+$
			or	[(2Hex,HexA,HexNAc,Thr)+Na]$^+$
829.267	829.212	11	65.8	[(2Hex,HexA,HexNAc,Ser)-H_2O+K]$^+$
813.224	813.239	16	-18.3	[(2Hex,HexA,HexNAc,Ser)-H_2O+Na]$^+$
510.115	510.122	15	-13.3	[(Hex,HexA,Ser,2OMe)+K]$^+$
			or	[(Hex,HexA,Thr,OMe)+K]$^+$
494.154	494.148	14	12.6	[(Hex,HexA,Ser,2OMe)+Na]$^+$
			or	[(Hex,HexA,Thr,OMe)+Na]$^+$
466.116	466.117	11	-1.7	[(Hex,HexA,Ser)+Na]$^+$
464.128	464.140	58	-25.0	[(Hex,HexA,Ser,2OMe)+CHO_2-2H_2O+Na]$^+$
			or	[(Hex,HexA,Thr,OMe)+CHO_2-2H_2O+Na]$^+$
448.150	448.143	43	15.5	[(Hex,HexNAc)+$C_2H_3O_2$+Na]$^+$
432.160	432.148	12	29.4	[(Hex,HexA,OMe)+C_2H_3ONAc-CO_2+Na]$^+$
422.113	422.106	17	16.3	[(Hex,HexNAc)+K]$^+$
406.130	406.132	15	-4.7	[(Hex,HexNAc)+Na]$^+$
404.082	404.095	40	-32.7	[(Hex,HexNAc)-H_2O+K]$^+$
388.121	388.122	100	-1.5	[(Hex,HexNAc)-H_2O+Na]$^+$
226.071	226.069	12	11.1	[(HexNAc)-H_2O+Na]$^+$
204.087	204.087	19	0.5	[(HexNAc)-H_2O+H]$^+$

In summary, the positive- and negative-ion spectra of *E. coli* K49 oligosaccharide suggests that the oligosaccharide is substituted with either a serine or a threonine residue. Some of the known *E. coli* capsular polysaccharides that are substituted with serine also partially incorporate threonine[206-207]. However, there was no indication of the relative abundance of the two substituted oligosaccharides. Although there were no fragments that could be used to locate the exact position of the amino acids, indirect evidence suggested that the linkage is via C-6 of the hexuronic acid. No positions of linkage could be identified from the spectra. Future m.s-m.s. experiments are planned to locate the exact positions of linkage for the oligosaccharide backbone and the positions of linkage of the amino acid substituent.

In conclusion, the negative- and positive-ion l.d.i.-F.t.-i.c.r. spectra of the sample suggest that there are two closely related oligosaccharides present. Both structures have the same tetrasaccharide backbone, and both are substituted at C-6 of the hexuronic acid with either a serine or a threonine residue. However, from the spectra it was not possible to distinguish whether the tetrasaccharide backbone is a linear or a 3+1 branched structures. The proposed structures of the oligosaccharides are therefore:

a)

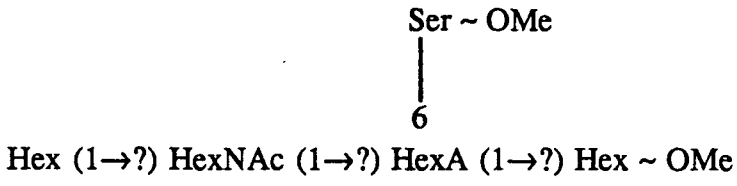

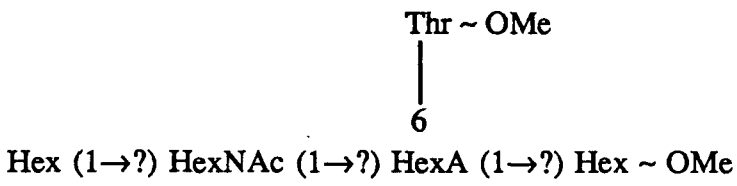

or

b)

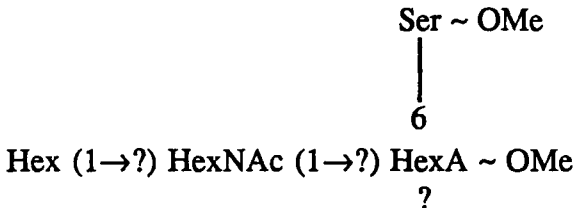

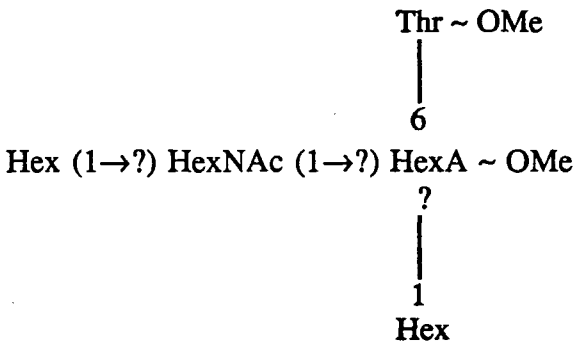

Although these negative- and positive-ion spectra would not distinguish whether this underivatized oligosaccharide was a linear or a 3+1 branched structure, a straight forward methylation analysis (Section II.3) would reveal the exact sequence of this tetrasaccharide backbone. A 3+1 branched structure would give two tetra-*O*-methylated hexitol acetates, while a linear structure would yield one tetra-*O*-methylated and one tri-*O*-methylated hexitol acetates.

Another approach to sequence this oligosaccharide is by permethylation. The series of permethylated oxonium ions for the proposed linear tetrasaccharide is m/z 219, 476, 694. Although the fragment ions m/z 219 and 476 would also be observed in the proposed 3+1 branched structure, m/z 694 would not be observed .

Subsequent to the development of the mass spectral analysis, the primary structure of this oligosaccharide was established independently by classical carbohydrate chemistry[208] and 2-D n.m.r. of the native capsular polysaccharide[209], and found to be a linear tetrasaccharide substituted with either threonine (75%) and serine (25%) through an amide bond to the C-6 of the glucuronic acid:

Glc (1→3) GalNAc (1→4) GlcA (NHCH(CH_2OH)COOMe) (1→6) Gal

Glc (1→3) GalNAc (1→4) GlcA (NHCH(CHOHCH_3)COOMe) (1→6) Gal

IV.4 GENERAL DISCUSSION

In the earlier Sections, it was proposed that for high molecular weight polysaccharides, fragmentation occurs principally in the solid or the solid-gas interface (selvedge), rather than in the gas phase, with ionization only arising before i.c.r. excitation and detection. This postulate implied that positive- and negative-ion mode laser desorption ionization of carbohydrates would give similar ring fragments. The ring fragments observed would therefore reflect the conformational integrity of the polysaccharide in the solid state. If this "macro-molecular" effect plays a major role in laser mass spectrometry, then the spectra of similar polysaccharides would have similar features. Furthermore, the ring fragments observed in negative-ion mass spectra can be used to interpret positive-ion mass spectra and *vice versa*. As illustrated in this thesis, most of the different types of ring-cleaved fragments are observed in both the positive- and negative-ion mass spectra, which support the proposed "fragmentation before ionization" model.

When a large number of oligosaccharides with different degrees of polymerization were observed in the mass spectra, they could have resulted from either sequential loss of one or more residues in the gas phase or selvedge, or the simultaneous desorption of a whole range of oligosaccharide fragments from the solid sample. If an oligosaccharide were to be "frozen" in a particular conformation in the solid, and fragmentation occurs in the selvedge, then the oligosaccharide spectrum would have similar features to that of the polysaccharide spectrum. However, once the oligosaccharides were desorbed into the gas phase, they would be energetic enough to take up different conformations. Consequently, some stereospecificity would be lost, and the spectra observed would reflect the most probable unimolecular or ion-molecule reactions in the gas phase.

This fragmentation model can explain the very similar spectra of the disaccharides, maltose and cellobiose. As both disaccharides are of low molecular weight, they can be easily be desorbed into the gas phase rather than fragmenting in the solid. Due to the similar structures of the disaccharides, they would have similar gas phase unimolecular and ion-molecule reactions, thereby giving identical mass spectra.

One possible way of encouraging low molecular weight oligosaccharides to fragment in the solid, would be to dope the sample with a large amount of alkali halide salt. The thermal energy absorbed by the oligosaccharide "trapped" in a alkali halide matrix could be dissipated either by vaporization followed by fragmentation in the gas phase or fragmentation in the solid or selvedge. Due to the biological nature of the sample, all the oligosaccharides investigated in this thesis contain a high abundance of attached alkali halide. Therefore, it is not possible to compare the spectra of a real "undoped" *vs* a heavily doped sample.

The Coates-Wilkins' mass spectral data on different polysaccharides (Table V.11) can be interpreted to strengthen the above "macro-molecular" model for laser mass spectrometry of polysaccharides. All the polysaccharides analyzed were of very high molecular weight. Therefore, if fragmentation occurred in the solid or selvedge, then the fragments observed from polysaccharides with different gross molecular structures would be different. This postulation also suggested that if two polysaccharides shared a similar tertiary structure, then their mass spectra would have a number of common features. Any differences observed in their spectra could have resulted from the differences at the "micro-molecular" level. Of the nine polysaccharide mass spectra obtained by Coates-Wilkins, several of them have a number of common gross molecular features. Their mass spectra are discussed below.

Cellulose is a polymer composed of 1,4-linked β-D-glucose in a straight chain. The gross molecular structure of cellulose is considered to be a number of long strand fibers running antiparallel to each other. Similarly, chitin is a fibrous polymer composed of 1,4-linked β-D-*N*-acetyl glucosamine. Therefore, the only difference in the "micro-molecular" structure is the difference in substitution at C-2 of the glucose residue. Both polysaccharides gave similar spectra, with the ion series A (X = 0), F (X = 60), G (X = 74), and Q (X = 144 or 185). The only ion series observed for cellulose but not for chitin, is the L-series (X = 102). This may reflect the subtle differences at the micro-molecular level. According to our interpretation, this L-series was derived from two ring fragments located at each end of the oligosaccharides. It may be that the acetamido substituent in chitin does not favor M_2-ring cleavage between the C-2, C-3 bond of the acetamido glucose.

Similarily, xanthan gum has a cellulose backbone, and should show fragmentation similar to cellulose. Both polysaccharides gave the ion series A (X = 0), F (X = 60), L (X = 102), and Q (X = 144). Although both spectra showed a number of similar features, there are some differences in their spectra, which may reflect the substitution pattern of xanthan gum. The differences in their spectra are: i) ion series C (X = 24) and P (X = 126) were observed for xanthan gum but not for cellulose; these two ion series correspond to two units of dehydration for glycosidic bond (P, X = 126) and ring cleavage between C-2 and C-3 (C, X = 24) reactions; ii) G (X = 74) was not observed for xanthan gum.

Starch is a poly- 1,4-linked α-D-glucose (with varying degree of branching by 1,6-linkage), while white dextrin is the acid/heat-treated lower molecular weight polymer of starch with a lower degree of branching. Except for glycosidic bond cleavages and M_2-reactions, the spectra obtained for starch and white dextrin are very different. Starch gave ion series of J (X = 88), M (X = 104) and R (X = 148); while white dextrin gave E (X = 44), L (X = 102) and N (X = 120). Both polysaccharides possess the same monosaccharide residues, position of linkage, anomeric configuration and α-helix structure. The differences in their mass spectra could be a reflection of the differences in the "macro-molecular" structure of the polysaccharide in the solid state; starch being more branched than white dextrin would have a "less ordered packing".

The same argument can also be used to account for the spectral differences observed for starch and cellulose. Starch gave ring fragments of ion series J (X = 88), M (X = 104) and R (X = 148); while cellulose gave G (X = 74) and L (X = 102). The differences in the mass spectra could have arisen from differences in the tertiary structure of the polysaccharides.

The proposed "macro-molecular" model requires that some glycosidic and ring cleavages occur in the solid state or at the solid-gas interface. The two main desorption techniques for depth profiling of solid materials are laser desorption and s.i.m.s. It is likely that the laser pulse removes the first layer of sample, causing pyrolysis, fragmentation and spontaneous desorption of the oligosaccharide. The energetic oligosaccharide could then

undergo further fragmentation in the gaseous phase, corresponding to losses of one or more monosaccharide residues, dehydration and further ring cleavages.

In the l.d.i.-F.t.-i.c.r. spectra, the same ring fragment structures are observed in both positive- and negative-ion mode. The only difference is that the carbohydrate structures are deprotonated in the negative-ion mode, and cationized by protonation or by alkali-ion attachment in the positive-ion spectra. If fragmentation occurs predominantly in the selvedge, then subsequent deprotonation or protonation will give the same structure in both the positive- and negative-ion spectra.

Although the application of l.d.i.-F.t.-i.c.r. to carbohydrates is relatively new compared to f.a.b or d.c.i., it has already shown a lot of potential. Although routine f.a.b. sequencing of both peptides and oligosaccharides is being carried out in most laboratories, it is still seen as backup or complementary techniques. This can be explained as follows:

i) High resolution f.a.b.-m.s.-m.s. are not routine experiments, and high resolution m.s.-m.s. is required to analyze a completely unknown sample. Often, by performing a limited amount of simple non-instrumental chemistry, some tentative composition data can be obtained. Therefore, most biological samples require only medium resolution m.s. analysis.

ii) Soft ionization techniques, such as f.a.b. and l.s.i.m.s., result in mainly glycosidic bond cleavages, thereby permitting only the sequencing of the sample. Consequently, some workers have attempted to use tandem m.s. to correlate these m.s.-m.s. data to additional structural features[118-121]. L.d.i.-F.t.-i.c.r. spectra are very rich, having both fragments derived from glycosidic bond and ring cleavages. We have shown that these ring fragments can be used for a tentative indication of positions of linkage and possibly a correlation to other stereochemical features. Further studies would have to be performed on a large number of model oligo- and poly-saccharides to ascertain the exact structures of the ring fragments proposed in this thesis.

From the five l.d.i.-F.t.-i.c.r. model oligosaccharide experiments described in this thesis. A few suggestions can be made with respect to the analysis of unknown oligosaccharides:

a) The first set of experiments (positive- and negative ion mode) should be performed on the underivatized material to obtain information on the component, as derivatization may cause loss of acid- or base-labile substituents. These experiments should also provide some tentative sequences and linkage information on most linear and some branched oligosaccharides.

b) The second set of experiments (positive- and negative ion mode) should be performed on the permethylated material to obtain complementary sequence information. This will provide: i) components information including base-stable substituents, and ii) sequencing from the non-reducing end.

c) The third set of experiments (positive- and negative ion mode) should be performed on the peracetylated or the pertrifluoroacetylated material to obtain complementary sequence information. This will provide: i) component information including acid-stable substituents, and ii) sequencing from the non-reducing end.

IV.5 CONCLUSION

In conclusion, the advantages of l.d.i.-F.t.-i.c.r. are as follows: i) underivatized oligosaccharides can be analyzed; ii) sequence information can be deduced from both the positive- and negative-ion spectra; iii) intense pseudo-molecular ions are obtained; iv) intense fragment ions from both glycosidic and ring cleavages are obtained; v) high resolution spectra can confirm the presence of unusual monosaccharides, such as deoxysugars, acetamido sugars, sialic acids and of labile substituents, such as *O*- & *N*-acetyls, pyruvic acid acetals and lactyls; vi) ring cleavage fragments may be used to distinguish alternative reducing-end structures; vii) ring cleavage fragments may also provide tentative information on the positions of linkage; viii) the characteristic fragmentation patterns seen in oligosaccharides can be used to analyze the characteristic fingerprint mass spectra of polysaccharides.

IV.6 FUTURE STUDIES

i) M.s.-m.s. studies of oligosaccharide fragments. Although l.d.i.-F.t.-i.c.r. provides abundant ring fragmentation, sometimes extensive ring cleavages can complicate the delineation of the oligosaccharide structures. Therefore, m.s.-m.s. studies may be useful to characterize some ambiguous oligosaccharide frements.

ii) Dopant *vs* fragment ion structures. For all our model oligosaccharides, addition of dopants (NaCl, NH_4Br and KBr) did not alter the structural features of the mass spectra in the positive-ion mode. With our sample preparation technique, the undoped oligosaccharides were analyzed first in both positive- and negative-ion modes, followed by addition of either NH_4Br or KBr and finally NaCl for re-examination if necessary. Although only pico-mole levels of samples were used for each laser shot, at the end of the experiments a substantial amount of the oligosaccharides had been used and a decrease in the intensity of the spectra was normally observed. Nevertheless, with the addition of halide ions, a slight increase in fragmentation was observed in the negative-ion spectra. Due to the complexity of these "halidated" spectra, they were not analyzed in detail. Exact mass measurement using the heterodyne mode should be performed on desalted as well as doped samples to determine the exact nature of the fragmentation, and the relationship between the degree of doping with increase in fragmentation.

iii) Laser intensity *vs* fragment ion structures of polysaccharides. It was noted by Coates during the experiments on polysaccharides that, except for overall intensity, the l.d.i.-F.t.-i.c.r. mass spectra did not change with laser power[171]. If fragmentation of the polysaccharides occurred in the selvedge, and the mass spectra reflect the macro-molecular structure in the solid state, then laser power should not substantially alter the fragmentation. Therefore, one aspect of further studies should concentrate on analyzing a series of homoglycans and simple linear heteroglycans to evaluate the different possible ring fragments observed under different laser power. The observed different ring fragments should be correlated with the primary and tertiary structure of the glycans to evaluate the proposed "macro-molecular" model for l.d.i.-F.t.-i.c.r. mass spectra.

iv) Laser intensity *vs* fragment ion structures of oligosaccharides. The mass spectra of oligosaccharides fragmenting in the gas-phase should be different from that of oligosaccharides undergoing pyrolysis and fragmentation in the solid state. If the oligosaccharides were desorbed into the gas-phase before fragmentation, then ion-molecule reactions would govern the fragmentation pathways. F.a.b.-m.s.-m.s. positive- and negative-ion spectra of monosaccharides have already shown different fragmentation patterns, and this is attributable to the different unimolecular and ion-molecule reactions occurring under the two different conditions[120]. In order to ascertain the site of fragmentation, a series of simple oligosaccharide repeating units derived from bacterial capsular polysaccharide (P1, P2, P3, P4, etc...) should be examined using different laser powers to determine the relationship between the degree of polymerization and the tendency for fragmentation to occur predominantly at the selvedge. Furthermore, m.s.-m.s. studies could be performed on the molecular and glycosidic bond cleaved ions to ascertain the exact nature of the fragmentation patterns of oligosaccharides in the gas phase.

v) The ring fragment structures of underivatized and permethylated oligosaccharides obtained by l.d.i.-F.t.-i.c.r. should be compared to the fragments obtained from f.a.b.-m.s.-m.s. studies.

CHAPTER V

BIBLIOGRAPHY

BIBLIOGRAPHY

1 G.O. Aspinall, in "*The Polysaccharides*" Vol. 2, 36-131, Ed. G.O. Aspinall, Academic Press, New York, 1983.

2 P.A. Sandford and J. Baird, in "*The Polysaccharides*". Vol. 2, 411-490, Ed. G.O. Aspinall, Academic Press, New York, 1983.

3 S. Hanessian, "*Total Synthesis of Natural Products: The 'Chiron' Approach*", Pergamon Press, New York, 1983.

4 "A Single Issue on AIDS" *Scientific America*, 259, 8 (1988).

5 C.T. Bishop and H.J. Jennings, in "*The Polysaccharides*" Vol. 2, 291-330, Ed. G.O. Aspinall, Academic Press, New York, 1982.

6 W.F. Dudman, in "*Surface Carbohydrates of the Prokaryotic Cell*" 357-414, Ed. I. Sutherland, Academic Press, London, 1977.

7 K. Jann and B Jann, *Prog. Allergy*, 33 (1983) 53-79.

8 H.J. Jenning, *Adv. Carbohydr. Chem. Biochem.*, 44 (1983) 155-208.

9 K. Jann and O. Westphal, in "*The Antigens*", Vol. 3., 1-125, Ed. M. Sela, Academic Press, New York, 1975.

10 M. Heidelberger and G.G.S. Dutton, *J. Immunol.*, 111 (1973) 857-859.

11 M. Heidelberger and W. Nimmich, *Immunochem.*, 13 (1976) 67-80.

12 Y.J. Lew and M. Heidelberger, *Carbohydr. Res.*, 52 (1976) 255-258.

13 M. Heidelberger, *Res. Immunochem. Immunobiol.*, 3 (1973) 1-40.

14 M. Heidelberger, *Trends Biochem. Sc.*, 7 (1982) 261-263.

15 R.L. Whistler, A.A. Bushway, P.P. Singh, I. Nakahara, and R. Tokuzen, *Adv. Carbohydr. Chem. Biochem.*, 32 (1976) 235-275.

16 J.R. Crook, W.K. Otto, and R.S. Jones, *Proc. Soc. Exp. Biol. Med.*, 109 (1962) 552-556.

17 K. Miyamoto, R. Koshiura, T. Hasegawe, and N. Kato, *Jpn. J. Pharmacol.*, 36 (1984) 51-57.

18 P.-E. Jannson, L. Kenne, H. Liedgren, B. Lindberg, and J. Lonngren, *Chem. Commun., Univ., Stockholm*, 8 (1976) 1-75.

19 J. Lönngren and S. Svensson, *Adv. Carbohydr. Chem. Biochem.*, 29 (1974) 84-106.

20 Z. Lam, M. Sc. Thesis, University of British Columbia, (1986).

21 O. Westphal and K. Jann, *Methods Carbohydr. Chem.*, 5 (1965) 83-91.

22 R.L. Whistler and J.L. Sannella, *Methods. Carbohydr. Chem.*, 5 (1965) 34-36.

23 T.J. Painter, *Methods Carbohydr. Chem.*, 5 (1965) 98-100.

24 G.O. Aspinal, J.A. Molloy, and J.W.T. Craig, *Can. J. Biochem.*, 47 (1969) 1063-1070.

25 J.E. Scott, *Methods Carbohydr. Chem.*, 5 (1965) 38-44.

26 K.A. Granath, *Methods Carbohydr. Chem.*, 5 (1965) 20-28.

27 Y.C. Yee and R. Montgomery, *Methods Carbohydr. Chem.*, 5 (1965) 28-34.

28 H. Neukon and W. Kuendig, *Methods Carbohydr. Chem.*, 5 (1965) 14-17.

29 I.J. Goldstein and C.E. Hayes, *Adv. Carbohydr. Chem. Biochem.*, 35 (1978) 127-340.

30 S. Narasimhan, J.R. Wilson, E. Martin, and H. Schachter, *Can. J. Biochem.*, 57 (1979) 83-96.

31 S.C. Churms, *Adv. Carbohydr. Chem. Biochem.*, 25 (1970) 13-51.

32 D.H. Northcote, *Methods Carbohydr. Chem.*, 5 (1965) 49-53.

33 M. Breen, H.G. Weinstein, L.J. Black, M.S. Borcherding, and R.A. Sittig, *Methods Carbohydr. Chem.*, 7 (1966) 101-115.

34 G.G.S. Dutton, *Adv. Carbohydr. Chem. Biochem.*, 28 (1973) 11-160.

35 P.J. Garegg and B. Lindberg, *Acta Chem. Scand.*, 14 (1960) 871-876.

36 P. Albersheim, D.J. Nevins, P.D. English, and A. Karr, *Carbohydr. Res.*, 5 (1967) 340-345.

37 C.G. Hellerqvist and A.A. Lindberg, *Carbohydr. Res.*, 16 (1971) 39-48.

38 A.J. Mort, and D.T.A. Lamport, *Anal. Biochem.*, 82 (1977) 289-309.

39 H.J. Jennings and C. Lugowski, *Can. J. Chem.*, 58 (1980) 2610-2612.

40 J.F. Codington, K.B. Linsley, and C. Silber, *Methods Carbohydr. Chem.*, 7 (1976) 226-232.

41 S. Inoue, G. Matsumura, and Y. Inoue, *Anal. Biochem.*, 125 (1982) 118-124.

42 G.G.S. Dutton and M.T. Yang, *Can. J. Chem.*, 51 (1973) 1826-1832.

43 Y.C. Lee and C.E. Ballou, *Biochem.*, 4 (1965) 257-264.

44 K. Macek, in "*Paper Chromatography*", Eds. I.M. Hais and K. Macek, Academic Press, New York, 1963.

45 K. Macek, in "*Chromatography*", 2nd Edit., Ed. E. Heftman, Reinhold Publishing Corporation, New York, 1967.

46 R.E. Wing and J.N. BeMiller, *Methods Carbohydr. Chem.*, 6 (1972) 42-64.

47 H. Weigel, *Adv. Carbohydr. Chem.*, 18 (1963) 61-97.

48 Z. Dische, *Methods Carbohydr. Chem.*, 1 (1962) 477-514.

49 D. Aminoff, W.W. Binkley, R. Schaffer, and R.W. Mowry, in "*The Carbohydrates*", 2nd Edit., Vol. 2B, 734-807, Eds. W. Pigman and D. Horton, Academic Press, New York, 1970.

50 G.G.S. Dutton, *Adv. Carbohydr. Chem. Biochem.*, 30 (1974) 9-110.

51 G.D. McGinnis and D. Fang, *Methods Carbohydr. Chem.*, 8 (1980) 33-43.

52 R.L. Taylor and H.E. Conrad, *Biochem.*, 11 (1972) 1383-1388.

53 J.K.N. Jones and M.B. Perry, *J. Am. Chem. Soc.*, 79 (1957) 2787-2793.

54 G.M. Bebault, J.M. Berry, Y.M. Choy, G.G.S. Dutton, N. Funnel, L.D. Hayward, and A.M. Stephen, *Can. J. Chem.*, 51 (1973) 324-326.

55 K. Leontin, B. Lindberg, and J. Lonngren, *Carbohydr. Res.*, 62 (1978) 359-362.

56 G.J. Gerwig, J.P. Kamerling, and J.F.G. Vliegenthart, *Carbohydr. Res.*, 77 (1979) 1-7.

57 J.H. Pazur, *Methods Enzymol.*, 9 (1966) 82-87.

58 D. Amaral, F. Kelly-Falcoz, and B.L. Horecker, *Methods Enzymol.*, 9 (1966) 87-92.

59 Y.T. Li and S.C. Li, *Methods Carbohydr. Chem.*, 7 (1976) 221-225.

60 S.J. Angyal and K. James, *Aust. J. Chem.*, 23 (1970) 1209-1215.

61 S.I. Hakomori, *J. Biochem. (Tokyo)*, 55 (1964) 205-208.

62 J.I. Brauman, J.A. Bryson, D.C. Kahl, and N.J. Nelson, *J. Am. Chem. Soc.*, 92 (1970) 6679-6680.

63 L.R. Phillips and B.A. Fraser, *Carbohydr. Res.*, 90 (1981) 149-152.

64 A.B. Blakeney and B.A. Stone, *Carbohydr. Res.*, 140 (1985) 319-324.

65 I. Ciucanu and F. Kerek, *Carbohydr. Res.*, 131 (1984) 209-217.

66 P. Prehm, *Carbohydr. Res.*, 78 (1980) 372-374.

67 T. Purdie and J.C. Irvin, *J. Chem. Soc.*, 83 (1903) 1021-1037.

68 M. Barber, R.S. Bordoli, G.J. Elliott, R.D. Sedgwick, and A.N. Tyler, *Biomed.Mass Spectrom.*, 8 (1981) 492-495.

69 A. Dell and P.R. Tiller, *Biochem. Biophys. Res. Comm.*, 135 (1986) 1126-1134.

70 A.N. de Belder and B. Normann, *Carbohydr. Res.*, 8 (1968) 1-6.

71 B. Lindberg, J. Lönngren, and J.L. Thompson, *Carbohydr. Res.*, 28 (1973) 351-357.

72 G.O. Aspinall and K.-G. Rosell, *Carbohydr. Res.*, 57 (1977) c23-c26.

73 L. Malaprade, *Bull. Soc. Chim. Fr.*, 43 (1928) 683-696.

74 H. Geyer, K. Himmelspach, N. Kwiatkowski, S. Schlect, and S. Stirm, *Pure Appl. Chem.*, 55 (1983) 637-653.

75 B. Capon, *Chem. Rev.*, 69 (1969) 407-498.

76 L.M. Beynon and G.G.S. Dutton, *Carbohydr. Res.*, 179 (1988) 419-423.

77 A.V.S. Lim, Ph. D. Thesis, University of British Columbia, (1987).

78 J.M. Bobbitt, *Adv. Carbohydr. Chem.*, 11 (1956) 1-40.

79 R.D. Guthrie, *Adv. Carbohydr. Chem.*, 16 (1961) 105-157.

80 G.O. Aspinall and R.J. Ferrier, *Chem. Ind. (London)* (1957) 1216.

81 P. Fleury and J. Lange, *J. Pharm. Chim.*, 17 (1933) 107-113.

82 I.J. Goldstein, G.W. Hay, B.A. Lewis, and F. Smith, *Methods Carbohydr. Chem.*, 5 (1965) 361-370.

83 G.G.S. Dutton and K.B. Gibney, *Carbohydr. Res.*, 25 (1972) 99-105.

84 M. Adams, "*Bacteriophages*", Interscience Publishers Inc., New York, 1957.

85 J. Douglas, "*Bacteriophages*", Chapman and Hall, London, 1975.

86 C.K. Mattews, "*Bacteriophages Biochemistry*", Van Nostrand Reinhold Co., N.Y. 1971.

87 A.A. Lindberg, in "*Surface Carbohydates of the Prokaryotic Cell.*", Ed. I. Sutherland, Academic Press, London, 1977.

88 D. Rieger-Hug and S.Stirm, *Virology*, 113 (1981) 363-378.

89 G.G.S. Dutton, G.K. Eigendorf, Z. Lam, and A.V.S. Lim, *Biomed. Environ. Mass Spectrom.*, 15 (1988) 459-460.

90 B. Coxon, *Adv. Carbohydr. Chem.*, 19 (1964) 51-93.

91 L.D. Hall, *Adv. Carbohydr. Chem. Biochem.*, 27 (1972) 7-83.

92 K. Bock and C. Pedersen, *Adv. Carbohydr. Chem. Biochem.*, 41 (1983) 27-66.

93 K. Dill, E. Bereman, and A.A. Pavia, *Adv. Carbohydr. Chem. Biochem.*, 43 (1985) 2-49.

94 P.E. Pferrer, *J. Carbohydr. Chem.*, 3 (1984) 613-639.

95 C.M. Preston and L.D. Hall, *Carbohydr. Res.*, 37 (1974) 267-282.

96 K. Bock, *Pure and Appl. Chem.*, 55 (1983) 605-622.

97 F. Michon, J.B. Brisson, R.Roy, F.E. Ashton, and H.J. Jennings, *Biochem.*, 24 (1985) 5592-5598.

98 J. Dabrowski, H. Egge, and U. Dabrowski, *Carbohydr. Res.*, 114 (1983) 1-9.

99 D.R. Bundle, M. Gerken, and M.B. Perry, *Can. J. Chem.*, 64 (1986) 225-264.

100 P.J. Garegg, P.E. Jansson, B. Lindberg, F. Lindh, J. Lönngren, I. Kvarnström, and W. Nimmich, *Carbohydr. Res.*, 78 (1980) 127-132.

101 M. Karplus, *J. Chem. Phys.*, 30 (1959) 11-15.

102 L. Hough, J.K.N. Jones, and W. Wadman, *J. Chem. Soc.*, (1950) 1702-1706.

103 W.F. Lehnherdt and R.J. Winzler, *J. Chrmatogr.*, 34 (1968) 471-479.

104 C.C. Sweeley, R. Bentley, M. Makita, and W.W. Wells, *J. Am. Chem. Soc.*, 85 (1963) 2497-2507.

105 D.P. Sweet, R.H. Shapiro, and P. Albershiem, *Carbohydr. Res.*, 40 (1975) 217-225.

106 D.P. Sweet, P. Albershiem, and R.H. Shapiro, *Carbohydr. Res.*, 40 (1975) 199-216.

107 B. Fournet, G. Strecker, Y. Leroy, and J. Montreuil, *Anal. Biochem.*, 161 (1981) 489-502.

108 R. Geyer, H. Geyer, S. Kühnhardt, W. Mink, and S. Strim, *Anal. Biochem.*, 121 (1982) 263-274.

109 H. Yamada, H. Yiyohara, and Y. Otsuka, *Carbohydr. Res.*, 170 (1987) 181-191.

110 H. Karlson and G.C. Hansson, *Proc. XIVth Int. Carbohydr. Symp.*, (1988) 107.

111 H.D. Beckey, *Int. J. Mass Spectrom. Ion Phys.*, 2 (1969) 500-503.

112 R.J. Cotter, *Anal. Chem.*, 52 (1980) 1589A-1606A.

113 R.D. Macfarlane and D.F. Torgerson, *Science*, 191 (1976) 920-925.

114 D.A. McCrery, E.B. Ledford, Jr., and M.L. Gross, *Anal. Chem.*, 54 (1982) 1435-1437.

115 C.R. Blakely, J.J. Carmody, and M.L. Vestal, *J. Am. Chem. Soc.*, 102 (1980) 5931-5933.

116 W. Aberth, K.M. Straub, and A.L. Burlingame, *Anal. Chem.*, 54 (1982) 2029-2034.

117 O.S. Chizhov and N.K. Kochetkov, *Adv. Carbohydr. Chem. Biochem.*, 21 (1966) 29-93.

118 G. Puzo, J. C. Promé ,and J. Fournier, *Carbohydr. Res.*, 140 (1985) 131-134.

119 E.G. de Jong, W. Heerma, and G. Dijkstra, *Biomed. Mass Spectrom.*, 7 (1980) 127-31.

120 J. W. Dallinga and W. Heerma, *Biomed. Environ. Mass Spectrom.*, 18 (1989) 363-372.

121 V. Kovacik, E. Petrakova, J. Hirsch, V. Mihalov, W. Heerma, and C. Versluis, *Biomed. Environ. Mass Spectrom.*, 17 (1988) 455-458.

122 Y.-Z. Chen, S. Hua, H. Li, and H. Yang, *Proc. 36th Con. Mass Spectrom. Allied Topics*, 36 (1988) 163-164.

123 N. Ravenscroft, Ph. D. Thesis, University of Cape Town, (1988).

124 B. Munson, *Anal. Chem.*, 43 (1971) 28A-43A.

125 A.G. Harrison, "*Chemical Ionization Mass Spectrometry*", CRC Press, Florida 1983.

126 V.N. Reinhold, *Methods Enzymol.*, 138 (Complex Carbohydr. Pt. E) (1988) 59-84.

127 H. Liebl, *Anal. Chem.*, 46 (1974) 22A-30A.

128 A. Benninghoven, *Surf. Sci.*, 35 (1973) 427-429.

129 A. Benninghoven and W.K. Sichtermann, *Anal. Chem.*, 50 (1978) 1180-1184.

130 R.J. Day, S.E. Unger, and R.G. Cook, *J. Am. Chem. Soc.*, 101 (1979) 1180-1182.

131 F.M. Devienne and J.C. Roustan, *Org. Mass Spectrom.*, 17 (1982) 173-181.

132 M.L. Vestal, *Mass Specrom. Rev.*, 2 (1983) 447-480.

133 R.S. Johnson and K. Biemann, *Biochemistry*, 26, (1987) 1209-1214.

134 H. Egge and J. Peter-Katalinic, in "*Mass Spectrometry in the Health and Life Sciences*" 401-450, Eds. A.L. Burlingame and N. Castagonli, Jr., Elsevier Science Publishers, Amsterdam, 1985.

135 V.N. Reinhold and S.A. Carr, *Mass Spec. Rev.*, 2 (1983) 153-221.

136 L. Poulter, R. Karrer, K. Jiang, K.; B.L. Gillece-Castro, and A.L. Burlingame, *Proc. 36th Con. Mass Spectrom. Allied Topics*, 36 (1988) 921-922.

137 M. Barber, R.S. Bordoli, G.J. Elliott, R.D. Sedgewick, and A.N. Tyler, *Anal. Chem.*, 54 (1982) 645A-657A.

138 F.H. Field, *J. Phys. Chem.*, 26 (1982) 5115-5123.

139 R.A.W. Johnson, I.A.S. Lewis, and M.E. Rose, *Tetrahedron*, 39 (1983) 1597-1603.

140 G. Puzo, and J.-C. Prome, *Org. Mass Spectrom.*, 19 (1984) 448-451.

141 R.M. Caprioli, *Anal. Chem.*, 55 (1983) 2387-2389.

142 R.M. Caprioli and L.A. Smith, *Biomed. Mass Spectrom.*, 11 (1984) 392-395.

143 M. Barber, R.S. Bordoli, G.J. Elliot, R.D. Sedwick, N. Tyler, *J. Chem. Soc., Faraday Trans. 1*, 79 (1983) 1249-1255.

144 E. de Pauw, G. Pelzer, V.D. Dao, and J. Marien, *Biochem. Biophys. Res. Comm.*, 123 (1984) 27-32.

145 J.L. Gower, *Biomed. Mass Spectrom.*, 12 (1985) 191-196.

146 M. Arita, M. Iwamori, T. Higuchi, Y. Nagai, *J. Biochem.*, 93 (1983) 319-322.

147 S.A. Martin, C.E. Costello, and K. Biemann, *Anal. Chem.*, 54 (1982) 2362-2368.

148 A. Dell, *Adv. Carbohydr. Chem. Biochem.*, 45 (1987) 19-72.

149 M.A. Postumus, P.G. Kistemaker, H.L.C. Meuzelaar, and M.C. Ten Noever de Brauw, *Anal. Chem.*, 50 (1978) 985-991.

150 F. Heresch, E.R. Schmid, and J.F.K. Huber, *Anal. Chem.*, 52 (1980) 1803-1807.

151 R. J. Cotter, *Anal. Chem.*, 52 (1980) 1767-1770.

152 H.J. Heinen, S. Meier, H. Vogt, and R. Wechsung, *Adv. Mass Spectrom.*, 8 (1980) 942-

153 D. Zakett, A.E. Svhoen, R.G. Cooks, and P.H. Hemberger, *J. Am. Chem. Soc.*, 103 (1981) 1295-1296.

154 K. Balasnmugan, R.A. Dang, R.J. Day, D.M. Hercules, *Anal. Chem.*, 53 (1981) 2296-2298.

155 G.J.Q. van der Peyl, K. Isa, J. Haverkamp, and P.G. Kistemaker, *Org. Mass Spectrom.*, 16 (1981) 416-420.

156 S.W. Gramham, P. Dowd and D.H. Hercules, *Anal. Chem.*, 54 (1982) 649-654.

157 R. Stoll and F.W. Röllgen, *Z. Naturforsch.*, 37A (1982) 9-14.

158 U. Seydel and B. Lindner, in *Ion Formation from Organic Solids, Springer Series in Chemical Physics 25*, 240-244, Ed. A. Benninghoven, Springer-Verlag, 1983.

159 K. Takayama, N. Qureshi, K. Hyver, J. Honovich, R.J. Cotter, P. Mascagni, and H. Schneider, *J. Biol. Chem.*, 261 (1986) 10624-10631.

160 R.J. Cotter, J. Honovich, N. Qureshi, and K. Takayama, *Biomed. Environ. Mass Spectrom.*, 14 (1987) 591-598.

161 F. Hillenkamp, in *Ion Formation from Organic Solids, Springer Series in Chemical Physics 25*, 190-205, Ed. A. Benninghoven, Springer-Verlag, 1983.

162 R.J. Cotter, J. Honovich, J. Olthoff, P. Demirev, and M. Alaim, in *Ion Formation from Organic Solids IFOS III, Springer Proceedings in Physics 9*, Springer-Verlag, 1986, 142-146, Ed. A. Benninghoven, Springer-Verlag, 1986.

163 D.M. Hercules, in *Ion Formation from Organic Solids IFOS III, Springer Proceedings in Physics 9*, Springer-Verlag, 1986, 147-152, Ed. A. Benninghoven, Springer-Verlag, 1986.

164 F. Hillenkamp, D. Holtkamp, M. Karas, and P. Klüsener, in *Ion Formation from Organic Solids IFOS III, Springer Proceedings in Physics 9*, Springer-Verlag, 1986, 153-167, Ed. A. Benninghoven, Springer-Verlag, 1986.

165 B. Lindner and U. Seydel, in *Ion Formation from Organic Solids IFOS III, Springer Proceedings in Physics 9*, Springer-Verlag, 1986, 158-162, Ed. A. Benninghoven, Springer-Verlag, 1986.

166 M.P. Chiarelli, D.A. McCrery, and M.L. Gross, in *Ion Formation from Organic Solids IFOS III, Springer Proceedings in Physics 9*, Springer-Verlag, 1986, 204-208, Ed. A. Benninghoven, Springer-Verlag, 1986.

167 M.P. Chiarelli and M.L. Gross, *Int. Mass Spectrom. Ion Proc.*, 78 (1987) 37-52.

168 M. Karas, D. Bachmann, U. Bahr, and F. Hillenkamp, *Int. Mass Spectrom. Ion Proc.*, 78 (1987) 53-68.

169 J. Grotemeyer, K. Walter, U. Boesl, and E.W. Schlag, *Int. Mass Spectrom. Ion Proc.*, 78 (1987) 69-84.

170 M.L. Coates and C.L.Wilkins, *Biomed. Mass Spectrom.*, 12 (1985)424-428.

171 M.L. Coates and C.L.Wilkins, *Anal. Chem.*, 159 (1987) 197-200.

172 Z. Lam, M.B. Comisarow, G.G.S. Dutton, D. Weil, and A. Bjarnason, *Rap. Commun. Mass Spectrom.*, 1 (1987) 83-87.

173 Z. Lam, M.B. Comisarow, and G.G.S. Dutton, *Anal. Chem.*, 60 (1988) 2304-2306.

174 E.W. Schlag and H.J. Neusser, *J. Am. Chem. Soc.*, 103 (1981) 5058-5061 and *Acc. Chem. Res.*, 16 (1983) 355-360.

175 J.F. Ready, "*Effect of High-Power Laser Radiation*", Academic Press, New York, 1971.

176 F. Hillenkamp, E. Unsold, R. Konfmann, and R. Nitsche, *Appl. Phys.*, 8 (1975) 341-348.

177 E.D. Hardin and M.L. Vestal, *Proc. 28th Con. Mass Spectrom. Allied Topics*, 28 (1980) 616-617.

178 G.D. Davis, *Adv. Mass Spectrom.*, 8 (1980) 1012-1013.

179 M.A. Postumus, *Anal. Chem.*, 50 (1978) 985-991.

180 M.B. Comisarow and A.G. Marshall, *Chem. Phys. Lett.*, 25 (1974) 282-283.

181 M.B. Comisarow and A.G. Marshall, *Chem. Phys. Lett.*, 26 (1974) 489-490.

182 D.A. McCrery and M.L. Gross, *Anal. Chim. Acta*, 178 (1985) 91-103.

183 M.B. Comisarow, *J. Chem. Phys.*, 69 (1978) 4097-4104.

184 M.B. Comisarow, *Adv. Mass Spectrom.*, 7 (1978) 1042-1046.

185 M.B. Comisarow, *Adv. Mass Spectrom.*, 8 (1980) 1698-1706.

186 F.W. McLafferty, *Interpretation of Mass Spectra*, 3rd Edit., University Science Book, New York, 1980.

187 B. Domon and C.E. Costello, *Glyconjugates*, 5 (1988) 397-409.

188 G.J.Q. van der Peyl, J. Haverkamp, P.G. Kistemaker, *Int. J. Mass Spectrom. Ion Phys.*, 42 (1982) 125-141.

189 R.J. Cotter and A.L. Yergey, *Anal. Chem.*, 53 (1981) 1306-1307.

190 G.J.Q. van der Peyl, W.J. van der Zonde, K. Bederski, A.J.H. Boerboom, and P.G. Kistemaker, *J. Int. Mass Spectrom. Ion Phys.*, 47 (1983) 7-10.

191 G.J.Q. van der Peyl, K. Isa, J. Haverkamp, and P.G. Kistemaker, *J. Int. Mass Spectrom. Ion Phys.*, 47 (1983) 11-14.

192 R.B. van Breemen, M. Snow, and R.J. Cotter, *Int. J. Mass Spectrom. Ion Phys.*, 49 (1983) 35-50.

193 R.J. Cotter, Anal. Chem., 53 (1981) 719-720.

194 F. Heresch, in *Ion Formation from Organic Solids, Springer Series in Chemical Physics 25*, Springer-Verlag, 1983, 217-221, Ed. A. Benninghoven, Springer-Verlag, 1983.

195 G.G.S. Dutton and T.E. Folkman, *Carbohydr. Res.*, 78 (1980) 305-15.

196 D.N. Karunaratne, Ph. D. Thesis, University of British Columbia, (1985).

197 G.G.S. Dutton, H. Parolis, J.-P. Joseleau, and M.-F. Marais, *Carbohydr. Res.*, 149 (1986) 411-424.

198 G.G.S. Dutton, H. Parolis, and L.A.S. Parolis, *Carbohydr. Res.*, 170 (1987) 193-206.

199 L.A.S. Parolis, H. Parolis, H. Niemann, and S. Strim, *Carbohydr. Res.*, 179 (1988) 301-314.

200 C.T. Greenwood, in "*The Carbohydrates*" Vol. 2B, 504, Eds., W. Pigman and D. Horton, Academic Press, New York, 1970.

201 P.A. Sandford and J. Baird, in "*The Polysaccharides*" Vol. 2, 471, Ed. G.O. Aspinall, Academic Press, New York, 1983.

202 A.J. Mort and W.D. Bauer, *J. Biol. Chem.*, 257 (1982) 1870-1875.

203 P.-E. Jannson, B. Lindberg, and P.A. Sandford, *Carbohydr. Res.*, 124 (1983) 135-139.

204 M.-S. Kuo and A.J. Mort, *Carbohydr. Res.*, 145 (1986) 247-265.

205 P. Mesner and F.M. Unger, *Biochem. Biophys. Res. Comm.*, 96 (1980) 1003-1010.

206 H.J. Jennings, K.-G. Rosell, and K.J. Johnson, *Carbohydr. Res.*, 105 (1982) 45-56.

207 M.A. Schmidt and K. Jann, *FEMS Microbiol. Lett.*, 14 (1982) 69-74.

208 W.F. Vann and K. Jann, *Infect. Immun.*, 25 (1979) 85-92.

209 W.F. Vann, T. Soderstrom, W. Egan, F.-P. Tsui, R. Scheerson, I. Ørskov, and F. Ørskov, *Infect. Immun.*, 39 (1983) 623-629.

210 B. Jann, P. Hofmann, and K. Jann, *Carbohydr. Res.*, 120 (1983) 131-141.

211 B. Jann, R. Ahrens, T. Dengler, and K. Jann, *Carbohydr. Res.*, 177 (1988) 273-277.

212 R. Ahrens, B. Jann, K. Jann, and H. Blades, *Carbohydr. Res.*, 179 (1988) 223-231.

213 T. Dengler, B. Jann, and K. Jann, *Carbohydr. Res.*, 142 (1985) 269-276.

214 E.J. McGurie and S.B. Binkley, *Biochem.*, 3 (1964) 247-251.

215 G.G.S. Dutton, H. Parolis, and L.A.S. Parolis, *Carbohydr. Res.*, 170 (1987) 193-206.

216 M.R. Lifely, J.C. Lindon, J.M. Williams, and C. Moreno, *Carbohydr. Res.*, 143 (1985) 191-205.

217 W. Egan, T.-Y. Liu, D. Dorow, J.S. Cohen. J.D. Robbins. E.C. Gotshich, and J.B. Robbins, *Biochem.*, 16 (1977) 3687-3692.

218 A.N. Anderson, H. Parolis, L.A.S. Parolis, *Carbohydr. Res.*, 163 (1987) 81-90.

219 K. Jann and M.A. Schmidt, *FEMS Microbiol. Lett.*, 7 (1980) 79-81.

220 W. Fischer, M.A. Schmidt, B. Jann, and K. Jann, *Biochem.*, 21 (1982) 1279-1284.

221 M.L. Rodriguez, B. Jann, and K. Jann, *Carbohydr. Res.*, 173 (1988) 243-253.

222 B. Jann, T. Dengler, K. Jann, *FEMS Microbiol. Lett.*, 29 (1985) 257-261.

223 P. Hofmann, B. Jan, and K. Jann, *Eur. J. Biochem.*, 147 (1985) 601-609.

224 F.-P. Tsui, W. Egan, M.F. Summers, R.A. Byrd, R. Schneerson, and J.B. Robbins, *Carbohydr. Res.*, 173 (1988) 65-74.

225 T. Dengler, B. Jann, and K. Jann, *Carbohydr. Res.*, 150 (1986) 233-240.

226 P. Hofmann, B. Jann, and K. Jann, *Carbohydr. Res.*, 139 (1985) 261-271.

227 L.M. Beynon, Ph. D. Thesis, University of British Columbia, (1988).

228 L.M. Beynon and G.G.S. Dutton, paper in preparation for *Carbohydr. Res.*

APPENDIX I

The structural elucidation of bacterial capsular polysaccharides using laser desorption ionization Fourier transform ion cyclotron resonance spectroscopy (l.d.i.-F.t.-i.c.r.).

The structural elucidation of bacterial capsular polysaccharides using laser desorption ionization Fourier transform ion cyclotron resonance spectroscopy (l.d.i.-F.t.-i.c.r.).

ZAMAS LAM, MELVIN B. COMISAROW, GUY G. S. DUTTON

Department of Chemistry, The University of British Columbia, Vancouver, B.C., V6T 1Y6 (Canada)

DAVID A. WEIL

Nicolet Analytical Instruments, 5225-1 Verona Road, Madison, WI 53711-0508 (USA)

AND ASGEIR BJARNASON

Science Institute, University of Iceland, Dunhaga 3, 107 Reykjavik, (Iceland)

SPONSOR REFEREE: Alma L. Burlingame, University of California, USA

Rapid Communication in Mass Spectrometry, 1 (1987) 83-86

(Received 1 Sept 1987; accepted 1 Sept 1987)

INTRODUCTION

Bacterial polysaccharides are important in immunology as potential vaccines[1] and it is desirable that the chemical structure of these biopolymers be established. An important aspect of such structural studies involves the determination of the sequence of the monosaccharide residues in the biopolymer. The molecular weights of these biopolymers are in the range of 10^6 daltons[1], obviating direct use of mass spectrometric methods for this sequencing.

It is now well documented[1] that the structures of most bacterial polysaccharides can be considered in terms of repeating units, which may contain two to seven monosaccharide residues, depending upon the species and the strain. Furthermore, there exist endoglycanases, associated with bacterial viruses (bacteriophages), capable of depolymerising the native polysaccharides into oligosaccharides corresponding to such repeating units[2-4]. The enzymatic depolymerisation reactions take place under neutral conditions and the oligosaccharides formed have the same sequence of monosaccharide residues as the native polymers. The molecular weight of, for example, a hexasaccharide repeating unit is approximately 10^3 daltons and within the mass range of modern mass spectrometers. The combination of bacteriophage degradation to form oligosaccharides and

mass spectrometric sequencing of these oligosaccharides thus has considerable potential for bacterial polysaccharide analysis.

Oligosaccharides are involatile compounds whose mass spectrometric analysis has been greatly facilitated by the development of desorption ionisation techniques. The two most frequently used desorption methods are desorption chemical ionisation (d.c.i.)[5,6] and fast atom bombardment (f.a.b.)[7,8]. These ionisation techniques usually give abundant sequence information on derivatised samples and we have recently sequenced a capsular antigen from *Escherichia coli* K44 using d.c.i.[9]. Unfortunately, these techniques provide little or no information on either the positions of linkage between the saccharide residues or the anomeric configuration of the linkage. Collision activation dissociation (c.a.d.) experiments[10] and mass ion kinetic energy (m.i.k.e.s.) experiments[11] have been carried out on either permethylated disaccharides or methyl glycosides to distinguish the position of linkage[10] and the anomeric configuration[11] with varying degrees of success.

It is obviously preferable, whenever possible, to sequence an oligosaccharide without derivatisation. Laser desorption ionisation (l.d.i.) has been shown to produce molecular or pseudomolecular ions from underivatised organic molecules, usually with time-of flight (t.o.f.) mass analysers. T.o.f. mass spectrometers give the entire mass spectrum from a single laser pulse, although the mass resolution is typically low[12,13]. Fourier transform ion cyclotron resonance (F.t.-i.c.r.) mass spectrometry[14,15] can be used to overcome this resolution limitation. F.t.-i.c.r. provides ultrahigh mass resolution[16-17], high mass capability[16-17] and is inherently a pulse experiment[16-17], and thus is well suited for l.d.i. experiments[19,20]. Unit-mass resolution l.d.i.-F.t.-i.c.r. mass spectrometry, using a Nicolet FTMS-1000 instrument, has shown the potential of the technique for carbohydrate analysis[21,22].

We report here a high resolution, accurate mass l.d.i.-F.t.-i.c.r. mass spectrum of an *underivatised* bacterial capsular oligosaccharide. This spectrum can be interpreted to give complete sequence information and also, in some cases, the linkage positions of the individual sugar residues.

The structure of the capsular polysaccharide of *Klebsiella* K44 (Figure 1) has been investigated previously[23,24]. The linear pentasaccharide repeating unit, generated by bacteriophage enzyme action on the polysaccharide, consists of a glucuronic acid residue, two rhamnose residues, two glucose residues and an *O*-acetyl group. F.a.b.-m.s. only provides total sequence information if this particular oligosaccharide, obtained from bacteriophage degradation, is reduced and peracetylated[25].

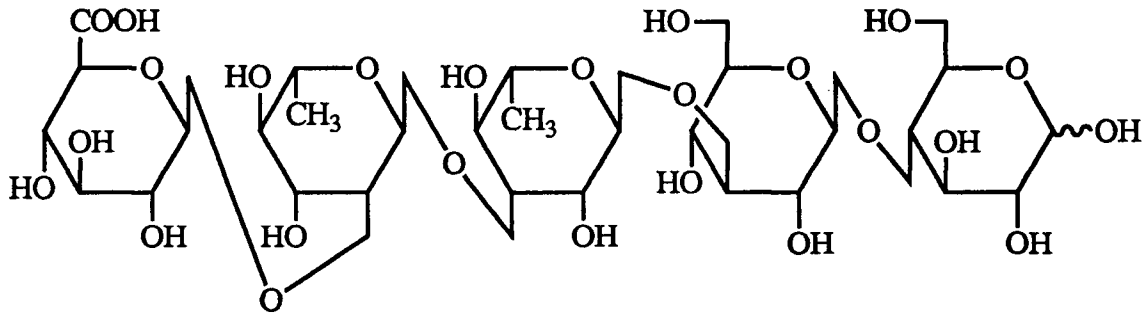

Glucuronic acid – Rhamnose – Rhamnose – Glucose – Glucose

Fig. 1. Structure of *O*–de–acetylated oligosaccharide obtained from *Klebsiella* K44 by bacteriophage degradation.

EXPERIMENTAL

Mass spectra were obtained with a Nicolet FTMS-2000 dual cell Fourier transform mass spectrometer equipped with a 3.0 T superconducting magnet and a Nicolet laser desorption interface. The laser was a Tachisto 216 pulse CO_2 laser operating as a stable resonator with aperture controlled beam characteristics. Equipped with a total reflector, the laser delivers up to 2 J in a 40 ns wide pulse emitting at 10.59 micron. Output energy can be controlled by adjusting the aperture and was estimated to be on the order of 0.05 J per pulse for this experiment. The spot size for the focus laser beam on the probe tip was on the order of 100 micron.

Approximately 1 mg of the sample was dissolved in 0.2 ml of methanol solution saturated with NaCl / KBr. A drop or two of water was added to completely dissolve the sample. This solution was transferred to and allowed to evaporate on the stainless steel

probe tip of the direct insertion probe of the mass spectrometer. The vacuum system was pumped down to ~$1x10^{-8}$ torr after insertion of the sample probe, prior to mass analysis.

Mass spectra were collected in the broadband mode[16] with a high frequency cutoff at 500 KHz (corresponding to a lower mass limit of ~90 amu). Normally, 64K data point transients were collected and when needed the spectra from several laser shots were averaged to increase the S/N ratio. After each laser pulse, the probe was rotated so that the laser always struck a fresh spot on the sample surface. After the laser pulse, a delay of 5-10 s was employed to reduce the pressure of neutrals in the cell before ion detection. For exact mass measurements, the series of ions corresponding to $K_nBr_{n-1}^+$ was used as an internal calibrant.

Results and Discussion

Table I contains a list of all the l.d.i.-F.t.-i.c.r. positive structural ions, above 5% of the base peak, of the *O*-de-acetylated oligosaccharide obtained from *Klebsiella* K44 by bacteriophage degradation. In the spectrum, pseudomolecular and fragment ions were observed in abundance, typically as the sodiated and potassiated ions. The calculated and observed masses in Table I agree within 30 ppm. Three distinct types of fragmentation pattern were observed as illustrated in Figures 2 and 3. These fragmentation routes do not belong to the classical A-K fragmentation series for permethylated methyl glycosides described by Kochetkov and Chizhov[26,27]. For convenience, the observed fragmentation pathways are labeled from L onwards to distinguish them from Kochetkov's series. The glycosidic bond cleavages (L-cleavage) provided some sequence information (Figure 2) while the ring cleavages (M- and N-cleavages) confirmed the sequence of the oligosaccharide and gave some positions of linkage between the individual sugar residues (Figure 3).

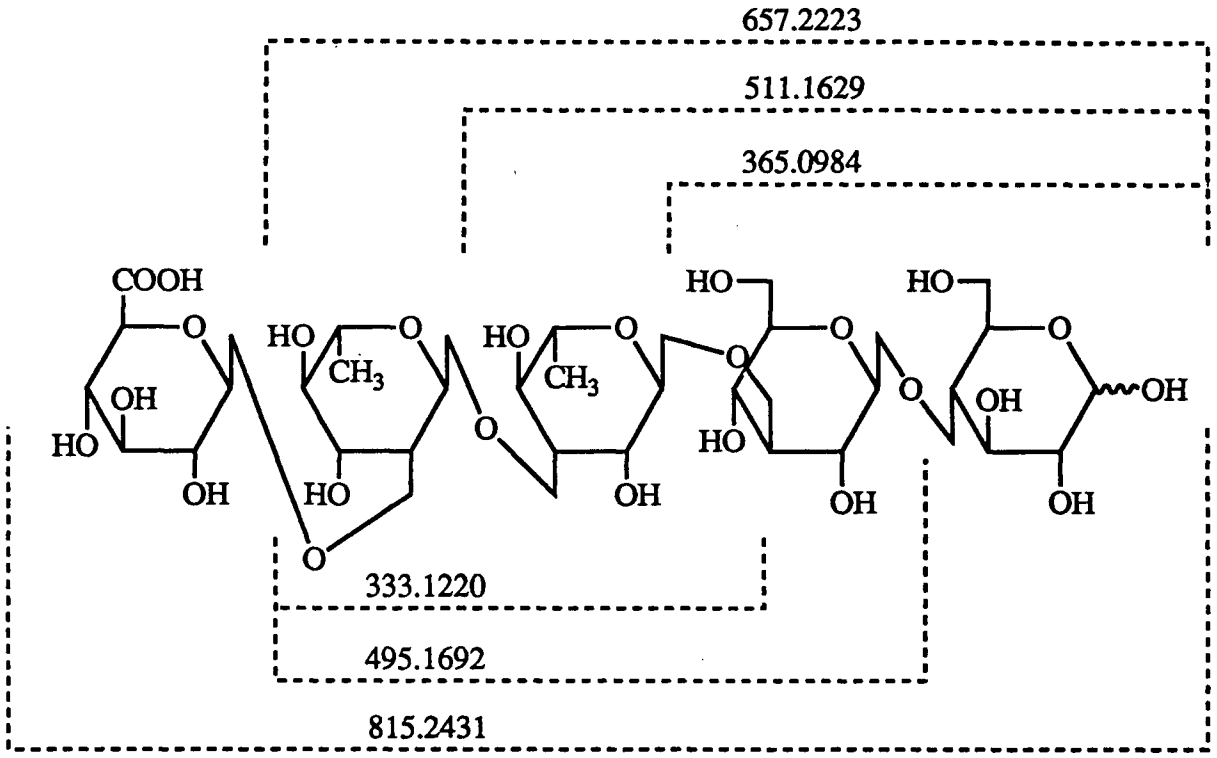

Fig. 2. Some fragment ions arising from glycosidic bond cleavages (L-cleavage) in the l.d.i.-F.t.-i.c.r. spectrum of the *O*-de-acetylated oligosaccharide obtained from *Klebsiella* K44 by bacteriophage degradation. Na^+ and K^+ have been omitted from the structures in this figure. The formulae of the cationised ions are assigned in Table I to specific masses .

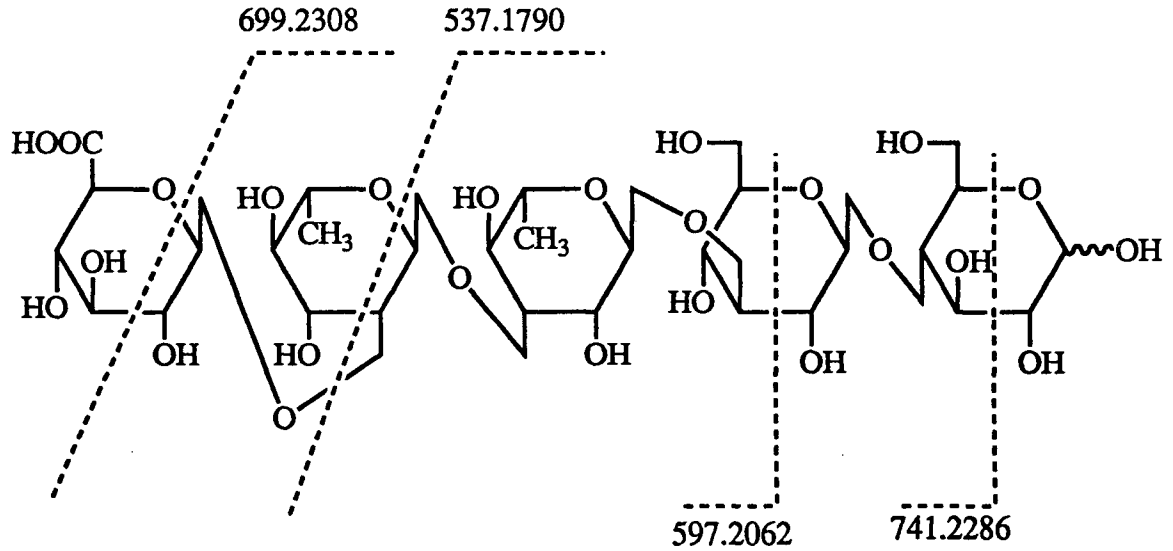

Fig. 3. Some fragment ions arising from ring cleavages (M- and N-cleavages) in the l.d.i.-F.t.-i.c.r. spectrum of the *O*-de-acetylated oligosaccharide obtained from *Klebsiella* K44 by bacteriophage degradation. Na^+ and K^+ have been omitted from the structures in this figure, as in Fig. 1.

TABLE I.

POSITIVE ION L.D.I.-F.T.-I.C.R. POSITIVE ION SPECTRUM OF THE *O*-DE-ACETYLATED OLIGOSACCHARIDE OBTAINED FROM *Klebsiella* K44 BY BACTERIOPHAGE DEGRADATION

Observed mass (amu)	*Calculated mass (amu)*	*Relative intensity (%)*	*Mass error (ppm)*	*Proposed structure (a)*
831.2297	831.2167	8.6	15.6	[(2Hex,2deoxyHex,HexA)-H_2O+K]$^+$
815.2431	815.2428	24.9	0.4	[(2Hex,2deoxyHex,HexA)-H_2O+Na]$^+$
771.2657	771.2530	9.7	16.5	[(2Hex,2deoxyHex,HexA)-H_2O-CO_2+Na]$^+$
741.2286	741.2430	6.0	-18.6	[(2deoxyHex,Hex,HexA)+$C_4H_7O_2$+Na]$^+$
715.2131	715.2058	11.1	10.2	[(2Hex,2deoxyHex)+$C_2H_3O_2$+K]$^+$
699.2308	699.2318	37.4	-1.4	[(2Hex,2deoxyHex)+$C_2H_3O_2$+Na]$^+$
697.2088	697.1952	5.9	19.4	[(2Hex,2deoxyHex)+$C_2H_3O_2$-H_2O+K]$^+$
681.2240	681.2213	25.0	4.0	[(2Hex,2deoxyHex)+$C_2H_3O_2$-H_2O+Na]$^+$
673.2067	673.1952	18.5	17.1	[(2Hex,2deoxyHex)+K]$^+$
657.2223	657.2213	47.9	1.6	[(2Hex,2deoxyHex)+Na]$^+$
655.1926	655.1846	26.0	12.2	[(2Hex,2deoxyHex)-H_2O+K]$^+$
639.2097	639.2107	100.0	-1.5	[(2Hex,2deoxyHex)-H_2O+Na]$^+$
613.1672	613.1741	13.4	11.2	[(2deoxyHex,HexA)+$C_4H_9O_3$+K]$^+$
597.2062	597.2001	32.8	10.1	[(2deoxyHex,HexA)+$C_4H_9O_3$+Na]$^+$
579.1959	579.1896	9.1	10.9	[(2deoxyHex,HexA)+$C_4H_9O_3$-H_2O+Na]$^+$
553.1681	553.1530	31.2	27.3	[(2Hex,deoxyHex)+C_2H_3O+K]$^+$
537.1790	537.1791	80.5	-0.2	[(2Hex,deoxyHex)+$C_2H_3O_2$+Na]$^+$
519.1643	519.1685	5.6	-8.0	[(2Hex,deoxyHex)+C_2H_3O-H_2O+Na]$^+$
511.1629	511.1634	17.6	1.0	[(2Hex,deoxyHex)+Na]$^+$
509.1300	509.1267	6.9	6.4	[(2Hex,deoxyHex)-H_2O+K]$^+$
495.1692	495.1684	27.4	1.6	[(2deoyHex,Hex)+Na]$^+$
493.1526	493.1526	27.2	-1.0	[(2Hex,deoxyHex)-H_2O+Na]$^+$
477.1580	477.1579	13.7	0.3	[(2deoxyHex,Hex)-H_2O+Na]$^+$
365.0984	365.1055	6.5	-19.3	[(2Hex)+Na]$^+$
349.1127	349.1105	6.9	6.2	[(Hex,deoxyHex)+Na]$^+$
347.0981	347.0949	18.4	9.3	[(2Hex)-H_2O+Na]$^+$
333.1220	333.1156	9.9	19.3	[(2deoxyHex)+Na]$^+$
315.1083	315.1050	6.3	10.4	[(2deoxyHex)-H_2O+Na]$^+$

(a) Hex = hexose, deoxyHex = deoxyhexose, HexA = hexuronic acid and the formation of each glycosidic bond involves the loss of a molecule of water.

For ring cleavage, two fragmentation routes were observed (Figure 4). The M-series fragments, with the positive charge residing on the reducing end, contain C-1 and C-2, while N–series fragments possibly hold C-3, C-4, C-5 and C-6.

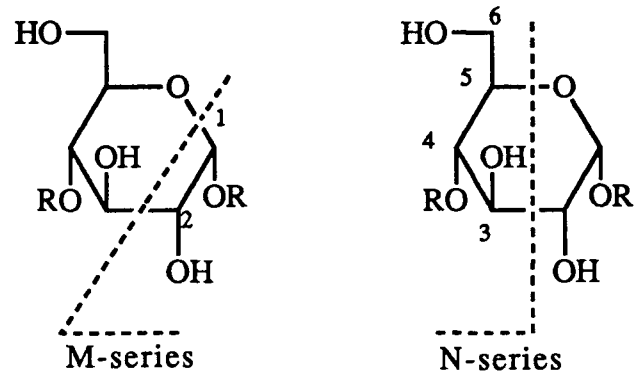

Fig. 4. Two different types of ring cleavages.

As both types of ring cleavage fragments were observed, the reducing end could be determined without reducing the oligosaccharide prior to mass spectrometric analysis (Figure 3). From the *Klebsiella* K44 oligosaccharide, two M-series fragments, m/z = 699.2308 and m/z = 537.1790 were observed. The first fragment corresponds to two hexoses plus two deoxyhexoses plus a $C_2H_3O_2$ ring fragment. The second corresponds to two hexoses plus one deoxyhexose plus a C_2H_3O ring fragment. The M-series fragment derived from the terminal glucuronic acid was $C_2H_3O_2$, while the 2-linked rhamnose gave a C_2H_3O fragment, presumably by a glycosidic oxygen loss (Figure 5).

Two N-series fragments were also observed from this oligosaccharide, m/z = 741.2286 and m/z = 597.2062. The first N-series fragment corresponds to an uronic acid, plus two deoxyhexoses plus a hexose, plus a $C_4H_7O_2$ ring fragment. The second N-series fragment corresponds to an uronic acid plus two deoxyhexoses plus a $C_4H_9O_3$ ring fragment. The 3-linked terminal glucose gave a $C_4H_7O_2$ fragment, while the adjacent 4-linked glucose gave a fragment of $C_4H_9O_3$ (Figure 6). This may indicate that 4-linked residues give a $C_4H_9O_3$ fragment, and 3-linked residues give a $C_4H_7O_2$ fragment. Dehydration of high molecular

weight oligosaccharides, however, is very facile, and further work is required to confirm these observations.

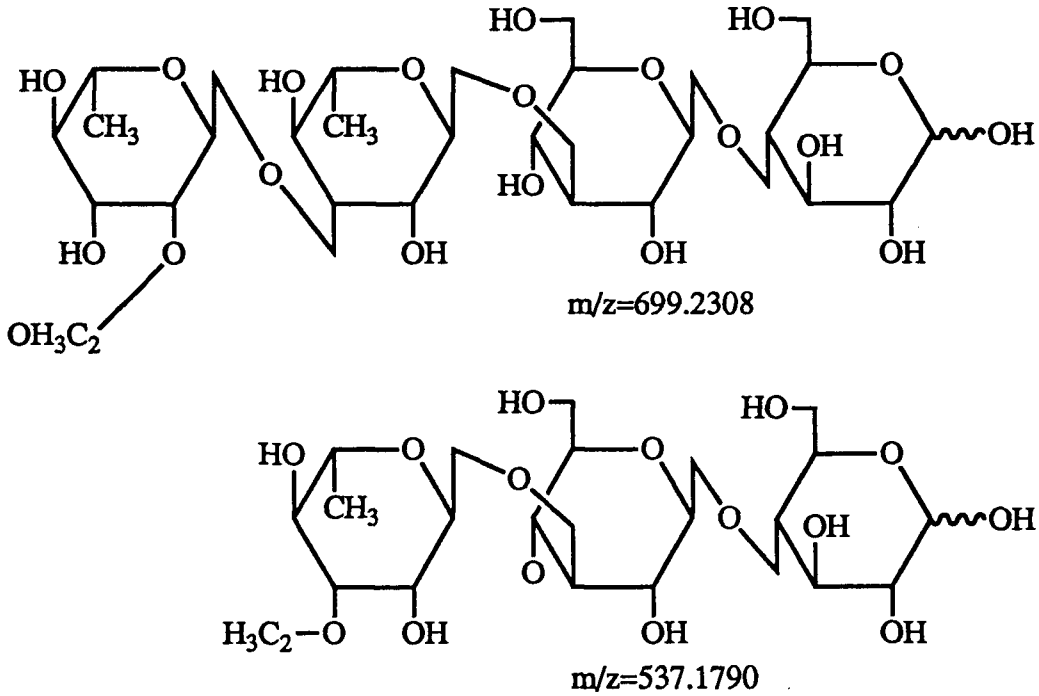

Fig. 5. M-series fragment ions observed for l.d.i.-F.t.-i.c.r. of *O*-de-acetylated oligosaccharide obtained from *Klebsiella* K44 by bacteriophage degradation.

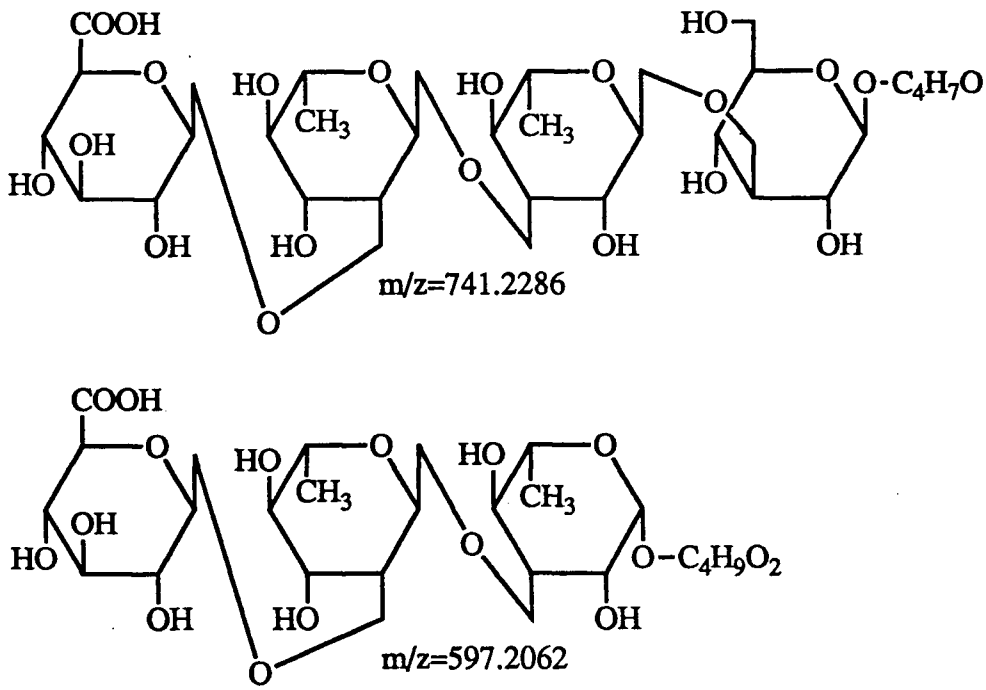

Fig. 6. N-series fragment ions observed for l.d.i.-F.t.-i.c.r. of *O*-de-acetylated oligosaccharide obtained from *Klebsiella* K44 by bacteriophage degradation.

High resolution l.d.i.-F.t.-i.c.r. shows promise for complete sequencing, and for determination of some linkage positions for the underivatised, linear oligosaccharide shown in Figure 1. Further work is in progress to confirm the generality of our proposed ring cleavage fragmentation patterns in other oligosaccharides.

ACKNOWLEDGMENT

This research was supported by the Natural Sciences and Engineering Research Council of Canada.

REFERENCES

1 L. Kenne and B. Lindberg, in G.O. Aspinall (Ed.), "*The Polysaccharides*," Vol. 1 and 2, Academic Press, New York (1983)

2 G.G.S. Dutton, J.L. di Fabio, D.M. Leek, E.H. Merrifield, J.R. Nunn and A.M. Stephen, *Carbohydr. Res.* **97**, 127-38 (1981)

3 H. Geyer, K. Himmelspach, B. Kwiatkowski, S. Schlecht and S. Strim, *Pure Appl. Chem.* **55**, 637-53 (1983)

4 D. Rieger-Hug and S. Stirm, *Virology* **113**, 363-78 (1981)

5 A.K. Ganguly, N.F. Cappuccino, H. Fujiwara and A.K. Bose, *J. Chem. Soc., Chem. Comm.* 148 (1979)

6 K.-I. Harada, S. Ito, N. Takeda, M. Suzuki and A. Tatematsu, *Biomed. Mass Spectrom.* **10**, 5-12, (1983)

7 H.R. Morris, A. Dell, M. Panico and R.A. McDowell, in A.L. Burlingame and N. Castagnoli, Jr. (Eds.), "*Mass Spectrometry in the Health and Life Sciences*", p. 363-78. Elsevier, Amsterdam (1985)

8 H. Egge and J. Peter-Katalinic, in A.L. Burlingame and N. Castagnoli, Jr. (Eds.), "*Mass Spectrometry in the Health and Life Sciences*", p. 401-24, Elsevier, Amsterdam (1985)

9 G.G.S. Dutton and A.V.S. Lim, submitted for publication

10 E.G. de Jong, W. Heerma and G. Dijkstra, *Biomed. Mass Spectrom.* **7**, 127-31 (1980)

11 G. Puzo, J.-C. Prome, and J.-J. Fournie, *Carbohydr. Res.* **140**, 131-34 (1985)

12 M.A. Posthumus, P.G. Kistemaker, H.L.C. Meuzelaar and M.C. Ten Noever de Brauw, *Anal Chem.* **50**, 985-91 (1978)

13 R J. Cotter and J.-C. Tabet *Anal., Chem.* **56**, 1662-67 (1984)

14 M.B. Comisarow and A.G. Marshall, *Chem. Phys. Lett.* **25**, 282-84 (1974)

15 M.B. Comisarow and A.G. Marshall, *Chem. Phys. Lett.* **26**, 489-90 (1974)

16 M.B. Comisarow, *Adv. Mass Spectrom.* **8** ,1698-706 (1980)

17 R.B. Cody, Jr., J.A. Kinsinga, S.G. Hadai, I.J. Austin and F.W. McLafferty, *Anal. Chim. Acta* **178**, 43-66 (1985)

18 D.A. Laude, Jr., C L. Johlman, R.S. Brown, D.A. Weil and C.L. Wilkins, *Mass Spectrom. Rev.* **5**, 107-66 (1986)

19 D.A. McCrery, E.B. Ledford, Jr. and M.L. Gross, *Anal. Chem.* **54**, 1435-37 (1982)

20 C.L. Wilkins, D.A. Weil, C.L.C. Yang and G.F. Ijames, *Anal. Chem.* **57**, 520-24 (1985)

21 M.L. Coates and C.L. Wilkins, *Biomed. Mass Spectrom.* **12**, 424-28 (1985)

22 M.L. Coates and C L. Wilkins, *Anal. Chem.* **59**, 197-200 (1987)

23 G.G.S. Dutton and T.E. Folkman, *Carbohydr. Res.* **78**, 305-15 (1980)

24 D.N. Karunaratne, Ph. D. Thesis, UBC, (1985)

25 A. Dell and P.R. Tiller, *Biochem. Biophys. Res. Comm.* **135**, 1126-34 (1986)

26 O.S. Chizhov and N.K. Kochetkov, *Advan. Carbohydr. Chem.* **21**, 39-93 (1966)

27 J. Lonngren and S. Svensson, *Advan. Carbohydr. Chem.* **29**, 41-106 (1974)

APPENDIX II

Laser desorption ionization Fourier transform ion cyclotron resonance mass spectra of underivatized oligosaccharides.

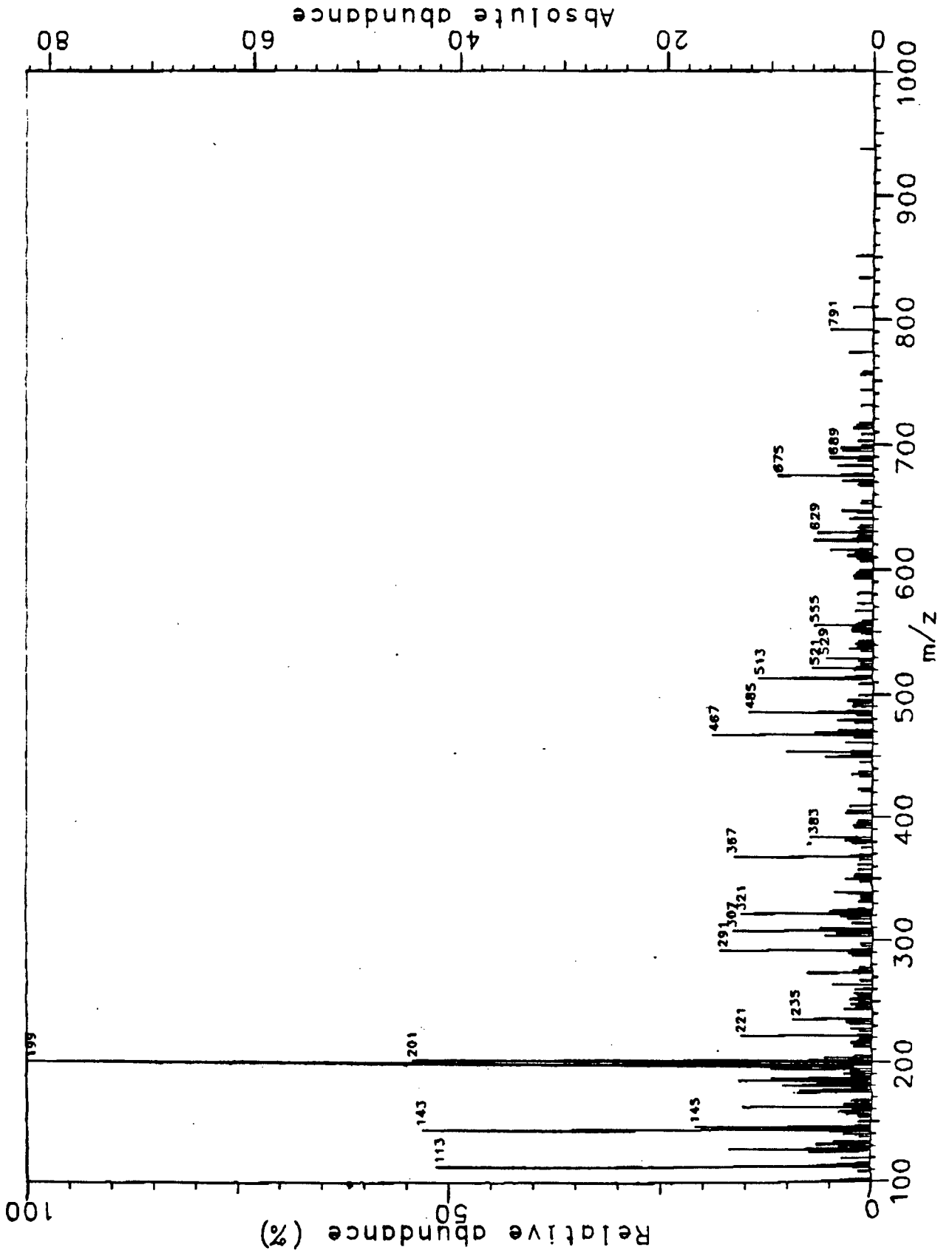

Spec. IV.1 Low resolution negative-ion l.d.i.-F.t.-i.c.r. spectrum of *Klebsiella* K44 de-*O*-acetylated oligosaccharide.

Nominal mass	Measured mass	Rel. intensity	Abs. intensity
100 amu	100.39799 amu	3.1432 %	2585.546875 m
101 amu	101.02504 amu	5.8857 %	4841.406250 m
108 amu	108.23066 amu	1.4945 %	1229.296875 m
111 amu	111.00949 amu	1.9883 %	1635.546875 m
112 amu	112.01785 amu	1.9812 %	1629.687500 m
113 amu	112.91869 amu	1.3363 %	1099.218750 m
113 amu	113.02414 amu	51.4519 %	42323.046875 m
114 amu	114.03139 amu	3.9292 %	3232.031250 m
115 amu	115.00537 amu	1.6203 %	1332.812500 m
115 amu	115.04182 amu	1.6493 %	1356.640625 m
119 amu	119.03660 amu	3.4168 %	2810.546875 m
125 amu	125.02448 amu	7.3421 %	6039.453125 m
126 amu	126.03230 amu	3.3674 %	2769.921875 m
127 amu	127.04004 amu	16.8654 %	13873.046875 m
128 amu	128.04697 amu	1.9608 %	1612.890625 m
129 amu	129.02072 amu	3.7601 %	3092.968750 m
131 amu	131.03692 amu	6.5524 %	5389.843750 m
131 amu	131.31233 amu	2.6418 %	2173.046875 m
133 amu	133.04733 amu	4.5641 %	3754.296875 m
137 amu	137.02520 amu	1.4384 %	1183.203125 m
139 amu	139.00274 amu	3.3075 %	2720.703125 m
139 amu	139.04021 amu	1.9841 %	1632.031250 m
141 amu	141.01996 amu	4.9122 %	4040.625008 m
142 amu	142.02819 amu	4.0954 %	3368.750000 m
143 amu	142.88925 amu	3.7919 %	3119.140625 m
143 amu	143.03526 amu	53.0271 %	43618.750000 m
144 amu	144.04105 amu	6.6018 %	5430.468750 m
145 amu	145.05173 amu	20.9147 %	17203.906250 m
146 amu	146.05591 amu	1.5614 %	1284.375000 m
149 amu	149.04416 amu	1.5681 %	1289.843750 m
153 amu	153.01888 amu	1.5286 %	1257.421875 m
154 amu	153.54873 amu	1.5571 %	1280.859375 m
155 amu	155.03429 amu	3.0084 %	2474.609375 m
157 amu	157.01365 amu	3.9738 %	3268.750000 m
159 amu	159.02930 amu	2.3820 %	1959.375000 m
161 amu	160.85783 amu	1.4099 %	1159.765625 m
161 amu	161.04565 amu	15.2845 %	12572.656250 m
162 amu	162.05137 amu	1.6711 %	1374.609375 m
163 amu	162.87879 amu	1.2979 %	1067.578125 m
163 amu	163.06320 amu	3.3759 %	2776.953125 m
165 amu	164.87663 amu	1.3335 %	1096.875000 m
166 amu	165.97945 amu	2.4841 %	2043.359375 m
167 amu	167.03378 amu	1.9850 %	1632.812500 m
173 amu	173.04790 amu	9.2673 %	7623.046875 m
175 amu	175.02766 amu	8.5859 %	7062.500000 m
177 amu	176.89859 amu	2.3274 %	1914.453125 m
179 amu	178.89672 amu	2.2538 %	1853.906250 m
179 amu	179.05863 amu	10.5481 %	8676.562500 m
181 amu	180.82961 amu	6.4299 %	5289.062500 m
183 amu	182.82529 amu	15.6867 %	12903.515625 m
185 amu	184.82379 amu	6.8112 %	5602.734375 m
185 amu	185.04501 amu	11.8915 %	9781.640625 m
186 amu	186.04913 amu	2.1018 %	1728.906250 m
187 amu	187.03633 amu	2.4604 %	2023.828125 m
189 amu	188.89590 amu	3.3560 %	2760.546875 m
189 amu	189.06228 amu	1.9940 %	1640.234375 m
191 amu	190.89556 amu	2.6004 %	2139.062500 m
193 amu	193.03628 amu	11.9836 %	9857.421875 m
197 amu	196.52167 amu	3.0616 %	2518.359375 m
197 amu	196.80179 amu	45.7220 %	37609.765625 m

Spec. IV.2 High resolution negative-ion l.d.i.-F.t.-i.c.r. spectrum of *Klebsiella* K44 de-*O*-acetylated oligosaccharide.

199	amu	198.57323	amu	1.4831	%	1219.921875	m
199	amu	198.79789	amu	100.0000	%	82257.421875	m
199	amu	199.17332	amu	2.3241	%	1911.718750	m
201	amu	200.50344	amu	3.2999	%	2714.453125	m
201	amu	200.79654	amu	54.2162	%	44596.875000	m
203	amu	202.80016	amu	2.7258	%	2242.187500	m
203	amu	203.05728	amu	5.7005	%	4689.062500	m
205	amu	205.05097	amu	2.0472	%	1683.984375	m
212	amu	212.07516	amu	2.0724	%	1704.687500	m
215	amu	215.05690	amu	2.3910	%	1966.796875	m
217	amu	217.03003	amu	1.6445	%	1352.734375	m
219	amu	219.17677	amu	1.4636	%	1203.906250	m
221	amu	221.06929	amu	15.5704	%	12807.812500	m
222	amu	222.07255	amu	1.7281	%	1421.484375	m
225	amu	225.19204	amu	1.5334	%	1261.328125	m
227	amu	227.20813	amu	2.5696	%	2113.671875	m
231	amu	230.90875	amu	2.6361	%	2168.359375	m
233	amu	232.90348	amu	3.1651	%	2603.515625	m
233	amu	233.07082	amu	1.8549	%	1525.781250	m
235	amu	235.04196	amu	9.4083	%	7739.062500	m
243	amu	243.19780	amu	3.3427	%	2749.609375	m
245	amu	245.06697	amu	1.9807	%	1629.296875	m
247	amu	247.06507	amu	2.4414	%	2008.203125	m
249	amu	249.06055	amu	1.5714	%	1292.578125	m
251	amu	251.07501	amu	2.5449	%	2093.359375	m
253	amu	253.07754	amu	1.5339	%	1261.718750	m
255	amu	255.01468	amu	1.6464	%	1354.296875	m
256	amu	256.24759	amu	2.1384	%	1758.984375	m
259	amu	259.08538	amu	2.0130	%	1655.859375	m
263	amu	263.08267	amu	4.7227	%	3884.765625	m
266	amu	266.21642	amu	1.4227	%	1170.312500	m
267	amu	267.07543	amu	1.4831	%	1219.921875	m
273	amu	273.01149	amu	7.7054	%	6338.281250	m
275	amu	275.07167	amu	2.2866	%	1880.859375	m
277	amu	277.09481	amu	1.5714	%	1292.578125	m
287	amu	287.08251	amu	2.2110	%	1818.750000	m
289	amu	289.09055	amu	2.7334	%	2248.437500	m
291	amu	290.54479	amu	1.6744	%	1377.343750	m
291	amu	291.10976	amu	17.9747	%	14785.546875	m
292	amu	292.12026	amu	2.3583	%	1939.843750	m
295	amu	294.69020	amu	1.3126	%	1079.687500	m
297	amu	296.69039	amu	1.4460	%	1189.453125	m
303	amu	303.07819	amu	5.7019	%	4690.234375	m
305	amu	305.08928	amu	4.3190	%	3552.734375	m
307	amu	307.10772	amu	16.5653	%	13626.171875	m
308	amu	308.13267	amu	2.6579	%	2186.328125	m
309	amu	309.12592	amu	6.1868	%	5089.062500	m
313	amu	313.10020	amu	2.3112	%	1901.171875	m
317	amu	316.67037	amu	2.8920	%	2378.906250	m
319	amu	318.67847	amu	3.5963	%	2958.203125	m
319	amu	319.11274	amu	3.6191	%	2976.953125	m
320	amu	320.22441	amu	2.8084	%	2310.156250	m
321	amu	321.08635	amu	15.5286	%	12773.437500	m
322	amu	322.10114	amu	2.1346	%	1755.859375	m
323	amu	323.10629	amu	4.9649	%	4083.984375	m
325	amu	325.11370	amu	2.9761	%	2448.046875	m
331	amu	331.09844	amu	1.7005	%	1398.828125	m
333	amu	333.13448	amu	1.3672	%	1124.609375	m
335	amu	335.12329	amu	1.4636	%	1203.906250	m
337	amu	337.10070	amu	1.3206	%	1086.328125	m
338	amu	338.23648	amu	2.8664	%	2357.812500	m
339	amu	339.10481	amu	4.5869	%	3773.046875	m
347	amu	347.09926	amu	1.2898	%	1060.937500	m

Spec. IV.2 High resolution negative-ion l.d.i.-F.t.-i.c.r. spectrum of *Klebsiella* K44 de-*O*-acetylated oligosaccharide, con't.

350 amu	350.21382 amu	1.3985 %	1150.390625 m
351 amu	351.15329 amu	2.0406 %	1678.515625 m
353 amu	353.10851 amu	2.0016 %	1646.484375 m
357 amu	357.01166 amu	1.6417 %	1350.390625 m
361 amu	361.12282 amu	1.8126 %	1491.015625 m
365 amu	365.11105 amu	1.5324 %	1260.546875 m
367 amu	367.12362 amu	16.3179 %	13422.656250 m
368 amu	368.12341 amu	2.5891 %	2129.687500 m
369 amu	369.13584 amu	1.5543 %	1278.515625 m
375 amu	375.09450 amu	1.3187 %	1084.765625 m
379 amu	379.11441 amu	2.4604 %	2023.828125 m
381 amu	381.13461 amu	3.0910 %	2542.578125 m
383 amu	383.11986 amu	7.2989 %	6003.906250 m
391 amu	391.06797 amu	2.0016 %	1646.484375 m
393 amu	393.10957 amu	2.2790 %	1874.609375 m
395 amu	395.12418 amu	1.8506 %	1522.265625 m
397 amu	397.10614 amu	1.7390 %	1430.468750 m
403 amu	403.12981 amu	3.1485 %	2589.843750 m
405 amu	405.15696 amu	2.9956 %	2464.062500 m
409 amu	409.12720 amu	2.5805 %	2122.656250 m
421 amu	421.11636 amu	1.3401 %	1102.343750 m
423 amu	423.15313 amu	1.6502 %	1357.421875 m
433 amu	433.14681 amu	1.5495 %	1274.609375 m
435 amu	435.12693 amu	2.4380 %	2005.468750 m
437 amu	437.14533 amu	1.7442 %	1434.765625 m
445 amu	445.14367 amu	1.4284 %	1175.000000 m
449 amu	449.11259 amu	5.5651 %	4577.734375 m
450 amu	450.11820 amu	1.3563 %	1115.625000 m
451 amu	451.12473 amu	2.4019 %	1975.781250 m
453 amu	453.13386 amu	10.1021 %	8309.765625 m
454 amu	454.14077 amu	2.1754 %	1789.453125 m
461 amu	461.14057 amu	3.3023 %	2716.406250 m
465 amu	465.12886 amu	2.2068 %	1815.234375 m
467 amu	467.13366 amu	18.9397 %	15579.296875 m
468 amu	468.13519 amu	4.2801 %	3520.703125 m
469 amu	469.15059 amu	6.8934 %	5670.312500 m
471 amu	471.17449 amu	4.0769 %	3353.515625 m
477 amu	477.13700 amu	2.2433 %	1845.312500 m
478 amu	478.16007 amu	1.3658 %	1123.437500 m
479 amu	479.13361 amu	4.1809 %	3439.062500 m
483 amu	483.12755 amu	1.8083 %	1487.500000 m
485 amu	485.15393 amu	14.6548 %	12054.687500 m
486 amu	486.15599 amu	3.1784 %	2614.453125 m
490 amu	490.22520 amu	2.4594 %	2023.046875 m
493 amu	493.15579 amu	2.1883 %	1800.000000 m
495 amu	495.14310 amu	3.0312 %	2493.359375 m
499 amu	499.18398 amu	1.6939 %	1393.359375 m
508 amu	508.19807 amu	1.8102 %	1489.062500 m
509 amu	509.19470 amu	1.4484 %	1191.406250 m
513 amu	513.15951 amu	13.5916 %	11180.078125 m
514 amu	514.16399 amu	3.2434 %	2667.968750 m
515 amu	515.17125 amu	1.6459 %	1353.906250 m
520 amu	520.14306 amu	2.1773 %	1791.015625 m
521 amu	521.17163 amu	7.1579 %	5887.890625 m
522 amu	522.17129 amu	2.0463 %	1683.203125 m
523 amu	523.10335 amu	1.4156 %	1164.453125 m
525 amu	525.14567 amu	1.5063 %	1239.062500 m
527 amu	527.16297 amu	1.7005 %	1398.828125 m
529 amu	529.17132 amu	5.6107 %	4615.234375 m
535 amu	535.08291 amu	1.5533 %	1277.734375 m
537 amu	537.14524 amu	2.8279 %	2326.171875 m
539 amu	539.16367 amu	1.8259 %	1501.953125 m
541 amu	541.16333 amu	2.1588 %	1775.781250 m

Spec. IV.2 High resolution negative-ion l.d.i.-F.t.-i.c.r. spectrum of *Klebsiella* K44 de-*O*-acetylated oligosaccharide, con't.

549	amu	549.07773	amu	1.2703	%	1044.921875	m
551	amu	551.08894	amu	2.4352	%	2003.124996	m
553	amu	553.08434	amu	2.3796	%	1957.421875	m
555	amu	555.19607	amu	6.9736	%	5736.328125	m
556	amu	556.16368	amu	2.0420	%	1679.687500	m
557	amu	557.16467	amu	1.7181	%	1413.281250	m
559	amu	559.17612	amu	1.2879	%	1059.375000	m
567	amu	567.18662	amu	2.1826	%	1795.312500	m
573	amu	573.21254	amu	1.8031	%	1483.203125	m
581	amu	581.17570	amu	1.6573	%	1363.281250	m
593	amu	593.03071	amu	2.1830	%	1795.703125	m
595	amu	595.04914	amu	2.3146	%	1903.906250	m
597	amu	597.12860	amu	1.9869	%	1634.375000	m
599	amu	599.22210	amu	1.6113	%	1325.390625	m
607	amu	607.12346	amu	1.4845	%	1221.093750	m
609	amu	609.14681	amu	1.7499	%	1439.453125	m
611	amu	611.12476	amu	2.9680	%	2441.406250	m
613	amu	613.21547	amu	2.0192	%	1660.937500	m
615	amu	615.22409	amu	4.9725	%	4090.234367	m
616	amu	616.23230	amu	1.5115	%	1243.359375	m
622	amu	622.17071	amu	1.7575	%	1445.703125	m
623	amu	623.17006	amu	7.0278	%	5780.859375	m
624	amu	624.17683	amu	2.4414	%	2008.203125	m
625	amu	625.19818	amu	1.8264	%	1502.343750	m
627	amu	627.20173	amu	1.7922	%	1474.218750	m
629	amu	629.17021	amu	6.5838	%	5415.625000	m
630	amu	630.11762	amu	2.1341	%	1755.468750	m
631	amu	631.16373	amu	1.4156	%	1164.453125	m
633	amu	633.27863	amu	1.8216	%	1498.437500	m
635	amu	635.17409	amu	1.4926	%	1227.734375	m
641	amu	641.15691	amu	2.8783	%	2367.578125	m
645	amu	645.12459	amu	1.7542	%	1442.968750	m
647	amu	647.11616	amu	3.7060	%	3048.437500	m
653	amu	653.06394	amu	1.4964	%	1230.859375	m
655	amu	655.10251	amu	1.4370	%	1182.031250	m
667	amu	667.20917	amu	1.5106	%	1242.578125	m
668	amu	668.13329	amu	1.9765	%	1625.781250	m
669	amu	669.23758	amu	1.5814	%	1300.781250	m
671	amu	671.21441	amu	3.8005	%	3126.171875	m
672	amu	672.16005	amu	1.9589	%	1611.328125	m
675	amu	675.21431	amu	11.3895	%	9368.750000	m
676	amu	676.23102	amu	3.8803	%	3191.796875	m
677	amu	677.19893	amu	1.3810	%	1135.937500	m
683	amu	683.21717	amu	4.2345	%	3483.203125	m
687	amu	687.25618	amu	1.8525	%	1523.828125	m
689	amu	689.21444	amu	5.1430	%	4230.468750	m
690	amu	690.32308	amu	1.7613	%	1448.828125	m
695	amu	695.13758	amu	3.6495	%	3001.953125	m
697	amu	697.12196	amu	3.9914	%	3283.203125	m
698	amu	698.12776	amu	1.3810	%	1135.937500	m
699	amu	699.21494	amu	1.4251	%	1172.265625	m
703	amu	703.23110	amu	1.9617	%	1613.671875	m
708	amu	708.43248	amu	1.4574	%	1198.828125	m
713	amu	713.13644	amu	2.3606	%	1941.796875	m
715	amu	715.20980	amu	1.9769	%	1626.171875	m
717	amu	717.22120	amu	1.6635	%	1368.359375	m
731	amu	731.18433	amu	1.4954	%	1230.078125	m
743	amu	743.08624	amu	1.5624	%	1285.156250	m
755	amu	755.08885	amu	1.5628	%	1285.546875	m
757	amu	757.15537	amu	1.2898	%	1060.937500	m
773	amu	773.23565	amu	2.8222	%	2321.484375	m
791	amu	791.31906	amu	5.1040	%	4198.437500	m
809	amu	809.34701	amu	2.3046	%	1895.703125	m

Spec. IV.2 High resolution negative-ion l.d.i.-F.t.-i.c.r. spectrum of *Klebsiella* K44 de-*O*-acetylated oligosaccharide, con't.

833 amu	833.40003 amu	1.7499 %	1439.453125 m
851 amu	851.32165 amu	2.0154 %	1657.812500 m
938 amu	937.58386 amu	1.7742 %	1459.375000 m

Spec. IV.2 High resolution negative-ion l.d.i.-F.t.-i.c.r. spectrum of *Klebsiella* K44 de-*O*-acetylated oligosaccharide, con't.

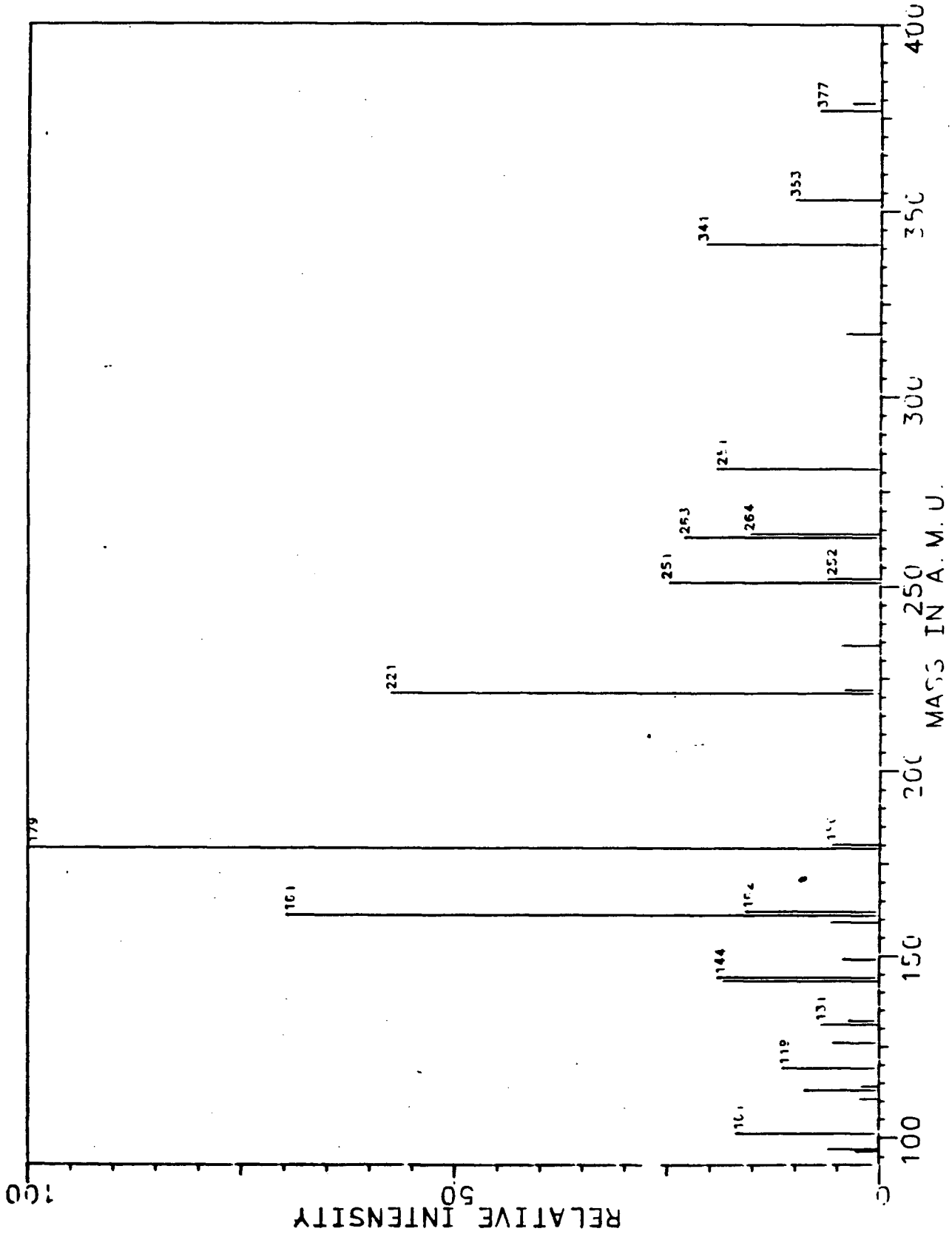

Spec. IV.3 Low resolution positive-ion l.d.i.-F.t.-i.c.r. spectrum of maltose.

Nominal mass	Measured mass	Rel. intensity	Abs. intensity
97. amu	97.02798 amu	31.0 %	10.9138
99. amu	99.04321 amu	7.1 %	2.5178
103. amu	103.03867 amu	11.6 %	4.0837
109. amu	109.02938 amu	4.1 %	1.4302
115. amu	115.03917 amu	5.1 %	1.7886
127. amu	127.03953 amu	41.9 %	14.7449
131. amu	131.03459 amu	6.1 %	2.1602
145. amu	145.04910 amu	100.0 %	35.2197
146. amu	146.05352 amu	7.5 %	2.6262
163. amu	163.06083 amu	56.0 %	19.7100
169. amu	169.05079 amu	10.6 %	3.7173
173. amu	173.04505 amu	2.9 %	1.0374
187. amu	187.06103 amu	17.3 %	6.1038
191. amu	191.05566 amu	4.5 %	1.5852
199. amu	199.06069 amu	3.9 %	1.3691
205. amu	205.07119 amu	9.7 %	3.4275
229. amu	229.07090 amu	23.8 %	8.3918
245. amu	245.06231 amu	8.4 %	2.9712
247. amu	247.08389 amu	12.7 %	4.4607
259. amu	259.08421 amu	4.2 %	1.4658
265. amu	265.09554 amu	13.6 %	4.8013
271. amu	271.08449 amu	12.3 %	4.3235
289. amu	289.09974 amu	5.5 %	1.9504
305. amu	305.08804 amu	33.2 %	11.7104
306. amu	306.08679 amu	5.3 %	1.8762
321. amu	321.05457 amu	16.1 %	5.6655
325. amu	325.11401 amu	24.0 %	8.4424
326. amu	326.11003 amu	4.8 %	1.7002
365. amu	365.10297 amu	71.7 %	25.2476
366. amu	366.11907 amu	9.6 %	3.3799
367. amu	367.11674 amu	6.0 %	2.1262
381. amu	381.08139 amu	23.8 %	8.3906

Spec. IV.4 High resolution positive-ion l.d.i.-F.t.-i.c.r. spectrum of maltose.

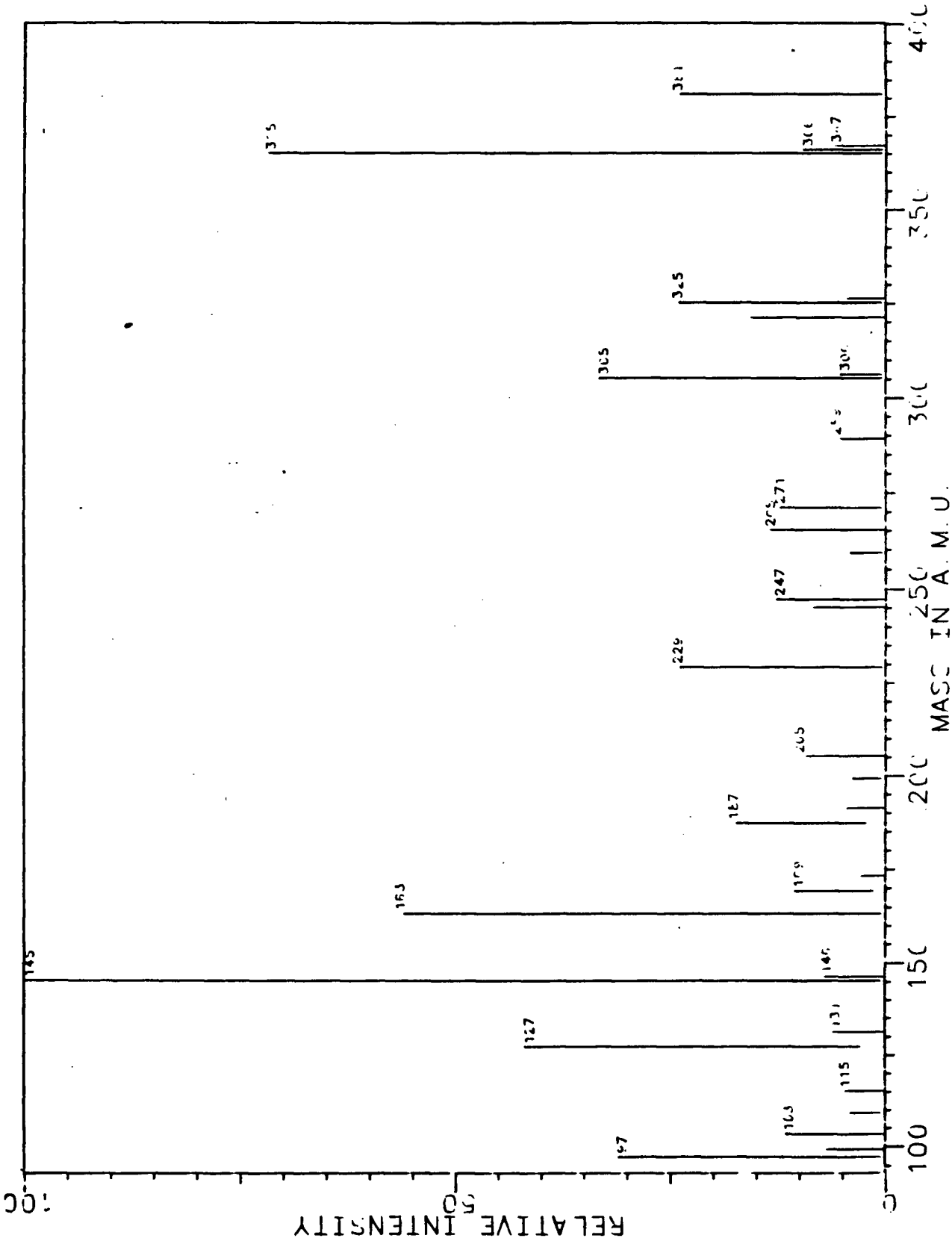

Spec. IV.5 Low resolution negative-ion l.d.i.-F.t.-i.c.r. spectrum of maltose.

Nominal mass	Measured mass	Rel. intensity	Abs. intensity
96. amu	96.39523 amu	2.7 %	1.0608
97. amu	97.03074 amu	6.1 %	2.3792
99. amu	99.00978 amu	2.1 %	805.1758 m
100. amu	100.01795 amu	2.1 %	817.3829 m
101. amu	101.02585 amu	16.9 %	6.5568
110. amu	109.58982 amu	2.0 %	784.7901 m
111. amu	110.53678 amu	2.4 %	931.2745 m
113. amu	113.02697 amu	8.8 %	3.4304
114. amu	114.03412 amu	2.5 %	964.2335 m
119. amu	119.03799 amu	11.4 %	4.4492
126. amu	126.03509 amu	5.5 %	2.1329
127. amu	127.04307 amu	1.6 %	635.6202 m
130. amu	130.02987 amu	1.9 %	757.2022 m
131. amu	131.03777 amu	6.9 %	2.6748
132. amu	132.04714 amu	3.6 %	1.4148
142. amu	142.03157 amu	1.3 %	504.6387 m
143. amu	143.03851 amu	18.4 %	7.1440
144. amu	144.04613 amu	19.1 %	7.4083
145. amu	145.05386 amu	2.1 %	817.5049 m
149. amu	149.04900 amu	4.3 %	1.6694
159. amu	159.03387 amu	5.8 %	2.2588
160. amu	160.04145 amu	1.5 %	585.9375 m
161. amu	160.94215 amu	3.2 %	1.2400
161. amu	161.04883 amu	69.6 %	27.0674
162. amu	162.05644 amu	15.8 %	6.1382
173. amu	173.04999 amu	1.3 %	519.1651 m
178. amu	178.05281 amu	2.4 %	949.9512 m
179. amu	178.92806 amu	3.4 %	1.3070
179. amu	179.05980 amu	100.0 %	38.8710
180. amu	180.06456 amu	6.1 %	2.3660
181. amu	181.06603 amu	1.4 %	559.5704 m
185. amu	185.05444 amu	1.5 %	600.4639 m
209. amu	208.64871 amu	1.2 %	483.5205 m
221. amu	220.86736 amu	2.0 %	791.6260 m
221. amu	221.07135 amu	57.4 %	22.3219
222. amu	222.07716 amu	4.2 %	1.6273
223. amu	223.08178 amu	1.3 %	523.6817 m
234. amu	234.08045 amu	4.7 %	1.8397
251. amu	251.08331 amu	24.8 %	9.6302
252. amu	252.08987 amu	6.3 %	2.4557
263. amu	263.08334 amu	23.0 %	8.9421
264. amu	264.09163 amu	15.4 %	5.9802
265. amu	265.09616 amu	1.6 %	604.8584 m
281. amu	281.09424 amu	19.3 %	7.5093
282. amu	282.09640 amu	2.2 %	845.2149 m
293. amu	293.10104 amu	2.3 %	904.0528 m
317. amu	317.08370 amu	4.2 %	1.6182
319. amu	319.07502 amu	2.3 %	907.8370 m
323. amu	323.12936 amu	1.1 %	440.5518 m
340. amu	340.12009 amu	1.9 %	736.8165 m
341. amu	341.12388 amu	20.5 %	7.9634
342. amu	342.12901 amu	2.8 %	1.0790

Spec. IV.6 High resolution negative-ion l.d.i.-F.t.-i.c.r. spectrum of maltose.

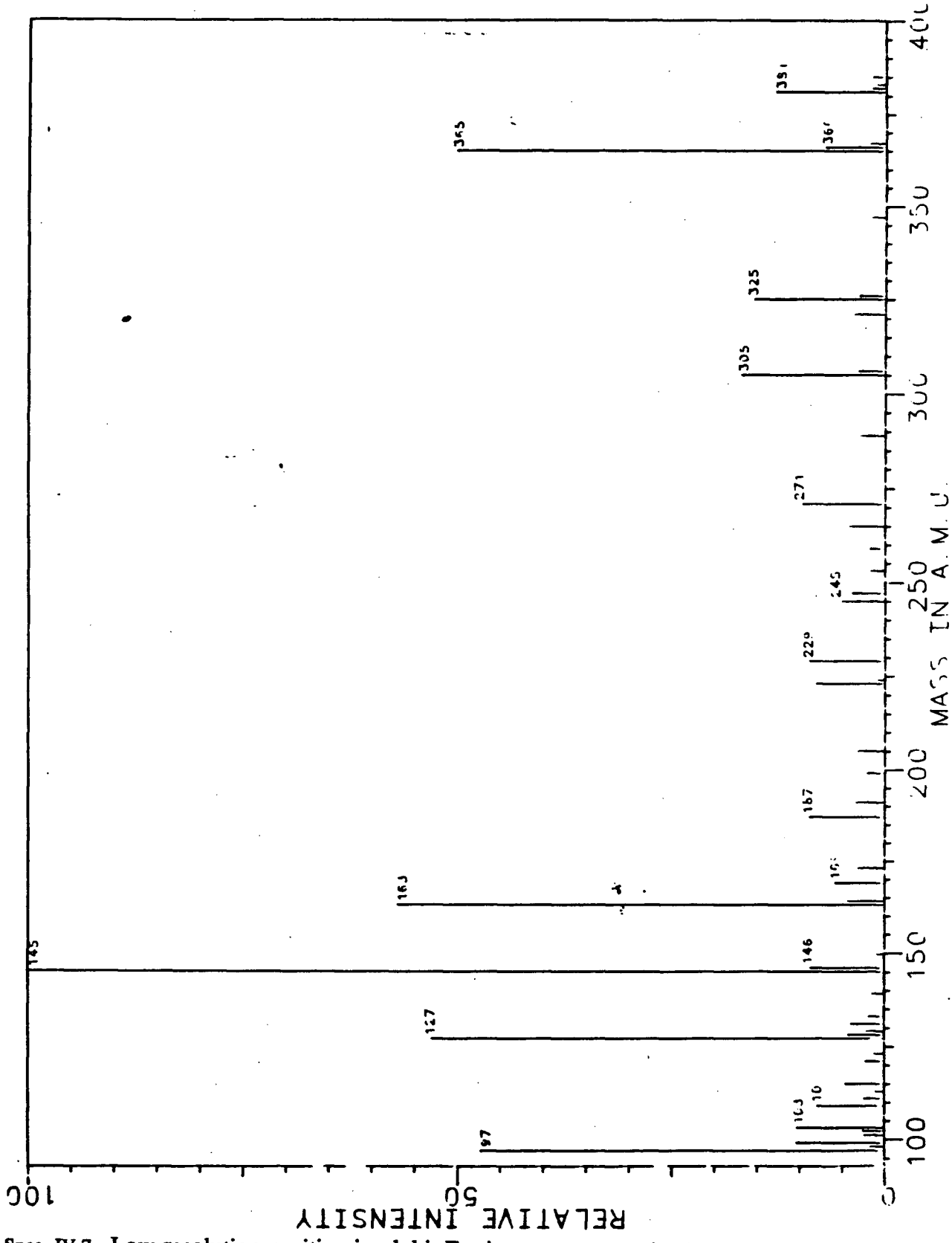

Spec. IV.7 Low resolution positive-ion l.d.i.-F.t.-i.c.r. spectrum of cellobiose.

Nominal mass	Measured mass	Rel. intensity	Abs. intensity
97. amu	97.02796 amu	47.3 %	14.9760
99. amu	99.04297 amu	10.3 %	3.2780
103. amu	103.03896 amu	10.7 %	3.3915
109. amu	109.02935 amu	7.9 %	2.5123
115. amu	115.03939 amu	4.6 %	1.4703
127. amu	127.03985 amu	53.0 %	16.7947
128. amu	128.04235 amu	4.3 %	1.3630
131. amu	131.03520 amu	3.9 %	1.2507
145. amu	145.04899 amu	100.0 %	31.6772
146. amu	146.05420 amu	8.7 %	2.7607
163. amu	163.06076 amu	56.9 %	18.0388
169. amu	169.05131 amu	5.8 %	1.8502
187. amu	187.06159 amu	8.9 %	2.8054
205. amu	205.06935 amu	3.2 %	1.0127
223. amu	223.09723 amu	8.1 %	2.5504
229. amu	229.07417 amu	8.9 %	2.8126
245. amu	245.06191 amu	5.6 %	1.7745
265. amu	265.09583 amu	4.3 %	1.3635
271. amu	271.08924 amu	9.7 %	3.0707
305. amu	305.09277 amu	16.9 %	5.3479
321. amu	321.05221 amu	3.9 %	1.2480
325. amu	325.12740 amu	15.4 %	4.8666
365. amu	365.11009 amu	50.0 %	15.8491
366. amu	366.12288 amu	7.1 %	2.2537
381. amu	381.07965 amu	12.9 %	4.0824

Spec. IV.8 High resolution positive-ion l.d.i.-F.t.-i.c.r. spectrum of cellobiose.

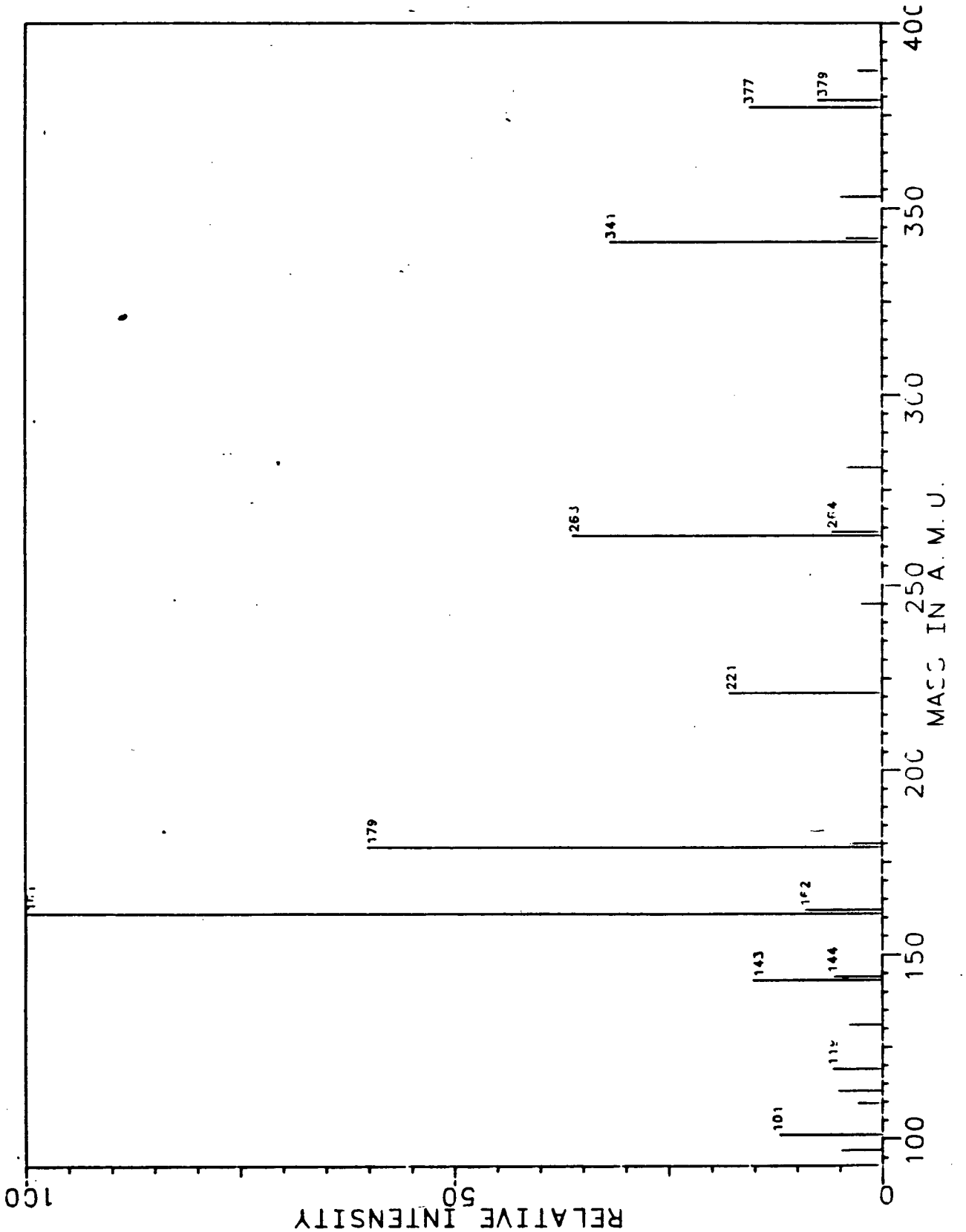

Spec. IV.9 Low resolution negative-ion l.d.i.-F.t.-i.c.r. spectrum of cellobiose.

Nominal mass	Measured mass	Rel. intensity	Abs. intensity
97. amu	97.03105 amu	4.8 %	2.6567
101. amu	101.02667 amu	12.0 %	6.6138
110. amu	109.59081 amu	2.9 %	1.5747
113. amu	113.02776 amu	5.6 %	3.0701
119. amu	119.03863 amu	5.8 %	3.1899
131. amu	131.03919 amu	4.3 %	2.3838
143. amu	143.04009 amu	15.0 %	8.2671
144. amu	144.04772 amu	5.7 %	3.1074
161. amu	161.05019 amu	100.0 %	54.9341
162. amu	162.05629 amu	9.0 %	4.9714
179. amu	179.06297 amu	60.0 %	32.9849
180. amu	180.06919 amu	3.8 %	2.1050
221. amu	221.07701 amu	17.9 %	9.8257
245. amu	245.08070 amu	2.8 %	1.5549
263. amu	263.09127 amu	36.2 %	19.8672
264. amu	264.09470 amu	5.9 %	3.2192
281. amu	281.10914 amu	4.3 %	2.3877
341. amu	341.14146 amu	31.8 %	17.4441
342. amu	342.15577 amu	4.2 %	2.2832
353. amu	353.13494 amu	4.8 %	2.6516
377. amu	377.12893 amu	15.5 %	8.4883
379. amu	379.11234 amu	7.5 %	4.1084
387. amu	387.16607 amu	2.7 %	1.4951

Spec. IV.10 High resolution negative-ion l.d.i.-F.t.-i.c.r. spectrum of cellobiose.

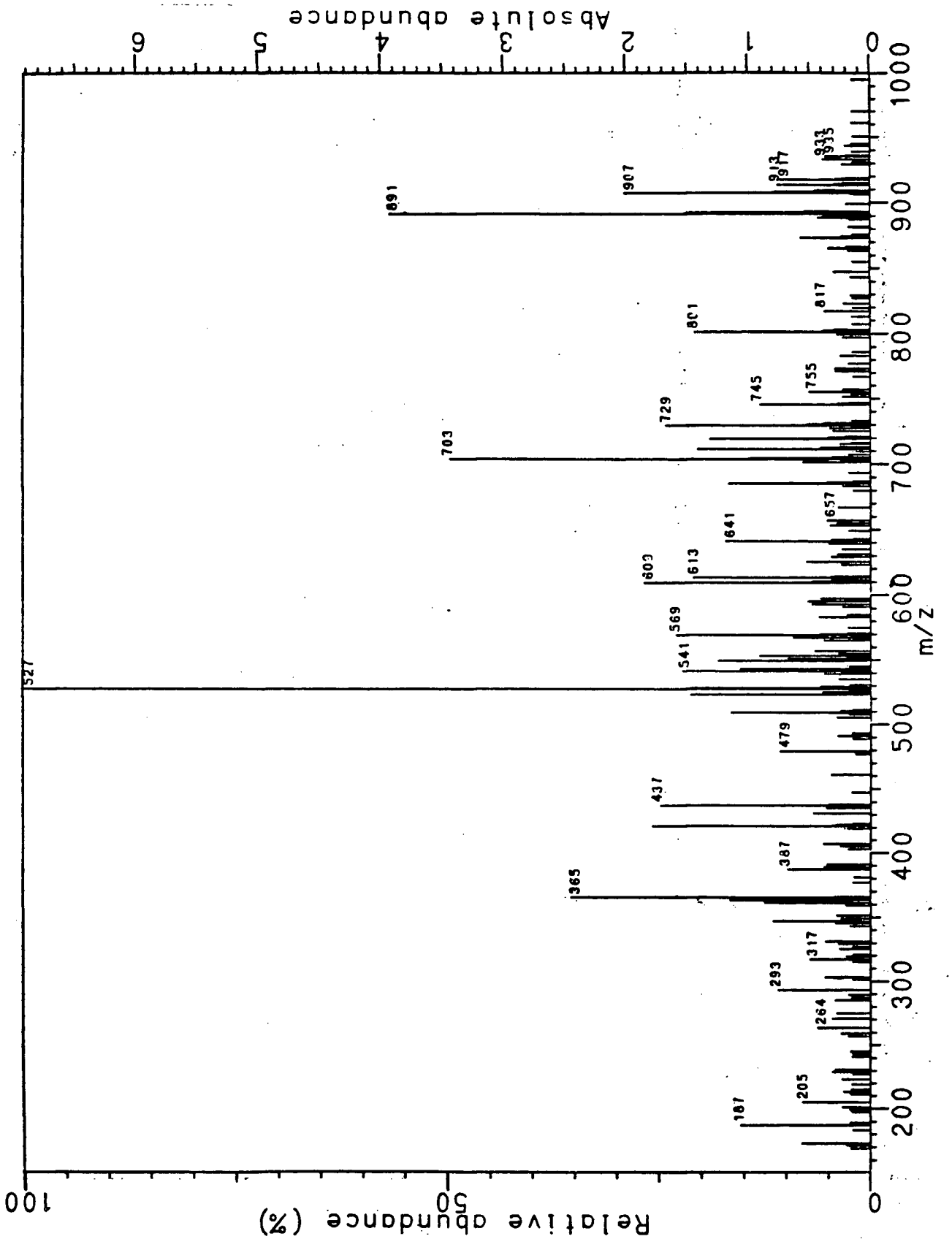

Spec. IV.11 Low resolution positive-ion l.d.i.-F.t.-i.c.r. spectrum of *Klebsiella* K3 oligosaccharide..

Nominal mass	Measured mass	Rel. intensity	Abs. intensity
173 amu	173.04755 amu	8.1151 %	560.974121 m
187 amu	187.06254 amu	15.3512 %	1061.187744 m
205 amu	205.07335 amu	7.9363 %	548.614502 m
264 amu	263.58277 amu	6.2022 %	428.741455 m
293 amu	293.09010 amu	10.9215 %	754.974365 m
303 amu	303.07414 amu	5.3819 %	372.039795 m
317 amu	317.08650 amu	7.1244 %	492.492676 m
331 amu	331.11122 amu	5.3899 %	372.589111 m
347 amu	347.09874 amu	11.4327 %	790.313721 m
361 amu	361.07915 amu	12.4472 %	860.443115 m
363 amu	363.09860 amu	16.5868 %	1146.606445 m
365 amu	365.10627 amu	35.3161 %	2441.314697 m
387 amu	387.08869 amu	9.7790 %	675.994873 m
389 amu	389.10813 amu	5.5325 %	382.446289 m
391 amu	391.13046 amu	5.1379 %	354.827881 m
407 amu	407.11124 amu	5.5625 %	384.521484 m
421 amu	421.09456 amu	25.7292 %	1778.594971 m
431 amu	431.07820 amu	6.7540 %	466.886420 m
435 amu	435.10978 amu	5.2822 %	365.142822 m
437 amu	437.12962 amu	24.7677 %	1712.127686 m
479 amu	479.14189 amu	10.7616 %	739.776611 m
509 amu	509.14977 amu	16.4707 %	1138.580322 m
523 amu	523.12701 amu	21.2536 %	1469.207764 m
524 amu	524.12893 amu	5.5960 %	386.840820 m
525 amu	525.13638 amu	5.6711 %	392.028809 m
527 amu	527.15790 amu	100.0000 %	6913.750244 m
528 amu	528.16895 amu	21.2730 %	1470.550537 m
529 amu	529.17321 amu	5.9364 %	410.369873 m
539 amu	539.09447 amu	5.4972 %	380.004883 m
541 amu	541.13721 amu	22.2010 %	1534.698486 m
543 amu	543.14342 amu	15.4253 %	1066.314697 m
549 amu	549.14199 amu	18.0062 %	1244.720459 m
551 amu	551.15695 amu	9.8187 %	678.741455 m

Spec. IV.12 High resolution positive-ion l.d.i.-F.t.-i.c.r. spectrum of *Klebsiella* K3 oligosaccharide.

553	amu	553.17603	amu	13.1037 %	905.822754 m
557	amu	557.12094	amu	6.6339 %	458.587646 m
565	amu	565.12821	amu	5.5585 %	384.246826 m
567	amu	567.15411	amu	9.1123 %	629.913330 m
569	amu	569.15959	amu	22.9528 %	1586.669922 m
570	amu	570.16926	amu	5.9541 %	411.590576 m
583	amu	583.13305	amu	6.0998 %	421.661377 m
593	amu	593.13605	amu	6.8230 %	471.679688 m
595	amu	595.15354	amu	7.3875 %	510.681152 m
597	amu	597.16117	amu	6.1360 %	424.163818 m
609	amu	609.15524	amu	26.7058 %	1846.069336 m
610	amu	610.16089	amu	6.9770 %	482.299805 m
613	amu	613.15712	amu	20.9591 %	1448.852539 m
625	amu	625.13763	amu	7.5169 %	519.622803 m
641	amu	641.18151	amu	17.0729 %	1180.206299 m
657	amu	657.16526	amu	5.1775 %	357.910156 m
685	amu	685.17414	amu	16.7391 %	1157.135010 m
686	amu	686.16901	amu	5.1056 %	355.010986 m
701	amu	701.14579	amu	8.0047 %	553.344727 m
703	amu	703.18614	amu	49.6855 %	3434.631348 m
704	amu	704.19624	amu	14.2749 %	986.785889 m
711	amu	711.18780	amu	20.4082 %	1410.766602 m
712	amu	712.17067	amu	5.8817 %	406.585693 m
719	amu	719.15531	amu	18.9359 %	1308.990479 m
720	amu	720.14605	amu	5.0107 %	346.374512 m
729	amu	729.20410	amu	24.1717 %	1670.928955 m
730	amu	730.20658	amu	7.4339 %	513.885498 m
731	amu	731.19078	amu	5.4910 %	379.577637 m
745	amu	745.18395	amu	13.0343 %	901.031494 m
755	amu	755.19028	amu	7.2599 %	501.861572 m
801	amu	801.21470	amu	20.7146 %	1431.945801 m
802	amu	802.21342	amu	5.5669 %	384.826660 m
817	amu	817.18921	amu	5.4226 %	374.847412 m
873	amu	873.23701	amu	8.1352 %	562.751221 m
888	amu	888.35460	amu	6.1576 %	425.659180 m
889	amu	889.20085	amu	5.5007 %	380.324219 m
891	amu	891.25044	amu	56.7251 %	3921.264648 m
892	amu	892.26040	amu	21.7869 %	1506.072998 m
893	amu	893.25237	amu	7.6875 %	531.402588 m
907	amu	907.20198	amu	28.9908 %	2004.058838 m
908	amu	908.22112	amu	11.2393 %	776.947021 m
909	amu	909.18495	amu	6.5329 %	451.599121 m
913	amu	913.19913	amu	10.9109 %	754.241943 m
917	amu	917.25661	amu	10.6177 %	733.978271 m
933	amu	933.25635	amu	5.6278 %	389.038086 m
935	amu	935.26465	amu	5.2945 %	365.997314 m

Spec. IV.12 High resolution positive-ion l.d.i.-F.t.-i.c.r. spectrum of *Klebsiella* K3 oligosaccharide, con't.

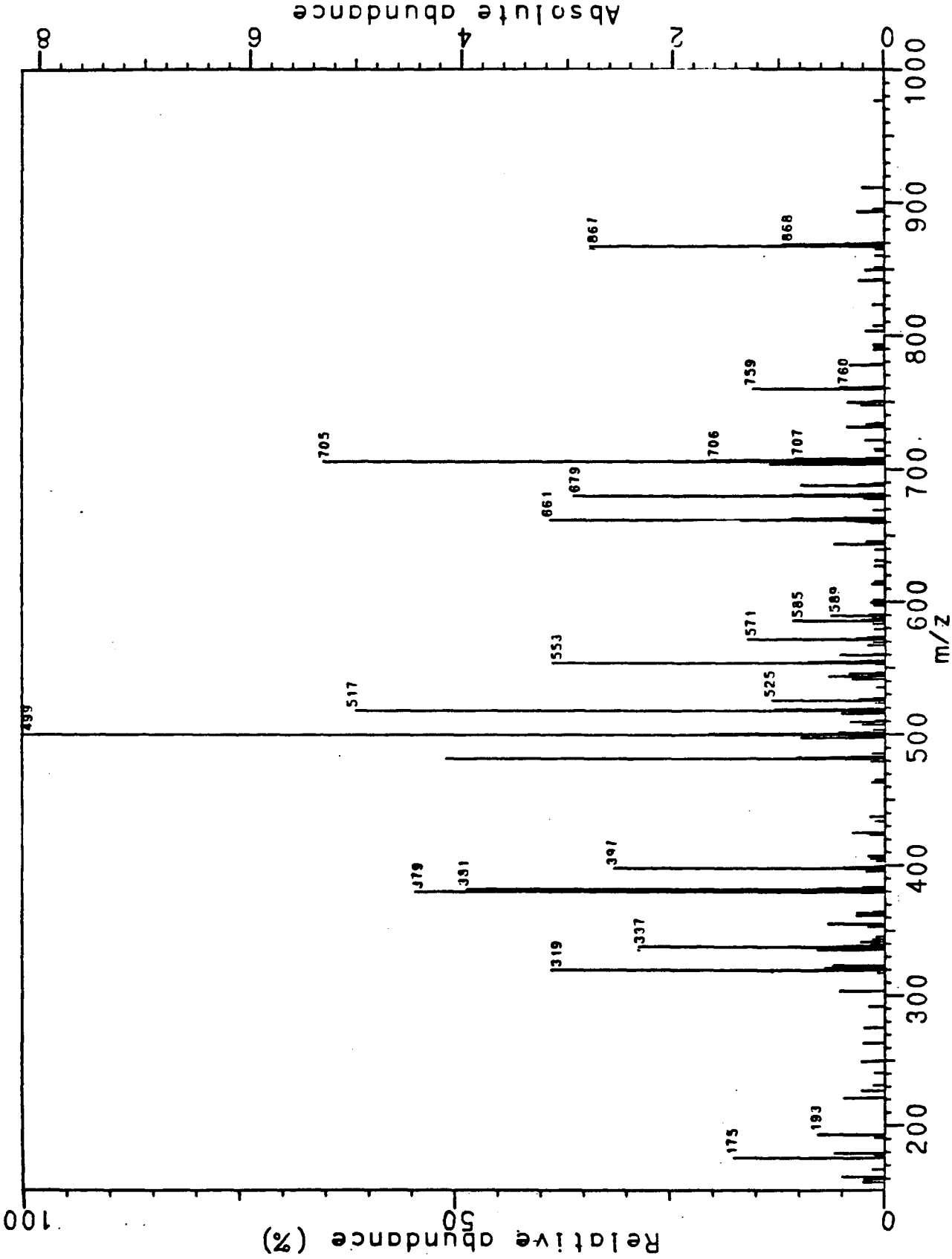

Spec. IV.13 Low resolution negative-ion l.d.i.-F.t.-i.c.r. spectrum of *Klebsiella* K3 oligosaccharide.

Nominal mass	Measured mass	Rel. intensity	Abs. intensity
157 amu	157.01535 amu	2.4756 %	202.099609 m
159 amu	159.03072 amu	2.4122 %	196.923828 m
161 amu	161.04631 amu	4.9613 %	405.029297 m
175 amu	175.02564 amu	17.5113 %	1429.589844 m
179 amu	179.05682 amu	5.8650 %	478.808594 m
193 amu	193.03643 amu	7.7760 %	634.814453 m
221 amu	221.06751 amu	4.7830 %	390.478516 m
227 amu	226.73973 amu	2.7142 %	221.582031 m
249 amu	249.06278 amu	2.7022 %	220.605469 m
263 amu	263.07834 amu	2.4965 %	203.808594 m
275 amu	275.07775 amu	2.3834 %	194.580078 m
303 amu	303.07325 amu	5.2496 %	428.564453 m
319 amu	319.06651 amu	38.6788 %	3157.666016 m
320 amu	320.06976 amu	4.7149 %	384.912109 m
321 amu	321.08369 amu	6.9859 %	570.312500 m
323 amu	323.10024 amu	5.9362 %	484.619141 m
335 amu	335.09930 amu	7.8782 %	643.164062 m
337 amu	337.07685 amu	28.5457 %	2330.419922 m
338 amu	338.08278 amu	4.7974 %	391.650391 m
341 amu	341.11144 amu	2.8518 %	232.812500 m
355 amu	355.08791 amu	6.5917 %	538.134766 m
361 amu	361.07876 amu	3.3536 %	273.779297 m
363 amu	363.09293 amu	3.2776 %	267.578125 m
379 amu	378.65965 amu	2.7794 %	226.904297 m
379 amu	379.08685 amu	54.5399 %	4452.539063 m
380 amu	380.09387 amu	10.3998 %	849.023437 m
381 amu	381.10510 amu	48.5158 %	3960.742187 m
382 amu	382.10787 amu	7.8232 %	638.671875 m
383 amu	383.11490 amu	2.5964 %	211.962891 m
395 amu	395.12164 amu	2.2273 %	181.835938 m
397 amu	397.09773 amu	31.3909 %	2562.695312 m
398 amu	398.10344 amu	4.8590 %	396.679688 m
425 amu	425.08926 amu	3.7992 %	310.156250 m
481 amu	481.12201 amu	50.9064 %	4155.908203 m
482 amu	482.12587 amu	10.2204 %	834.375000 m
483 amu	483.13049 amu	3.9499 %	322.460938 m
497 amu	497.10992 amu	9.8813 %	806.689453 m
498 amu	498.12282 amu	2.2309 %	182.128906 m
498 amu	498.38577 amu	3.7854 %	309.033203 m
499 amu	498.97976 amu	2.0599 %	168.164063 m
499 amu	499.12956 amu	100.0000 %	8163.818359 m
500 amu	500.13698 amu	20.4127 %	1666.455078 m
501 amu	501.14006 amu	5.4918 %	448.339844 m
507 amu	507.13586 amu	2.6263 %	214.404297 m
509 amu	509.15291 amu	4.0922 %	334.082031 m
515 amu	515.12249 amu	5.1485 %	420.312500 m
516 amu	516.36078 amu	4.1622 %	339.794922 m
517 amu	517.13834 amu	61.4151 %	5013.818359 m
518 amu	518.14706 amu	12.8730 %	1050.927734 m
519 amu	519.14561 amu	4.1544 %	339.160156 m
525 amu	525.14819 amu	13.1661 %	1074.853516 m
526 amu	526.15408 amu	3.0031 %	245.166016 m
541 amu	541.14005 amu	3.8105 %	311.083984 m
543 amu	543.15747 amu	6.5863 %	537.695313 m
545 amu	545.13705 amu	4.2459 %	346.630859 m
553 amu	553.14154 amu	38.6232 %	3153.125000 m

Spec. IV.14 High resolution negative-ion l.d.i.-F.t.-i.c.r. spectrum of *Klebsiella* K3 oligosaccharide.

554	amu	554.14677	amu	8.9596	%	731.445312	m
555	amu	555.15359	amu	2.8314	%	231.152344	m
559	amu	559.15472	amu	5.2705	%	430.273438	m
567	amu	567.15365	amu	2.1053	%	171.875000	m
571	amu	571.14206	amu	15.9975	%	1306.005859	m
572	amu	572.14603	amu	3.3661	%	274.804688	m
573	amu	573.15420	amu	2.0120	%	164.257813	m
585	amu	585.16400	amu	10.7234	%	875.439453	m
586	amu	586.17451	amu	2.7698	%	226.123047	m
589	amu	589.16560	amu	6.3106	%	515.185547	m
643	amu	643.17917	amu	5.9380	%	484.765625	m
645	amu	645.19567	amu	2.1580	%	176.171875	m
660	amu	659.90122	amu	3.3667	%	274.853516	m
661	amu	661.18173	amu	38.9043	%	3176.074219	m
662	amu	662.18508	amu	10.8622	%	886.767578	m
663	amu	663.18934	amu	4.7968	%	391.601563	m
678	amu	677.84485	amu	2.4648	%	201.220703	m
679	amu	678.90380	amu	2.1861	%	178.466797	m
679	amu	679.19605	amu	36.1757	%	2953.320312	m
680	amu	680.20202	amu	10.5960	%	865.039063	m
681	amu	681.19835	amu	2.9995	%	244.873047	m
687	amu	687.20232	amu	9.7766	%	798.144531	m
688	amu	688.20417	amu	3.1484	%	257.031250	m
703	amu	703.19243	amu	13.3712	%	1091.601563	m
704	amu	703.75996	amu	5.7687	%	470.947266	m
704	amu	704.20106	amu	4.3034	%	351.318359	m
705	amu	705.20224	amu	65.1036	%	5314.941406	m
706	amu	706.21032	amu	20.1250	%	1642.968750	m
707	amu	707.20407	amu	10.5165	%	858.544922	m
708	amu	708.20853	amu	2.2435	%	183.154297	m
721	amu	721.19356	amu	2.2118	%	180.566406	m
731	amu	731.22004	amu	4.4194	%	360.791016	m
733	amu	733.18738	amu	2.1693	%	177.099609	m
747	amu	747.22866	amu	2.6957	%	220.068359	m
749	amu	749.20120	amu	4.2992	%	350.976563	m
759	amu	759.23024	amu	15.3234	%	1250.976563	m
760	amu	760.23156	amu	5.2484	%	428.466797	m
777	amu	777.21992	amu	4.0910	%	333.984375	m
803	amu	803.20610	amu	2.1215	%	173.193359	m
841	amu	841.25590	amu	2.9624	%	241.845703	m
849	amu	849.24959	amu	2.2112	%	180.517578	m
867	amu	867.28056	amu	34.1362	%	2786.816406	m
868	amu	868.28306	amu	11.8167	%	964.697266	m
869	amu	869.28911	amu	4.4481	%	363.134766	m
893	amu	893.26589	amu	3.1777	%	259.423828	m
911	amu	911.22090	amu	2.5653	%	209.423828	m

Spec. IV.14 High resolution negative-ion l.d.i.-F.t.-i.c.r. spectrum of *Klebsiella* K3 oligosaccharide, con't.

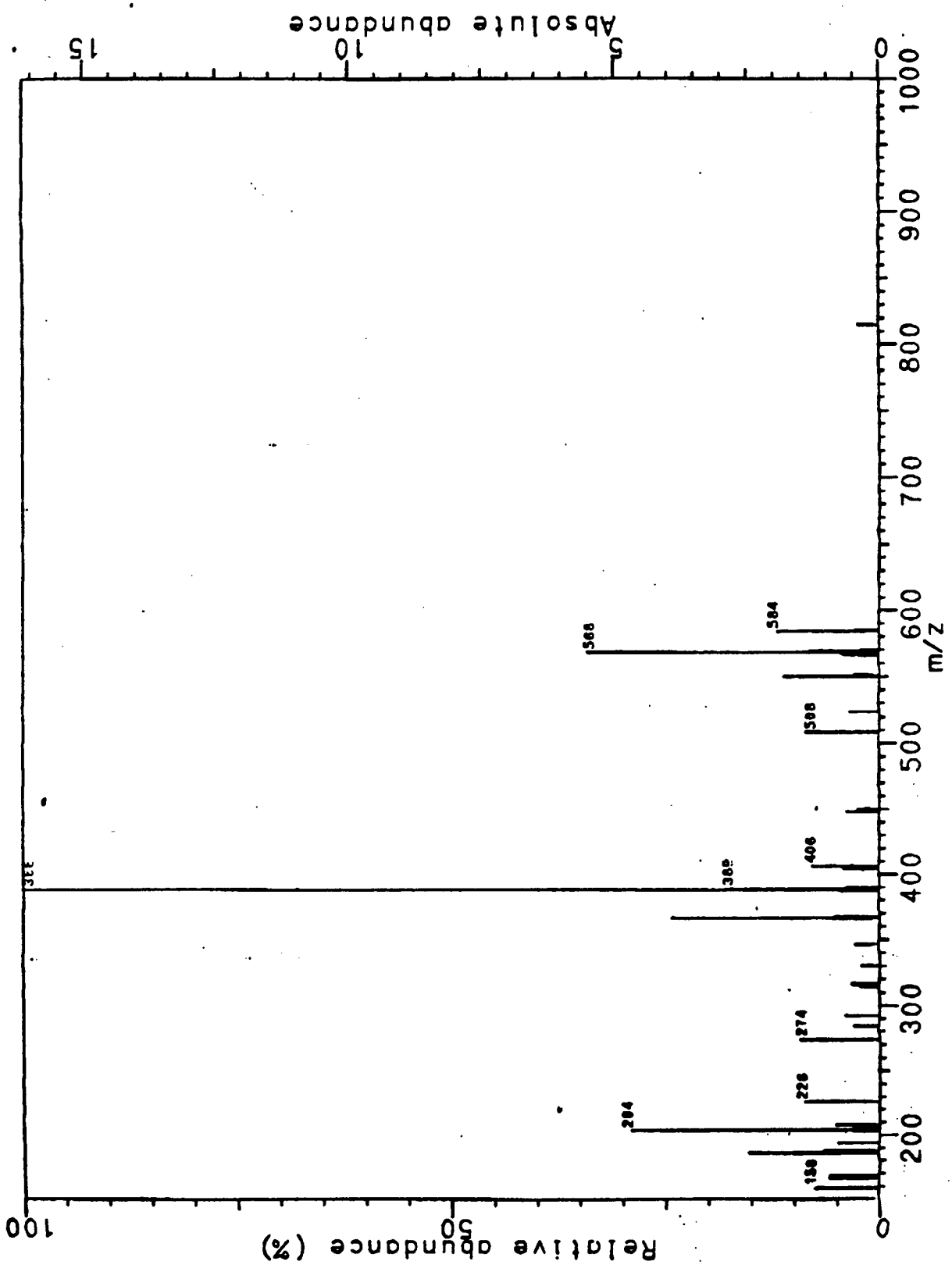

Spec. IV.15 Low resolution positive-ion l.d.i.-F.t.-i.c.r. spectrum of *E. coli* K9 oligosaccharide..

Nominal mass	Measured mass	Rel. intensity	Abs. intensity
158 amu	158.30813 amu	7.5522 %	1219.921875 m
166 amu	166.26356 amu	5.8383 %	943.066406 m
168 amu	168.06632 amu	5.6708 %	916.015625 m
186 amu	186.07621 amu	15.3009 %	2471.582031 m
188 amu	187.79268 amu	6.3920 %	1032.519531 m
204 amu	204.08645 amu	29.0625 %	4694.531250 m
208 amu	208.05762 amu	5.1073 %	825.000000 m
226 amu	226.06826 amu	8.7559 %	1414.355469 m
274 amu	274.09083 amu	9.2909 %	1500.781250 m
366 amu	366.13965 amu	24.3106 %	3926.953125 m
367 amu	367.14015 amu	5.2313 %	845.019531 m
388 amu	387.68734 amu	7.1737 %	1158.789063 m
388 amu	388.11952 amu	100.0000 %	16153.222687 m
389 amu	389.12455 amu	17.3908 %	2809.179687 m
406 amu	406.13025 amu	7.8055 %	1260.839844 m
508 amu	508.16437 amu	8.5854 %	1386.816406 m
550 amu	550.17634 amu	11.1814 %	1806.152344 m
568 amu	568.18814 amu	34.0973 %	5507.812500 m
569 amu	569.19233 amu	8.0927 %	1307.226563 m
584 amu	584.17066 amu	11.8778 %	1918.652344 m

Spec. IV.16 High resolution positive-ion l.d.i.-F.t.-i.c.r. spectrum of *E. coli* K9 oligosaccharide.

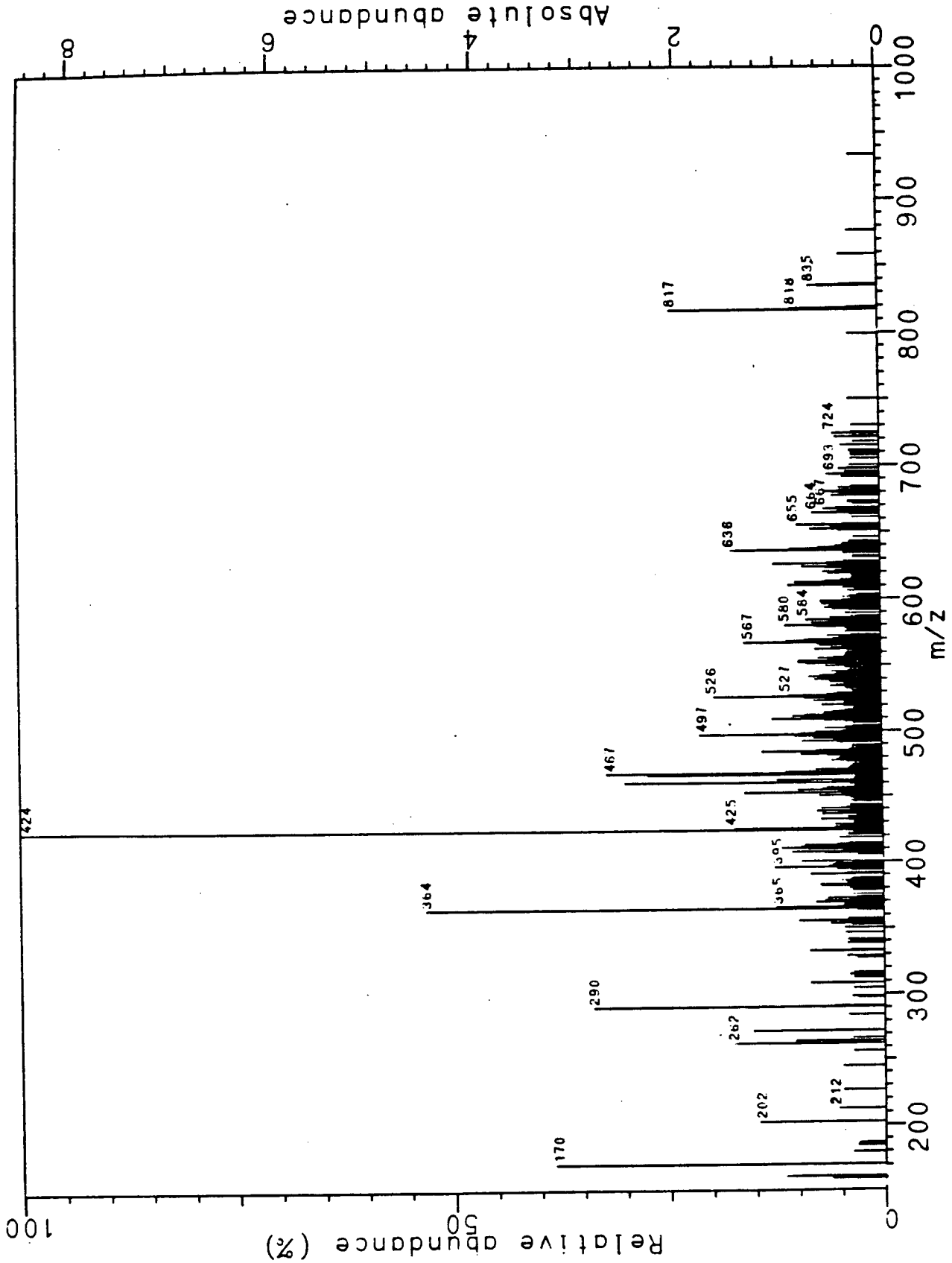

Spec. IV.17 Low resolution negative-ion l.d.i.-F.t.-i.c.r. spectrum of *E. coli* K9 oligosaccharide.

Nominal mass	Measured mass	Rel. intensity	Abs. intensity
159 amu	159.49366 amu	6.2559 %	530.371094 m
161 amu	160.73590 amu	11.7061 %	992.431641 m
170 amu	170.04480 amu	38.3633 %	3252.392578 m
202 amu	202.07084 amu	14.6694 %	1243.652344 m
212 amu	212.07860 amu	5.5112 %	467.236328 m
262 amu	262.08791 amu	17.6395 %	1495.458984 m
264 amu	264.09414 amu	10.4223 %	883.593750 m
272 amu	272.07474 amu	15.2926 %	1296.484375 m
290 amu	290.08815 amu	33.8496 %	2869.726562 m
291 amu	291.08508 amu	5.8113 %	492.675781 m
308 amu	308.09403 amu	8.5856 %	727.880859 m
332 amu	332.08634 amu	8.6265 %	731.347656 m
353 amu	353.13939 amu	6.1580 %	522.070313 m
355 amu	355.15804 amu	9.8810 %	837.695313 m
364 amu	364.11388 amu	53.1939 %	4509.716797 m
365 amu	365.11853 amu	12.5614 %	1064.941406 m
369 amu	369.14954 amu	7.9112 %	670.703125 m
370 amu	370.14022 amu	6.8325 %	579.248047 m
372 amu	372.09508 amu	6.5307 %	553.662109 m
381 amu	381.17351 amu	7.0847 %	600.634766 m
382 amu	382.12471 amu	7.3548 %	623.535156 m
390 amu	390.10935 amu	8.5033 %	720.898437 m
394 amu	394.12061 amu	5.3926 %	457.177734 m
395 amu	395.15934 amu	12.6570 %	1073.046875 m
396 amu	396.16276 amu	6.3245 %	536.181641 m
397 amu	397.17559 amu	5.9363 %	503.271484 m
398 amu	398.16979 amu	5.6564 %	479.541016 m
400 amu	400.08613 amu	9.5187 %	806.982422 m
406 amu	406.16413 amu	6.7950 %	576.074219 m
407 amu	407.15304 amu	10.6366 %	901.757812 m
409 amu	409.16689 amu	8.6288 %	731.542969 m
7-'88 16:34 ID:NICOLET INSTRUMENTS ... TEL NO:1608-...		... %	... m
411 amu	411.17614 amu	9.5561 %	810.156250 m
412 amu	412.17435 amu	9.1409 %	774.951172 m
413 amu	413.16830 amu	5.3724 %	455.468750 m
418 amu	418.11402 amu	5.1392 %	435.693359 m
424 amu	424.13016 amu	100.0000 %	8477.880859 m
425 amu	425.14126 amu	17.2859 %	1465.478516 m
426 amu	426.13883 amu	5.5579 %	471.191406 m
428 amu	428.17097 amu	5.6374 %	477.929688 m
432 amu	432.12512 amu	7.1884 %	609.423828 m
436 amu	436.15662 amu	7.0387 %	596.728516 m
437 amu	437.19004 amu	5.0591 %	428.906250 m
438 amu	438.17940 amu	7.6762 %	650.781250 m
440 amu	440.18018 amu	7.1158 %	603.271484 m
450 amu	450.14200 amu	7.3848 %	626.074219 m
452 amu	452.13349 amu	16.0655 %	1362.011719 m
453 amu	453.12806 amu	5.0557 %	428.613281 m
454 amu	454.16195 amu	9.8556 %	835.546875 m
455 amu	455.17506 amu	6.9822 %	591.943359 m
456 amu	456.17697 amu	6.4662 %	548.193359 m
460 amu	460.12225 amu	29.9412 %	2538.378906 m
461 amu	461.10968 amu	5.5723 %	472.412109 m
462 amu	462.11058 amu	12.2959 %	1042.431641 m
466 amu	466.15643 amu	27.2561 %	2310.742187 m
467 amu	467.17213 amu	32.0924 %	2720.751953 m

Spec. IV.18 High resolution negative-ion l.d.i.-F.t.-i.c.r. spectrum of *E. coli* K9 oligosaccharide.

468	amu	468.18183	amu	11.2845	%	956.689453	m
469	amu	469.16860	amu	6.3855	%	541.357422	m
470	amu	470.14403	amu	7.7442	%	656.542969	m
477	amu	477.17352	amu	5.9236	%	502.197266	m
478	amu	478.20777	amu	5.3183	%	450.878906	m
479	amu	479.19326	amu	5.0465	%	427.832031	m
481	amu	481.18539	amu	6.2790	%	532.324219	m
482	amu	482.19320	amu	9.4461	%	800.830078	m
483	amu	483.20342	amu	9.0942	%	770.996094	m
484	amu	484.16614	amu	13.9541	%	1183.007812	m
485	amu	485.19501	amu	7.6981	%	652.636719	m
491	amu	491.16165	amu	5.2417	%	444.384766	m
492	amu	492.15000	amu	9.3062	%	788.964844	m
493	amu	493.18692	amu	5.6748	%	481.103516	m
494	amu	494.21875	amu	7.8997	%	669.726562	m
495	amu	495.21210	amu	7.9579	%	674.658203	m
496	amu	496.19645	amu	10.2087	%	865.478516	m
497	amu	497.19203	amu	21.2461	%	1801.220703	m
498	amu	498.19956	amu	9.4185	%	798.486328	m
499	amu	499.20624	amu	7.7413	%	656.298828	m
502	amu	502.12117	amu	6.7017	%	568.164063	m
508	amu	508.19450	amu	6.7011	%	568.115234	m
509	amu	509.20630	amu	12.7353	%	1079.687500	m
510	amu	510.21371	amu	9.3079	%	789.111328	m
511	amu	511.22722	amu	10.3158	%	874.560547	m
512	amu	512.20962	amu	8.9232	%	756.494141	m
513	amu	513.22677	amu	6.6436	%	563.232422	m
514	amu	514.21232	amu	6.6850	%	566.748047	m
515	amu	515.20298	amu	5.6477	%	478.808594	m
520	amu	520.12551	amu	6.9338	%	587.841797	m
523	amu	523.22170	amu	7.8888	%	668.798828	m
524	amu	524.21320	amu	6.5399	%	554.443359	m
525	amu	525.20958	amu	8.9715	%	760.595703	m
526	amu	526.17757	amu	19.5045	%	1653.564453	m
527	amu	527.19454	amu	10.8670	%	921.289062	m
528	amu	528.20073	amu	6.3815	%	541.015625	m
529	amu	529.21390	amu	5.1881	%	439.843750	m
534	amu	534.19370	amu	5.9973	%	508.447266	m
535	amu	535.18408	amu	5.2763	%	447.314453	m
538	amu	538.22064	amu	6.1016	%	517.285156	m
539	amu	539.24760	amu	7.7701	%	658.740234	m
540	amu	540.23895	amu	7.2621	%	615.673828	m
541	amu	541.21125	amu	8.4319	%	714.843750	m
542	amu	542.19985	amu	7.1631	%	607.275391	m
543	amu	543.17664	amu	5.5164	%	467.675781	m
544	amu	544.19368	amu	5.2849	%	448.046875	m
545	amu	545.18600	amu	5.8320	%	494.433594	m
549	amu	549.21626	amu	6.5024	%	551.269531	m
550	amu	550.25027	amu	5.1207	%	434.130859	m
551	amu	551.24158	amu	8.5995	%	729.052734	m
552	amu	552.18347	amu	9.6869	%	821.240234	m
553	amu	553.23551	amu	9.5924	%	813.232422	m
554	amu	554.23845	amu	6.2277	%	527.978516	m
555	amu	555.19666	amu	7.3658	%	624.462891	m
556	amu	556.20750	amu	5.5936	%	474.218750	m
562	amu	562.15277	amu	7.7355	%	655.810547	m
563	amu	563.23968	amu	5.8545	%	496.337891	m
565	amu	565.27364	amu	7.1556	%	606.640625	m
566	amu	566.28549	amu	7.3848	%	626.074219	m

Spec. IV.18 High resolution negative-ion l.d.i.-F.t.-i.c.r. spectrum of *E. coli* K9 oligosaccharide, con't.

567	amu	567.25886	amu	15.9416	%	1351.513672	m
568	amu	568.24310	amu	11.0012	%	932.666016	m
569	amu	569.24199	amu	8.8650	%	751.562500	m
570	amu	570.22537	amu	5.5418	%	469.824219	m
572	amu	572.22374	amu	6.3141	%	535.302734	m
579	amu	579.26379	amu	7.6636	%	649.707031	m
580	amu	580.16251	amu	11.1699	%	946.972656	m
581	amu	581.21563	amu	7.4700	%	633.300781	m
582	amu	582.17991	amu	7.9654	%	675.292969	m
583	amu	583.22092	amu	5.9829	%	507.226562	m
584	amu	584.22680	amu	8.7400	%	740.966797	m
586	amu	586.17518	amu	5.9426	%	503.808594	m
592	amu	592.25132	amu	5.6259	%	476.953125	m
593	amu	593.24039	amu	6.5825	%	558.056641	m
594	amu	594.27166	amu	6.0423	%	512.255859	m
596	amu	596.24197	amu	6.8762	%	582.958984	m
597	amu	597.26007	amu	6.8065	%	577.050781	m
598	amu	598.24926	amu	7.0974	%	601.708984	m
610	amu	610.25418	amu	10.7339	%	910.009766	m
611	amu	611.26193	amu	9.2872	%	787.353516	m
612	amu	612.22248	amu	9.9581	%	844.238281	m
613	amu	613.22044	amu	6.4944	%	550.585938	m
619	amu	619.22210	amu	6.0682	%	514.453125	m
620	amu	620.27371	amu	6.7484	%	572.119141	m
621	amu	621.24261	amu	5.2123	%	441.894531	m
623	amu	623.23474	amu	6.4408	%	546.044922	m
624	amu	624.09377	amu	9.1662	%	777.099609	m
625	amu	625.24137	amu	5.9086	%	500.927735	m
626	amu	626.10181	amu	12.4911	%	1058.984375	m
627	amu	627.21042	amu	6.2162	%	527.001953	m
636	amu	636.31231	amu	17.4702	%	1481.103516	m
637	amu	637.29440	amu	10.5001	%	890.185547	m
638	amu	638.26519	amu	7.1786	%	608.593750	m
639	amu	639.30133	amu	5.2659	%	446.435547	m
652	amu	652.32108	amu	8.1704	%	692.675781	m
653	amu	653.28205	amu	5.7295	%	485.742188	m
655	amu	655.23636	amu	9.6886	%	821.386719	m
664	amu	664.34188	amu	7.8755	%	667.675781	m
667	amu	667.27066	amu	6.6004	%	559.570313	m
668	amu	668.25821	amu	5.0856	%	431.152344	m
677	amu	677.27166	amu	5.6195	%	476.416016	m
679	amu	679.25608	amu	5.4980	%	466.113281	m
680	amu	680.27322	amu	6.4034	%	542.871094	m
721	amu	721.39881	amu	5.1599	%	437.451172	m
724	amu	724.29827	amu	5.4790	%	464.501953	m
817	amu	817.27382	amu	24.2480	%	2055.712891	m
818	amu	818.28671	amu	10.2271	%	867.041016	m
835	amu	835.28946	amu	8.0909	%	685.937500	m

Spec. IV.18 High resolution negative-ion l.d.i.-F.t.-i.c.r. spectrum of *E. coli* K9 oligosaccharide, con't.

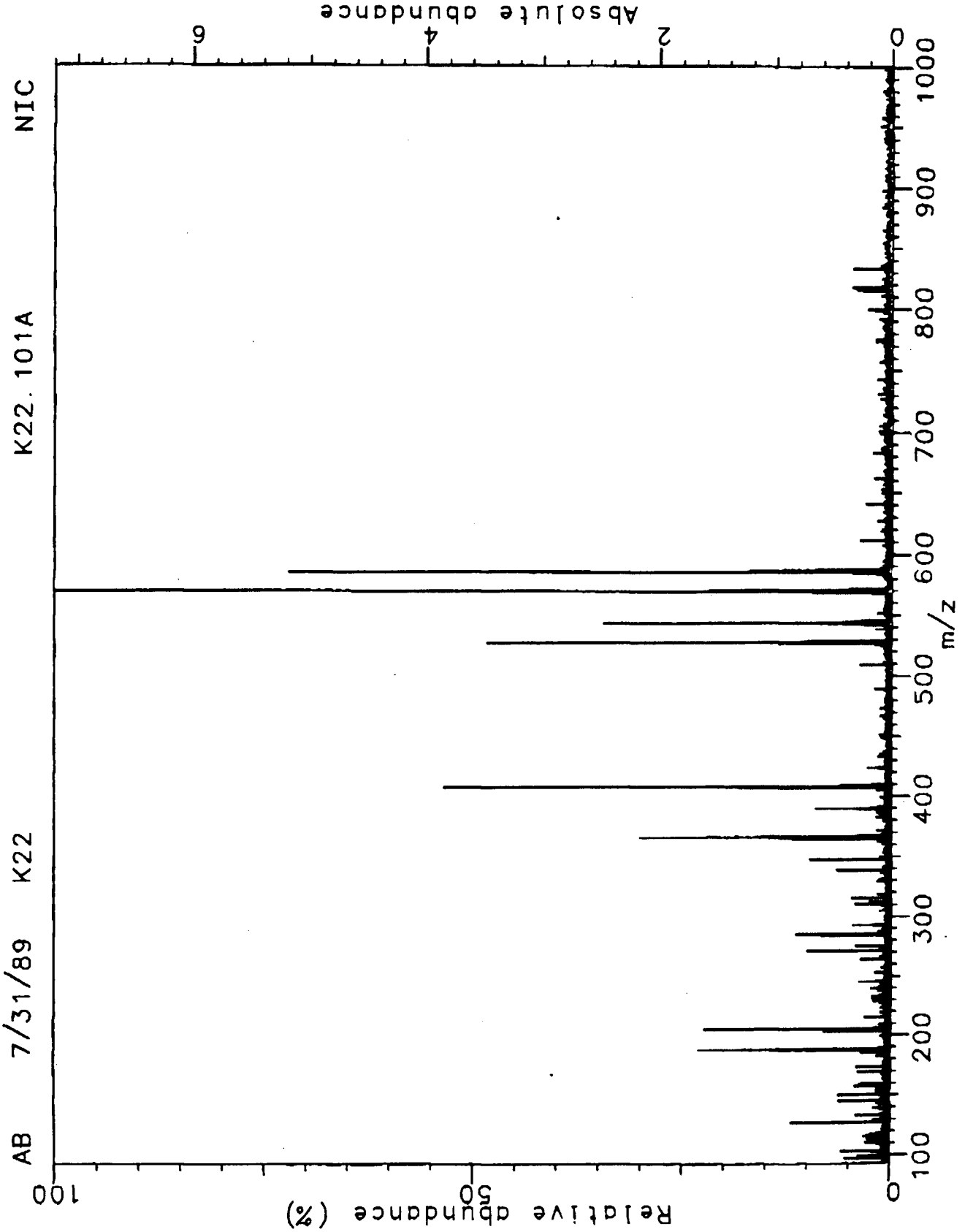

Spec. IV.19 Low resolution positive-ion l.d.i.-F.t.-i.c.r. spectrum of *Klebsiella* K22 oligosaccharide..

Nominal mass	Measured mass	Rel. intensity	Abs. intensity
94 amu	93.53036 amu	1.4387 %	253.784180 m
97 amu	97.02904 amu	2.5279 %	445.922852 m
99 amu	99.04397 amu	1.8366 %	323.974609 m
102 amu	102.21946 amu	1.4242 %	251.220703 m
103 amu	102.53582 amu	1.8601 %	328.125000 m
103 amu	103.03929 amu	3.6026 %	635.498047 m
110 amu	110.48207 amu	2.1522 %	379.638672 m
115 amu	115.03884 amu	2.0809 %	367.065430 m
127 amu	127.03945 amu	8.0800 %	1425.292969 m
129 amu	129.05383 amu	1.4885 %	262.573242 m
133 amu	132.90525 amu	3.7161 %	655.517578 m
133 amu	133.04978 amu	1.6276 %	287.109375 m
145 amu	145.04929 amu	4.0227 %	709.594727 m
150 amu	149.71473 amu	3.8788 %	684.204102 m
153 amu	153.05544 amu	1.5390 %	271.484375 m
155 amu	155.03154 amu	1.4366 %	253.417969 m
157 amu	157.05030 amu	3.4456 %	607.788086 m
159 amu	159.02939 amu	2.3729 %	418.579102 m
169 amu	169.04912 amu	3.7826 %	667.236328 m
173 amu	173.04386 amu	3.3404 %	589.233398 m
185 amu	185.04306 amu	3.3051 %	583.007813 m
187 amu	187.06018 amu	23.4116 %	4129.760742 m
188 amu	188.06247 amu	1.8311 %	322.998047 m
203 amu	203.05276 amu	9.4191 %	1661.499023 m
205 amu	204.92232 amu	2.2705 %	400.512695 m
205 amu	205.07030 amu	26.3306 %	4644.653320 m
206 amu	206.07386 amu	1.9688 %	347.290039 m
209 amu	209.03993 amu	1.7591 %	310.302734 m
215 amu	215.05613 amu	2.9556 %	521.362305 m
227 amu	227.05096 amu	2.0338 %	358.764648 m
229 amu	229.07024 amu	2.1252 %	374.877930 m
231 amu	231.05149 amu	1.6442 %	290.039063 m
233 amu	233.06574 amu	2.2968 %	405.151367 m
245 amu	245.06185 amu	3.1736 %	559.814453 m
253 amu	253.03845 amu	1.8034 %	318.115234 m
257 amu	257.06274 amu	1.4214 %	250.732422 m
264 amu	263.57396 amu	3.3680 %	594.116211 m
271 amu	271.04263 amu	12.7061 %	2241.333008 m
275 amu	275.07516 amu	2.8248 %	498.291016 m
285 amu	284.58033 amu	11.2833 %	1990.356445 m
285 amu	285.08217 amu	3.1148 %	549.438477 m
293 amu	292.57330 amu	1.7051 %	300.781250 m
329 amu	329.09107 amu	1.5785 %	278.442383 m
347 amu	347.09418 amu	9.0371 %	1594.116211 m
349 amu	349.11490 amu	1.9051 %	336.059570 m
365 amu	364.62844 amu	2.8317 %	499.511719 m
365 amu	365.10536 amu	23.8864 %	4213.500977 m
366 amu	366.10968 amu	3.0476 %	537.597656 m
375 amu	375.02189 amu	1.5550 %	274.291992 m
389 amu	389.10226 amu	8.1457 %	1436.889648 m
390 amu	390.10495 amu	1.4000 %	246.948242 m
407 amu	406.52575 amu	2.8539 %	503.417969 m
407 amu	407.11523 amu	41.9556 %	7400.878906 m
408 amu	408.11672 amu	6.5942 %	1163.208008 m
409 amu	409.11058 amu	1.6781 %	296.020508 m
435 amu	435.10268 amu	1.4442 %	254.760742 m

Spec. IV.20 High resolution positive-ion l.d.i.-F.t.-i.c.r. spectrum of *Klebsiella* K22 oligosaccharide.

509	amu	509.14772	amu	3.4961	%	616.699219	m
526	amu	526.17843	amu	2.6110	%	460.571289	m
527	amu	526.64842	amu	1.7446	%	307.739258	m
527	amu	527.15477	amu	50.5720	%	8920.776367	m
528	amu	528.15965	amu	11.2314	%	1981.201172	m
529	amu	529.14901	amu	3.0553	%	538.940430	m
543	amu	543.12971	amu	15.0977	%	2663.208008	m
544	amu	544.12788	amu	2.7750	%	489.501953	m
545	amu	545.13283	amu	1.7231	%	303.955078	m
551	amu	551.14761	amu	1.8228	%	321.533203	m
568	amu	567.97008	amu	1.9356	%	341.430664	m
569	amu	568.60685	amu	3.2386	%	571.289063	m
569	amu	569.16087	amu	100.0000	%	17639.770508	m
570	amu	570.16937	amu	21.4602	%	3785.522461	m
571	amu	571.17809	amu	5.6088	%	989.379883	m
584	amu	583.97258	amu	2.2110	%	390.014648	m
585	amu	585.14293	amu	29.1935	%	5149.658203	m
586	amu	586.14278	amu	6.9742	%	1230.224609	m
587	amu	587.15141	amu	4.2504	%	749.755859	m
611	amu	611.17594	amu	3.8933	%	686.767578	m
641	amu	641.17731	amu	3.6082	%	636.474609	m
683	amu	683.23459	amu	2.4470	%	431.640625	m
685	amu	685.18407	amu	1.7411	%	307.128906	m
727	amu	727.20140	amu	1.5605	%	275.268555	m
731	amu	731.24246	amu	1.5245	%	268.920898	m
757	amu	757.18150	amu	1.7563	%	309.814453	m
799	amu	799.25831	amu	3.4324	%	605.468750	m
815	amu	815.23083	amu	1.9729	%	348.022461	m
817	amu	817.22371	amu	4.4504	%	785.034180	m
833	amu	833.16937	amu	2.0186	%	356.079102	m

Spec. IV.20 High resolution positive-ion l.d.i.-F.t.-i.c.r. spectrum of *Klebsiella* K22 oligosaccharide, con't.

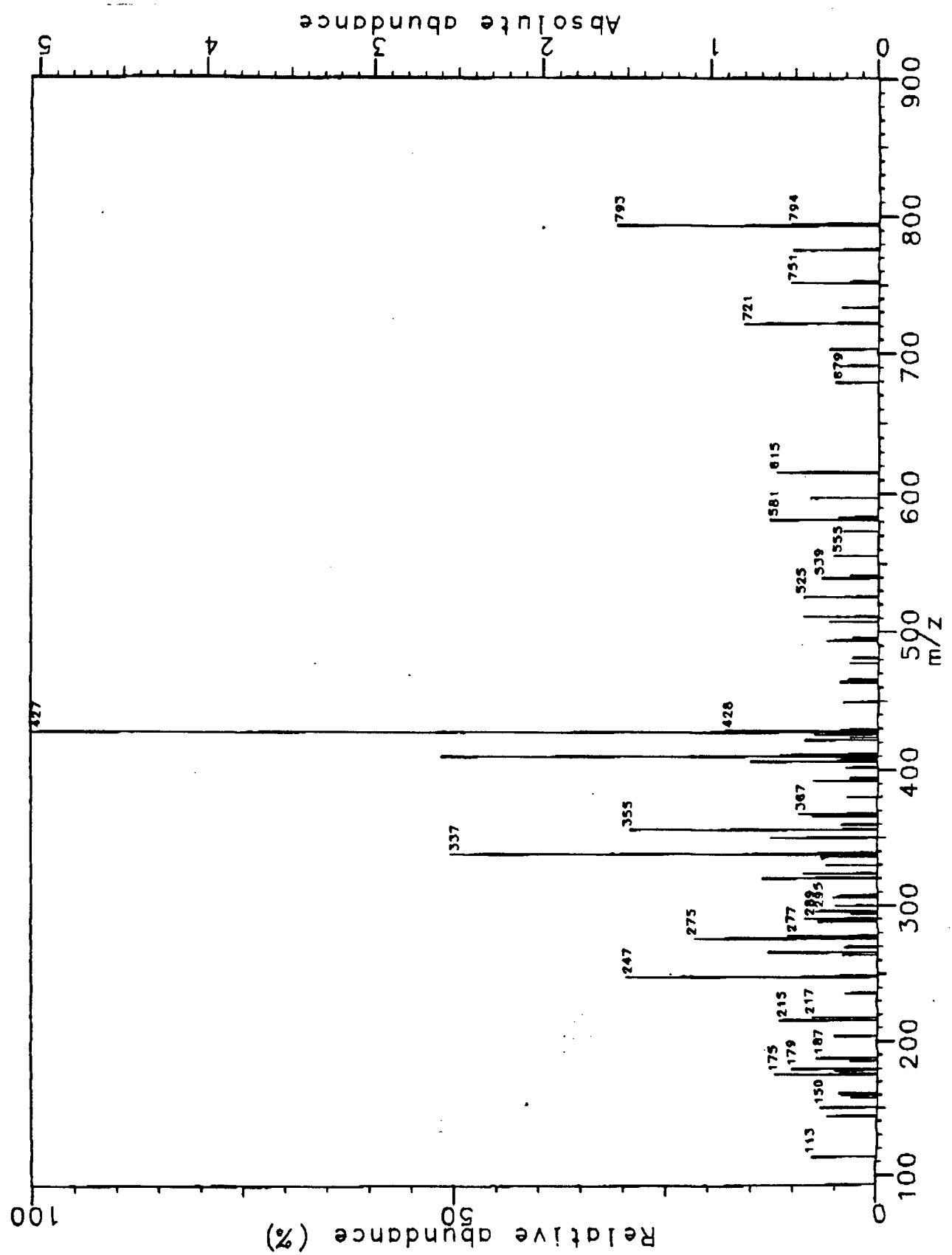

Spec. IV.21 Low resolution negative-ion l.d.i.-F.t.-i.c.r. spectrum of *Klebsiella* K22 oligosaccharide.

Nominal mass	Measured mass	Rel. intensity	Abs. intensity
113 amu	113.02327 amu	7.6821 %	387.939453 m
143 amu	143.03333 amu	5.8140 %	293.599446 m
150 amu	149.72364 amu	6.7877 %	342.773438 m
157 amu	157.01422 amu	3.0579 %	154.418945 m
159 amu	159.03148 amu	4.2729 %	215.779623 m
161 amu	161.04603 amu	4.4643 %	225.443522 m
175 amu	175.02329 amu	12.1641 %	614.278158 m
178 amu	178.04629 amu	4.9449 %	249.715169 m
179 amu	179.05487 amu	10.1570 %	512.919107 m
185 amu	185.04541 amu	3.2859 %	165.934245 m
187 amu	187.06000 amu	7.2265 %	364.929199 m
203 amu	203.05633 amu	5.0485 %	254.943848 m
215 amu	215.03153 amu	11.5445 %	582.987467 m
217 amu	217.03336 amu	7.7409 %	390.909831 m
235 amu	235.04647 amu	3.6960 %	186.645508 m
247 amu	247.04399 amu	29.6878 %	1499.206543 m
248 amu	248.05043 amu	4.4857 %	226.521810 m
263 amu	263.07355 amu	3.9736 %	200.663249 m
265 amu	265.05646 amu	12.9171 %	652.303061 m
269 amu	269.08194 amu	3.7871 %	191.243490 m
275 amu	275.07676 amu	21.5766 %	1089.599609 m
276 amu	276.08304 amu	3.8572 %	194.783529 m
277 amu	277.05552 amu	10.5659 %	533.569336 m
287 amu	287.03629 amu	7.0202 %	354.512532 m
288 amu	288.08288 amu	4.1154 %	207.824707 m
289 amu	289.05273 amu	8.5697 %	432.759603 m
293 amu	293.08495 amu	3.1392 %	158.528646 m
295 amu	295.06693 amu	7.3804 %	372.701009 m
299 amu	299.04892 amu	5.0146 %	253.234863 m
305 amu	305.09000 amu	5.2390 %	264.567058 m
306 amu	306.08941 amu	4.7608 %	240.417480 m
307 amu	307.05482 amu	4.3132 %	217.814127 m
319 amu	319.06568 amu	13.5247 %	682.983398 m
320 amu	320.07485 amu	7.0923 %	358.154297 m
323 amu	323.09707 amu	8.7663 %	442.687988 m
329 amu	329.04188 amu	5.9300 %	299.458821 m
335 amu	335.05683 amu	6.6979 %	338.236491 m
337 amu	336.70920 amu	2.9491 %	148.925781 m
337 amu	337.07562 amu	50.4168 %	2546.000160 m
338 amu	338.07879 amu	7.0963 %	358.357747 m
349 amu	349.07469 amu	12.5461 %	633.565268 m
355 amu	355.08649 amu	29.2241 %	1475.789387 m
356 amu	356.08625 amu	4.1029 %	207.194010 m
359 amu	359.05648 amu	4.0191 %	202.962240 m
359 amu	359.12087 amu	4.1960 %	211.893717 m
365 amu	365.10350 amu	7.7288 %	390.299479 m
366 amu	366.11443 amu	3.5977 %	181.681315 m
367 amu	367.08368 amu	9.3247 %	470.886230 m
379 amu	379.08487 amu	3.4225 %	172.831217 m
391 amu	391.08665 amu	7.5733 %	382.446289 m
393 amu	393.09877 amu	3.3044 %	166.870117 m
401 amu	401.07614 amu	3.6900 %	186.340332 m
405 amu	405.10474 amu	14.9444 %	754.679361 m
406 amu	406.10491 amu	3.4378 %	173.604330 m
407 amu	407.07869 amu	4.2246 %	213.338216 m

Spec. IV.22 High resolution negative-ion l.d.i.-F.t.-i.c.r. spectrum of *Klebsiella* K22 oligosaccharide.

409 amu	409.09895 amu	51.5352 %	2602.478027 m
410 amu	410.10311 amu	11.4466 %	578.043619 m
411 amu	411.11287 amu	3.3608 %	169.718424 m
421 amu	421.10048 amu	8.6341 %	436.014812 m
423 amu	423.12063 amu	3.2359 %	163.411458 m
425 amu	425.08669 amu	7.5540 %	381.469727 m
427 amu	426.52266 amu	6.1919 %	312.683105 m
427 amu	427.10978 amu	100.0000 %	5049.906418 m
428 amu	428.11567 amu	18.0192 %	909.952799 m
429 amu	429.11678 amu	4.4011 %	222.249349 m
449 amu	449.08971 amu	3.9369 %	198.811849 m
463 amu	463.09710 amu	4.4152 %	222.961426 m
465 amu	465.13098 amu	3.4358 %	173.502604 m
477 amu	477.13950 amu	3.3669 %	170.023600 m
481 amu	481.11229 amu	2.9531 %	149.129232 m
493 amu	493.12016 amu	6.0621 %	306.131999 m
495 amu	495.13158 amu	2.9386 %	148.396810 m
507 amu	507.14363 amu	5.6161 %	283.610026 m
511 amu	511.12571 amu	8.7804 %	443.400065 m
525 amu	525.14990 amu	8.6281 %	435.709636 m
539 amu	539.11301 amu	6.6225 %	334.431966 m
541 amu	541.12177 amu	3.1582 %	159.484863 m
555 amu	555.15096 amu	5.2419 %	264.709473 m
573 amu	573.17500 amu	3.9909 %	201.538086 m
581 amu	581.13754 amu	12.7894 %	645.853678 m
583 amu	583.12633 amu	4.5948 %	232.035319 m
597 amu	597.16319 amu	7.8747 %	397.664388 m
615 amu	615.16897 amu	11.9406 %	602.986654 m
679 amu	679.18124 amu	5.1029 %	257.690430 m
691 amu	691.36671 amu	4.5356 %	229.044596 m
703 amu	703.19201 amu	5.6488 %	285.257976 m
721 amu	721.18972 amu	15.8964 %	802.754721 m
722 amu	722.16838 amu	4.9514 %	250.040690 m
733 amu	733.20234 amu	4.1843 %	211.303711 m
751 amu	751.21309 amu	10.4116 %	525.777182 m
752 amu	752.19484 amu	3.3016 %	166.727702 m
775 amu	775.20791 amu	10.1417 %	512.145996 m
776 amu	776.22393 amu	4.0872 %	206.400553 m
793 amu	793.22478 amu	30.9210 %	1561.482746 m
794 amu	794.23952 amu	10.3887 %	524.617514 m
795 amu	795.16052 amu	3.2226 %	162.740072 m

Spec. IV.22 High resolution negative-ion l.d.i.-F.t.-i.c.r. spectrum of *Klebsiella* K22 oligosaccharide, con't.

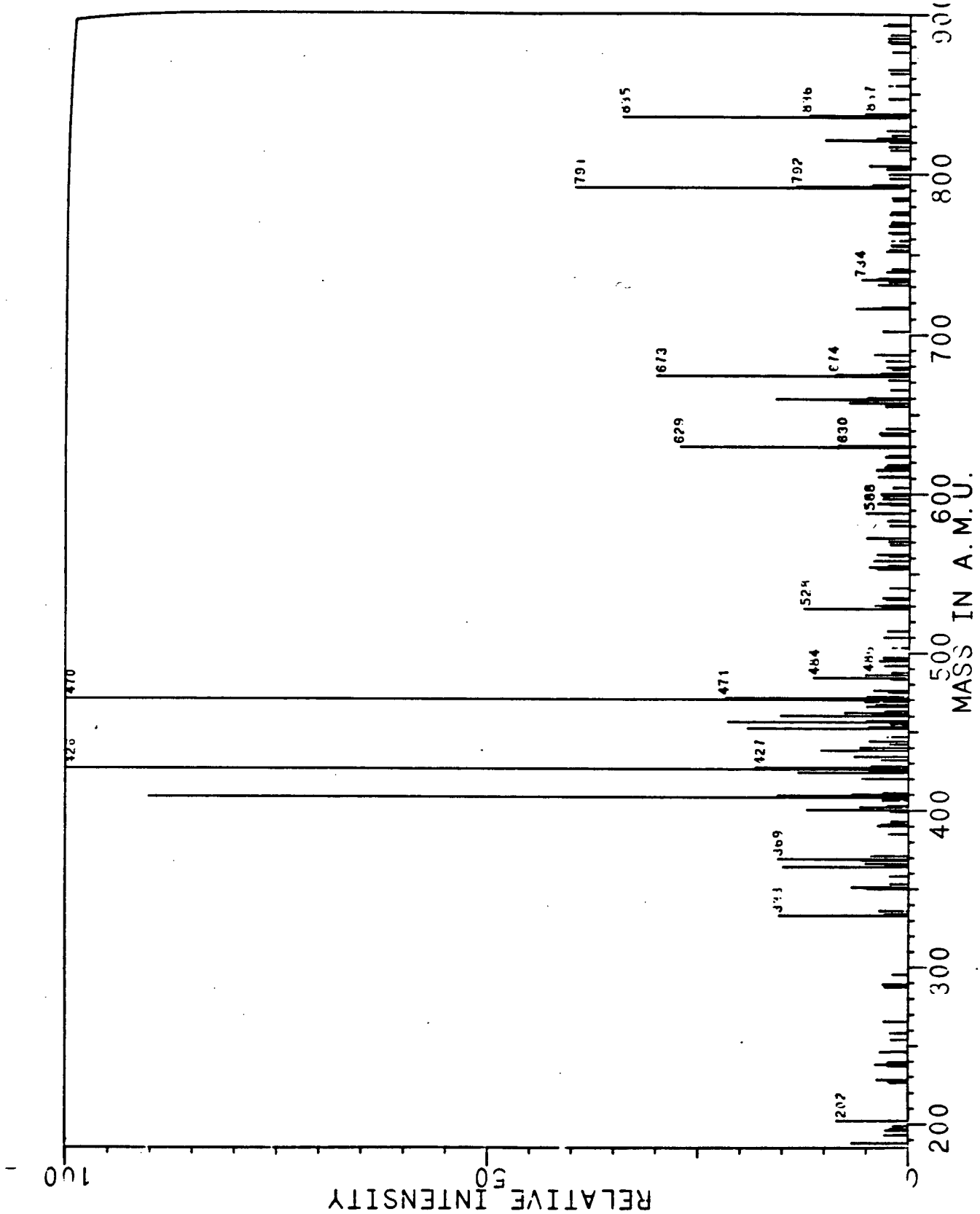

Spec. IV.23 Low resolution **negative-ion** l.d.i.-F.t.-i.c.r. spectrum of *E. coli* K49 oligosaccharide..

Nominal mass	Measured mass	Rel. intensity	Abs. intensity
188 amu	188.05702 amu	6.7795 %	621.044922 m
202 amu	202.07237 amu	8.4905 %	777.783203 m
333 amu	333.07777 amu	15.3319 %	1404.492187 m
351 amu	351.08551 amu	6.7630 %	619.531250 m
364 amu	364.12315 amu	14.9183 %	1366.601563 m
366 amu	366.10456 amu	5.2434 %	480.322266 m
368 amu	368.12358 amu	5.7806 %	529.541016 m
369 amu	369.01619 amu	5.7449 %	526.269531 m
369 amu	369.10702 amu	15.6789 %	1436.279297 m
400 amu	400.08572 amu	11.9696 %	1096.484375 m
402 amu	402.08656 amu	5.8185 %	533.007813 m
408 amu	408.10979 amu	90.1780 %	8260.839844 m
409 amu	409.10914 amu	15.5765 %	1426.904297 m
410 amu	410.10927 amu	6.7401 %	617.431641 m
420 amu	420.10804 amu	5.5088 %	504.638672 m
424 amu	424.13403 amu	13.2749 %	1216.064453 m
426 amu	426.11463 amu	99.8342 %	9145.410156 m
427 amu	427.12305 amu	18.2694 %	1673.583984 m
434 amu	434.12144 amu	6.4954 %	595.019531 m
438 amu	438.11596 amu	10.3972 %	952.441406 m
440 amu	440.12333 amu	5.8713 %	537.841797 m
452 amu	452.13133 amu	19.2262 %	1761.230469 m
456 amu	456.12985 amu	21.5427 %	1973.437500 m
460 amu	460.10650 amu	15.0451 %	1378.222656 m
462 amu	462.09651 amu	7.6105 %	697.167969 m
466 amu	466.01652 amu	5.1101 %	468.115234 m
469 amu	468.81784 amu	5.3537 %	490.429688 m
470 amu	470.14345 amu	100.0000 %	9160.595703 m
471 amu	471.14614 amu	21.8641 %	2002.880856 m
484 amu	484.06001 amu	11.4787 %	1051.513672 m
486 amu	486.05056 amu	5.1069 %	467.822266 m
528 amu	528.09480 amu	12.5639 %	1150.927734 m
572 amu	572.20427 amu	5.1554 %	472.265625 m
588 amu	588.17213 amu	5.1767 %	474.218750 m
629 amu	629.21419 amu	27.3713 %	2507.373047 m
630 amu	630.22390 amu	8.5646 %	784.570312 m
657 amu	657.19213 amu	7.1457 %	654.589844 m
659 amu	659.20014 amu	15.9219 %	1458.544922 m
660 amu	660.23585 amu	5.0248 %	460.302734 m
673 amu	673.24735 amu	30.1873 %	2765.332031 m
674 amu	674.24813 amu	8.8844 %	813.867187 m
716 amu	716.20160 amu	6.2220 %	569.970703 m
734 amu	734.25780 amu	5.7428 %	526.074219 m
791 amu	791.24591 amu	39.9267 %	3657.519531 m
792 amu	792.22926 amu	13.4311 %	1230.371094 m
821 amu	821.26808 amu	10.0805 %	923.437500 m
835 amu	835.28005 amu	33.9205 %	3107.324219 m
836 amu	836.23190 amu	11.8225 %	1083.007813 m
837 amu	837.30852 amu	5.3046 %	485.937500 m

Spec. IV.24 High resolution **negative-ion** l.d.i.-F.t.-i.c.r. spectrum of *E. coli* K49 oligosaccharide.

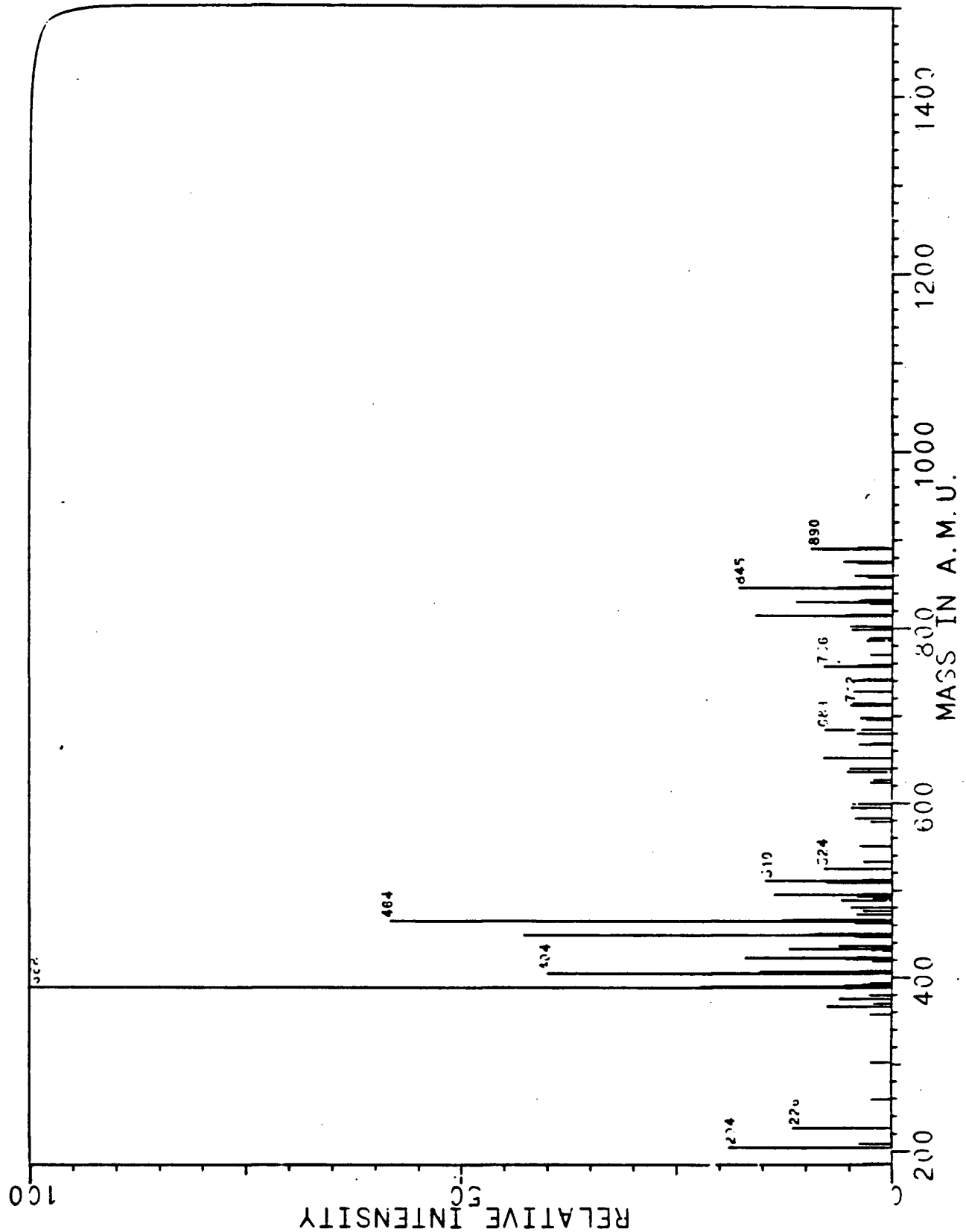

Spec. IV.25 Low resolution **positive-ion** l.d.i.-F.t.-i.c.r. spectrum of *E. coli* K49 oligosaccharide.

Nominal mass	Measured mass	Rel. intensity	Abs. intensity
204 amu	204.08675 amu	19.0477 %	1578.320312 m
226 amu	226.07116 amu	11.6337 %	963.984375 m
366 amu	366.13983 amu	7.4895 %	620.585938 m
375 amu	375.10968 amu	5.9672 %	494.453125 m
388 amu	388.12091 amu	100.0000 %	8286.132812 m
389 amu	389.13688 amu	22.2138 %	1840.664062 m
390 amu	390.13884 amu	5.5571 %	460.468750 m
404 amu	404.08224 amu	39.8713 %	3303.789062 m
405 amu	405.09224 amu	7.9920 %	662.226562 m
406 amu	406.13010 amu	15.4230 %	1277.968750 m
420 amu	420.16247 amu	5.2464 %	434.726563 m
422 amu	422.11281 amu	17.0319 %	1411.289062 m
432 amu	432.16040 amu	11.9166 %	987.421875 m
436 amu	436.12385 amu	6.1384 %	508.632813 m
448 amu	448.14951 amu	42.8563 %	3551.132812 m
449 amu	449.14350 amu	9.5566 %	791.875000 m
450 amu	450.13256 amu	8.5992 %	712.539062 m
464 amu	464.12825 amu	57.9093 %	4798.437500 m
465 amu	465.12927 amu	12.7778 %	1058.789062 m
466 amu	466.11601 amu	11.4381 %	947.773437 m
488 amu	488.11823 amu	5.8140 %	481.757812 m
494 amu	494.15428 amu	13.6981 %	1135.039063 m
508 amu	508.18300 amu	7.7549 %	642.578125 m
510 amu	510.11520 amu	14.7116 %	1219.023437 m
524 amu	524.17479 amu	7.8317 %	648.945312 m
635 amu	635.23124 amu	5.1720 %	428.554688 m
651 amu	651.15376 amu	7.8308 %	648.867188 m
683 amu	683.21279 amu	7.7256 %	640.156250 m
711 amu	711.30716 amu	5.0895 %	421.718750 m
756 amu	756.10590 amu	7.8015 %	646.445312 m
813 amu	813.22359 amu	15.6342 %	1295.468750 m
814 amu	814.19814 amu	5.4487 %	451.484375 m
829 amu	829.26689 amu	11.1387 %	922.968750 m
845 amu	845.02400 amu	18.0219 %	1493.320312 m
846 amu	846.04426 amu	6.4047 %	530.703125 m
875 amu	875.06413 amu	5.8343 %	483.437500 m
889 amu	889.10161 amu	7.8025 %	646.523437 m
889 amu	889.46572 amu	9.4642 %	784.218750 m

Spec. IV.26 High resolution **positive-ion** l.d.i.-F.t.-i.c.r. spectrum of *E. coli* K49 oligosaccharide.